UNIVERSITY OF OKLAHOMA

GRADUATE COLLEGE

ASSESSMENT OF PARTIAL JOINT PENETRATION WELDS ON BOLTED END-PLATE CONNECTIONS FOR USE IN INTERMEDIATE MOMENT FRAMES

A THESIS

SUBMITTED TO THE GRADUATE FACULTY

in partial fulfillment of the requirements for the

Degree of

MASTER OF SCIENCE

By

SAMUEL T. SHERRY
Norman, Oklahoma
2016

ASSESSMENT OF PARTIAL JOINT PENETRATION WELDS ON BOLTED END-PLATE CONNECTIONS FOR USE IN INTERMEDIATE MOMENT FRAMES

A THESIS APPROVED FOR THE
SCHOOL OF CIVIL ENGINEERING AND ENVIROMENTAL SCIENCE

BY

_____
Dr. Chris Ramseyer, Chair

_____
Dr. Jeffery Volz

_____
Dr. Philip Scott Harvey Jr

© Copyright by SAMUEL T. SHERRY 2016
All Rights Reserved.

Acknowledgements

This research could not have been completed without the support from BC Steel Building Inc. The entire staff's help is deeply appreciated. The materials and fabrication associated with this project were all generously donated by BC Steel Buildings Inc. A special thank you to the owner of the company Mary Webber for continuing to invest in the future of the metal building industry. Also a big thank you to Dennis Watson, whose insight and help throughout the project was instrumental to the success of this work. His support is greatly appreciated on this project.

I would like to thank and express my admiration to my committee chairman, Dr. Chris Ramseyer. His guidance, patience, and the lessons he taught me will follow me wherever I go. His passion for research is infectious and it is a quality I hope to emulate. I would also like to thank Dr. Jeffery Volz, and Dr. Philip Scott Harvey Jr for their guidance in the development of this thesis.

I would like to express my gratitude to Mike Schmitz Fears Laboratory's outstanding lab technician. He showed me the value of "teaching a man to fish", something that will not be forgotten.

Finally, I would like to thank my Mother and Father. The encouragement, sound advice and love they show me is deeply appreciated.

Table of Contents

Acknowledgements iv

Table of Contents v

List of Tables ix

List of Figures x

Abstract xiii

Chapters 1

1. Introduction and Literature Review 1

1.1. Introduction: 1

1.2. Literature Review 3

1.2.1. Welding Overview 3

1.2.2. End-Plate Connections 9

1.2.3. Partial Joint Penetration Welding 16

1.2.4. Literature Review Testing Summary 28

2. Objectives 29

3. Experimental Investigation 30

3.1. Introduction 30

3.2. Test Specimen Overview 32

3.3. Overall Design Considerations 33

3.3.1. Test Specimen Design Considerations 34

3.3.2. Modified PJP Weld 35

3.3.2.1. Design of Modified PJP Welds 35

3.3.2.2. Fabrication of Modified PJP Welds 39

3.4. Materials 40

3.4.1. Tensile Coupon Tests 40

3.4.1. Weld Metal Tests 42

4. Experimental Testing 43

4.1. Testing Setup 43

4.2. Instrumentation 55

4.2.1. Overall Instrumentation 55

4.2.2. Real Time Data Processing, Collection & Overview 59

4.2.3. Instrumentation Differences 60

4.2.3.1. King End Bolt Instrumentation: 61

4.2.3.2.2. Jack End Strain Gauge Instrumentation 66

4.3. Testing Procedures 68

4.3.1. Testing Procedures, Specifications & Loading Sequence 68

4.3.2. King End Testing Procedures 68

4.3.2.1. King End Snug Tight Bolt Installation Procedure 68

4.3.2.2. King End Snug Tight Testing Procedures 69

4.3.2.3. King End Pre-tensioned Bolt Installation Procedures 70

4.3.2.4. King End Pre-tensioned Testing Procedures 72

4.3.3. Jack End Testing Procedures 73

4.3.3.1. Jack End Pre-tensioned Bolt Installation Procedures 73

4.3.3.2. Jack End Pre-tensioned Testing Procedures 73

5. Experimental Results and Discussion 75

5.1. Overview 75

5.1.1. King End Overview 76

5.1.2. Jack End Overview 80

5.2. Rafters' Performance 84

5.3. Specimens Connection Performance 88

5.3.1. Inspection of Flange to End-plate Welds 89

5.3.1.1. Directly Measured Weld Throats 89

5.3.1.2. Theoretical Weld Throats 96

5.3.2. Examination of Flange to End-plate's Connections Strength 99

5.3.3. Discussion of Fillet Welds 103

5.3.4. Discussion of Root Face and LOP 104

5.3.5. Discussion of Size Effects on Connection 107

5.3.6. Final Remarks on Connection Performance 107

6. Summary and Conclusions 109

7. Further PJP Weld Design Considerations / Recommendations 111

References: 112

Appendix A – Design Calculations 115

A.1 – Test Specimen Design 115

A.2 – Weld Design 123

Appendix B – Material Properties 124

Appendix C – King End Plots & Photos 127

Appendix D - Jack End Plots & Photos 134

Appendix E – Bottom Side of Jack End Weld Cuts 140

Appendix F - Top Side of Jack End Weld Cuts 157

Appendix G - Bottom Side of King End Weld Cuts 174

Appendix H - Top Side of King End Weld Cuts..... 191

List of Tables

Table 1. Sumner's Testing Matrix 13

Table 2. Sumner's Test Results 14

Table 3. Summary of Literature Review's Test Specimen Sizes 28

Table 4. Test Specimen's Dimensions 32

Table 5. Predicted Design Strength 35

Table 6. Optimum Weld Sizes 37

Table 7. Theoretical Flange Force & Weld Design Strength 38

Table 8. Tensile Material Properties 41

Table 9. Weld Metal Material Properties 42

Table 10. Loading Sequences 68

Table 11. King End Test Data Summary 78

Table 12. King End Strain Gauge Data Summary 79

Table 13. Jack End Test Data Summary 82

Table 14. Jack End Strain Gauge Data Summary 83

Table 15. Predicted & Tested Beam Strength 85

Table 16. Average Dimensions of the Compiled Cut Section Properties 93

Table 17. Average Ratio of the Compiled Cut Section Properties 93

Table 18. Averaged Fillet Sizes of Flange to End-plate Welds Measured from Gauges 98

Table 19. Averaged Strengths of Flange to End-plate Welds 102

Table 20. True Strength (Measured Throat) / Design Strength of Flange to End-plate Welds 102

List of Figures

Figure 1. Typical Bolted End-plate Moment Connections 1

Figure 2. Typical CJP Weld 4

Figure 3. Typical PJP Weld 5

Figure 4. Typical Fillet Weld 6

Figure 5. Loading of Fillet Welds 7

Figure 6. Fillet Weld Load Deformation Relationship 7

Figure 7. Modified PJP Weld 9

Figure 8. End-plate Behavior 10

Figure 9. Sumner 2003 Test Specimens 11

Figure 10. Sumner's Testing Setup 12

Figure 11. Profile View of Koji Azuma et al.'s Connections 18

Figure 12. Kurobane et al.'s Testing Configuration 20

Figure 13. Profile View of Kurobane et al.'s Connections 21

Figure 14. Profile View of Kurobane et al.'s Failed Weld 22

Figure 15. Myers et al.'s Specimens Connections 23

Figure 16. Myers et al.'s Testing Configuration 23

Figure 17. Myers et al.'s Loading Protocol 24

Figure 18. End-plate Configuration of Chen et al.'s PJP Specimens 26

Figure 19. Chen et al.'s PJP Specimens 26

Figure 20. Chen et al.'s Testing Configuration 27

Figure 21. End-plate Typical Sheet 31

Figure 22. Test Specimen with Location Labeling 32

Figure 23. Test Specimen Naming Layout (Plan View) 33

Figure 24. Flange's Welding Callout Sheet 38

Figure 25. Examples of Test Specimen Welds..... 40

Figure 26. Idealized Test Setup 43

Figure 27. Overview of the Test Specimen 44

Figure 28. Level 1: Strong Floor 45

Figure 29. Level 2 Bottom Bracing 47

Figure 30. Lateral Torsional Buckling Cage 48

Figure 31. Rafter's Lateral Torsional Buckling Cage in Testing Setup 48

Figure 32. Column's Lateral Torsional Buckling Cage in Testing Setup 49

Figure 33. Test Specimens Tip Configuration 50

Figure 34. Level 3 Test Specimen and Loading Fixture 51

Figure 35. Level 4 Top Bracing Layout 53

Figure 36. Testing Setup Overlay..... 54

Figure 37. Instrument Layout Overview 56

Figure 38. Panel Zone Deflection Measurement Setup, Invar Rods (A), LVDT (B)..... 56

Figure 39. Wire Pot Measuring Column Deflection 57

Figure 40. Wire Pot at Rafter's Tip..... 57

Figure 41. Hydraulic Cylinder (A), and Load Cell (B) 58

Figure 42. Test Specimen's Rafter with a Fresh Coat of White Wash..... 58

Figure 43. Gauged Bolt Cross Section 61

Figure 44. Fully Gauged Bolt..... 62

Figure 45. Bolt Being Calibrated..... 63

Figure 46. Flat Strain Gauge 64

Figure 47. Strain Gauge Location on King End Specimen 65

Figure 48. Strain Gauge Naming System: King End 66

Figure 49. Strain Gauge Location on Jack End Specimen 67

Figure 50. Strain Gauge Naming System: Jack End 67

Figure 51. Strain Gauged Bolts Numbering System 69

Figure 52. Norbar Pneutorque PT5, Pneumatic Torque Wrench 71

Figure 53. Pneumatic Torque Wrench Regulator 71

Figure 54. King's End-plate to Rafter Connection Prior to Testing 80

Figure 55. King's End-plate to Rafter Connection at Testing Termination 80

Figure 56. Jack's End-plate to Rafter Connection Prior to Testing 84

Figure 57. Jack's End-plate to Rafter Connection at Testing Termination 84

Figure 58. Mn/Mp vs Rotation: King End 86

Figure 59. Mn/Mp vs Rotation: Jack End 87

Figure 60. Design Sheet for Cuts on JB Flange 90

Figure 61. Cut Flange Specimens 90

Figure 62. Typical Polished and Etched Weld Cut Specimen 92

Figure 63. KT- Cross Sectional Weld PenetrationView 94

Figure 64. KB- Cross Sectional Weld PenetrationView 95

Figure 65. JT- Cross Sectional Weld PenetrationView 95

Figure 66. JB- Cross Sectional Weld PenetrationView 96

Figure 67. Labeling System for the Measured Fillets 98

Figure 68. Stress at Crack's Tip 105

Abstract

ASSESSMENT OF PARTIAL JOINT PENETRATION WELDS ON BOLTED END-PLATE CONNECTIONS FOR USE IN INTERMEDIATE MOMENT FRAMES

End-plate moment connections are a very common connection type used in the metal building industry today. Bolted end-plate connections are found where a rafter is joined to a column and consist of a steel plate welded to the end of a rafter. The steel plate contains pre-drilled holes which allow the rafter to be easily bolted to a column in the field. Improved weld quality resulting from a controlled manufacturing environment and the cost effectiveness of these connections has made bolted end-plates very popular. Bolted end-plate connections can be engineered to meet design requirements for moment resisting connections used in seismically active areas and in structures that require a higher level of dependability. The current industry standard is to use complete joint penetration (CJP) welds when making the end-plate to flange welds. CJP welds connect the entire thickness of the joining metals. An alternative to CJP is partial joint penetration (PJP), which leaves some portion of the base metals' thickness unfused. PJP welds save time and money in the fabrication of end-plate connections, but the use of PJP in this application is currently not accepted by the code. The objective of this research is to evaluate the effectiveness of properly detailed built-up PJP flange welds on end-plate connections when subjected to seismic loading. The results of testing the built-up PJP welds on the six-bolt multiple row extended end-plate connections should

provide the basis for prequalification of this connection by the American Institute of Steel Construction (AISC).

Two multiple row extended end-plate moment connection tests were conducted at the University of Oklahoma's Donald G. Fears Structural Engineering Laboratory. The test specimens were 44 inch deep, cantilevered beams connected to a column via a bolted end-plates. A load was applied at the beam's tip creating a moment at the beam to column connection and created a force acting on the flange welds. The test specimens were tested in accordance with the *2010 AISC Seismic Provision's* criteria on cyclic loading sequences for beam to column moment connections.

The six-bolt multiple row extended end-plate connection with built-up PJP welds passed all the prequalification criteria for use on demand critical welds on intermediate moment frames. No weld failures were observed during testing. Built-up PJP welds used on bolted end-plate connections built according to specific design requirements identified by this testing, should be acceptable as pre-qualified connections according the *2010 AISC Seismic Provision* when used for demand critical welds in intermediate moment frames and less stringent connections. The 44 inch deep test sections are to our knowledge the deepest PJP weld tests performed to date.

Chapters

1. Introduction and Literature Review

1.1. Introduction:

End-plate moment connections are a very common joining technology used in the metal building industry today. A typical example of a bolted end-plate connection is found when joining a rafter to a column; however end-plate moment connections may also be used to splice rafters together. Typical bolted end-plate connections, as shown in Figure 1, consist of a steel plate which is welded to the end of a rafter. The steel plate contains pre-drilled holes which allows the end-plate-rafter combination to be easily bolted to a column in the field. End-plate connections come in many shapes, sizes, and bolt configurations to meet the intended application. Multiple row extended (MRE) end-plates are common due to the fact they require no field welding and yet still provide a desired semi-rigid seismic connection.

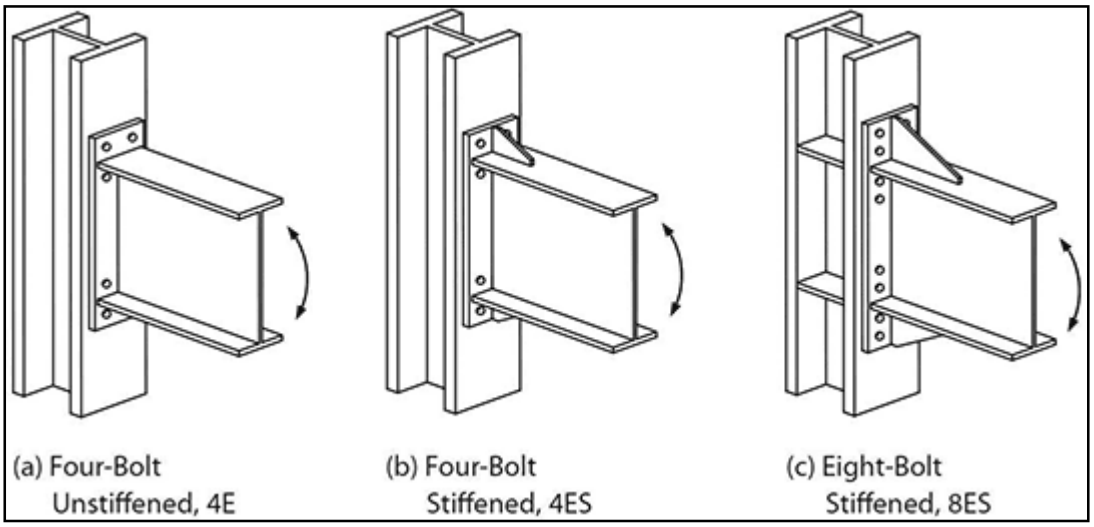

Figure 1. Typical Bolted End-plate Moment Connections (Murry, Summner, 2003)

Today the metal building industry requires specific moment resisting connections to meet intended seismic design applications. While these connections have been utilized for over fifty years, the aim of this research is to study in greater depth the weld strength of flange to end-plate connection under seismic loading. Specifically this work will examine a six-bolt extended multiple-row moment end-plate connection. This MRE end-plate is classified as a seismic force resisting system (SFRS) by the 2010 *AISC Seismic Provision,* and more specifically under that group as an intermediate moment frame (IMF). Designers like utilizing MRE connections in SFRSs because these connections enable them to meet moment resistance requirements, at a generally lower cost, and typically faster assembly in the field. The reduced installation time is due to the fact all welding can be completed in the shop. This is not the case for a fully welded rafter to column connection, which must be welded in the field. Welding in the shop is not only more economical due to cheaper labor, but assembly control in the shop enables a higher quality weld than can be typically achieved in the field. Variables such as work environment, structural alignment of elements, equipment and welders access are controlled in a shop, whereas field welding has less control over the assembly process. In shops, MRE connections are typically all completed in a continuous pass in the down hand welding or flat position. These are some of the easier welds to preform, and as a result, generally produce much better quality welds. According to the *Federal Emergency Management Agency* (FEMA) *350 Design Aid*, fully welded field welds on beam to column connections are made in the following manner:

Joints between the bottom beam flange and the column flange are typically made as a down hand field weld, often by a welder sitting on top of the beam top flange,

in a so-called “wildcat” position. To make the weld from this position each pass must be interrupted at the beam web, with either a start or stop of the weld at this location. This welding technique often results in poor quality welding at this critical location, with slag inclusions, lack of fusion and other defects. These defects can serve as crack initiators when the connection is subjected to severe stress and strain demands (FEMA 350).

While other types of connections are available to make these moment resisting connections (e.g., fully welded, fully bolted, mixed welds and bolts), it is not the aim of this research to examine different design practices; only connections consisting of flange welds are relevant to this research.

The purpose of this research is to test partial join penetration weld strength with the implementation of the six-bolt MRE end-plate connection to demonstrate that this joining technology should be considered by the American Institute of Steel Construction (AISC) as a viable, prequalified connection. Ultimately, these welds and end-plates could be used in practice once the connections are fully tested and proven acceptable. The criteria for validating this connection will be discussed further in the objectives portion of this paper.

1.2. Literature Review

1.2.1. Welding Overview

This research investigates the use of many different types of welds. An understanding of each weld and the accompanying properties is crucial to understanding key points that will later be examined. When designing connections of this nature, three

main types of welds are to be considered: complete joint penetration (CJP), partial joint penetration (PJP), and fillet welds.

CJP welds are typically used on thicker sections, and when used penetrate all the way through the material being connected. An example of a CJP weld can be seen in Figure 2. Typically, the metal being connected is “grooved”, in that, part of the metal is removed to provide access so weld metal can take its place and connect the adjoining metals. Typically the CJP welding process makes use of back-gouging, which is a process where typically an angle grinder or plasma cutter is used on the back side of the weld creating a gouge to remove any inclusions or flaws that might have been produced during the welding process. Upon completion of the weld, the entire thickness of the adjoining metals are fused, which allows the materials being joined to reach their full strength. In fact the deposited weld metal is stronger than the metal being joined. CJP welds are costly because they are labor intensive and require significant preparation work. However these welds require very little engineering effort when it comes to design, and their ease of use has made CJP welds common practice. These welds also typically require some non-destructive testing (NDT) to ensure that the welds pass inspection and are qualified for use.

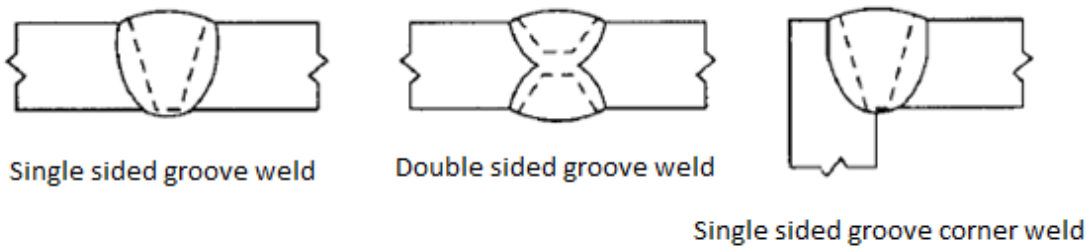

Figure 2. Typical CJP Weld (McCormac and Csernak, 2012)

The next type of weld to be examined is a PJP weld. An example of a PJP weld can be seen in Figure 3. PJP, as the name implies, has some portion of the metal being connected that is unfused, or not welded. PJP welds are similar to CJP welds in the sense that they are both typically grooved. The unfused face of the PJP weld has been the focus of much discussion (e.g., Ricles et al., 2002; Myers et al., 2009; Chen and Wang, 2009), as cracks often propagate from unfused locations, in turn causing the weld to fail. While this idea of crack initiation and propagation may be accurate, not enough research has been conducted on this area of study to quantify the true performance of PJP welds. The earliest advancement in PJP welds connection strength research was completed in the 70s and 80s, (Satoh et al., 1974; Gagnon and Kennedy, 1989). Recently however new research interests have been focusing on PJP welded columns to baseplate connections (e.g., Myers et al., 2009; Gomez, 2010) and column splices (Shaw, 2013).

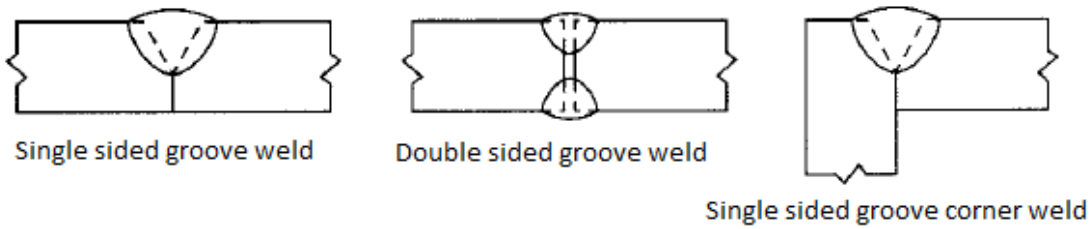

Figure 3. Typical PJP Weld (McCormac and Csernak, 2012)

Fillet welds are used to join thinner sections of steel. An example of a typical fillet weld can be seen in Figure 4. The advantage of using fillet welds is that no prep work is required on the metal being joined. This typically means no grooving of the metal is required prior to welding. These types of welds are used to connect thinner

thicknesses of metal due to the fact they cannot penetrate extreme depths, and because they become less cost effective to make as the welds become larger.

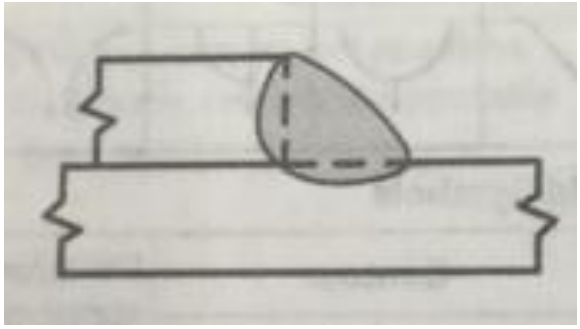

Figure 4. Typical Fillet Weld (AISC's 14th Edition of the Steel Construction Manual, 2012)

It is worth noting that a fillet weld strength is dependent upon the direction in which it is loaded. This variation in strength is due to the weld orientation under load and how this affects the stress and strain of the welds. In Figure 5(a) the fillet welds are being loaded parallel to the weld and in Figure 5(b) they are being loaded perpendicularly to the weld. In both cases the same amount of weld metal has been placed. When welds are loaded along the line of the weld as seen in Figure 5(a), they are more ductile then when they are loaded perpendicular to the weld. This is due to the fact the entire length of the welds is being pulled, allowing for elongation. However when one pulls on a weld perpendicular to the load as seen in Figure 5(b), less metal is able to elongate. This property allows perpendicularly loaded fillet welds to receive a strength increase, as shown in Figure 6. Each line on the graph represents a different angle measured from the direction of the weld's length. Meaning the 0° line is being loaded parallel to the length of the weld as seen in Figure 5(a), while the 90° line is being loaded perpendicular to the length of the weld as seen in Figure 5(b),. Assuming

the welds in Figure 5(a) and 5(b) are the same size and length, the latter receives a fifty percent strength increase. This strength increase is dependent on the angle of the load to that of the weld. The AISC's *14th Edition of the Steel Construction Manual* (2012) recognizes this strength increase and allows designers to utilize these strength increases on fillet welds.

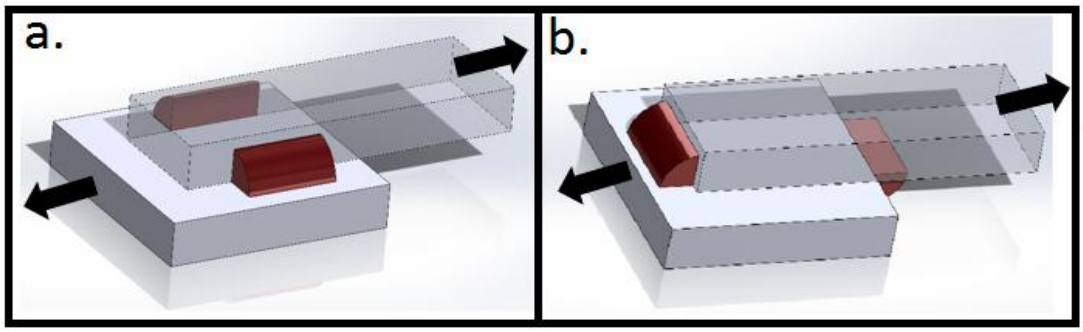

Figure 5. Loading of Fillet Welds

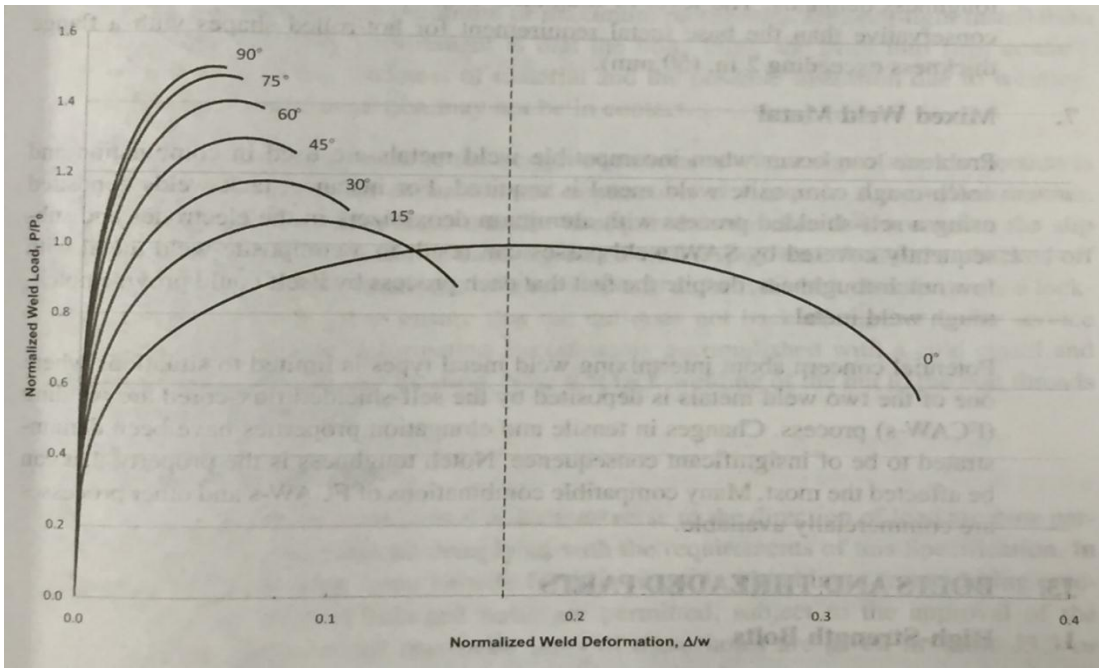

Figure 6. Fillet Weld Load Deformation Relationship (AISC's 14th Edition of the Steel Construction Manual, 2012)

While ample design aids, such as the *AISC Design Guide 4*, *AISC Design Guide 16* and *FEMA 350*, are available for practicing engineers to help design MRE end-plate connections, these aids neglect PJP welds. The current design standard is to use CJP welds on larger MRE connections and double sided fillet welds on the smaller connections. The *AISC Design Guide 4* and *AISC Design Guide 16* are the standards for bolted end-plate connections and neglect to mention the use of PJP welds to make the connection between a rafter's flanges and the end-plate. The *FEMA 350* design aid states that only CJP welds are prequalified, and are the recommended weld type. The omission of PJP welds in these design guides is likely because PJP welds are thought to be less effective and more problematic than CJP and fillet welds. Engineers have a preconceived notion that any unfused portion of the weld will cause crack propagation and this in turn makes the weld deficient. In general these welds are not used in common design practice.

Even though PJP welds were neglected from the design guides, designers are allowed to use their engineering judgment and knowledge to design these connections and meet needed strength criteria. Theoretically this should allow them to use PJP welds. However, PJP welds must first be validated through testing before becoming an acceptable standard. It is believed that testing can show that the use of modified PJP welds with built-up fillets on the PJP portion of the weld and reinforcing fillets on the other side will be more than sufficient to meet the *AISC 2010 Seismic Provision's* requirements for semi-rigid connection. When a modified PJP weld is referred to in this paper, it is referring to the modified PJP weld just described. An example of this modified PJP weld can be seen Figure 7 .

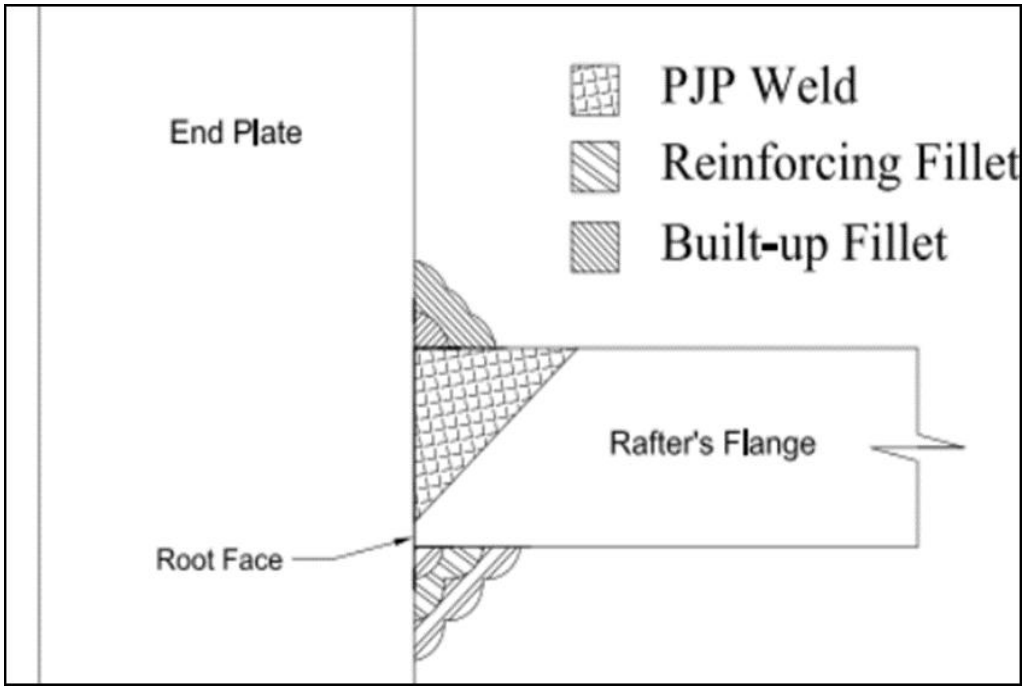

Figure 7. Modified PJP Weld

1.2.2. End-Plate Connections

The development of moment end-plate connections has a rich history dating back to research from the 1950s. The connection was not a new concept, but more of an evolution of the much-used split tee connection whose initial credit goes to R.O. Disque (Murray and Shoemaker 2002). Since then, extensive research has been conducted on end-plate connections (e.g., Kennedy et al., 1981; Srouji et al., 1983; Bond and Murray, 1989). This research focused on the yield line behavior of end-plates and the effect that plate thickness has on the prying action of the plate and bolt forces. It is known that there are three controlling failure stages when it comes to end-plate strength. These are thick plate behavior, intermediate plate behavior and thin plate behavior. An example and a reference of these three stages can be seen in Figure 8.

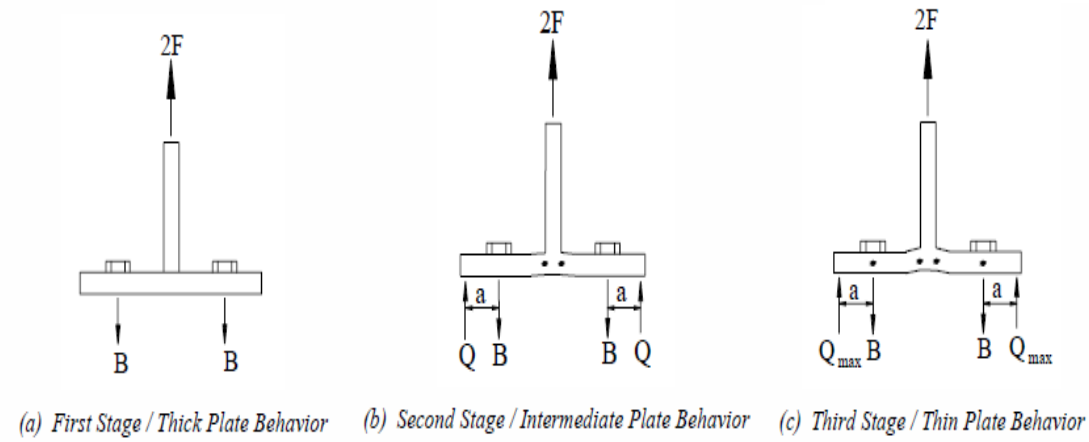

Figure 8. End-plate Behavior (Murry and Shoemaker, 2002)

In thick end-plate behavior no plastic hinges are formed and the applied force gets distributed to the bolts. Here the end-plate is thick enough to resist prying action. If enough force is applied the bolts may rupture; however, the end-plates do not yield. This is typically the case for which engineers design, but care is taken to ensure that the bolts are strong enough to resist rupture. Next is intermediate plate behavior. As the force is increased two plastic hinges are formed where the end-plate and the web intersect. At this point two things could happen: the bolts rupture or loading continues to increase and the next stage is observed. The final stage is thin plate behavior. As the force is increased two additional plastic hinges are formed at the center line of the bolts. At this stage one typically sees failure of the end-plate. It is important to note the difference between thick and thin plate behavior because it greatly affects the design of our specimen.

Coupled with this research and his own Murray, (1990) published the first edition of the *AISC Design Guide Series 4, Extended End-Plate Moment Connections.* This document is important in the fact it was published by the AISC and it was the first

of its kind. This document examined past research and published a design guide for extended bolted end-plate connections.

In 2003 Emmett Sumner published his dissertation which provided a unified design for extended end-plate connections subject to seismic loading. His research had four parts: an extensive literature review, an experimental testing portion, a comparison of these new versus old results, and design recommendations. His literature review examined the past forty years of bolted end-plate connection research. The literature review looked at a combination of eighteen journal and research papers, which in total examined the results of ninety end-plate moment connections. Using a combination of the previous research three connection configurations were selected for design / verification when subject to seismic loading. These connections can be seen in Figure 9. "The three connection configurations are as follows: 4E for the four bolt extended unstiffened connection (Figure 9a), 8ES for the eight bolt extended stiffened connection (Figure 9b), 8E-4W for the eight bolt extended, four bolts wide connection (Figure 9c)" (Sumner, 2003).

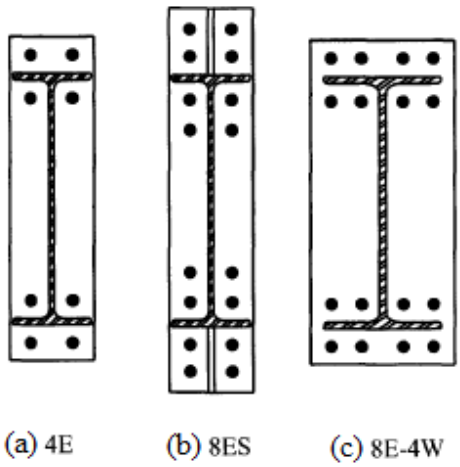

Figure 9. Sumner 2003 Test Specimens (Sumner, 2003)

Eleven beam to column connection tests were performed in this study. The testing setup can be seen in

Figure 10. The specimens were loaded in a quasi-static manner in accordance with SAC which is a joint venture of the following organizations: Structural Engineers Association of California, Applied Technology Center, and the California Universities for Research in Earthquake Engineering. The depth of the tested rafters ranged from 24 inches to 36 inches. The end-plates are classified here as weak plate or strong plate which is the equivalent of thick plate or thin plate behavior. The testing matrix can be seen in Table 1.

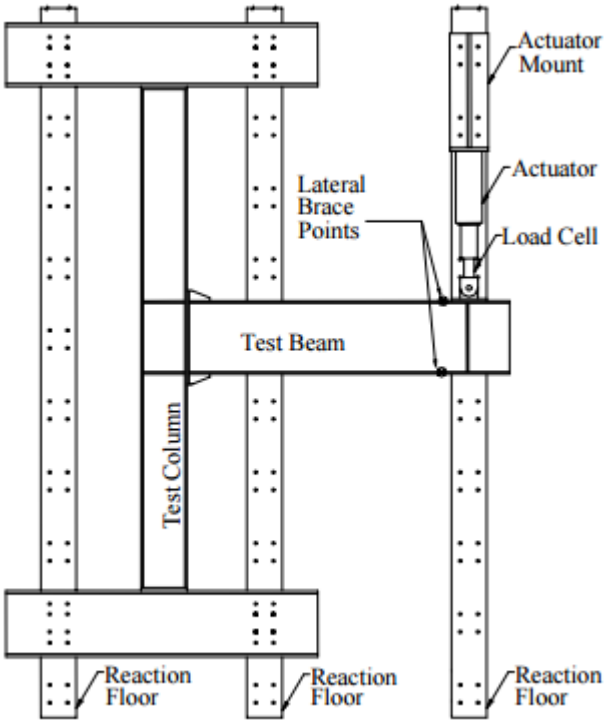

Figure 10. Sumner's Testing Setup (Sumner, 2003)

Table 1. Sumner's Testing Matrix (Sumner, 2003)

Specimen Identification*	Beam / Column	No. of Connection Bolts** (Material)	End-Plate Thickness (in)
4E-1 1/4 -1 1/2-24	W24x68 / W14x120	8 (A490)	1 1/2
4E-1 1/4-1 1/8-24	W24x68 / W14x120	8 (A325)	1 1/8
4E-1 1/4-1 3/8-24 with 5 in. composite slab	(2) W24x68 / W14x257	8 (A490)	1 3/8
8ES-1 1/4-1 3/4-30	W30x99 / W14x193	16 (A490)	1 3/4
8ES-1 1/4-1-30	W30x99 / W14x193	16 (A325)	1
8ES-1 1/4-2 1/2-36	W36x150 / W14x257	16 (A490)	2 1/2
8ES-1 1/4-1 1/4-36	W36x150 / W14x257	16 (A325)	1 1/4

* 4E designates a four bolt extended unstiffened connection
8ES designates an eight bolt extended stiffened connection
** 1 1/4 in. diameter

The test results from Sumner (2003) can be seen in Table 2. The weak plate connections were controlled by yielding of the end-plate and then bolt rupture. These connections did not perform as well as the strong plate connections. The strong plate connections typically failed due to local beam buckling. Both connection types showed good ductility but it was clear that the strong plate connections provided the best energy dissipation. The maximum sustained rotation can be seen in Table 2.

Table 2. Sumner's Test Results (Sumner, 2003)

Test Identification		M_{max} / $M_{n\ BEAM}$*	$\theta_{Total\ Sustained}$ (rad)	$\theta_{P\ Max\ Sustained}$ (rad)
4E-1 1/4-1 1/2-24 (Strong Plate)		1.00	0.052	0.038
4E-1 1/4-1 1/8-24 (Weak Plate)		0.95	0.040	0.021
4E-1 1/4-1 3/8-24 with 5" composite slab (Strong Plate)	North Beam	1.28	0.050	0.025
	South Beam	1.27	0.060	0.035
8ES-1 1/4-1 3/4-30 (Strong Plate)		1.00	0.050	0.036
8ES-1 1/4-1-30 (Weak Plate)		1.06	0.056	0.039
8ES-1 1/4-2 1/2-36 (Strong Plate)		1.06	0.050	0.028
8ES-1 1/4-1 1/4-36 (Weak Plate)		0.89	0.030	0.011

* M_{max} = Maximum applied moment at the face of column

$M_{n\ BEAM} = R_y\ [(F_y + F_u)/2]\ Z_x = 1.1[(50+65)/2]\ Z_x$

Sumner's (2003) study provided a unified body of work for cyclic testing on bolted end-plate connections and then compared that to previous testing. He found that his work was closely aligned with past researchers' test results. This was extremely important in the fact that not all strength predictions completed by previous researchers were tested in a cyclic manner.

As more and more research was completed, the AISC utilized this extensive database on the subject and in 2002 the *AISC Design Guide 16: Flush and Extended Multiple-Row Moment End-Plate Moment Connections* was published (Murray and

Shoemaker, 2002). A years later the AISC published the second edition of *Design Guide 4: Extended End-Plate Moment Connections Seismic and Wind Applications* which highlighted the work done by Sumner in 2003 (Murray and Sumner, 2003). These two design guides are the current industry standards used to design moment resisting end-plates. While very inclusive and good references, these guides do not discuss the use of PJP welds to make the connection between the flanges of the rafters to the end-plate of these connections. After a detailed review of the *AISC Design Guide 4, AISC Design Guide 16*, and the *FEMA 350 Recommended Seismic Design Criteria* about the connection of the rafters' flanges to an end-plate, some important information can be summarized. *AISC Design Guide* 16 suggests that flange welds should be designed as follows:

Normally, the beam flange to end-plate weld is designed to develop the yield strength of the connected beam flange. This is usually done with full penetration welds but alternatively, fillet welds may be used for thin flanges. When the applied moment is less than the design flexural strength of the beam, the beam flange to end-plate weld can be designed for the required moment strength but not less than 60 percent of the specified minimum yield strength of the connected beam flange (Murray and Shoemaker, 2002).

Concerning flange welds *AISC Design Guide* 4 states: "The beam flange to end-plate connection should be made using a CJP weld if the flange thickness is greater than 3/8 inch. Fillet welds on both sides of the beam flange may be acceptable for thinner flanges" (Murray and Summner 2003). Yet, both design guides entirely neglect the use of PJP welds. However these design guides do note that as long as welds can

meet the required moment strength of the connection any type of welding is acceptable. The *FEMA 350 Reference Design Guide* only states that CJP welds are prequalified, and offers no further insight on the flange welds (FEMA, 2000).

The above information provides background that specifically addresses the end-plate side of this research. It shows a lack of information regarding the use and design of PJP welds for MRE end-plate connections. The remaining portion of this literature review will examine research on welded connections which specifically implement PJP welds.

1.2.3. Partial Joint Penetration Welding

The initial research that examined PJP welds and developed design equations is credited to Satoh and colleagues. Satoh et al. (1974) developed complex charts and design equations for PJP weld strength. They also tested many specimens and found the optimum ratio of depth penetration to outside fillet leg size. Their seminal work provided the basis for further research in the field of PJP welds. The next major research breakthrough regarding PJP welding is credited to Gagnon and colleagues. Gagnon et al. (1989) proposed simplified design strength equations for PJP welds. Their research also determined what percent penetration of the weld was required to achieve failure in the base metal.

Five years later, in response to the 1995 Kobe earthquakes in Japan, Koji, Azuma et al. (2000) investigated weld defects in beam to column connections that were subject to cyclic loading (seismic). The researchers were interested in the effect of weld defects in the beam flange to column flange connections on its overall strength. Ideally the connections strength would be able to resist flange forces associated with the beam

achieving its plastic moment; but, due to weld flaw inclusion it was unknown if this was possible.

Four beam to column connections were tested in their research. All beams and columns were the same size. Of these four specimens two were PJP flange to column connection (BS specimens), and the other two were single sided CJP flange splices (BH specimens). The BH specimens had a steel bar inserted into the groove that would serve as its flaw. While the BS specimens had a root face where no weld penetration was present. Examples of the test beams profiles and test setup can be seen in Figure 11. The 350 x 357 x 19 x 19 mm beams are equivalent to: 13.78” deep sections, with 14.06” wide flanges, 0.74” thick webs, and 0.74” thick flanges. The BH specimens had two variations of flaw size, one where the root face, L, was 4mm or 0.16”, and 8mm or 0.32”. The BS specimens had two different length of flaw inclusion; but, here it was the length from the centerline of the web to some distance L away from the web. These lengths were 50mm or 1.97”, and 100mm or 3.94”. The width of the rectangular steel bar that was included in the weld was the same for both specimens, 10mm or 0.393”. The thickness of the steel bar was not reported. It is also of note that the backing bar used to make the weld in specimens BS was not removed.

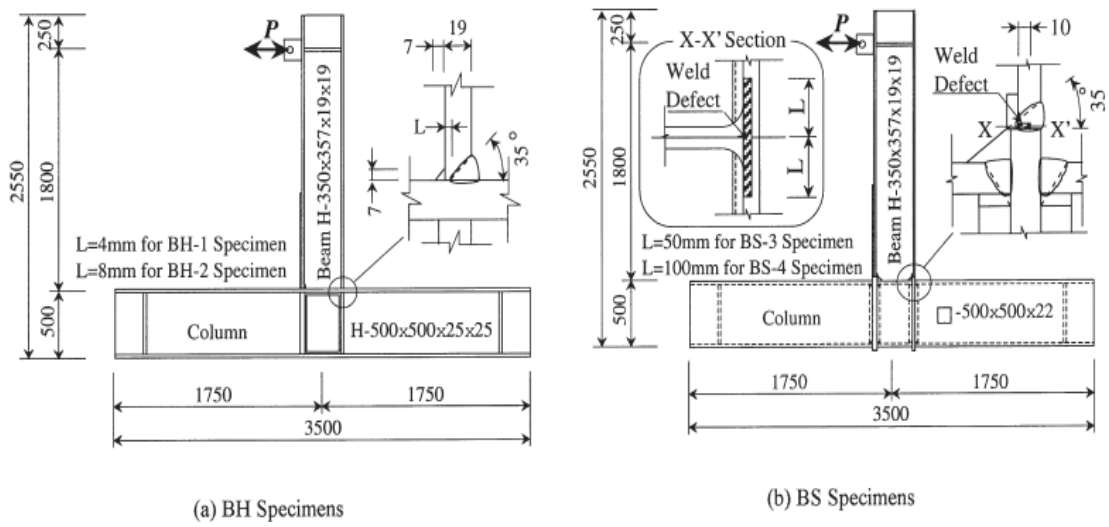

Figure 11. Profile View of Koji Azuma et al.'s Connections (Koji Azuma et al., 2000)

The cyclic loading protocol for these specimens looked at the rotation of the beam when it achieved plastic rotation, θp. This rotation, θp was the benchmark for further cycles. Further testing used this benchmark rotation, and multiples of 2 for the next set of cycles (e.g. 2θp, 4θp, 6θp, etc.); this loading protocol was run until failure. Each stroke consisted of positive and negative deflection.

Both BH specimens failed due to local and lateral buckling. Nevertheless ductile cracks did extend from the welds' toes, and included defects. However these cracks did not cause the welds to rupture or fail. The BS specimens did not preform as well. These specimens failed due to tensile rupture of the flange. Ductile crack iniated in the weld flaw and extended to the point that they became brittle fractures running across the beams flanges.

A few major points can be taken from their research: First, even though an initial well-defined defect existed in the PJP weld, ductile crack initiation started at either the toe of the welds or in the unfused portion of the weld. Also the cracking

observed in the PJP welds were just surface cracks while the cracking in the CJP welds were through the entire cross section of the flange. Second, the observed cracks in the PJP welds were small and grew stably with the loading increase. When the unfused portions of this PJP weld were examined, notably lower strains were observed in this location than in other portions of this connection, a result of the larger cross-sectional area here due to the reinforcing fillets. Lastly, the use of high toughness weld metal and the low demand strains in this area relieved concerns regarding the occurrence of brittle fracture. Conversely the inclusion of such large defects as in the case of BS specimens and lack of penetration, i.e., no reinforcing fillets, at the weld root caused severe strain concentrations. The weld metal was not sufficient to resist these large stresses and the result was crack propagation and brittle fracture. The findings of their paper demonstrated that concerns about incomplete or partial weld penetration can be eased with the inclusion of reinforcing fillets and ductile weld material.

One of the first examinations of beam to column connections that strictly investigated PJP welds with reinforcing fillets on end-plate connection was conducted by Kurobane et al. in 2004. Their research wanted to validate PJP welds with reinforcing fillets as a means to achieve the strength of beam to column connections that were subject to cyclic loading. In total, four specimens were tested in cyclic loading, with all tested beams being the same size. In cyclically testing these specimens the loading procedures

were controlled by the displacement at the free end of the cantilever beam. A setup of their testing layout can be seen in Figure 12.

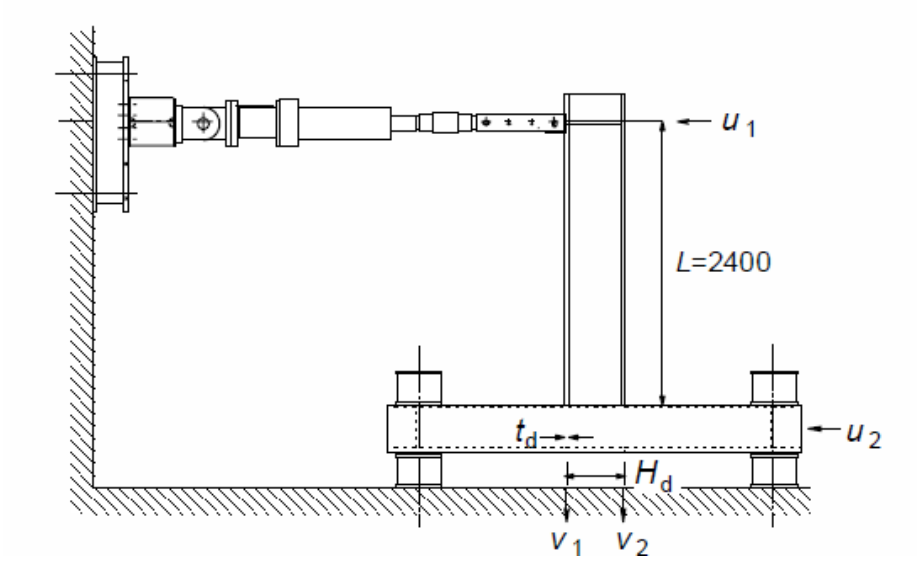

Figure 12. Kurobane et al.'s Testing Configuration (Kurobane et al., 2004)

Each flange to column weld on these connections utilized different sized PJP welds. Examples of the tested beam profiles can be seen in Figure 13. The 500 x 200 x 100 x 16 mm beams tested are equivalent to: 19.68” deep sections, with 8.87” wide flanges, 0.39” thick webs, and 0.69” thick flanges. During the loading protocol two cycles of load application were applied during testing. Initially the specimen were loaded in the elastic range for a few cycles. Once the beam saw plastic rotation, θp, this was the benchmark for further cycles. Further testing used this benchmark rotation and

multiples of 2 for the next set of cycle (e.g. 2θp, 4θp, 6θp, etc.), this loading protocol was run until failure.

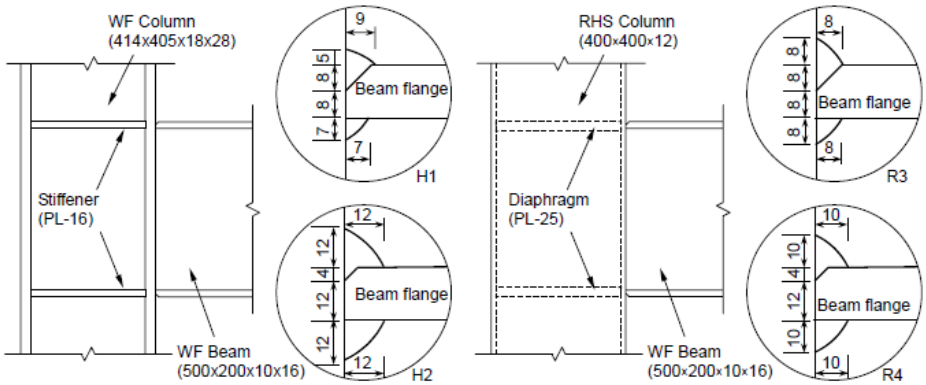

Figure 13. Profile View of Kurobane et al.'s Connections (Kurobane et al., 2004)

Out of these four connections one failed due to weld failure caused by a lack of weld penetration. The other three specimens exhibited good strength and plastic deformation capabilities; these specimens failed due to local flange buckling. A few major points can be taken from their research: First, even though an initial well-defined defect existed in the PJP weld, ductile crack initiation started at either the toe of the welds or at edges of the beams flanges. See Figure 14 for a reference of the weld toe and root face. Second, the observed cracks were small and grew stably with increased loading. The use of high toughness weld metal and the low demand strains in this area relieved concerns about the occurrence of brittle fracture. A non-linear finite element analysis conducted by these researchers showed that the tip of the root face did not induce a high enough stress to cause brittle fracture, and their experimental results back these findings. Again here proper PJP welds, with the use of high toughness electrodes, and reinforcing fillets were sufficient in achieving the beams' plastic capacity.

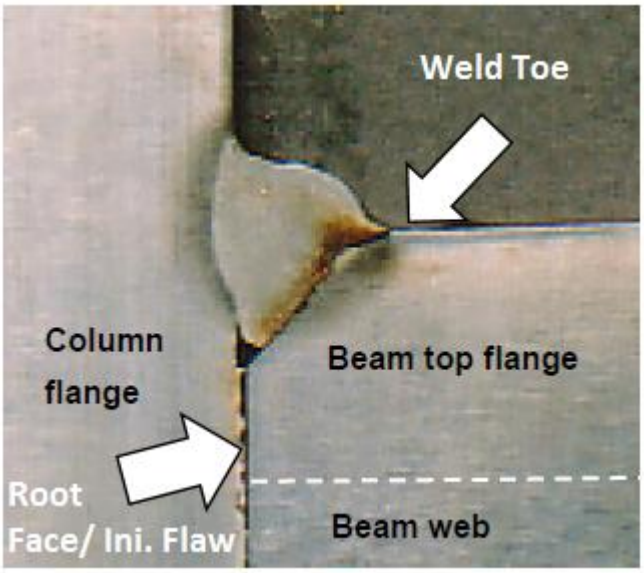

Figure 14. Profile View of Kurobane et al.'s Failed Weld (Kurobane et al., 2004)

The next application of PJP welds with reinforcing fillets was used on column to baseplate connections. Myers et al. (2009) investigated both PJP and CJP welded connections. These connections were designed for seismic activity and the yielding of the column. The column sections were W8 X 67 and detailed to be 2/3 scale models of typical first floor column sections. This column section was selected because it has both compact flanges and webs, which typically lends itself to ductile behavior. Meaning that a plastic hinge of the beam is most likely to occur before any local bucking. In total 6 specimens were fabricated, 4 had CJP flange to baseplate connections and 2 used PJP welds with reinforcing fillets. Figure 15 shows the specimens detailed flange to baseplate connections with the CJP specimen on the left and the PJP on the right.

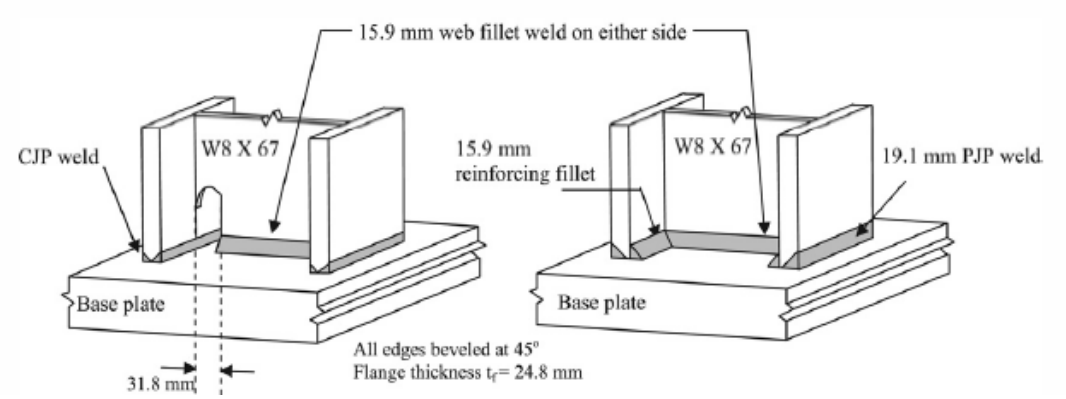

Figure 15. Myers et al.'s Specimens Connections (Myers et al., 2009)

The cyclic loading of these specimens was controlled by the displacement at the free end of the cantilever column being tested. The testing configuration for this column to baseplate connection can be seen in Figure 16.

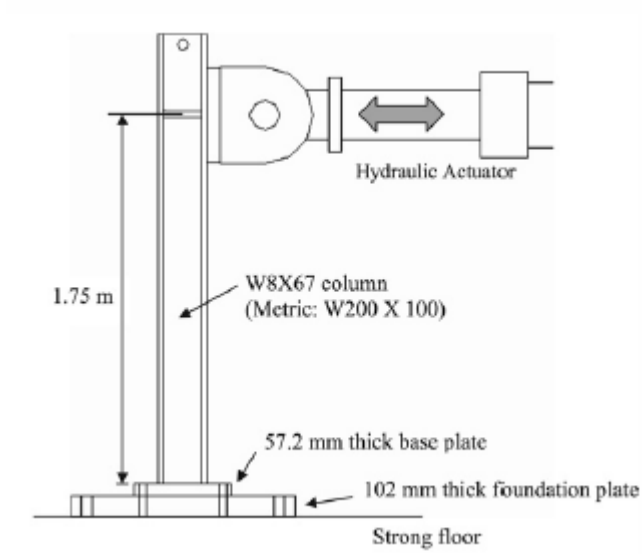

Figure 16. Myers et al.'s Testing Configuration (Myers et al., 2009)

The cyclic loading protocol used in this testing was adopted from the SAC. A plot of the measured drift versus load cycles can be seen in Figure 17.

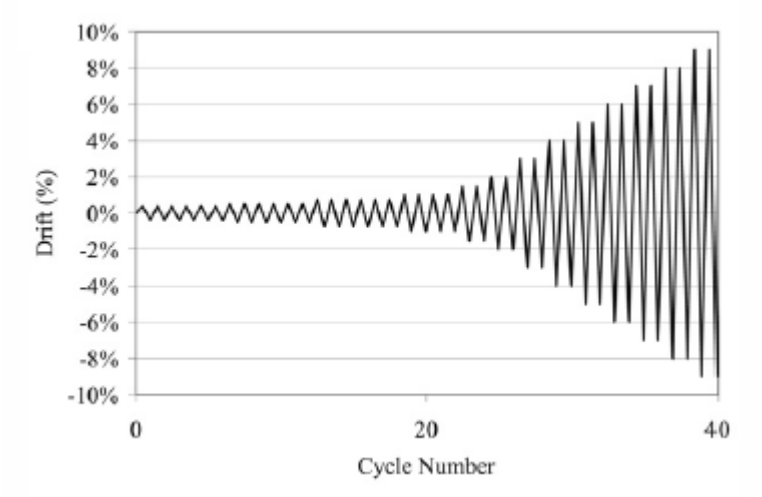

Figure 17. Myers et al.'s Loading Protocol (Myers et al., 2009)

A majority of their specimens show fracture initiation and failure in the heat effected zone near the fusion line between the weld and the column flange. While this type of behavior was expected for CJP weld specimens, it was expected that PJP welds would fail due to their initial defect. However, the test results clearly indicate that the combination of the extra strength provided by the fillet weld reinforcement and the weld toughness was sufficient to resist fracture at the weld root and to concentrate yielding in the column flange. Myers et al. (2009) concluded that "Overall, specimens with PJP welds performed better than those with CJP welds, with the PJP details sustaining drifts as large as 8%-9% before failure, as compared to 5%-6% drifts for the tests with the CJP detail." It should be noted that the typical maximum seismic design is based upon a 4%-5% drift for the column.

Lastly, and the most relevant to our research, modified PJP welds in MRE end-plate connections was a study completed by Chen and colleagues. Chen et al. (2009) focused their research on achieving the beam's plastic moment capacity when subject to

cyclic or monotonic loading. These researchers wanted to show that PJP and double sided fillet welds could be used to make flange to end-plate connections for seismic force resisting system's intermediate moment frame. This research examined 30 specimens, 11 of which had PJP welds, 9 had double sided fillet welds, and the remaining 10 were full penetration welds. Out of those 11 PJP weld specimens, only 2 were loaded cyclically; the rest were monotonically loaded. These 2 cyclically loaded PJP specimens were the largest of all the tested specimens, and of most relevance to this thesis. These specimens were 24.6" deep sections, with 7.87" wide flanges, 0.31" thick webs, and 0.47" thick flanges. These parameters define both the flange and the web as compact sections, which typically lends itself to ductile behavior. An end-plate thickness of 1" was used, which maintained the end-plate in its elastic deformation zone, avoiding any end-plate plastic yielding during their testing. As previously discussed this is a first stage thick end-plate behavior as defined by Murry and Shoemaker, 2002. In total, 14 0.95"-diameter bolts were used on these connections; these bolts were pre-tensioned to 60% of their ultimate strength. A profile of these end-plates can be seen in Figure 18. It should be noted that this bolting pattern is not prequalified for use by the AISC.

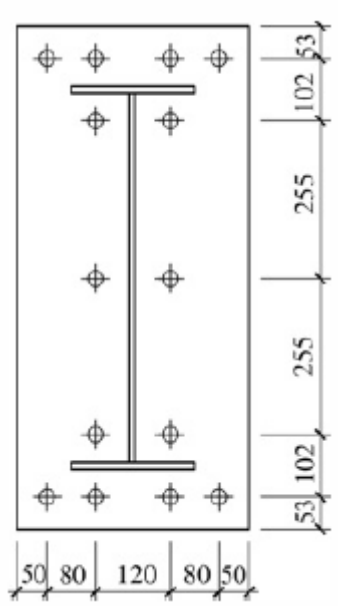

Figure 18. End-plate Configuration of Chen et al.'s PJP Specimens (Chen et al., 2009)

The flange to end-plate connection made use of built-up PJP welds and reinforcing fillets. A side profile of the PJP welds can be seen in Figure 19. The S value is the throat of the weld, and is 0.44". The groove of the PJP side, α, is 60°. The reinforcing fillets on the inside of the flanges measured 0.315" along the length of the end-plate.

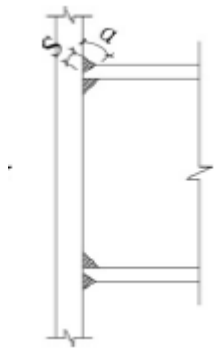

Figure 19. Chen et al.'s PJP Specimens (Chen et al., 2009)

In monotonic loading the specimens were loaded until the ultimate state of the specimens were observed. In cyclically testing of these specimens the loading procedure was controlled by the displacement at the free end of the cantilever beam. Three deflection levels were observed, δe, 2δe, and 3δe, where δe was the free end displacement of the cantilever beam tip at beam yielding. Each deflection set contained deflections in both the positive and negative direction three times each. If all 3 deflection levels were completed the last deflection would be the beams length/25; after this, testing was terminated. The testing configuration for these beam to end-plate connections can be seen in Figure 20.

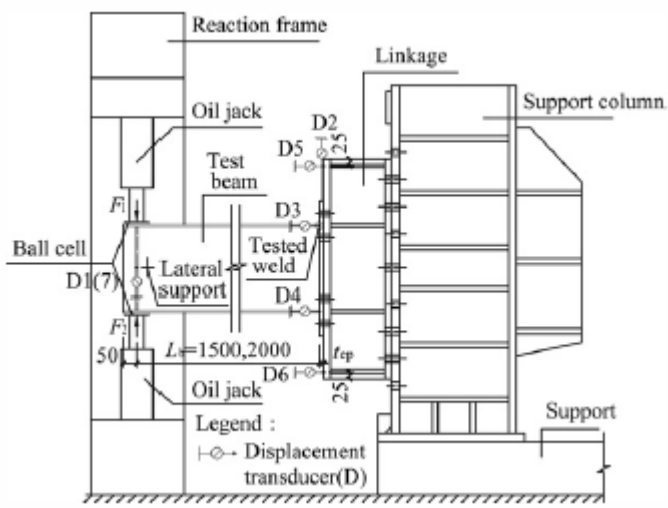

Figure 20. Chen et al.'s Testing Configuration (Chen et al., 2009)

All of the 30 tested specimens failed due to local buckling or plastic buckling. No weld failures were observed in any of the specimens. These results helps to demonstrate that as long as one uses reinforcing fillet welds, proper weld penetration, and adequately

tough weld metal the use of PJP welds can meet the design requirements of seismic force resisting systems' connections.

1.2.4. Literature Review Testing Summary

Table 3 provides a summary of the most pertinent articles related to this research that were discussed in the literature review. Table 3 highlights the fact that to our knowledge the use of PJP welds on flange to end-plate connections for seismic design has been limited to 10 specimens with a maximum rafter size of 24.6 inches.

Table 3. Summary of Literature Review's Test Specimen Sizes

Research	Area of Interest	Connection Type:	Max Specimen Depth (in)	Max Flange Thickness (in)	Failure Mode
Sumner (2003)	Bolted End-plate Connections with CJP Welds	Beam Flange to End-plate / Column	36.00	0.90	Flange Buckling
Azuma et al. (2000)	Weld Defects / PJP Welds	Beam Flange to Column Flange	13.87	0.74	2 out of 2 Local & Lateral Buckling
Kurobane et al. (2004)	Built-up PJP Weld with Reinforcing Fillets	Beam Flange to Column Flange	19.68	0.69	3 out of 4 Local Flange Buckling 1 Weld Rupture
Myers et al. (2009)	PJP Welds with Reinforcing Fillets	Column Flange to Baseplate	8.00	0.97	2 out of 2 Flange Fracture After Significant Buckling
Chen et al. (2009)	Built-up PJP Weld with Reinforcing Fillets	Beam Flange to End-plate / Column	24.60	0.47	2 out of 2 Local Buckling

2. Objectives

The objective of this research is to provide test data to evaluate the effectiveness of properly detailed modified PJP flange welds on end-plates connections when subject to seismic loading. The results of testing the modified PJP welds using the 6-bolt MRE end-plate connections should provide the basis for prequalification of this connection by AISC simplifying future use. This research will further provide important groundwork for examining the true capabilities of PJP welds.

The main requirement to proving any design to be capable of being a standard practice in seismic regions is to meet *2010 AISC Seismic Provision's Criteria*. In particular this research was focused on qualifying this connections for use as an Intermediate Moment Frame (IMF). The requirements for this IMF end-pate connection validation can be found in the *2010 AISC Seismic Provision*. The provision states: "beam-to-column connections used in the SFRS shall satisfy the following requirements:

(1) The connection shall be capable of accommodating a story drift angle of at least 0.02 rad.

(2) The measured flexural resistance of the connection, determined at the column face, shall equal at least 0.80M of the connected beam at a story drift angle of 0.02 rad."

3. Experimental Investigation

3.1. Introduction

The details of the experimental work conducted in this research are presented in this chapter. Included are a description of the test specimen overview, design considerations, material properties, test setup, test procedures, and test results for each specimen. Two MRE end-plate moment connection tests were conducted at the University of Oklahoma's Donald G. Fears Structural Engineering Laboratory. This research implemented the use of the six-bolt, multiple-row extended, unstiffened moment end-plate consisting of three rows of two bolts in both the tension, and compression zones of the bolted end-plate, for a total of twelve bolts. A full typical sheet with dimensions of this end-plate can be found in Figure 21.

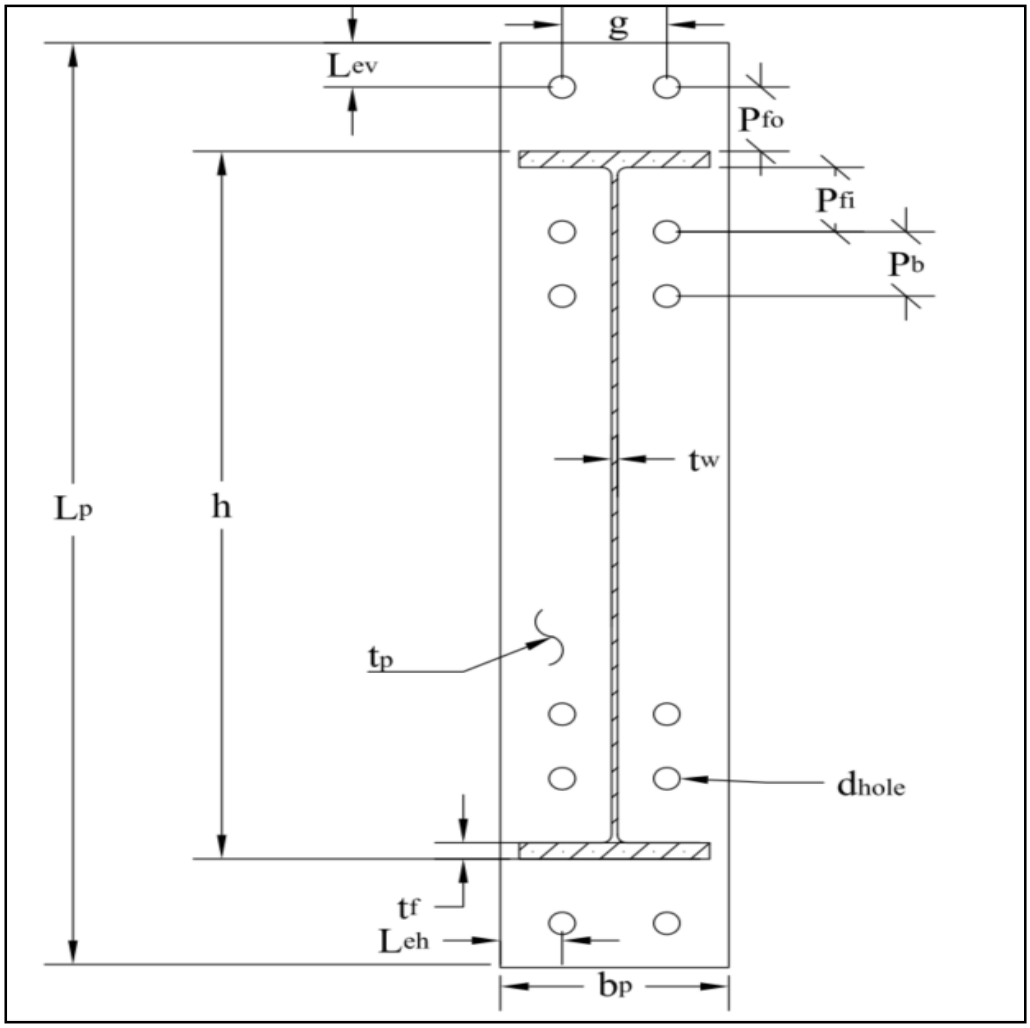

End-plate Thickness, t_p:	2.0 in.
End-plate Width, b_p	12.0 in.
End-plate Length, L_p:	57.5 in.
End-plate Vertical Edge Distance, L_{ev}:	2.75 in.
End-plate Horizontal Edge Distance, L_{eh}:	3.25 in.
Outer Pitch, Bolt to Flange, p_{fo}:	4.0 in.
Inner Pitch, Bolt to Flange, p_{fi}:	4.0 in.
Outer Pitch, Bolt to Bolt, p_b:	4.0 in.
Bolt Hole Diameter, d_{hole}:	1.5 in.
Flange Thickness, t_f:	1.0 in.
Web Thickness, t_w:	0.375 in.
Beam Depth, h:	42.0 in.
Gauge, g:	5.5 in.

Figure 21. End-plate Typical Sheet

3.2. Test Specimen Overview

Figure 22 shows the test specimen with a bolted end-plate on each end. This allows the specimen to be tested twice. The built-up section's dimensions are shown in Table 4.

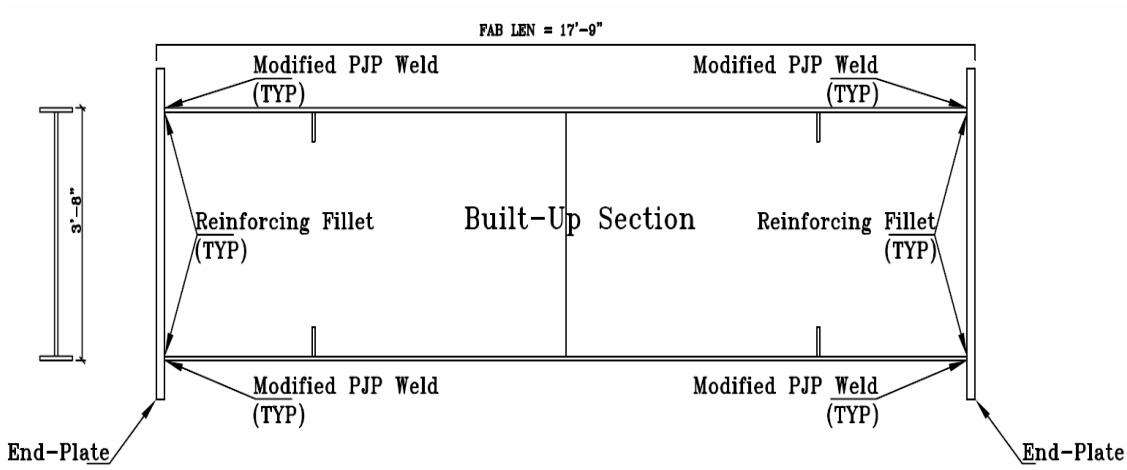

Figure 22. Test Specimen with Location Labeling

Table 4. Test Specimen's Dimensions

Location	Dimension
Beam Depth (d)	44.0 in.
Flange Thickness (t_f)	1.0 in.
Flange Width (b_f)	10.0 in.
Web Thickness (t_w)	0.3125 in.

The end-plate thickness of our specimens was two inches, which ensured "thick end-plate" behavior. The gauge (g) of our bolt pattern was 5.5". The inside bolt pitch (p_{fi}), outside bolt pitch (p_{fo}), and inside bolt spacing (p_b) were all 4". These values are shown in Figure 21. The spacing of the inner and outer pitch was implemented in the

event these end-plates would be used for pitched rafter splices. All bolts used on the end-plates in these tests were grade A490, and were 1 & 3/8 inches in diameter.

The naming convention of the test connection is: King end and Jack end. Besides the ends being named, each flange is labeled either top or bottom, and left or right depending on location relative to the web. This perspective is from the center of the beam looking towards each respective ends, with your line of sight running parallel to the flanges. To better understand the naming convention please refer to Figure 23. For example looking at the top left flange to end-plate connection in Figure 23, it can be seen that this is Jack Bottom (JB). Depending on which side of the web we are looking it is either left (JBL) or right (JBR).

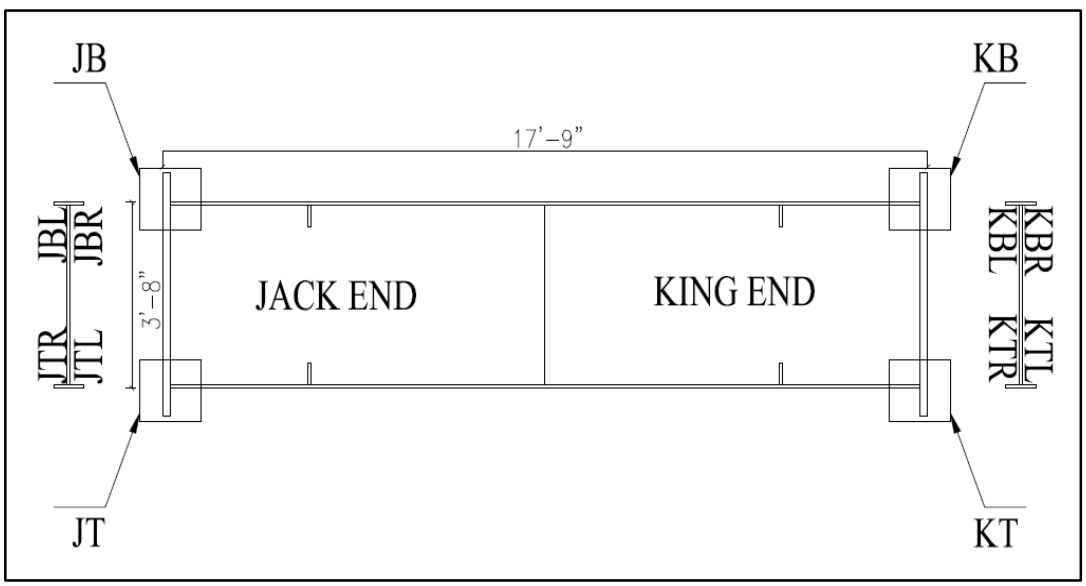

Figure 23. Test Specimen Naming Layout (Plan View)

3.3. Overall Design Considerations

Standard engineering practices were followed to design and manufacture the modified PJP weld on our specimens. *AISC Steel Design Guide 16* standard was

followed for designing these connections. Research has shown that MRE end-plates connections can fail in the following ways:

- Weld Failure
- Excessive End-plate Deformation
- Bolt Failure
- Column Failure
- Rafter Failure

Knowing these different modes of failure and how one can control these allowed the specimen to be designed for a failure mode that is nearly ideal. Rafter failure will be the desired failure mode in this study. The next section will further look at the above failure modes and how the design achieved a determined type of failure.

3.3.1. Test Specimen Design Considerations

The plastic strength of the beam was used as the controlling factor in designing the test specimen. That is to say that every component in this testing setup is designed so that the beam will achieve a plastic hinge at failure. As long as lateral torsional buckling is controlled with adequate bracing it can be predicted that this rafter will see a plastic hinge form at half the rafter's depth (d), or 22 inches away from the connection. Table 5 shows the predicted design strengths for our test specimen. The beam expected plastic strength in the Table 5 includes a term "Ass. Fy" which is the assumed yield strength of our material, in this case 50 ksi. This study was concerned with achieving the beam's plastic strength and everything was designed to be greater than this value, which reflects the values in Table 5. The values in Table 5 and any calculations used to design the rafter, connection and column of the testing setup can be viewed in Appendix A.

Table 5. Predicted Design Strength

Predicted Strengths:	
Beam Expected Yield Strength (Ass.Fy), M_{YA}:	2134 Kip*ft.
Beam Expected Plastic Strength (Ass.Fy) @ d/2, M_{PA}:	2602 Kip*ft.
End-plate Strength, M_{PL}:	5818 Kip*ft.
Bolt Tension Rupture (w/o prying action), M_{NP}:	3370 Kip*ft.

While the entire design of the testing setup is important, the design of the modified PJP welds is the primary focus of this research. The next section will discuss the design process for sizing the critical PJP flange welds and provide an overview of the welding procedures.

3.3.2. Modified PJP Weld

3.3.2.1. Design of Modified PJP Welds

The welds used on this test specimen were designed in accordance with the *AISC's 14th Edition of the Steel Construction Manual* (2012) for weld design. A root face of an eighth of an inch was selected. It was felt that an eighth of an inch is something one can easily discern with the naked eye, fabricate without difficulty, and was a substantial unfused region in the weld. The welds were then sized to optimize strength and minimize the number of welding passes.

When designing the critical PJP flange welds for a seismic force resisting system our primary design objective was to meet the flange forces at the beam's flexural strength, (M_d). This was done in accordance with the *2010 AISC Seismic Provisions for Structural Steel Buildings*. The expected flexural strength (M_d) of the beam is:

$$M_d = R_y * M_{EP} \qquad \text{[E1.0]}$$

$M_d = Expected\ Flexural\ Strength\ of\ Beam$
$M_{EP} = Beam\ Expected\ Plastic\ Moment$
$R_y = Ratio\ of\ Expected\ Yield\ Stress\ to\ Specified\ Minimum\ Yiled\ Stress$

The expected flexural strength was used as the baseline to determine the sizes for the modified PJP welds. With this information this allowed for the test specimens maximum flange forces (F_f) to be calculated:

$$F_f = \frac{M_d}{(d_b - t_f)} \qquad \text{[E2.0]}$$

$F_f = Flange\ Force$
$d_b = Depth\ of\ Beam$
$t_f = Flange\ Thickness$

It is known that the total strength of our flange welds (R_n), needs to be equal to or greater than that of our flange forces (F_f). In equation form this is written as:

$$R_n \geq F_f \qquad \text{[E3.0]}$$

$R_n = Total\ Strength\ of\ Flange\ Weld$

The strength of the outside flange weld (R_{no}) and the strength of the inside flange weld (R_{ni}) sum to the total strength of the flange weld (R_n). In equation form this is written as:

$$R_n = R_{no} + R_{ni} \qquad \text{[E4.0]}$$

$R_{ni} = Strength\ of\ Fillet\ Weld$
$R_{no} = Strength\ of\ PJP\ \&\ Built - up\ Fillet$

Lastly the strength of the flange welds can be solved. This is done by solving for the strength of the weld on the outside of the flange (R_{no}) and the strength of the welds on the inside of the flange (R_{ni}). Those equations for these welds' strengths are as follows:

$$R_{no} = .6 * F_{EXX} * \sqrt{(P)^2 + (F_{built})^2} * L \qquad [E5.0]$$

$$R_{ni} = .6 * F_{EXX} * (0.707) * F_{rein} * (L - t_{web}) * F_{SF} \qquad [E6.0]$$

$F_{built} = Length\ of\ Built - up\ Fillets\ Leg$
$F_{EXX} = Strength\ of\ Weld\ Electrode$
$F_{rein} = Length\ of\ Reinforcing\ Fillets\ Leg$
F_{SF}= *1.5 Strength Factor Increase for Transversely Loaded Fillet Welds*
$L = Length\ of\ Weld\ Along\ Width\ of\ Flange$
$P = Length\ of\ Groove$
$R_y = Ratio\ of\ Expected\ Yield\ Stress\ to\ Specified\ Minimum\ Yiled\ Stress$
$t_{web} = Thickness\ of\ Beam's\ Web$

Equations E1.0 though E6.0 were used to design the specimen welds. Working through these equations it allows one to calculate the expected flange forces and then solve for the size of the flange to end-plate welds through an iterative process. Using these equations the optimum weld sizes in Table 6 were calculated.

Table 6. Optimum Weld Sizes

Welds	(in)
Groove Side	7/8
Built-up Fillet	1/2
Reinforcing Fillet	5/8

A cross sectional view of our dimensioned flange to end-plate welds to accommodate these weld sizes can be seen in Figure 24.

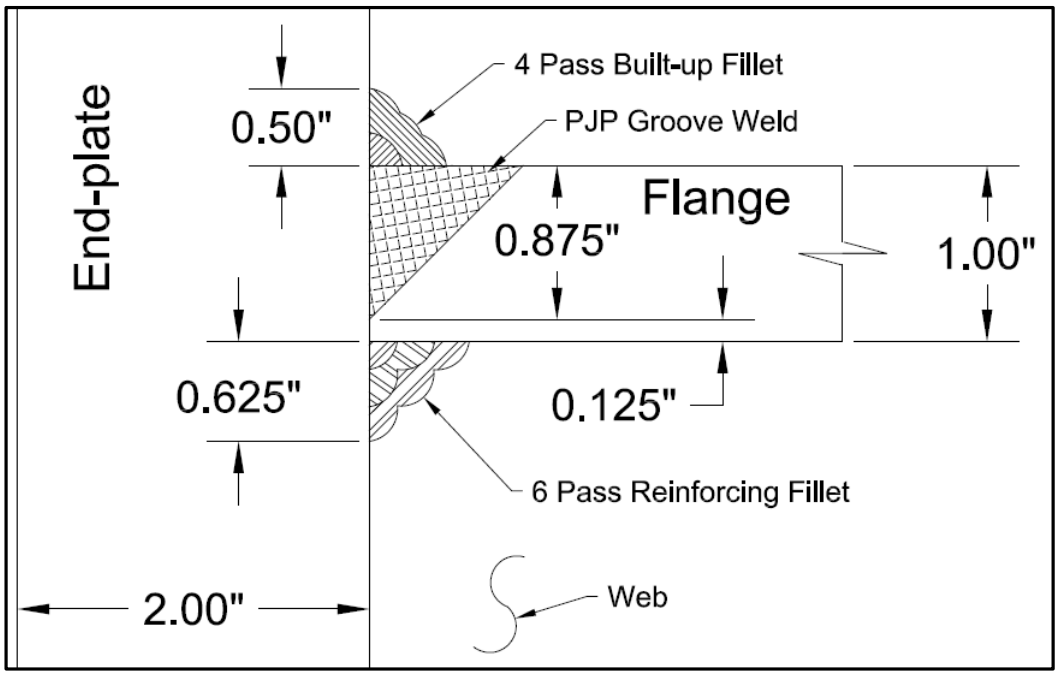

Figure 24. Flange's Welding Callout Sheet

The calculated flange forces, and strength of the welds can be seen in Table 7. The detailed design sheets and calculations for the flange's welds are presented in Appendix A.2.

Table 7. Theoretical Flange Force & Weld Design Strength

Parameter	Force	Units	Description
F_f for Md :	**726.25**	Kips.	Flange Force.
Rni :	269.68	Kips.	Developed Using a 5/8" Fillet.
Rno :	423.26	Kips.	Developed Using a 45° 7/8" Groove weld and 1/2" Built-up Fillet.
Rn :	**692.95**	Kips.	Designed Flange Force of Flange Welds.

It should be noted that wrapped ends of the PJP welds were not included in the design strength equation; however, if these were included the design strength of these welds would be equal to 748.63 kips, as opposed to 692.95 kips. It is not typical practice to include these values.

3.3.2.2. Fabrication of Modified PJP Welds

All flange to end-plate welds were made by a certified AWS welder in the flat position with a gas metal arc welder (GMAW) and 70 ksi bare wire electrodes. The connection of the flange to the end-plate utilized a 0.875” 45° groove weld. This groove was cut using an oxyacetylene torch on the 1” thick rafter flange. This groove was cut so that the opening was facing the outside of the rafter’s flange, away from the web. This left a 0.125” root opening on the rafter’s flange.

The rafter was then fit up to the end-plate, making sure that the root opening was flush with the end-plate. Once in place appropriate tack welds were made. During the entire welding process no cleaning or back gouging of the welds or the weld’s roots were performed.

Pictures of typical test specimens welds are presented in Figure 25. The flange to end-plate weld was manufactured in the following manner; the first step in the welding process was to place a reinforcing fillet weld on the inside of the rafters flange (Figure 25. Location A). Next the groove opening was filled with weld metal, fusing the rafters flange to the end-plate. This groove weld was then built up with an additional fillet weld (Figure 25.Location C). The fillet welds on the inside of the rafters were wrapped around from the underside of the flange to the sides of the flange and into the welds on the top side (Figure 25. Location B). Essentially these are wrapped fillet welds on the flanges’ sides. These wrapped fillets were included for uniformity and to alleviated concerns about stress risers and the creation of sites where crack initiation could potentially occur.

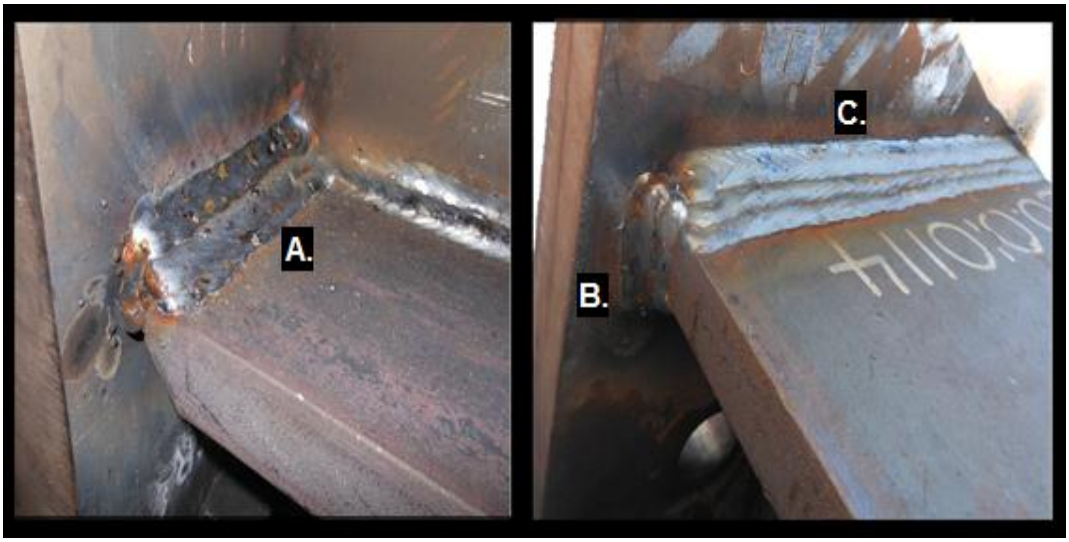

Figure 25. Examples of Test Specimen Welds

3.4. Materials

3.4.1. Tensile Coupon Tests

Tensile coupon tests were performed for the following materials: end-plate, rafter flanges & web, column flanges & web, and weld metal. Table 8 below presents the type of steel, location of sample, thickness, assumed grade, and test results. The preparation and testing of samples were conducted in accordance with ASTM A370. Testing was performed by Metalab-McClure Engineering Inc. It is important to note that the tensile properties of the demand critical weld metal passed the *American Welding Society's Structural Welding Code –Seismic Supplement* (AWS D1.8/D1.8M). The test reports from which the data in Table 8 below was derived can be found in Appendix B **.**

Table 8. Tensile Material Properties

		Assumed Design Strength		Avg. Tested Strength			% Change	
Location:	**Type of Steel:**	**Fy (ksi)**	**Fu (ksi)**	**Fy* (ksi)**	**Fu (ksi)**	**Elongation (% in 2 ")**	**Fy**	**Fu**
End-plate t= 2"	ASTM A 36	36	58	50.5	72	31	40.3	24.1
Rafter & Column Flanges t= 1"	ASTM A 572	50	65	62.5	79	32	25.0	21.5
Columns Web t= 1/2"	ASTM A 572	50	65	64	78.5	35	28.0	20.8
Rafter Web t= 5/16"	ASTM A 572	50	65	78	80	31	56.0	23.1
Flange to End-plate Welds	E70 Weld Metal	-	70	66.5	77	33	---	10.0
1-3/8 " Bolts	ASTM A490	113	150	---	---	---	---	---

* Determined at 0.2% offset.

It can be observed from Table 8 that overall the strength of the metal and weld metal were stronger than assumed design values. This is particularly evidenced in our end-plate and rafter webs. In the case of our end-plate strength this is not important because our end-plate strength is so much larger than the rupture strength of our bolts. However the increase in the rafter's materials strength is important because the beams true plastic capacity is needed for analysis. The beam's plastic strength will be recalculated below in the experimental results portion of this thesis.

3.4.1. Weld Metal Tests

Charpy Impact Tests were performed on the demand critical weld metal. Table 9 below presents the results of testing. The preparation and testing of samples were done in accordance with ASTM A370. Testing was completed by Metalab-McClure Engineering Inc. Following standards, five samples were tested and two outliers were thrown out. The toughness of the tested demand critical weld metal passed the AWS D1.8/D1.8M requirements. The test reports from which the data in Table 9 were derived can be found in Appendix B**.**

Table 9. Weld Metal Material Properties

Sample I.D.	Sample 1	Sample 2	Sample 3
Temperature (◦F)	-20	-20	-20
Energy Absorbed (ft-lbs.)	161	178	173
Lateral Expansion (in.)	0.091	0.081	0.088
Percent Shear	80	80	80

4. Experimental Testing

4.1. Testing Setup

The idealized layout of our test setup can be seen in Figure 26. Our test specimen consists of a cantilevered beam connected to a column via a bolted end-plate. Location A in Figure 26 shows the location of the flange to end-plate welds which was the area of interest in testing this connection. The columns' pinned connections B and C in Figure 26 were achieved by connecting the ends of the column to supports that were connected to the lab's strong floor. Location D in Figure 26 shows where the load was applied. It should be noted that since the test specimen's rafter was loaded on both sides of its tip the testing setup is mirrored along the rafter's center line.

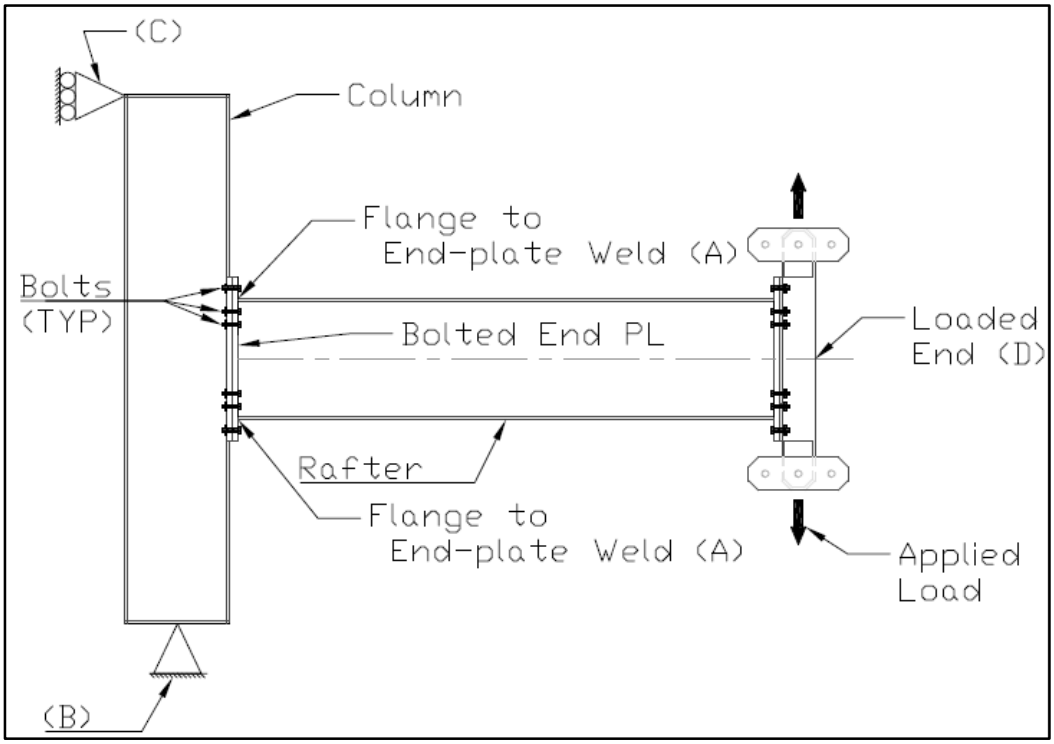

Figure 26. Idealized Test Setup

The actual implementation of the testing required a multitude of lateral bracing, miscellaneous pieces, and connections to transfer the applied force to the labs strong floor. An overview photo of the test specimen, its bottom bracing and connection to the strong floor can be seen below in Figure 27.

Figure 27. Overview of the Test Specimen

The easiest way to explain the testing layout is to break it down into layers. There were a total of four layers in our test setup. The first layer is the strong floor. This level can be observed in Figure 28. The strong floor is comprised of a 60’ x 25’ x 3’ concrete slab that has four W-sections imbedded into the concrete. These W-sections are 8’ on center of each other. The W-sections have holes drilled into the top flanges so items may be connected to the strong floor.

Figure 28. Level 1: Strong Floor

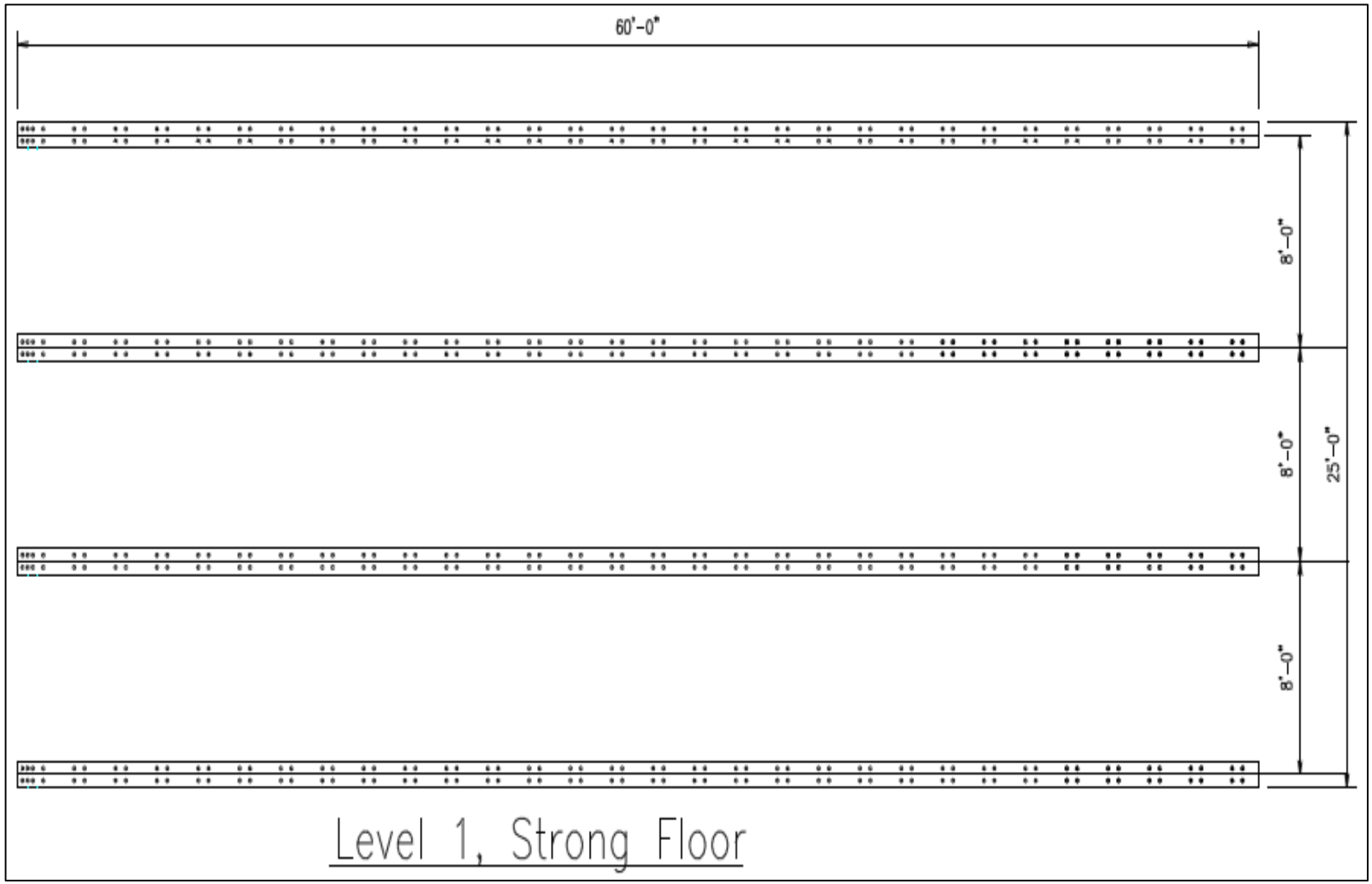

Level 2 consists of the bottom portion of the lateral torsional bracing for the column and rafter, connections that connect the test specimen to the strong floor, and the connections that connect the hydraulic ram to the strong floor. Figure 29 shows the second level of the testing setup. The lateral torsional bracing BRC-2 are W-sections whose bottom flanges are connect to the strong floor via bolts. The top flanges of BRC-2 provide the bottom of our test rafter with lateral torsional bracing. BRC-3 are short W-sections with end-plates on both ends that run perpendicular (out of the page in Figure 29) to the strong floor. The end-plates are bolted to BRC-2, and then on level 4 bolted to BRC-1. These W-sections essentially make a cage that confines our test beam; this cross sectional view is A1/E2, Figure 30. A photograph of the rafter's lateral torsional bucking cage in our testing setup can be seen in Figure 31. This cage provides brace points which are needed to meet design requirements for lateral torsional buckling of the test specimen. The controlling unbraced length of our test beam was 8.8'; see Appendix A.1 for these calculations. An actual braced length of 4' was maintained for the beam test specimen during this test.

Figure 29. Level 2 Bottom Bracing

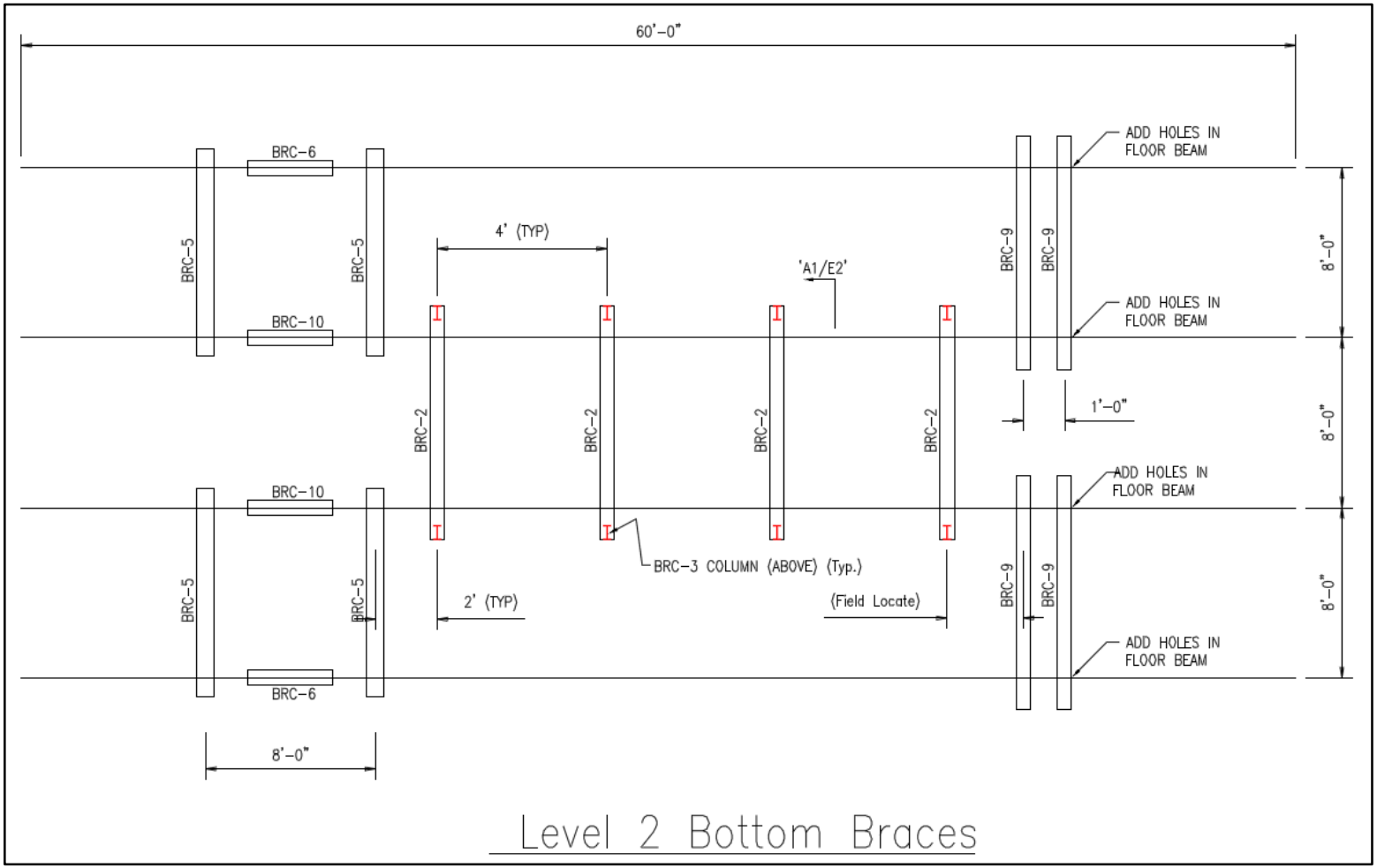

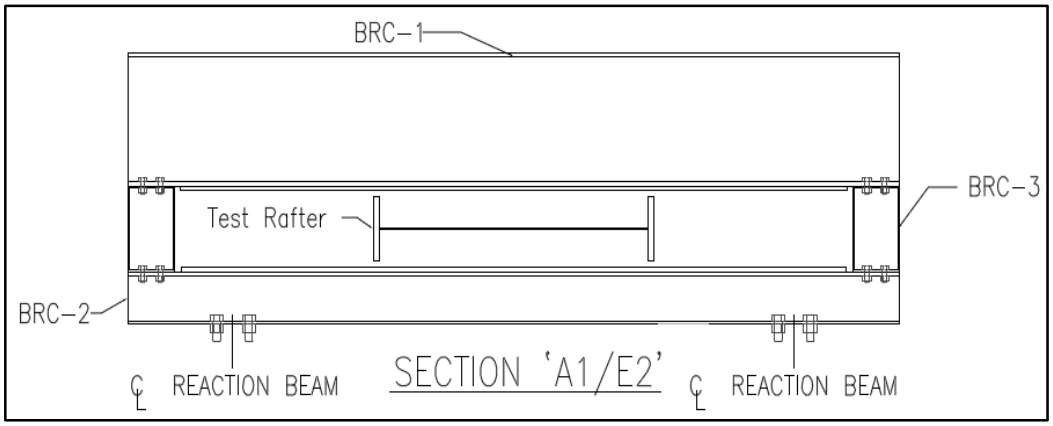

Figure 30. Lateral Torsional Buckling Cage

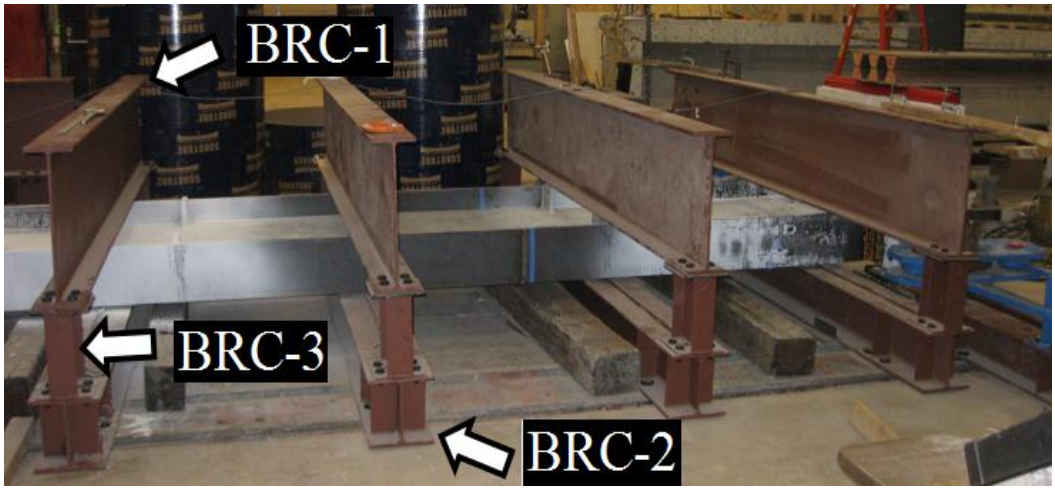

Figure 31. Rafter's Lateral Torsional Buckling Cage in Testing Setup

This lateral torsional buckling cage concept was also implemented with our column. However in this case the bottom portion of the cage was BRC-10 and the top portion was BRC-11. A photograph of the column's lateral torsional bucking cage used in our testing setup can be seen in Figure 32.

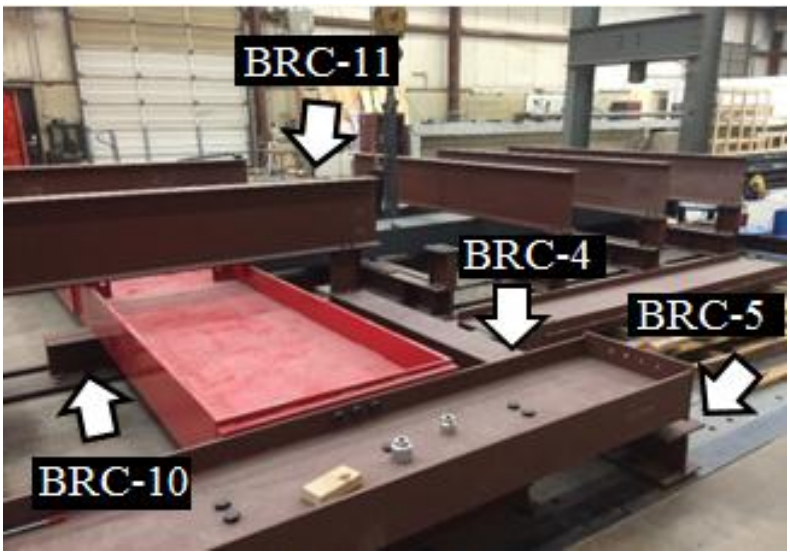

Figure 32. Column's Lateral Torsional Buckling Cage in Testing Setup

BRC-4 is a W-section whose bottom flange was connected to the strong floor via bolts. The top flanges of BRC-4 connect to BRC-5 which in turn was connected to the test specimen's column. A photograph of this configuration is shown in Figure 32.

BRC-9 is a W-sections whose bottom flange was connect to the strong floor via bolts. Two of these beams who were placed side by side of each other. These beam top flanges bolt to the hydraulic cylinders backing, BRC-7. Figure 33 shows this portion of the testing configuration.

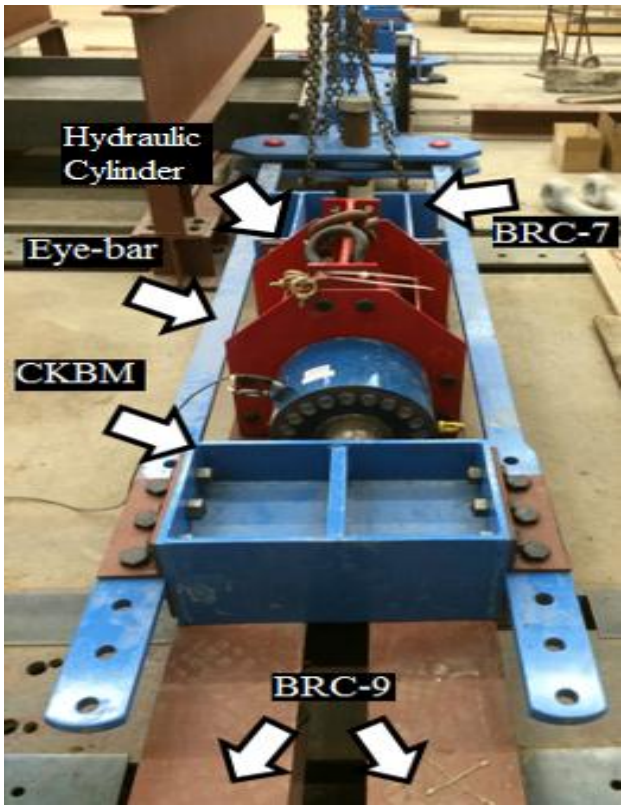

Figure 33. Test Specimens Tip Configuration

Level 3 consists of the test specimen, and the configuration used for loading the specimen. Figure 34 shows the third level of the testing setup. Figure 33 shows in detail the tips loading configuration. As a load is applied through the hydraulic cylinder, BRC-7 braces the back side of the cylinder and transfers this load to the strong floor. This provides a stationary point for the hydraulic cylinder to be backed against. The front end of the hydraulic cylinder is pushing on is CKBM. CKBM takes this load and transfers it into the eye-bars; which is connected to the specimens tip. This load puts the eye-bars in tension and pulls the specimens tip towards the hydraulic cylinder. Simply put, CKBM pulls the eye-bars which in turn pulls the specimens tip.

Figure 34. Level 3 Test Specimen and Loading Fixture

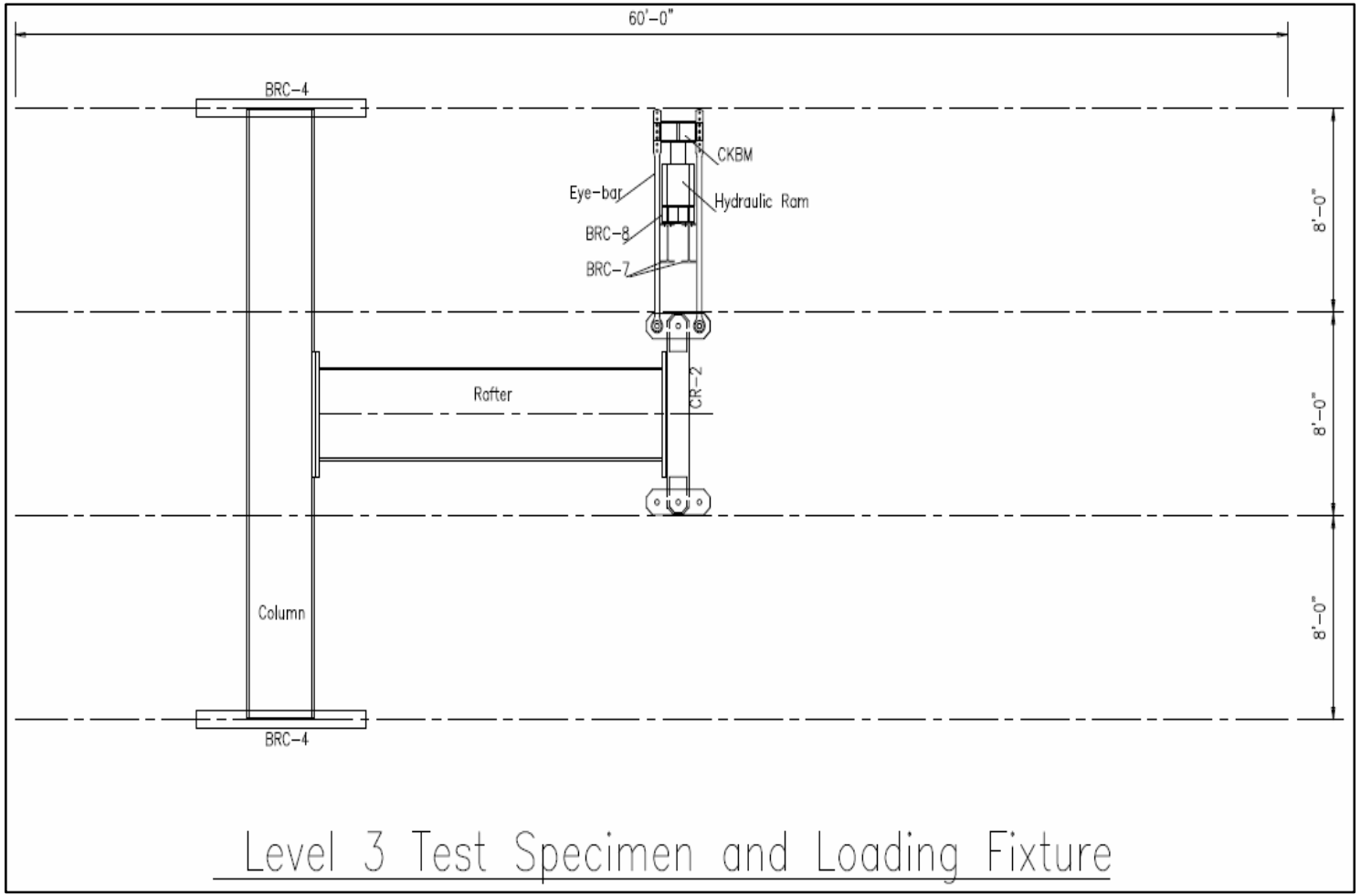

Level 4 consists of the top portion of the lateral torsional bracing for the column and rafter. BRC-1 is the top portion of the bracing cage which confined the rafter. BRC-11 is the top portion of the bracing cage which confined the column. Figure 35 shows the fourth level of the testing setup. Figure 31 shows in detail the lateral torsional bracing cage used to confine the rafter. Figure 32 shows in detail the lateral torsional bracing cage used to confine the column. A superimposed drawing of the 4 layers of the testing setup can be seen in Figure 36.

Figure 35. Level 4 Top Bracing Layout

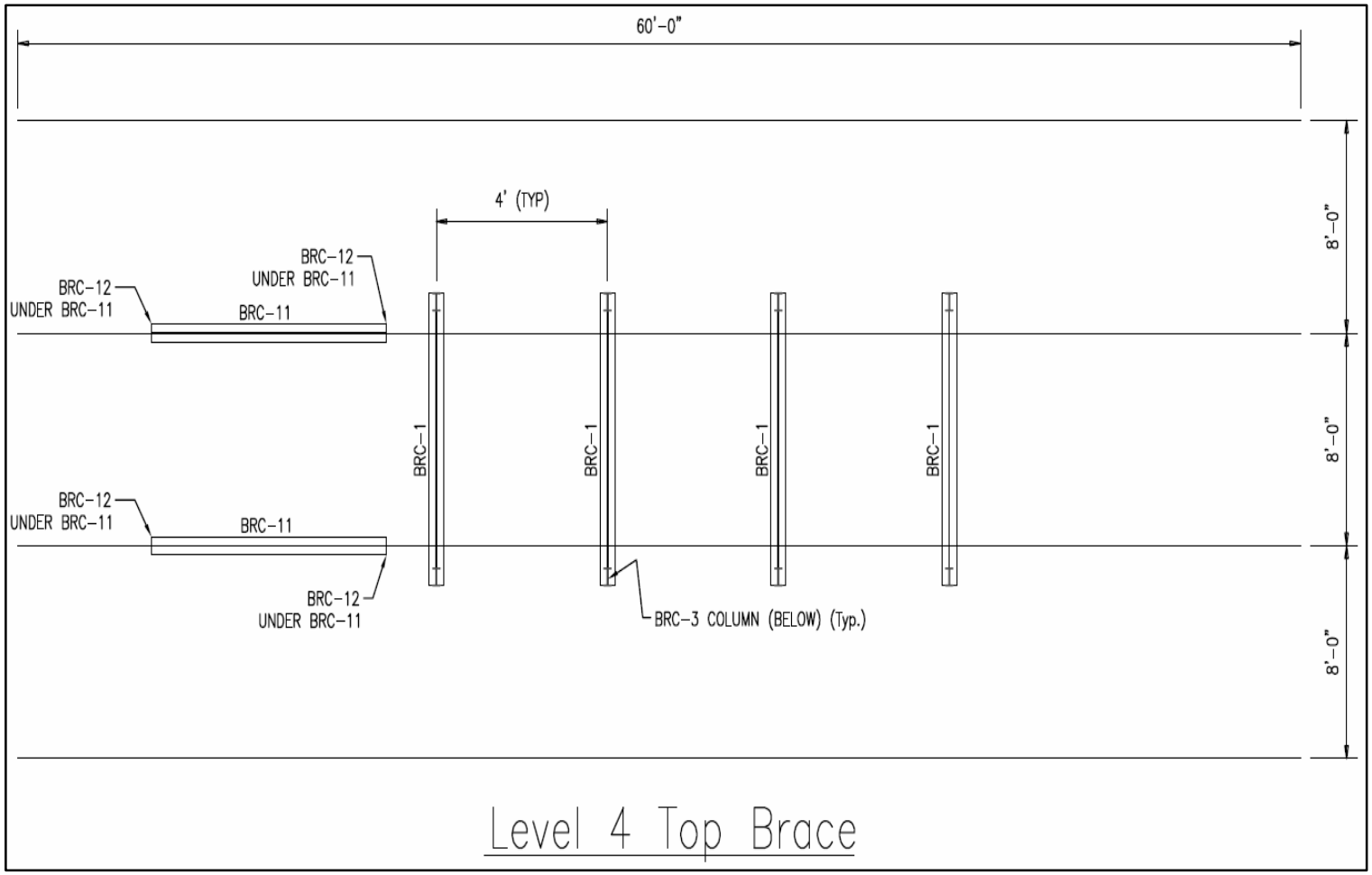

Figure 36. Testing Setup Overlay

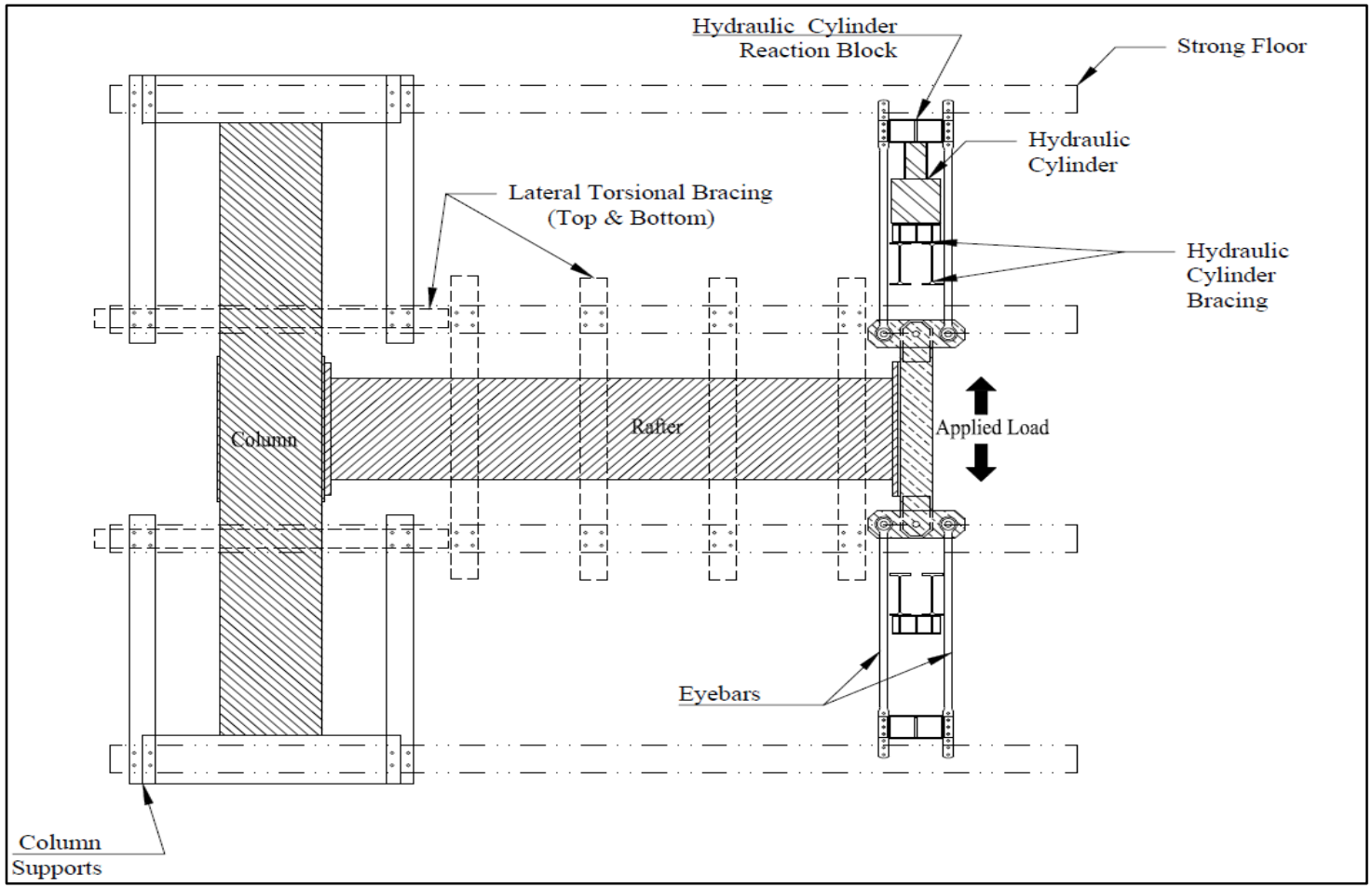

4.2. Instrumentation

4.2.1. Overall Instrumentation

Load cells, linear variable differential transformers (LVDTs), temperature compensating strain gauges, and white wash were utilized in the instrumentation and assessment of these specimens. While the load cell and the displacement transducers were used in the exact same location on both tests, the use of strain gauged bolts, location and number of strain gauges varied for each test. Figure 37 shows the test configuration and approximate instrumentation location.

The following instrumentation was utilized in the same manner on both specimens:

- LVDTs @ the panel zone of the column to measured panel zone distortion. (Figure 38)
- Wire Pots @ the end of columns to measure column rotation/deflection. (Figure 39)
- Wire Pot @ the end of rafter to measure tip deflection & rotation. (Figure 40)
- Load Cell @ the beam tip to measure applied load. (Figure 41)

In Figure 38 the use of Invar (64FeNi) rods were employed in the measurement of the panel zone distortion of the column. Invar is a metal that is made up of about 40% nickel and 60 % iron. Its composition gives it a low coefficient of thermal expansion. This property was utilized in testing due to varying temperatures in the lab. It was believed this would alleviate concerns about thermal expansion of the rod and in doing so provide researchers with the best possible results.

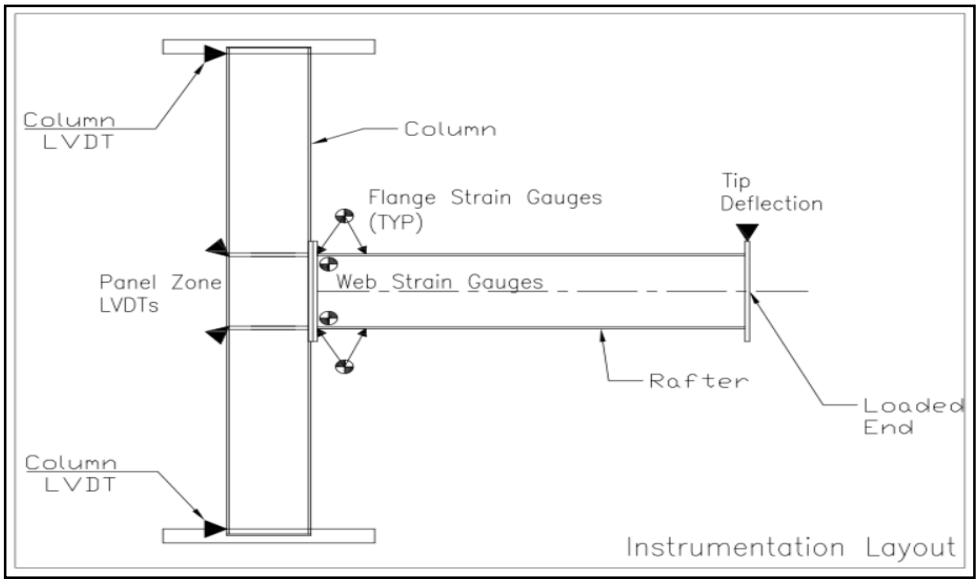

Figure 37. Instrument Layout Overview

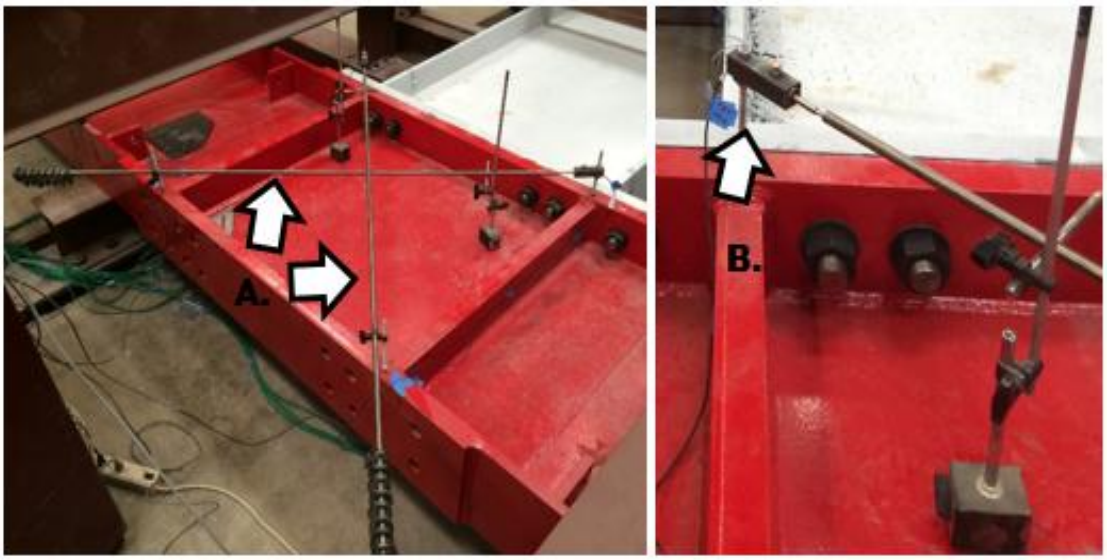

Figure 38. Panel Zone Deflection Measurement Setup, Invar Rods (A), LVDT (B)

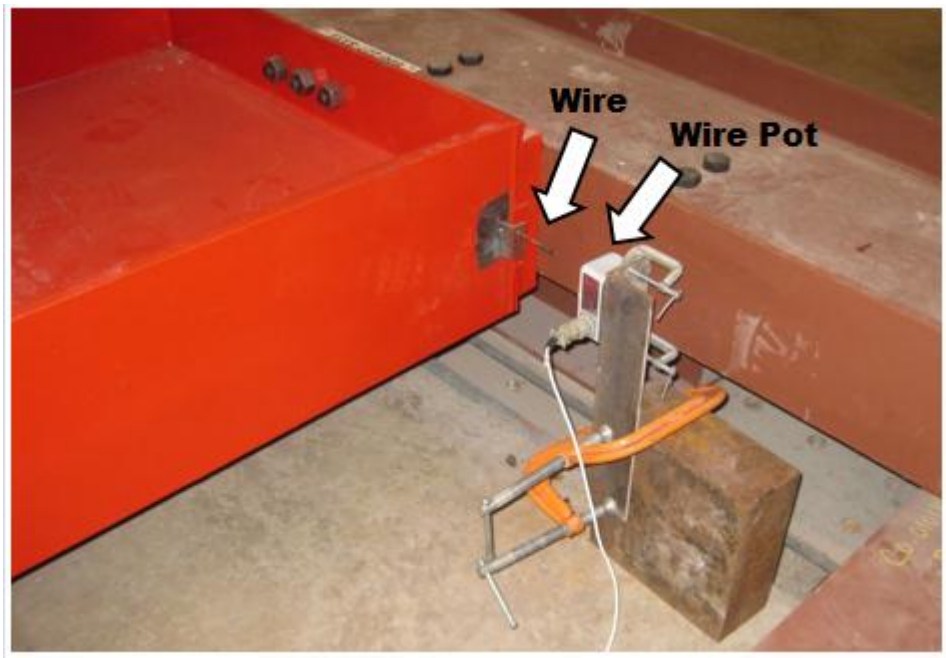

Figure 39. Wire Pot Measuring Column Deflection

Figure 40. Wire Pot at Rafter's Tip

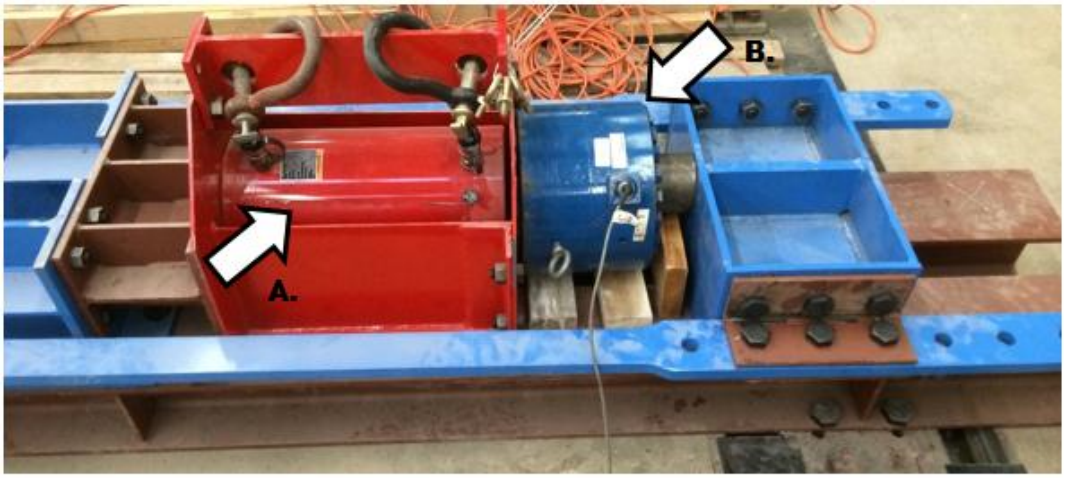

Figure 41. Hydraulic Cylinder (A), and Load Cell (B)

A coating of white wash was applied to the rafter near the connection where we expected to observe plastic deformation. A picture of the white washed rafter can be observed in Figure 42. Pictures were taken before and after each loading cycle so that when strain lines appear in the white wash we would know what at cycle plastic deformation occurred in the rafter.

Figure 42. Test Specimen's Rafter with a Fresh Coat of White Wash

All the displacement transducers were calibrated prior to use and connected to a PC-based data acquisition system. Data was collected for each instrument listed above at a sampling rate of 1 Hz. Utilizing this data acquisition system allowed for real time analysis of incoming data.

4.2.2. Real Time Data Processing, Collection & Overview

The main concern of this research was achieving specified rafter rotations at each displacement step. The rafter rotations had to be developed through the bending/yielding of the beam and any slippage/rotation in the end-plate connection. Any rotation due to the slippage in the column connections or distortion of the panel zone of the column had to be subtracted from this total rafter rotation. This "corrected rafter rotation" had to meet the specified rafter rotation per the testing protocol. To solve for the corrected rafter rotation, the column rotation and panel zone rotation were subtracted from raw tip rotation. The equation used to solve for corrected rafter rotation is presented below, E7.0.

$$Corrected\ Rafter\ Rotation = \left(\tan\frac{Tip\Delta}{R}\right) - \left(\tan\frac{Adv\ Col\Delta}{C/2}\right) - \left(\tan\frac{PZ\Delta}{R}\right) \quad \text{[E7.0]}$$

R = distance from col. face to center of loading pt.
C = from CL of rafter to col. ends
$Tip\Delta =$ ‖tip deflection at R‖

$$Adv\ Col\Delta = \frac{(\|Col\ \Delta\ at\ end\ 1\| + \|Col\ \Delta\ at\ end\ 2\|)}{2}$$

$$PZ\Delta = \left\|\|Panel\ Zone\ \Delta\ at\ end\ 1\| + \|Panel\ Zone\ \Delta\ at\ end\ 2\|\right\| * \gamma * R$$

$$\gamma = \frac{\sqrt{a^2 + b^2}}{2 * a * b} \quad From\ Sato\ et.al\ (2008)$$

$a = Panel\ Zone\ Width$
$b = Panel\ Zone\ Length$

Equation E7.0 makes use of the corrected tip deflections ($Tip\Delta$) and this must be solved for before rotation can be determined. The corrected tip deflection is found by taking the raw tip deflection and subtracting scaled average column deflection and panel zone deformation. The equation used to solve for corrected tip deflection is as follows:

$$Corrected\ Tip\ Deflection = (Tip\Delta) - \left(\frac{Adv\ Col\Delta}{C/2}\right) - (PZ\Delta) \qquad [E8.0]$$

Utilizing theses equations in the data acquisition software allowed for this corrected rafter rotation to be viewed in real time which provided researchers with accurate data during testing

4.2.3. Instrumentation Differences

The difference between the instrumentation on the two tests conducted for this research is the use of strain gauged bolts and the location of flat strain gauges. Flat strain gauges were used to measure strain at various locations on each test specimen; their locations are discussed below in their respective section. The King end testing utilized strain gauged bolts, while the Jack end did not. This was so that bolt distribution forces could be examined for “snug tightened” bolts at the lower stress level testing, as well as to validate the procedures used for pre-tensioning bolts. It is of note that once plastic deformation of the test specimen was expected the snug tightened bolts were pre-tensioned. Both snug tight and pre-tensioned bolt testing were completed at this rotation so a comparison could be made concerning the effect of bolt pretension. The use of strain gauged bolts allowed for validation of the pre-tensioning tightening procedures.

4.2.3.1. King End Bolt Instrumentation:

Specialty strain gauges were inserted in the bolts to enable us to calculate the imposed bolt forces. Tokyo Sokki Kenkyujo Company's BTM-6C strain gauges were installed in the shafts of the one and three-eighths inch diameter bolts. Before the strain gauges could be installed in the bolts this required drilling a five-sixty-fourths inch dia. hole, to a depth of two and a quarter inches. After drilling the bolts were cleaned and filled with a two part epoxy. The bolts were placed in a vacuum to release voids in the epoxy, and the gauges were installed. Care was taken to ensure the required gap between the bottom of the hole and the end of the strain gauge was achieved. In Figure 43 the cross-section of a fully strain gauged bolt is presented.

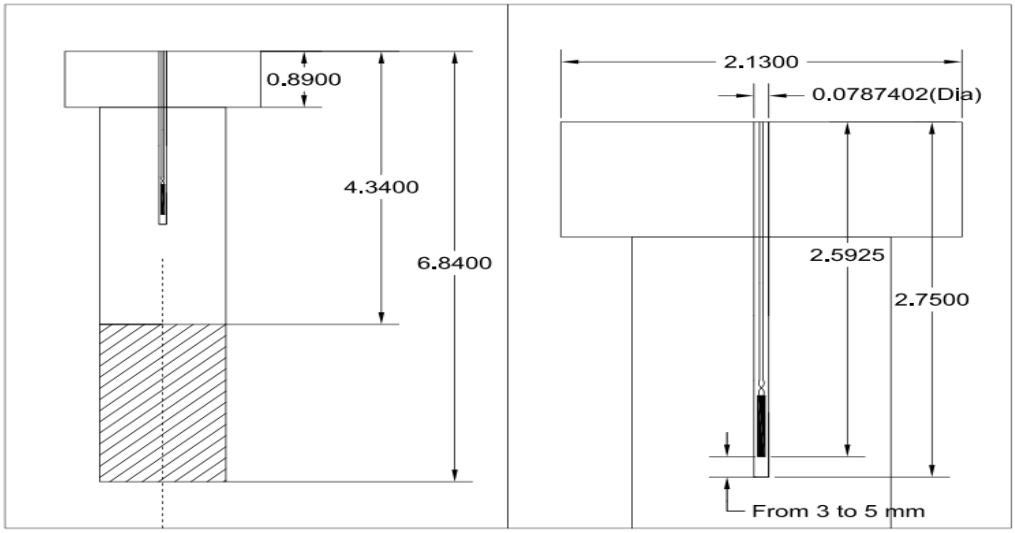

Figure 43. Gauged Bolt Cross Section

The bolts were then allowed to cure. Once the epoxy cured, heat shrink tubing was installed over the non-insulated portion of the strain gauge wires. This was to increase durability of the wire and prevent the possibility of a short. Next a dab of commercial

grade silicone sealer was added to the top of the bolts as a strain relief. A picture of a finalized bolt can be seen in Figure 44.

Figure 44. Fully Gauged Bolt

Once all the bolts had strain gauges installed, each was calibrated. The calibration process involved placing each bolt in a tension testing machine and then loading them to 50 kips. The load calibration setup can be seen in Figure 45. A data acquisition system reported a voltage for each applied load. Using the output voltage at each given load allowed us to determine a calibration factor. This relationship is linear, and thus points above and below this point were extrapolated. Each bolt then had its own calibration factor. Once calibrated, each bolt was reloaded at intermittent points up to 50 kips. If the expected load on the bolts data acquisition system was off by more

than 2% the bolts were recalibrated or thrown out. This process was repeated until 12 bolts were validated for use in the experiment.

Figure 45. Bolt Being Calibrated

4.2.3.2. Flat Strain Gauge Instrumentation

Strain at various locations on the rafter were measured using flat strain gauges. Tokyo Sokki Kenkyujo Company's FLA-5-11 strain gauges were installed on the surface of the test rafters. Tokyo Sokki Kenkyujo's instructions on strain gauge installation were followed. Once the desired location of strain gauge placement was determined a 2" x 2" square was centered on this spot and outlined in soap stone. The

mill-scale on this square was removed with the use of a hand held angle grinder. Once the mill scale was removed an 80-grit sand paper grinding wheel was applied to this area to smooth over deep scratches. Once major scratches were removed, successively finer grit sand paper were applied until the surface was smooth to the touch of a finger nail. Once the surface was free of blemishes a clean paper towel saturated in a cleaning solution was wiped over the area to remove any residual dirt. Next Vishay solution A on a paper tower was wiped over the effective area in one pass, followed by Vishay solution B. The flat strain gauges were then applied to this polished, dirt free area by means of Vishay M-Bond 200 adhesive. Lastly these gauges were covered with a protective coating of Vishay M-Coat A. This process was repeated for all flat strain gauges. Calibrating the strain gauges was completed automatically using the data acquisition system and the provided strain gauge calibration factor. A completely installed strain gauge can be seen in Figure 46.

Figure 46. Flat Strain Gauge

4.2.3.2.1. King End Strain Gauge Instrumentation

Strain gauge locations and naming of locations for the King end testing can be seen in Figure 47 and Figure 48, respectively. Strain gauges are shown in red and are not to scale. In total, 12 strain gauges were installed to measure strain on both the rafter's outside flanges and web.

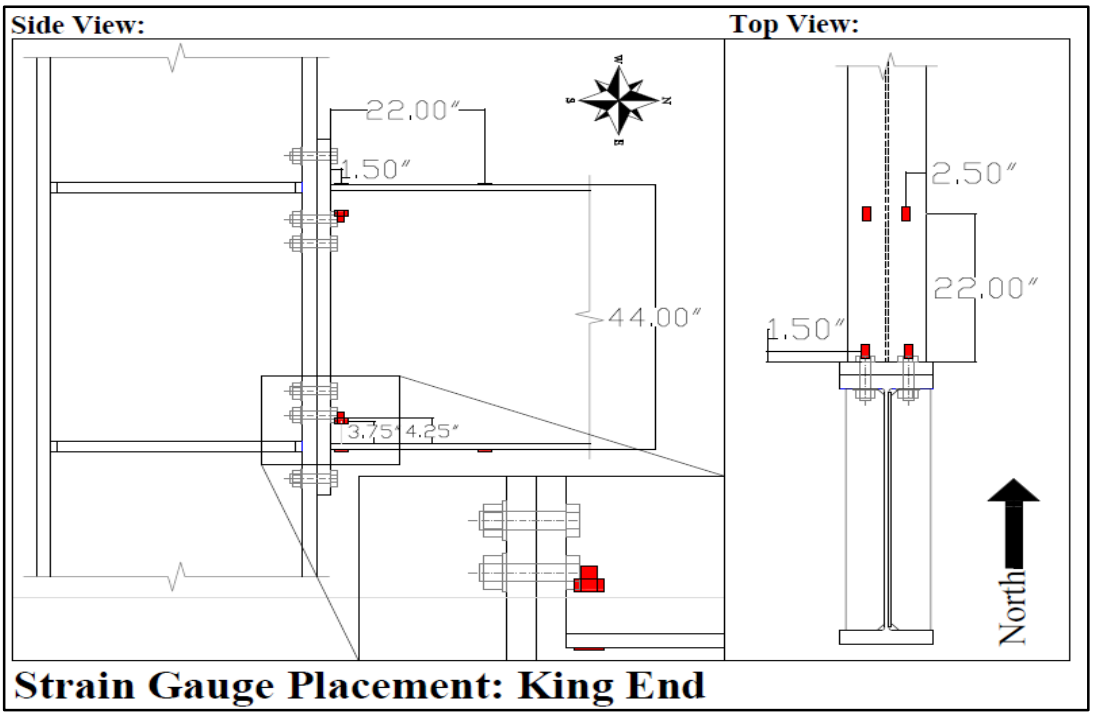

Figure 47. Strain Gauge Location on King End Specimen

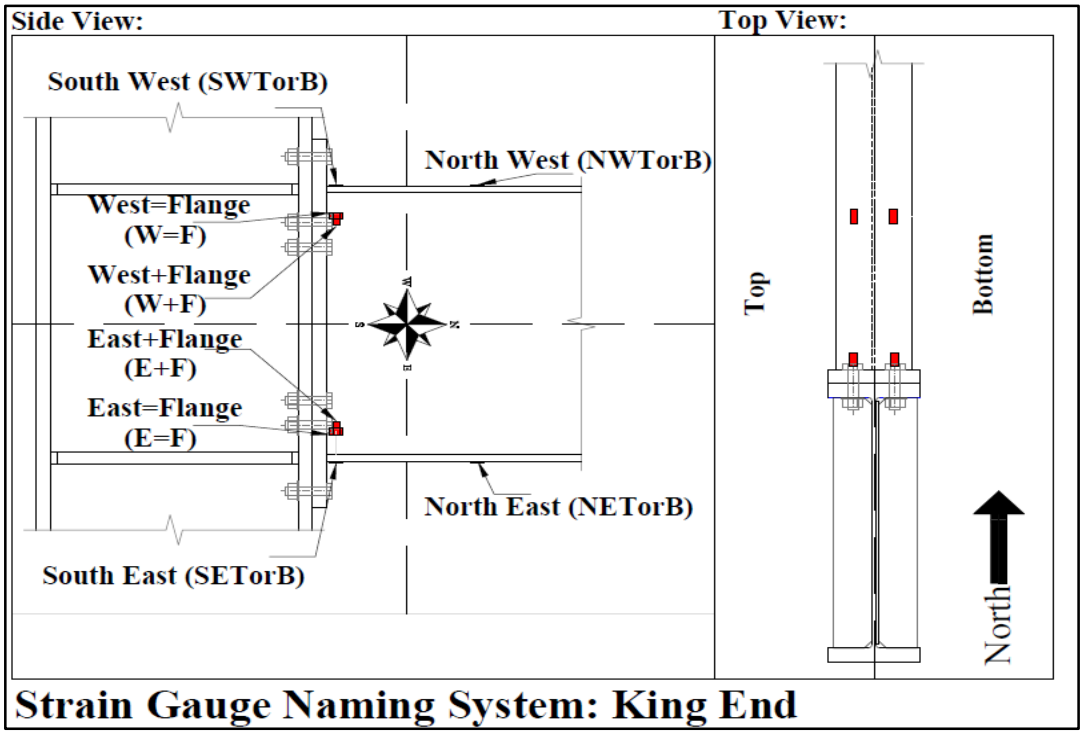

Figure 48. Strain Gauge Naming System: King End

4.2.3.2.2. Jack End Strain Gauge Instrumentation

Strain gauge locations and naming conventions for the Jack End testing can be seen in Figure 49 and Figure 50, respectively. Strain gauges are shown in red and are not to scale. In total, 16 strain gauges were installed to measure strain on both the rafter outside flanges and web.

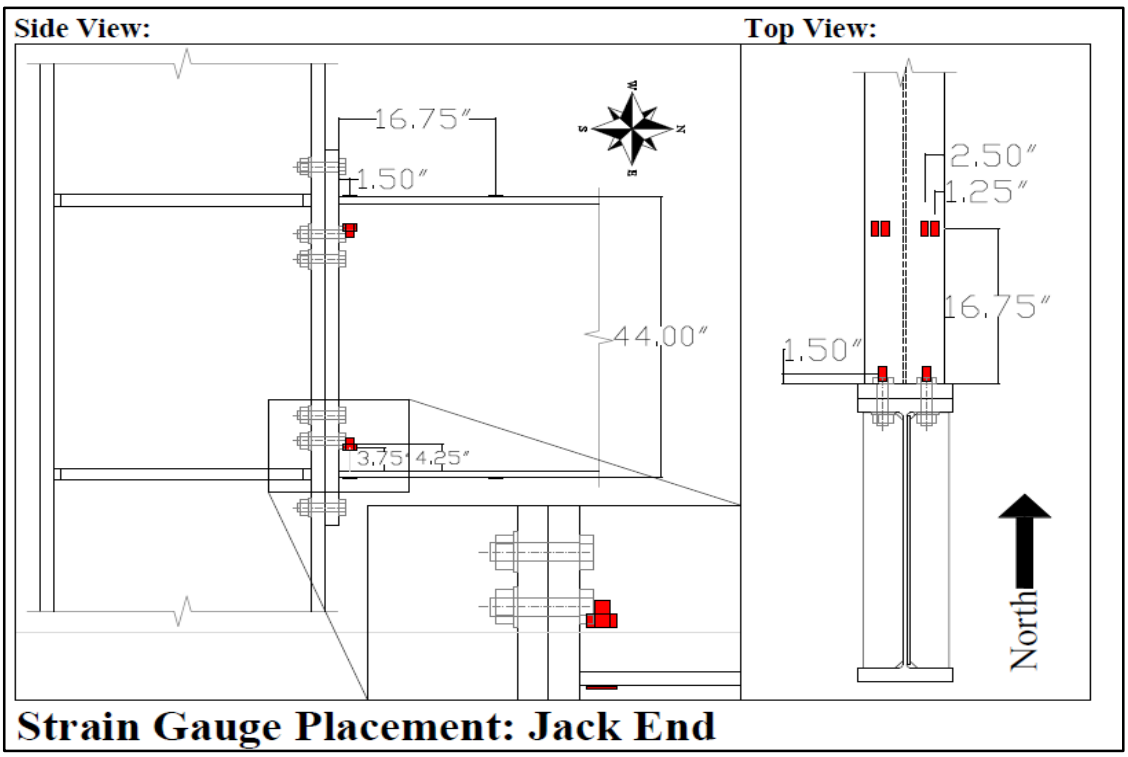

Figure 49. Strain Gauge Location on Jack End Specimen

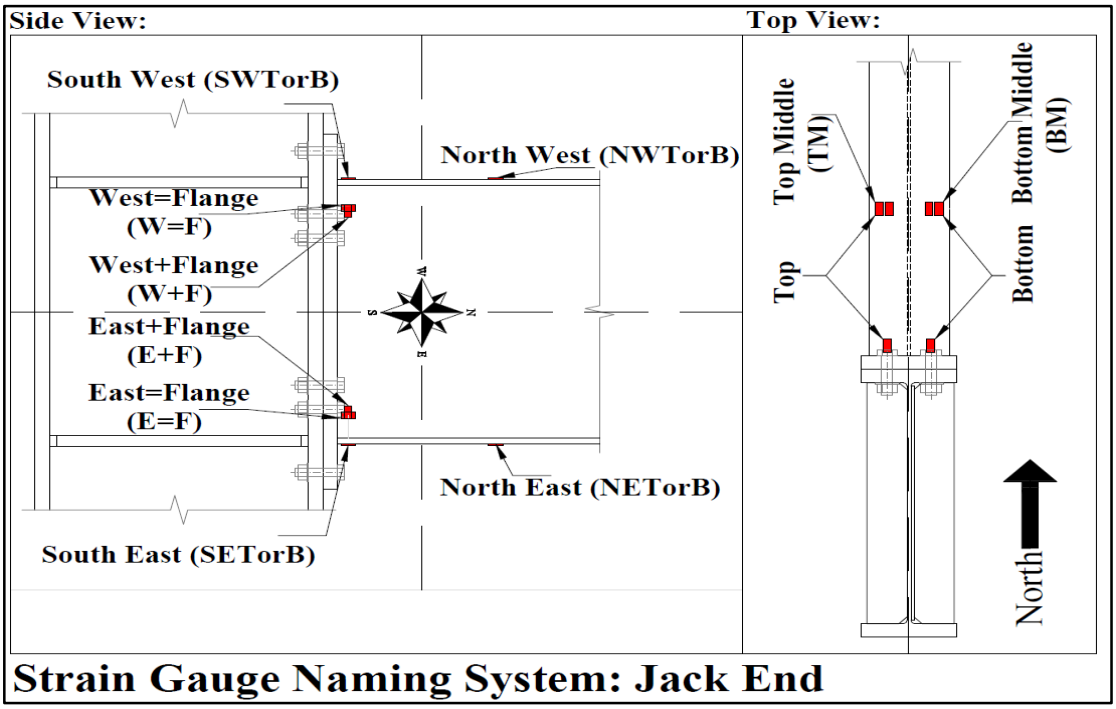

Figure 50. Strain Gauge Naming System: Jack End

4.3. Testing Procedures

4.3.1. Testing Procedures, Specifications & Loading Sequence

The rafters were tested in accordance to the *2010 AISC Seismic Provision's* criteria on loading sequences for beam to column moment connections. These require achieving a specified rotation of the rafter for given number of cycles. The *2010 AISC Seismic Provision* defines a *cycle* as "a full tension and full compression excursion to a prescribed deformation" (2010). The required number of cycles and the accompanying rotations for each cycle can be found in Table 10. These predetermined cycles and rotations were utilized during the testing of each specimen.

Table 10. Loading Sequences

# of Cycles:	Rafter Rotation (Radians) :
6	0.00375
6	0.005
6	0.0075
4	0.01
2	0.015
2	0.02†
2	0.03
2	0.04

† Minimum rotation required for consideration as intermediate moment frame (IMF)

4.3.2. King End Testing Procedures

4.3.2.1. King End Snug Tight Bolt Installation Procedure

Once the test rafter was installed inside of the lateral torsional cage the strain gauged bolts were installed. All twelve bolts were installed, backed with washers and nuts and finger tightened. Referencing Figure 51, the tightening sequence started with

the most north east bolt labeled 2, and this process continued along the topside, working left until the last bolt on that row was tightened.

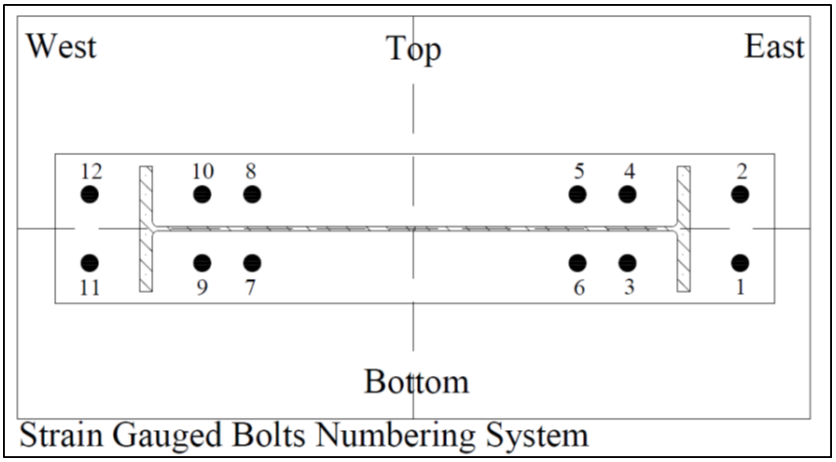

Figure 51. Strain Gauged Bolts Numbering System

Next the bottom row was tightened, starting with bolt 11 and working right. Each nut was rotated with a standard socket wrench until resistance was met and hand tightening was no longer possible. After all nuts had been tightened using this method, the force in each bolt was checked against the strain readings on the data acquisition system. The bolt with the highest force was the benchmark to which the other bolts would now be tightened. The remaining bolts were tightened on an as needed basis until all bolts had achieved a similar bolt force of 2 kips.

4.3.2.2. King End Snug Tight Testing Procedures

Once all the instrumented bolts were installed and pre-tensioned to the same level the gauges were zeroed so that any additional force applied to the bolts would be easily measured. All displacement transducers were placed in the middle of their stroke to enable the largest range possible. Once the data acquisition system was fully functional all the instrumentation was zeroed. The system was then left to run for five

minutes to verify that no voltage drift existed in our system. Upon verifying our system was in good working order the testing started.

The snug tight test was run in accordance with the *2010 AISC Seismic Provision*, shown in Table 10. This testing protocol was followed until the end of the 0.01 radians cycle. At the end 0.01 radians cycle the applied load was close to the expected yield moment and a small amount of white wash flaking was observed. This was a good indication to terminate the snug tight portion of the testing. The desire was to keep the snug tight portion of our testing within the elastic range.

4.3.2.3. King End Pre-tensioned Bolt Installation Procedures

Following the completion of the snug tight portion of testing the bolts on our specimen needed to be fully pre-tensioned. Following the *AISC Steel Construction Manual's* requirements on pretension levels for bolts the inch and three-eighths inch diameter bolts were pre-tensioned to force of one hundred and twenty-seven kips. Pre-tension levels were achieved using a Norbar Pneutorque PT5, pneumatic torque wrench. A photo of the Norbar Pneutorque PT5 pneumatic torque wrench can be seen in Figure 52. The pneumatic torque wrench was hooked up to a regulator, which can be seen in Figure 53. The regulator allows the user to controls the amount of torque that is applied to the bolts. The regulator was then hooked up to a source of compressed air.

Figure 52. Norbar Pneutorque PT5, Pneumatic Torque Wrench

Figure 53. Pneumatic Torque Wrench Regulator

When a pneumatic torque wrench is properly calibrated the input air pressure correlates to an applied torque. Using the manufacture's supplied psi to torque conversion chart the desired psi was determined, and used to achieve the desired

pretention force. In accordance with the manufactures specifications the tensioned bolts were tightened until the torque wrench stalled out; thereby ensuring the bolts were completely tightened. After each bolt was tightened results were checked against the data acquisition system. An upper extension limit exists on the bolt strain gauges, beyond which the strain gauges in the bolts no longer provided meaningful data. The tightening sequence is shown in Figure 51. The tightening sequence started with the most north east bolt labeled 2, and this process continued along the topside, working west until the last bolt on the top row was tightened. Next the bottom row was tightened, starting with bolt 11 and working east.

4.3.2.4. King End Pre-tensioned Testing Procedures

Once all the bolts were pretension to 127 kips and the gauges were zeroed testing was ready to begin. Displacement transducers were not moved, but were left in the position from the previous test.

The pre-tensioned test was run in accordance with the *2010 AISC Seismic Provision*, shown in Table 10. The first cycle that was run following the snug tight tests was the 0.01 radians cycle, this cycle was repeated so comparisons could be made between snug tight and pretention testing. Photos were taken of the specimen after each cycle so comparisons of the white wash flaking could be made between each cycle. These photos can be seen in Appendix C. Once the test specimen achieved all cycles of the 0.02 radianss rotation, the testing cycle deviated from the *2010 AISC Seismic Provision*. The next cycle conducted was 0.0225 radians of rotation. While the test specimen probably could have continued to achieve larger rotations and tip deflection, concerns about the specimen's structural integrity for testing the other end caused

termination of the test at this point. While a substantial failure of the beam would have been interesting, the need to test the opposite end of the rafter was more important.

4.3.3. Jack End Testing Procedures

4.3.3.1. Jack End Pre-tensioned Bolt Installation Procedures

After the test specimen was contained inside of its lateral torsional cage the bolts were installed. All twelve bolts were placed in their holes and backed with washers and nuts. The same installation procedures were followed for this process as were in the section 4.3.2.3. The only difference between these installations procedures is that the bolts were installed with an initial pretension of 127 kips. Since the bolts were not gauged for this round of testing, validation through the data acquisition system was not possible and for this reason the snug tight bolt installation was not used.

4.3.3.2. Jack End Pre-tensioned Testing Procedures

Once all the bolts were installed and pre-tensioned to 127 kips the flat strain gauges were then zeroed. All displacement transducers were placed in the middle of their stroke to enable the largest range possible. Once the data acquisition system was fully functional all the instrumentation was zeroed. The system was then run for five minutes to verify no voltage drift existed in our system. Upon verifying our system was in good working order the test was begun.

Photos were taken of the specimen after each cycle so comparisons of the white wash flaking could be made between each cycle. These photos can be seen in Appendix C and Appendix D. Once the test specimen achieved all cycles of the 0.02 radians rotation, the testing cycle deviated from the *2010 AISC Seismic Provision*. The next cycle conducted was 0.0225 radians of rotation. While the test specimen probably could

have continued to achieve larger rotations and tip deflection, the test was terminated due to concerns about testing conditions and safety.

5. Experimental Results and Discussion

5.1. Overview

An overview of the results for each test, King and Jack end testing, are included in the next two sections 5.1.1 and 5.1.2. The following can be found in each section:

- Test summary sheet
- Compiled tables of max recorded testing values
- Tables of compiled strain gauge data
- Photographs of the specimens before testing and at the end of testing

The test summary sheet provides details on the test specimens, design strengths, and experimental results. The compiled testing tables shows max corrected tip deflection, max load, max moment, and the max corrected rotation for each load step and cycle. The summary tables for strain show the max positive and max negative values for each location at each of the load steps. The strain tables also show the max positive and max negative set for each of the load cycles.

The following additional information can be found in Appendix C and Appendix D:

- Plots of moment vs rafter rotation, and load vs tip deflection
- Photographs of the specimens before testing and at different cycles during testing

The moment vs rafter rotation plots show the corrected rotation vs Mn/M_p, (normalized beam moment at the column face / plastic beam moment capacity). The

load vs tip deflection charts provide information on yielding of the specimen, and corrected tip displacement with applied load.

5.1.1. King End Overview

This section includes the following:

- Test summary: King End Strength
- Compiled tables of max recorded testing values (Table 11)
- Tables of compiled strain gauge data (Table 12)
- Photographs of the specimens before testing and at the end of testing (Figure 54 and Figure 55)

Test Summary: King End Strength

Connection Description:	
Type:	Multiple Row Extended (MRE)
Number of Tension Bolts:	6 (2 Outside, 4 Inside)
Number of Compression Bolts:	6 (2 Outside, 4 Inside)
Beam Data:	
Section Type:	Built-up
Depth, h:	44.0 in.
Flange Width, b_f:	10.0 in.
Flange Thickness, t_f:	1.0 in.
Web Thickness, t_w:	0.3125 in.
Moment of Inertia, I:	11,176 in^4.
Nominal Yield Stress Flange, $F_{yf.spec}$:	50.0 ksi.
Measured Yield Stress Flange, $F_{yf.}$:	60.0 ksi.
Nominal Yield Stress Web, $F_{yw.spec}$:	50.0 ksi.
Measured Yield Stress Web, $F_{yw.}$:	55.0 ksi.
End-plate Data:	
End-plate Thickness, t_p:	2.0 in.
End-plate Width, b_p	12.0 in.
End-plate Length, L_p:	57.5 in.
End-plate Vertical Edge Distance, L_{ev}:	2.75 in.
End-plate Horizontal Edge Distance, L_{eh}:	3.25 in.
Outer Pitch, Bolt to Flange, p_{fo}:	4.0 in.
Inner Pitch, Bolt to Flange, p_{fi}:	4.0 in.
Outer Pitch, Bolt to Bolt, p_b:	4.0 in.
Gauge, g:	5.5 in.
Nominal Yield Stress, $F_{yp.spec}$:	36.0 ksi.
Measured Yield Stress, $F_{yp.}$:	41.0 ksi.
Bolt Data:	
Bolt Diameter, d_b:	1.375 in.
Bolt Length, L_b	6.0 in.
Bolt Type:	ASTM A490
Bolt Pretension, T_b:	127 kips.
Nominal Bolt Yield Strength, F_{yb}:	130 ksi.
Experimental Results:	
Maximum Applied Moment, M_{max}:	2742 kip*ft.
Yield Moment, M_y:	2619 kip*ft.
Failure Mode:	N/A
Predicted Strengths:	
End-plate Strength, M_{PL}:	5818 kip*ft.
Bolt Tension Rupture(w/o Prying), M_{NP}:	3369 kip*ft.
Beam Expected Yield Strength (Ass.Fy), M_{PE}:	2134 kip*ft.
Beam Expected Yield Strength (Tested.Fy), M_{PE}:	2786 kip*ft.
Beam Expected Plastic Strength (Ass.Fy) @ d/2, M_{PE} :	2602 kip*ft.
Beam Expected Plastic Strength (Tested.Fy) @ d/2, M_{PE}:	3135 kip*ft.
Controlling Condition: **M_n:**	2602 kip*ft.

Table 11. King End Test Data Summary

CYCLIC LOADING DATA
TEST NAME: King End Test

	LoadStep	Cycle	Cycle A: Corrected Max Tip Def. (in)	Cycle A: Max Pos. Load (Kips)	Cycle A: Max Moment (kip-in)	Cycle A: Max Rotation: (rads)	Cycle B: Corrected Max Tip Def. (in)	Cycle B: Max Neg. Load (kip)	Cycle B: Max Moment (kip-in)	Cycle B: Max Rotation: (rads)
Snug Tight	I	1	0.67782	27.71414	6097.11080	0.00305	-0.75176	-24.66682	-5426.70040	-0.00346
	(0.00375 rad)	2	0.68006	27.67296	6088.05120	0.00306	-0.74887	-24.15207	-5313.45540	-0.00345
	Avg. Disp. = 0.7033275	3	0.66998	27.77591	6110.70020	0.00302	-0.73520	-23.55496	-5182.09120	-0.00338
	Avg. Load = 25.643129	4	0.67005	27.42588	6033.69360	0.00302	-0.72584	-23.22552	-5109.61440	-0.00335
		5	0.67402	27.79650	6115.23000	0.00304	-0.70712	-22.85490	-5028.07800	-0.00327
		6	0.67963	28.24948	6214.88560	0.00306	-0.71957	-22.62841	-4978.25020	-0.00332
	II	1	0.87077	33.29403	7324.68660	0.00392	-0.91091	-31.13208	-6849.05760	-0.00413
	(0.005 rad)	2	0.86761	34.98241	7696.13020	0.00391	-0.91386	-30.74087	-6762.99140	-0.00413
	Avg. Disp. = 0.8894273	3	0.86420	34.77651	7650.83220	0.00389	-0.91820	-30.61733	-6735.81260	-0.00416
	Avg. Load = 32.648877	4	0.86008	35.04418	7709.71960	0.00387	-0.91362	-30.30848	-6667.86560	-0.00414
		5	0.86430	35.14713	7732.36860	0.00389	-0.91631	-30.16435	-6636.15700	-0.00415
		6	0.84634	34.81769	7659.89180	0.00381	-0.92692	-30.76146	-6767.52120	-0.00421
	III	1	1.51514	60.47283	13304.02260	0.00682	-1.65482	-62.73773	-13802.30060	-0.00753
	(0.0075 rad)	2	1.47468	60.74050	13362.91000	0.00664	-1.64868	-62.51124	-13752.47280	-0.00751
	Avg. Disp. = 1.5886261	3	1.47182	60.18457	13240.60540	0.00663	-1.66900	-60.98758	-13417.26760	-0.00760
	Avg. Load = 59.755612	4	1.50045	52.89571	11637.05620	0.00676	-1.72139	-62.38770	-13725.29400	-0.00775
		5	1.47247	54.68704	12031.14880	0.00663	-1.72761	-62.82009	-13820.41980	-0.00778
		6	1.45955	54.54291	11999.44020	0.00657	-1.74789	-62.09944	-13661.87680	-0.00787
	IV	1	2.25137	78.22141	17208.71020	0.01014	-2.24311	-79.97156	-17593.74320	-0.01010
	(0.01 rad)	2	2.23730	72.80624	16017.37280	0.01008	-2.21270	-81.82466	-18001.42520	-0.00997
	Avg. Disp. = 2.2263157	3	2.22452	74.51521	16393.34620	0.01002	-2.20670	-83.43068	-18354.74960	-0.00994
	Avg. Load = 79.377024	4	2.22803	79.45681	17480.49820	0.01004	-2.20680	-84.78962	-18653.71640	-0.00994
Pre-Tensioned	V	1	2.20736	93.29329	20524.52380	0.00994	-2.18669	-84.68667	-18631.06740	-0.00985
	(0.01 rad)	2	2.23163	90.51364	19913.00080	0.01005	-2.21568	-88.61936	-19496.25920	-0.00998
	Avg. Disp. = 2.2108789	3	2.23426	85.79853	18875.67660	0.01006	-2.20438	-91.17252	-20057.95440	-0.00993
	Avg. Load = 89.592238	4	2.22913	82.77180	18209.79600	0.01004	-2.17789	-99.88209	-21974.05980	-0.00981
	VI	1	3.33809	121.48100	26725.82000	0.01504	-3.27933	-130.93181	-28804.99820	-0.01477
	(0.015 rad)	2	3.31233	120.73976	26562.74720	0.01492	-3.29189	-140.91796	-31001.95120	-0.01483
	Avg. Disp. = 3.305411									
	Avg. Load = 128.51763									
	VII	1	4.41976	142.70929	31396.04380	0.01991	-4.41311	-143.61525	-31595.35500	-0.01988
	(0.02 rad)	2	4.43022	140.05318	30811.69960	0.01996	-4.43445	-144.72711	-31839.96420	-0.01988
	Avg. Disp. = 4.4243848									
	Avg. Load = 142.77621									
	VIII	1	5.17732	142.83283	31423.22260	0.02335	-5.00648	-144.06823	-31695.01060	-0.02256
	(0.0225 rad)	2	4.99953	143.51230	31572.70600	0.02252	-4.99718	-147.91856	-32542.08320	-0.02251
	Avg. Disp. = 5.0451268									
	Avg. Load = 144.58298									

Table 12. King End Strain Gauge Data Summary

Compiled Strain Gauge Data													
Test ID: King End													
Location :	NWB	NEB	E=F	W=F	W+F	SW	SWT	NWT	SET	SEB	NET	E+F	Load Cycle:
Min	-1.28E+02	-1.14E+02	-4.89E+00	-3.24E+01	-5.04E+02	-1.15E+02	-2.94E+02	-3.68E+02	-3.79E+02	-1.20E+02	-3.97E+02	-3.99E+02	0.00375
Max	1.18E+02	1.06E+02	2.60E+01	1.07E+02	6.13E+01	5.18E+02	6.98E+02	3.38E+02	5.80E+02	4.21E+02	3.51E+02	1.19E+02	
Max + Set:	1.44E+01	-3.62E+00	2.17E+00	-1.62E+01	3.51E+00	-2.23E+01	1.97E+01	-2.17E+01	8.77E+01	2.43E+01	4.26E+01	-1.11E+01	
Max - Set:	1.03E+01	-8.38E+00	-2.32E+00	-3.01E+01	-1.54E+01	-5.14E+01	-3.87E+01	-5.10E+01	2.16E+01	-1.02E+01	1.06E+01	-1.95E+01	
Min	-1.76E+02	-1.49E+02	-1.30E+01	-2.75E+01	-7.03E+02	-1.28E+02	-3.63E+02	-4.30E+02	-5.08E+02	-1.95E+02	-5.22E+02	-5.28E+02	0.005
Max	1.57E+02	1.53E+02	2.81E+01	1.39E+02	8.25E+01	7.13E+02	8.42E+02	4.50E+02	6.76E+02	5.41E+02	4.20E+02	1.67E+02	
Max + Set:	1.72E+01	-3.62E+00	-6.54E+00	-9.97E+00	-7.79E+01	2.08E+01	1.47E+01	-5.61E+00	4.55E+01	2.05E+01	2.02E+01	-1.12E+01	
Max - Set:	1.23E+01	-8.83E+00	-1.24E+01	-2.36E+01	-9.30E+01	-7.30E+00	-3.59E+01	-3.25E+01	-1.65E+01	-1.36E+01	-7.20E+00	-2.35E+01	
Min	-3.46E+02	-3.33E+02	-6.34E+00	-4.79E+01	-1.48E+03	-5.66E+02	-7.73E+02	-8.16E+02	-1.08E+03	-6.06E+02	-8.43E+02	-9.32E+02	0.0075
Max	3.59E+02	3.13E+02	3.59E+01	1.88E+02	3.02E+02	1.21E+03	1.29E+03	7.69E+02	1.23E+03	1.13E+03	7.95E+02	4.40E+02	
Max + Set:	1.58E+01	1.17E+00	-4.69E+00	3.86E+00	-7.53E+01	7.99E+00	-5.39E+00	-3.15E+00	2.61E+01	7.15E+00	9.80E+00	4.75E+00	
Max - Set:	1.10E+01	-4.05E+00	-5.70E+00	1.66E+00	-9.06E+01	-7.05E-01	-2.28E+01	-1.87E+01	5.50E+00	-5.67E+00	-1.65E+00	1.87E-01	
Min	-4.58E+02	-4.85E+02	-1.08E+01	-4.79E+01	-1.60E+03	-1.10E+03	-1.28E+03	-1.11E+03	-1.40E+03	-1.02E+03	-1.11E+03	-9.98E+02	0.01 Snug Tight
Max	4.98E+02	4.46E+02	3.59E+01	1.88E+02	4.98E+02	1.48E+03	1.56E+03	9.95E+02	1.39E+03	1.52E+03	1.09E+03	8.00E+02	
Max + Set:	5.93E+00	-1.13E+01	4.66E+00	8.27E+00	-3.33E+02	-4.45E+01	-5.13E+01	5.99E+00	-8.90E+01	2.12E+01	4.44E+01	6.66E+01	
Max - Set:	-1.24E-01	-1.89E+01	-4.59E+00	3.88E+00	-3.68E+02	-4.51E+01	-5.31E+01	-1.08E+01	-1.36E+02	1.46E+01	3.18E+01	1.52E+01	
Min	-5.74E+02	-5.92E+02	-1.00E+02	-2.77E+02	-8.88E+02	-1.08E+03	-5.64E+02	-1.26E+03	-1.62E+03	-1.77E+03	-1.20E+03	-9.13E+02	0.01 Pre-Tensioned
Max	6.14E+02	5.86E+02	7.31E+00	1.35E+01	1.37E+03	2.48E+03	2.84E+03	1.15E+03	1.53E+03	2.86E+03	1.23E+03	1.19E+03	
Max + Set:	1.20E+00	1.46E+01	-2.03E+01	-9.66E+01	1.50E+02	8.67E+02	1.33E+03	1.71E+01	-8.47E+01	8.99E+02	2.95E+01	-6.74E+01	
Max - Set:	-3.48E+00	-1.95E+00	-3.58E+01	-1.37E+02	1.05E+02	7.26E+02	1.21E+03	-4.49E+00	-1.26E+02	1.11E+03	2.45E+01	-9.48E+01	
Min	-7.56E+02	-8.41E+02	-3.27E+02	-4.52E+02	-2.99E+03	-2.99E+03	-3.00E+03	-2.59E+03	-2.14E+03	-3.00E+03	-1.70E+03	-2.44E+03	0.015
Max	8.66E+02	7.56E+02	1.08E+02	1.53E+02	2.98E+03	2.99E+03	2.54E+03	1.48E+03	1.94E+03	2.61E+03	1.69E+03	2.99E+03	
Max + Set:	-1.10E+01	1.47E+01	9.46E+01	1.08E+02	7.83E+02	1.13E+03	6.79E+02	3.78E+01	1.43E+02	3.02E+00	6.73E+01	2.99E+03	
Max - Set:	-1.61E+01	-2.99E+01	-1.73E+02	-2.07E+02	-2.95E+03	-2.80E+03	-1.38E+02	-7.29E+02	-1.37E+02	-6.64E+02	-5.35E+01	-1.14E+03	
Min	-9.01E+02	-8.35E+02	-3.80E+02	-7.89E+02	-2.40E+03	-2.99E+03	-3.00E+03	-2.98E+03	-2.99E+03	-3.00E+03	-2.99E+03	-2.99E+03	0.02
Max	1.03E+03	1.14E+03	2.07E+02	1.67E+02	2.99E+03	2.99E+03	3.00E+03	2.29E+03	2.99E+03	3.00E+03	1.73E+03	2.94E+03	
Max + Set:	1.10E+02	2.37E+02	1.73E+02	1.44E+00	2.99E+03	2.99E+03	1.63E+03	5.88E+02	7.51E+02	2.04E+03	-4.79E+01	1.62E+03	
Max - Set:	-7.74E+01	-4.39E+01	-3.44E+02	-7.60E+02	1.01E+02	-1.48E+03	-7.93E+02	-2.98E+03	-1.83E+03	-3.00E+03	-1.01E+03	-2.99E+03	
Min	-9.61E+02	-1.87E+03	-4.28E+02	-8.89E+02	-2.99E+03	-2.99E+03	-3.00E+03	-2.98E+03	-2.99E+03	-3.00E+03	-2.99E+03	-2.99E+03	0.0225
Max	1.56E+03	2.12E+03	4.30E+02	8.30E+02	2.99E+03	2.99E+03	3.00E+03	2.98E+03	2.99E+03	3.00E+03	3.00E+03	2.99E+03	
Max + Set:	7.25E+01	7.11E+01	3.20E+01	6.39E+02	1.02E+03	6.27E+02	1.83E+02	2.78E+02	1.43E+03	3.00E+03	3.00E+03	2.99E+03	
Max - Set:	-2.87E+01	-1.01E+03	-3.13E+02	-1.87E+02	-2.99E+03	-2.99E+03	-2.72E+03	-2.98E+03	-2.31E+02	-7.56E+02	3.12E+02	-3.27E+02	
Values shown are in micro strain													

Figure 54. King's End-plate to Rafter Connection Prior to Testing

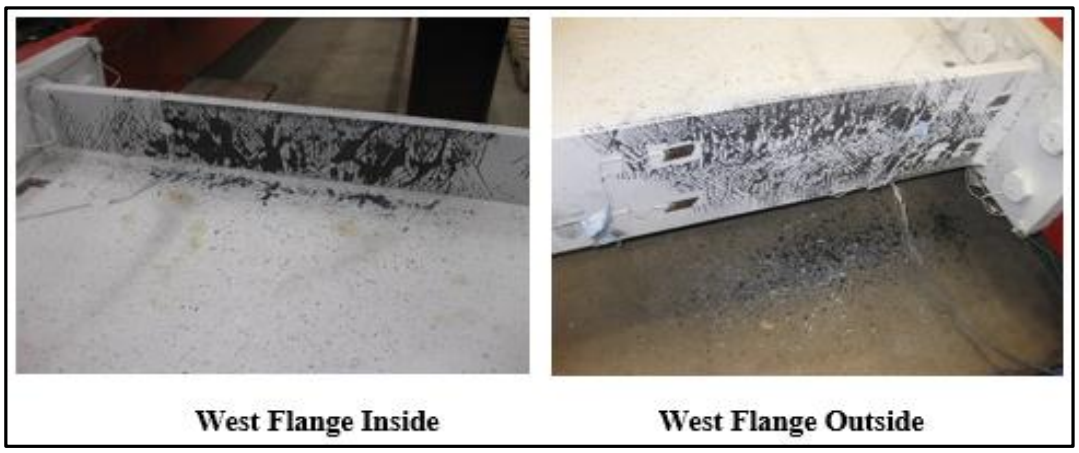

Figure 55. King's End-plate to Rafter Connection at Testing Termination

5.1.2. Jack End Overview

This section includes the following:

- Test summary: Jack End Strength
- Compiled tables of max recorded testing values (Table 13)
- Tables of compiled strain gauge data (Table 14)
- Photographs of the specimens before testing and at the end of testing (Figure 56 and Figure 57)

Test Summary: Jack End

Connection Description:	
Type:	Multiple Row Extended (MRE)
Number of Tension Bolts:	6 (2 Outside, 4 Inside)
Number of Compression Bolts:	6 (2 Outside, 4 Inside)
Beam Data:	
Section Type:	Built-up
Depth, h:	44.0 in.
Flange Width, b_f:	10.0 in.
Flange Thickness, t_f:	1.0 in.
Web Thickness, t_w:	0.3125 in.
Moment of Inertia, I:	11,176 in^4.
Nominal Yield Stress Flange, $F_{yf.spec}$:	50.0 ksi.
Measured Yield Stress Flange, $F_{yf.}$:	62.5 ksi.
Nominal Yield Stress Web, $F_{yw.spec}$:	50.0 ksi.
Measured Yield Stress Web, $F_{yw.}$:	78.0 ksi.
End-plate Data:	
End-plate Thickness, t_p:	2.0 in.
End-plate Width, b_p	12.0 in.
End-plate Length, L_p:	57.5 in.
End-plate Vertical Edge Distance, L_{ev}:	2.75 in.
End-plate Horizontal Edge Distance, L_{eh}:	3.25 in.
Outer Pitch, Bolt to Flange, p_{fo}:	4.0 in.
Inner Pitch, Bolt to Flange, p_{fi}:	4.0 in.
Outer Pitch, Bolt to Bolt, p_b:	4.0 in.
Gauge, g:	5.5 in.
Nominal Yield Stress, $F_{yp.spec}$:	36.0 ksi.
Measured Yield Stress, $F_{yp.}$:	50.5 ksi.
Bolt Data:	
Bolt Diameter, d_b:	1.375 in.
Bolt Length, L_b	6.0 in.
Bolt Type:	ASTM A490
Bolt Pretension, T_b:	127 kips.
Nominal Bolt Yield Strength, F_{yb}:	130 ksi.
Experimental Results:	
Maximum Applied Moment, M_{max}:	2786 kip*ft.
Yield Moment, M_y:	2678 kip*ft.
Failure Mode:	N/A
Predicted Strengths:	
End-plate Strength, M_{PL}:	5818 kip*ft.
Bolt Tension Rupture(w/o Prying), M_{NP}:	3369 kip*ft.
Beam Expected Yield Strength (Ass.Fy), M_{PE}:	2134 kip*ft.
Beam Expected Yield Strength (Tested.Fy), M_{PE}:	2786 kip*ft.
Beam Expected Plastic Strength (Ass.Fy) @ d/2, M_{PE} :	2602 kip*ft.
Beam Expected Plastic Strength (Tested.Fy) @ d/2, M_{PE}:	3135 kip*ft.
Controlling Condition: **M_n:**	2602 kip*ft.

Table 13. Jack End Test Data Summary

CYCLIC LOADING DATA
TEST NAME: Jack End Test

			Cycle A				Cycle B			
	LoadStep	Cycle	Corrected Max Tip Def. (in)	Max Pos. Load (Kips)	Max Moment (kip-in)	Max Rotation: (rads)	Corrected Max Tip Def. (in)	Max Neg. Load (kip)	Max Moment (kip-in)	Max Rotation: (rads)
Pre-Tensioned	I	1	0.83561	33.78819	7433.40180	0.00376	-0.84344	-33.66465	-7406.22300	-0.00380
	(0.00375 rad)	2	0.83577	34.73533	7641.77260	0.00376	-0.84856	-39.53280	-8697.21600	-0.00382
	Avg. Disp. = 0.8419242	3	0.84459	37.92678	8343.89160	0.00380	-0.84395	-35.72365	-7859.20300	-0.00380
	Avg. Load = 36.274433	4	0.84640	36.77374	8090.22280	0.00381	-0.85099	-38.44153	-8457.13660	-0.00383
		5	0.83850	38.54448	8479.78560	0.00378	-0.83919	-33.82937	-7442.46140	-0.00378
		6	0.83748	37.94737	8348.42140	0.00377	-0.83861	-34.38530	-7564.76600	-0.00378
	II	1	1.11473	48.34532	10635.97040	0.00502	-1.12001	-49.06597	-10794.51340	-0.00504
	(0.005 rad)	2	1.12707	50.36314	11079.89080	0.00508	-1.11711	-42.68307	-9390.27540	-0.00503
	Avg. Disp. = 1.1215191	3	1.11328	49.12774	10808.10280	0.00501	-1.11856	-49.29246	-10844.34120	-0.00504
	Avg. Load = 49.484633	4	1.13307	50.87789	11193.13580	0.00510	-1.12017	-42.35363	-9317.79860	-0.00504
		5	1.11669	49.33364	10853.40080	0.00503	-1.12327	-49.82780	-10962.11600	-0.00506
		6	1.12928	64.36434	14160.15480	0.00509	-1.12497	-48.18060	-10599.73200	-0.00507
	III	1	1.67800	85.71617	18857.55740	0.00756	-1.66690	-58.39324	-12846.51280	-0.00751
	(0.0075 rad)	2	1.67094	84.87198	18671.83560	0.00753	-1.66765	-58.68150	-12909.93000	-0.00751
	Avg. Disp. = 1.6744801	3	1.67677	85.46909	18803.19980	0.00755	-1.68084	-59.50510	-13091.12200	-0.00757
	Avg. Load = 72.318943	4	1.67105	85.13965	18730.72300	0.00753	-1.67752	-60.67873	-13349.32060	-0.00755
		5	1.67635	84.46018	18581.23960	0.00755	-1.67168	-60.30811	-13267.78420	-0.00753
		6	1.67410	84.31605	18549.53100	0.00754	-1.68196	-60.28752	-13263.25440	-0.00757
	IV	1	2.23499	105.95614	23310.35080	0.01007	-2.22501	-80.75398	-17765.87560	-0.01002
	(0.01 rad)	2	2.23705	105.85319	23287.70180	0.01008	-2.22808	-80.54808	-17720.57760	-0.01003
	Avg. Disp. = 2.2298085	3	2.23320	105.85319	23287.70180	0.01006	-2.22592	-80.34218	-17675.27960	-0.01002
	Avg. Load = 93.092538	4	2.22670	105.11195	23124.62900	0.01003	-2.22752	-80.32159	-17670.74980	-0.01003
	V	1	3.33138	140.30026	30866.05720	0.01501	-3.33175	-124.11652	-27305.63440	-0.01501
	(0.015 rad)	2	3.33235	140.87678	30992.89160	0.01501	-3.33748	-123.91062	-27260.33640	-0.01503
	Avg. Disp. = 3.3332389									
	Avg. Load = 132.30105									
	VI	1	4.44181	143.49171	31568.17620	0.02001	-4.45496	-145.03596	-31907.91120	-0.02007
	(0.02 rad)	2	4.44161	145.30363	31966.79860	0.02001	-4.46854	-144.50062	-31790.13640	-0.02013
	Avg. Disp. = 4.4517293									
	Avg. Load = 144.58298									
	VII	1	5.01198	149.60694	32913.52680	0.02258	-5.01904	-142.70929	-31396.04380	-0.02261
	(0.0225 rad)	2	5.00530	151.48063	33325.73860	0.02252	-5.01315	-144.10941	-31704.07020	-0.02259
	Avg. Disp. = 5.0123658									
	Avg. Load = 146.97657									

Table 14. Jack End Strain Gauge Data

Compiled Strain Gauge Data

Test ID: Jack End

Location :	NWB	NWBM	NWT	NWTM	SWB	SWT	W+F	W45	W=F	NEB	NEBM	NET	NETM	SET	SEB	E=F	E+F	E45	Load Cycle:
Min	-2.58E+02	-4.98E+02	-4.62E+02	-4.68E+02	-7.74E+02	-7.10E+02	-1.02E+02	-3.62E+02	-3.37E+02	-2.63E+02	-4.40E+02	-4.98E+02	-4.84E+02	-6.34E+02	-6.59E+02	-3.57E+02	-6.34E+01	-2.16E+02	0.00375
Max	2.37E+02	4.79E+02	5.22E+02	5.16E+02	5.53E+02	6.22E+02	6.23E+01	3.21E+02	3.39E+02	2.18E+02	5.16E+02	4.89E+02	4.89E+02	6.71E+02	5.61E+02	3.59E+02	2.78E+01	1.44E+02	
Max + Set:	7.00E+00	1.59E+01	3.77E+01	3.44E+01	-7.52E+01	-3.29E+01	-4.06E+00	1.18E+01	8.79E+00	-5.04E+00	1.67E+01	1.87E+01	1.84E+01	3.11E+01	-7.10E+01	-1.19E+01	-1.35E+01	3.90E+01	
Max - Set:	3.90E+00	1.37E+01	2.10E+01	2.21E+01	-8.38E+01	-3.87E+01	-1.97E+01	9.65E+00	-6.90E+00	-7.42E+00	1.24E+01	1.45E+01	1.43E+01	2.14E+01	-7.37E+01	-1.95E+01	-2.36E+01	3.30E+01	
Min	-3.23E+02	-6.15E+02	-6.02E+02	-5.99E+02	-1.08E+03	-9.50E+02	-1.38E+02	-4.52E+02	-4.26E+02	-3.31E+02	-8.13E+02	-8.64E+02	-8.39E+02	-1.14E+03	-1.08E+03	-6.64E+02	-8.09E+01	-4.55E+02	0.005
Max	4.27E+02	8.41E+02	8.20E+02	8.25E+02	9.69E+02	1.03E+03	9.81E+01	4.18E+02	5.86E+02	4.08E+02	6.54E+02	6.18E+02	6.16E+02	8.84E+02	7.48E+02	4.54E+02	7.56E+01	1.57E+02	
Max + Set:	1.35E+01	3.59E+01	5.89E+01	5.92E+01	-1.57E+02	-6.46E+01	-6.59E+00	2.56E+01	6.61E+00	-5.59E+00	3.12E+01	3.42E+01	3.31E+01	5.82E+01	-8.29E+01	-1.85E+01	-2.03E+01	6.00E+01	
Max - Set:	1.04E+01	3.44E+01	3.54E+01	4.05E+01	-1.68E+02	-7.27E+01	-2.65E+01	2.20E+01	-1.13E+01	-1.11E+01	2.22E+01	3.33E+01	3.02E+01	3.78E+01	-9.14E+01	-2.68E+01	-3.59E+01	4.84E+01	
Min	-3.70E+02	-7.33E+02	-7.61E+02	-7.56E+02	-1.04E+03	-1.03E+03	-1.53E+02	-6.08E+02	-5.26E+02	-3.71E+02	-1.09E+03	-1.19E+03	-1.15E+03	-1.69E+03	-1.52E+03	-1.08E+03	-9.10E+01	-7.17E+02	0.0075
Max	5.78E+02	1.14E+03	1.09E+03	1.11E+03	1.49E+03	1.41E+03	1.57E+02	4.27E+02	9.24E+02	5.44E+02	7.28E+02	7.26E+02	7.37E+02	9.55E+02	8.96E+02	5.68E+02	9.99E+01	9.59E+01	
Max + Set:	6.19E-01	3.01E+00	2.01E+01	1.49E+01	1.88E+01	1.25E+01	1.51E+01	-7.65E+00	4.87E+00	1.08E+01	9.44E+00	1.97E+01	2.24E+01	-4.58E+01	-3.19E+01	2.72E+01	-1.49E-01	1.57E+00	
Max - Set:	2.54E-01	-3.85E-01	-3.88E+00	-2.94E+00	-2.39E+01	1.18E+01	-2.53E+01	-2.33E+01	-1.93E+01	-6.22E+00	-1.62E+01	1.98E+00	1.18E+01	-7.98E+01	-5.38E+01	-7.31E-01	-2.94E+01	-1.40E+00	
Min	-4.98E+02	-9.87E+02	-1.02E+03	-1.01E+03	-1.20E+03	-1.58E+03	-2.92E+02	-7.31E+02	-4.36E+02	-4.96E+02	-1.31E+03	-1.44E+03	-1.39E+03	-2.09E+03	-1.93E+03	-1.12E+03	-2.00E+02	-8.67E+02	0.01
Max	6.71E+02	1.31E+03	1.23E+03	1.25E+03	2.10E+03	1.56E+03	1.65E+02	3.26E+02	1.28E+03	6.51E+02	9.71E+02	9.76E+02	9.84E+02	1.39E+03	1.15E+03	7.66E+02	9.57E+01	1.48E+00	
Max + Set:	8.65E+00	2.05E+01	3.63E+01	3.18E+01	2.09E+02	-1.39E+02	-8.48E+01	9.78E+01	3.78E+02	6.97E+00	1.14E+01	3.79E+01	4.70E+01	1.56E+02	-1.53E+02	5.74E+01	-9.33E+01	-5.92E+01	
Max - Set:	3.54E+00	8.78E+00	9.73E+00	8.39E+00	1.68E+02	-1.85E+02	-1.55E+02	7.90E+01	2.96E+02	-7.32E+00	-1.15E+01	3.68E+01	4.52E+01	-5.75E+01	-1.70E+02	-1.41E+01	-1.49E+02	-7.25E+01	
Min	-7.60E+02	-1.52E+03	-1.58E+03	-1.57E+03	-2.46E+03	-2.68E+03	-3.67E+02	-6.39E+02	1.57E+02	-8.13E+02	-1.94E+03	-2.46E+03	-1.86E+03	-3.00E+03	-3.00E+03	-2.79E+03	-3.82E+02	-2.17E+03	0.015
Max	9.33E+02	1.81E+03	1.62E+03	1.65E+03	2.99E+03	1.59E+03	1.27E+02	9.21E+02	2.97E+03	8.38E+02	1.40E+03	1.25E+03	1.55E+03	1.80E+03	1.49E+03	9.03E+02	2.24E+02	-1.66E+02	
Max + Set:	6.51E+01	1.27E+02	9.88E+01	1.04E+02	1.52E+03	-4.11E+02	-8.79E+01	8.86E+02	2.16E+03	-7.11E+01	-5.54E+01	-1.75E+02	1.21E+02	-1.28E+02	-7.32E+02	3.09E+01	1.07E+02	-1.02E+03	
Max - Set:	2.86E+01	4.29E+01	1.18E+01	1.55E+01	-1.46E+02	-5.94E+02	-2.90E+02	6.10E+02	1.50E+03	-8.99E+01	-1.24E+02	-4.86E+02	9.78E+01	-4.68E+02	-7.99E+02	-1.50E+03	-3.60E+02	-1.16E+03	
Min	-8.54E+02	-2.79E+03	-2.99E+03	-2.99E+03	-2.99E+03	-3.00E+03	-4.04E+02	-2.95E+03	-2.97E+03	-9.46E+02	-3.01E+03	-2.99E+03	-2.99E+03	-3.00E+03	-3.00E+03	-2.96E+03	-3.99E+02	-2.95E+03	0.02
Max	1.04E+03	2.00E+03	1.79E+03	1.83E+03	2.99E+03	2.99E+03	2.82E+02	2.03E+03	2.97E+03	9.99E+02	1.66E+03	-1.88E+02	9.44E+02	3.00E+03	3.00E+03	2.96E+03	5.31E+02	-1.10E+03	
Max + Set:	2.33E+02	3.93E+01	-7.60E+01	-6.24E+01	2.99E+03	5.73E+02	-1.10E+02	1.91E+03	2.97E+03	-1.46E+01	-9.10E+01	-2.32E+03	-1.06E+03	6.08E+02	1.27E+02	2.80E+03	1.24E+02	-1.66E+03	
Max - Set:	4.85E+01	-7.90E+02	-2.99E+03	-2.99E+03	-2.39E+03	-3.00E+03	-1.99E+02	-2.95E+03	-1.49E+03	-7.24E+01	-1.32E+03	-2.99E+03	-2.99E+03	-8.04E+02	-3.00E+03	-1.90E+03	-1.48E+02	-2.18E+03	
Min	-2.59E+03	-3.00E+03	-2.99E+03	-2.99E+03	Damaged		-5.43E+02	-2.95E+03	-2.97E+03	-9.37E+02	-3.00E+03	-2.99E+03	-2.99E+03	Damaged		-2.65E+03	-4.79E+02	-9.22E+02	0.0225
Max	1.31E+03	3.00E+03	2.18E+03	2.91E+03			2.64E+02	8.85E+02	2.95E+03	1.41E+03	2.63E+03	2.99E+03	2.99E+03			2.96E+03	6.32E+02	8.17E+02	
Max + Set:	4.42E+02	3.00E+03	-3.75E+02	-9.77E+01			-3.73E+01	-1.66E+02	1.67E+03	4.05E+02	8.17E+02	2.99E+03	2.91E+03			2.96E+03	2.02E+02	2.47E+02	
Max - Set:	-2.19E+01	-2.43E+03	-2.99E+03	-2.99E+03			-3.25E+02	-2.04E+03	-2.48E+03	-4.73E+01	-1.25E+03	-2.99E+03	-2.99E+03			-1.26E+02	-1.51E+02	-1.90E+02	

Values shown are in micro strain

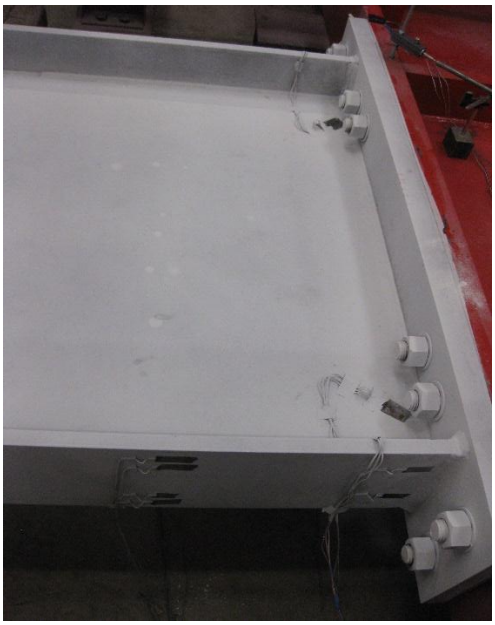

Figure 56. Jack's End-plate to Rafter Connection Prior to Testing

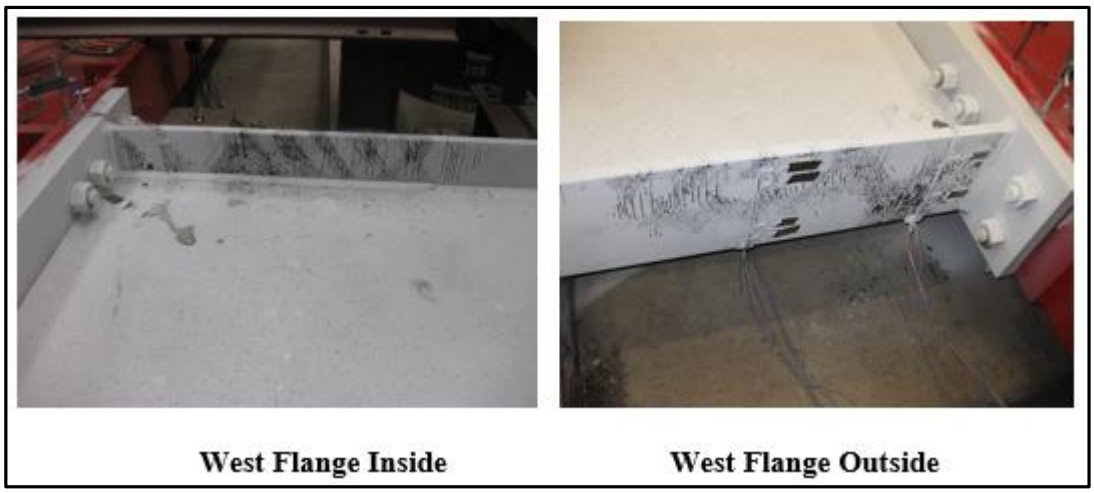

Figure 57. Jack's End-plate to Rafter Connection at Testing Termination

5.2. Rafters' Performance

At the end of testing both the Jack End and King End of the test beam achieved 0.0225 radians of rotation, and reached over 85 percent of the beam's plastic capacity moment. The predicted beam strength and the experimental beam strength for both tests

can be seen in Table 15. The beam experimental yield strength (M_{YE}) was the moment observed through testing at which the beam started to yield. The largest collected experimental moment (M_L) was the largest moment observed through testing. The predicted beam strengths were calculated using both the actual tested materials values (Tested Fy), and assumed values (Ass. Fy). This is to highlight the difference the steel's grade has on the specimen's strength. For the purpose of this thesis the values of importance are the specimen's strength calculated with tested material values. The supporting equations for these values can be found in Appendix A.

Table 15. Predicted & Tested Beam Strength

Tested Strengths:		**Jack End (Kip*ft.):**	**King End (Kip*ft.):**
Beam Experimental Yield Strength M_{YE}:		2678	2619
Largest Collected Experimental Moment M_L:		2786	2743
Predicted Strengths (Kip*ft.):		$M_{Experimental}/M_{Predicted}$	$M_{Experimental}/M_{Predicted}$
Beam Expected Yield Strength (Ass.Fy), M_{YA}:	2134	1.25	1.23
Beam Expected Yield Strength (Tested.Fy), M_{YT}:	2786	**0.96**	**0.94**
Beam Expected Plastic Strength (Ass.Fy) @ d/2, M_{PA}:	2602	1.07	1.05
Beam Expected Plastic Strength (Tested.Fy) @ d/2, M_{PT}:	3135	**0.89**	**0.87**

A figure of each specimen's experimental moment/expected plastic moment (tested) vs total plastic rotation can be viewed in Figure 58 and Figure 59.

Figure 58. Mn/Mp vs Rotation: King End

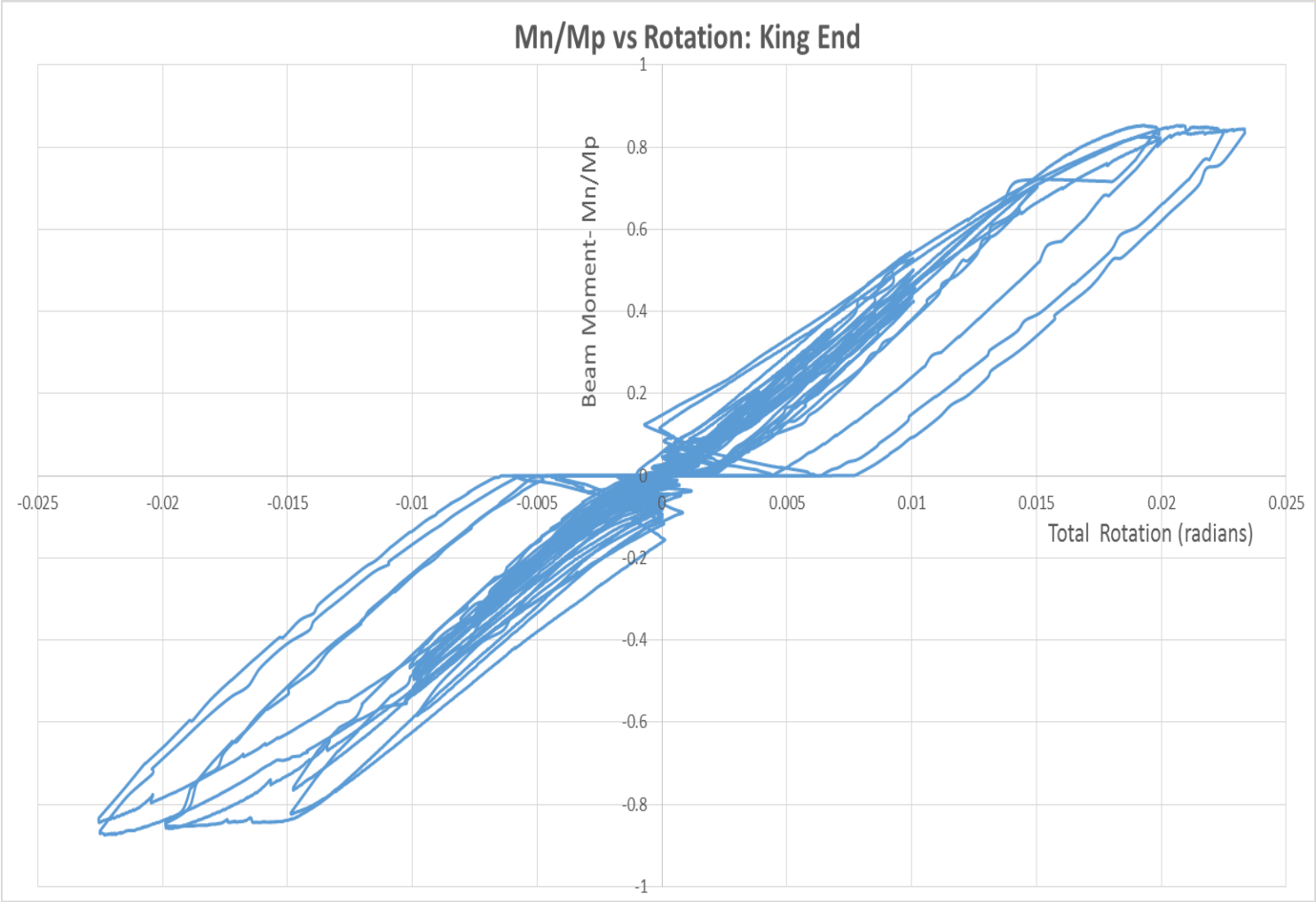

Figure 59. Mn/Mp vs Rotation: Jack End

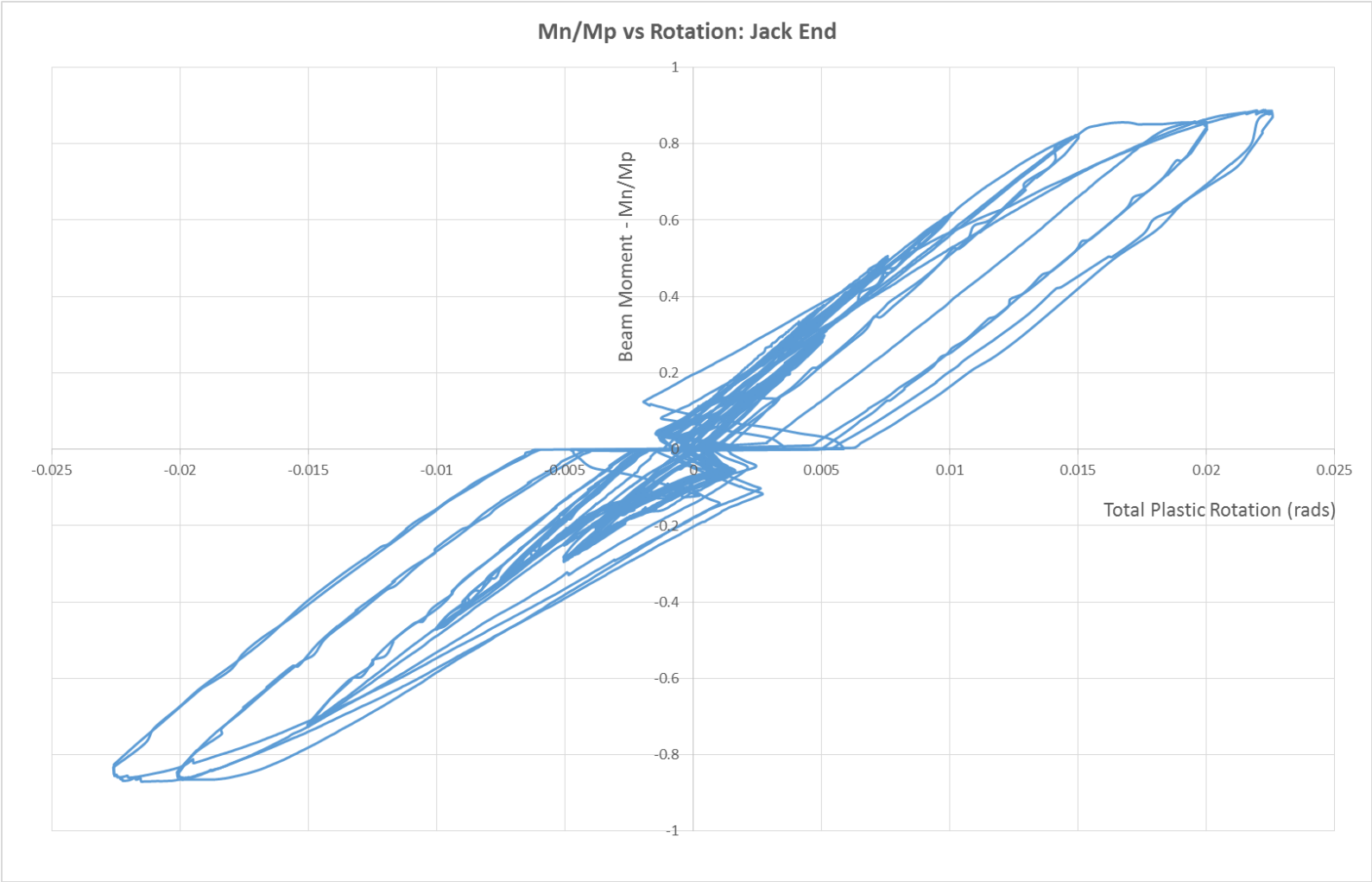

The King and Jack ends both saw a plastic hinge form around seventeen inches from the end-plate. This hinge location was close to the expected location of twenty-two inches. Along with plastic flange deformation, plastic buckling of the web was observed. Over an inch of out of plane web deformation was observed during the final cycles at 0.0225 radians. These are best observed by viewing the pictures supplied in Appendix C and in Appendix D.

5.3. Specimens Connection Performance

The four modified PJP welds were able to withstand all steps of the loading cycles with no loss of strength or degradation to the connection. While the desired results of these modified PJP welds were achieved, concern remained that while designed correctly the welds may have been incorrectly fabricated. In this section these concerns will be addressed and alleviated.

In order to validate the fact these modified PJP welds were fabricated according to design specifications, a physical examination was performed on the flange to end-plate welds. A destructive and non-destructive analysis was performed on the weld dimensions to provide details of the weld's construction.

The destructive analysis measured the internal portion of the flange to end-plate connection by examining the weld penetration and weld root at deliberate cross sections of the PJP welds. This analysis was called the "directly measured weld throats". Multiple cross sectional cuts were made through the depth of the flange to end-plate connections. The cut faces were then mechanically polished and acid etched to reveal the material structure. The etching revealed the penetration of the built-up fillet weld, the reinforcing fillet, root face of the flange, and any lack of penetration (LOP) that was

present at the interface. With these dimensions a realistic estimate could be made of the actual design strength of the welds.

The nondestructive examination of the welds was accomplished by measuring the exposed legs of the fillet welds on the flange to end-plate connection. This analysis was called the "theoretical weld throats". With these measured lengths the theoretical design strength of the welds could be estimated. The two different examinations were completed so industry standard/practical examination of the welds could be compared to the actual measured values.

5.3.1. Inspection of Flange to End-plate Welds

5.3.1.1. Directly Measured Weld Throats

In total twelve cuts were made along the ten inch wide flange, using a band saw. The design sheet for making these cuts can be seen in Figure 60. An example of a completely cut flange to end-plate section can be seen in Figure 61. The naming convention of the slices was taken from section 3.2. The slices got their names from the locations that they were taken. Slices were taken on both sides of the specimen's web. The web slices is the point where the naming/numbering system changes. Starting from the outside edged of the flanges, the slices are numbered 1 to 7. Number 1 being at the edge of the flange and number 7 being the web slice. On both sides of the web there should be 6 slices, and they both share the web slice.

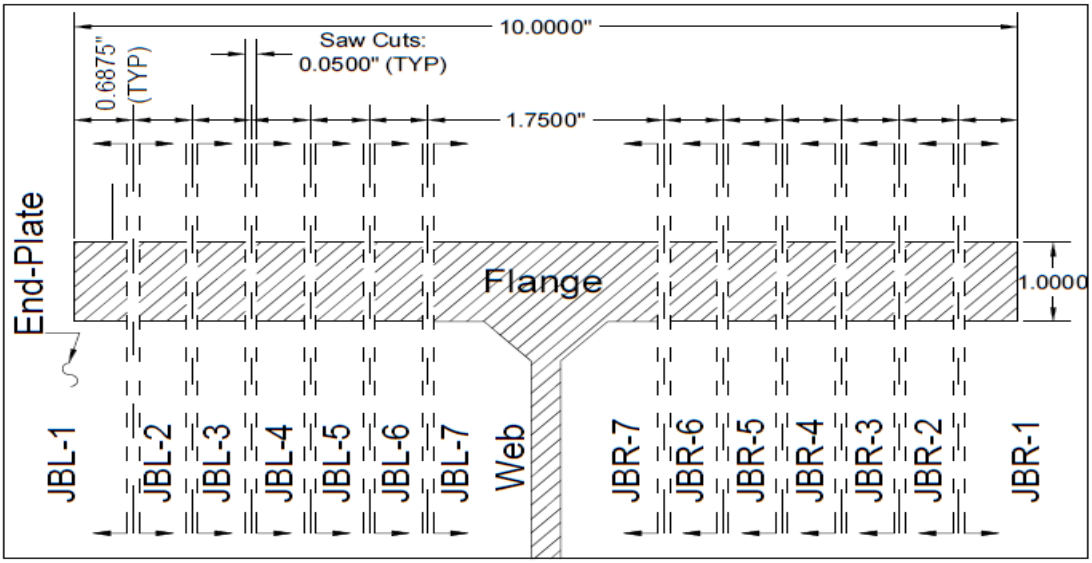

Figure 60. Design Sheet for Cuts on JB Flange

Figure 61. Cut Flange Specimens

The center cut section that included the web was approximately 1-1/2 inches wide, and the remaining samples were approximately 11/16 of an inch wide. Approximately 1/16 of an inch of material was removed due to the width of the saw blade. In total thirteen samples were manufactured and of those samples fourteen faces would be polished and chemically etched for examination. The faces to be polished and etched are denoted with cross sectional black arrows with arrow tips pointing at the face that was to be polished and etched (Figure 60). This process was repeated for all four flanges of the test specimen.

After all of the surfaces were polished, acid etched, and photographed, the photographs were imported into Autocad where the images were scaled and dimensioned. The areas for characterization were the built-up PJP fillets (A), LOP (B), reinforcing fillets (C), effective throats of the PJP (T_{fo}) effective throats reinforcing fillet welds (T_{fi}) as shown in Figure 62.

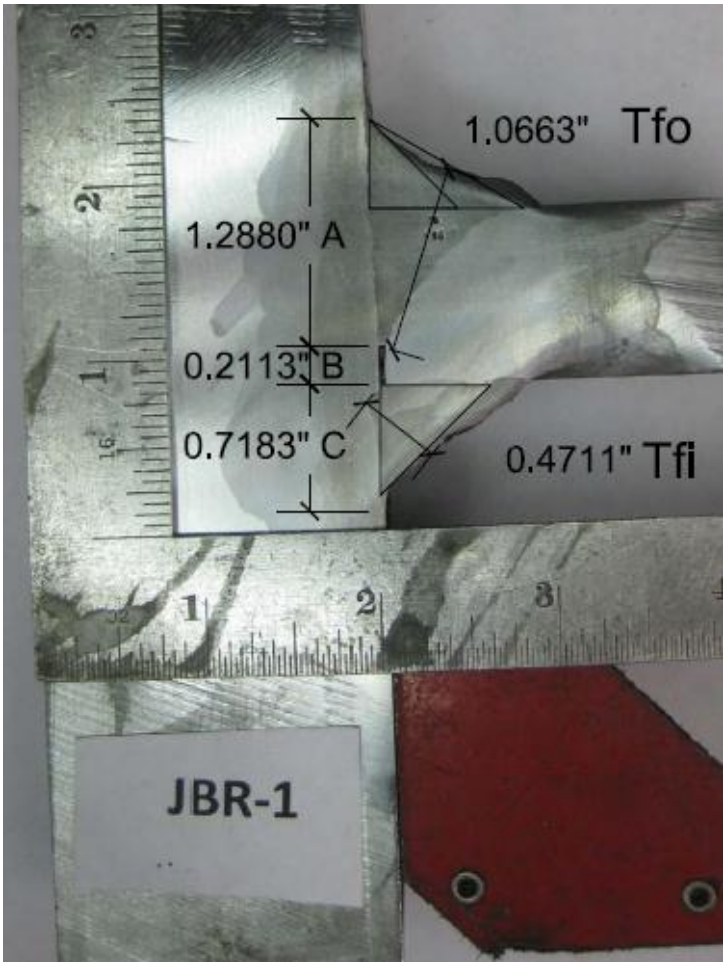

A = Built-up PJP Fillets
B = Lack of Penetration, LOP , Weld Root
C = Reinforcing Fillet
T_{fo} = Throat of A, PJP Fillets
T_{fi} = Throat of C, Reinforcing Fillets

Figure 62. Typical Polished and Etched Weld Cut Specimen

These dimensioned photographs and compiled data for each flange can be found in Appendix E, Appendix F, Appendix G, and Appendix H. The average for each measured dimensions, can be seen in

Table 16. A comparison between the actual measured values divided by the design value can be seen in Table 17.

Table 16. Average Dimensions of the Compiled Cut Section Properties

Weld Cut Location:	Avg. Built-up PJP Weld Leg A (in.)	Avg. Root Face & Lack of Penetration B (in.)	Avg. Reinforcing Fillet Leg C (in.)	Avg. Measured Effective Throat T_{fo} (in.)	Avg. Measured Effictive Throat T_{fi} (in.)	Avg. LOP Measured Along EP (in.)	Avg. Approx. Measured Root Face Along EP (in.)
Designed Vals.	**1.375**	**0.125**	**0.625**	**1.007**	**0.442**	**0.000**	**0.125**
Jack Bottom	1.240	0.241	0.673	1.056	0.475	0.150	0.170
Jack Top	1.119	0.308	0.713	0.947	0.506	0.131	0.247
King Bottom	1.121	0.305	0.699	0.904	0.526	0.172	0.198
King Top	1.170	0.256	0.711	0.943	0.523	0.105	0.189
Total Avg:	**1.162**	**0.277**	**0.699**	**0.963**	**0.507**	**0.140**	**0.201**

Table 17. Average Ratio of the Compiled Cut Section Properties

Weld Cut Location:	Avg. Built-up PJP Weld Leg A	Avg. Root Face & Lack of Penetration B	Avg. Reinforcing Fillet Leg C	Avg. Measured Effective Throat T_{fo}	Avg. Measured Effictive Throat T_{fi}	Avg. Approx. Measured Root Face Along EP
Jack Bottom Actual / Design	0.902	1.927	1.076	1.048	1.074	1.363
Jack Top Actual / Design	0.814	2.463	1.141	0.941	1.146	1.980
King Bottom Actual / Design	0.815	2.438	1.119	0.898	1.191	1.581
King Top Actual / Design	0.851	2.045	1.138	0.937	1.183	1.508
Total Avg:	**0.845**	**2.218**	**1.118**	**0.956**	**1.148**	**1.608**

As can be seen in Table 17 most of the measured values are close to designed values (ratio near 1.0), with the exception of the average root face and LOP, where the actual is nearly 2.2 times the designed value. The expected reasoning for this large inconsistency will be discussed in the next section. The other values of significance in reference to design strength are the T_{fo} and T_{fi} values. The T_{fo} is 95.6% of the design value, meaning it is a little under the designed value. The T_{fi} is 14.8 % larger than the design value, meaning it is a little over the designed value.

Knowing the properties of each weld at intermittent points along our flanges allows us to create a fairly accurate pictorial plan view of the weld penetration. Figure 63 through Figure 66 show the sizes of weld legs and LOP along the flange to end-plate connection.

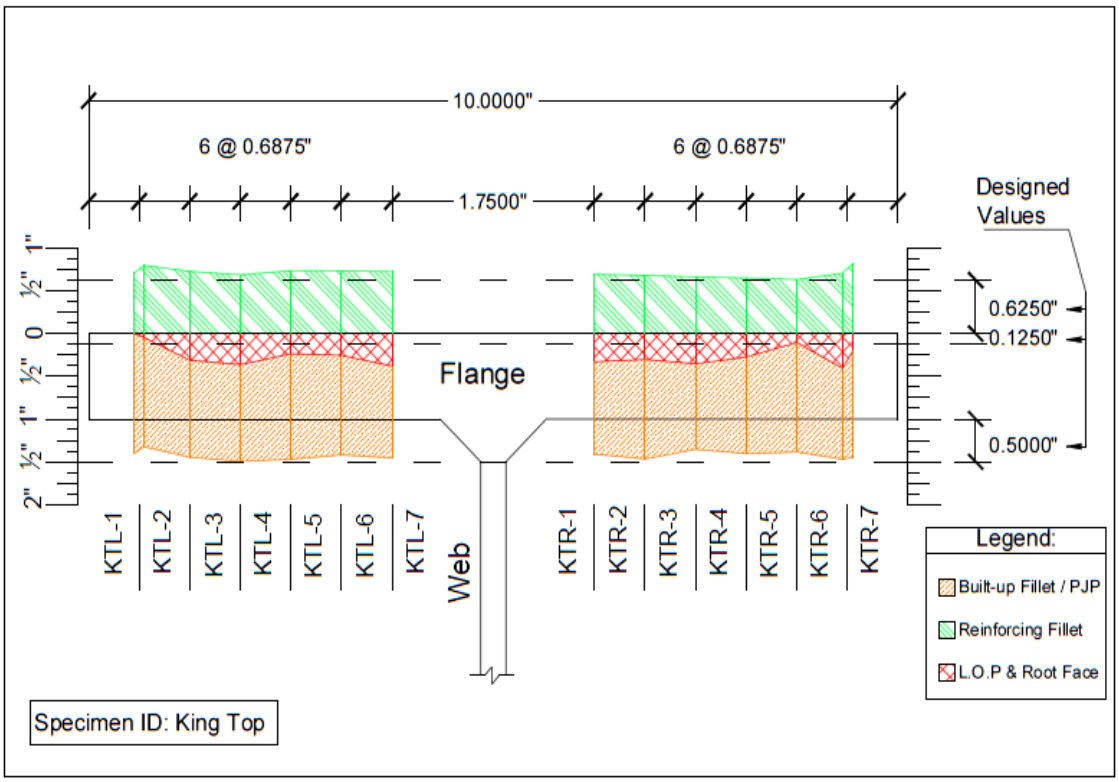

Figure 63. KT- Cross Sectional Weld PenetrationView

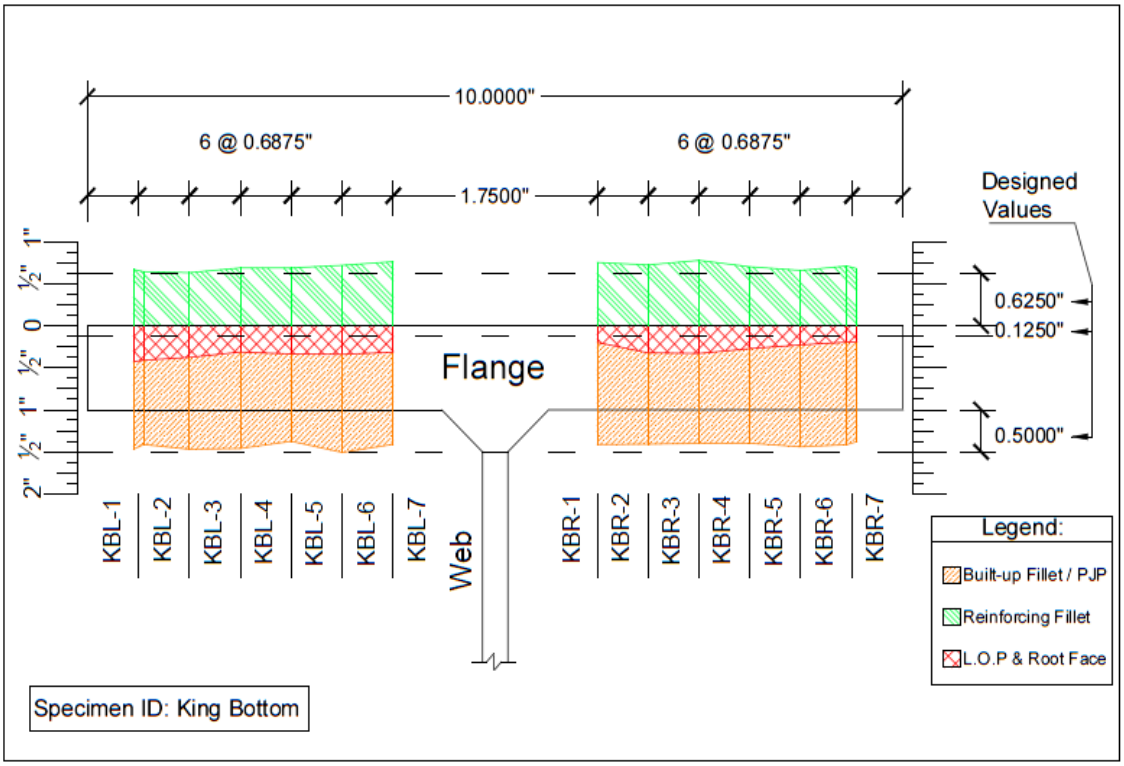

Figure 64. KB- Cross Sectional Weld PenetrationView

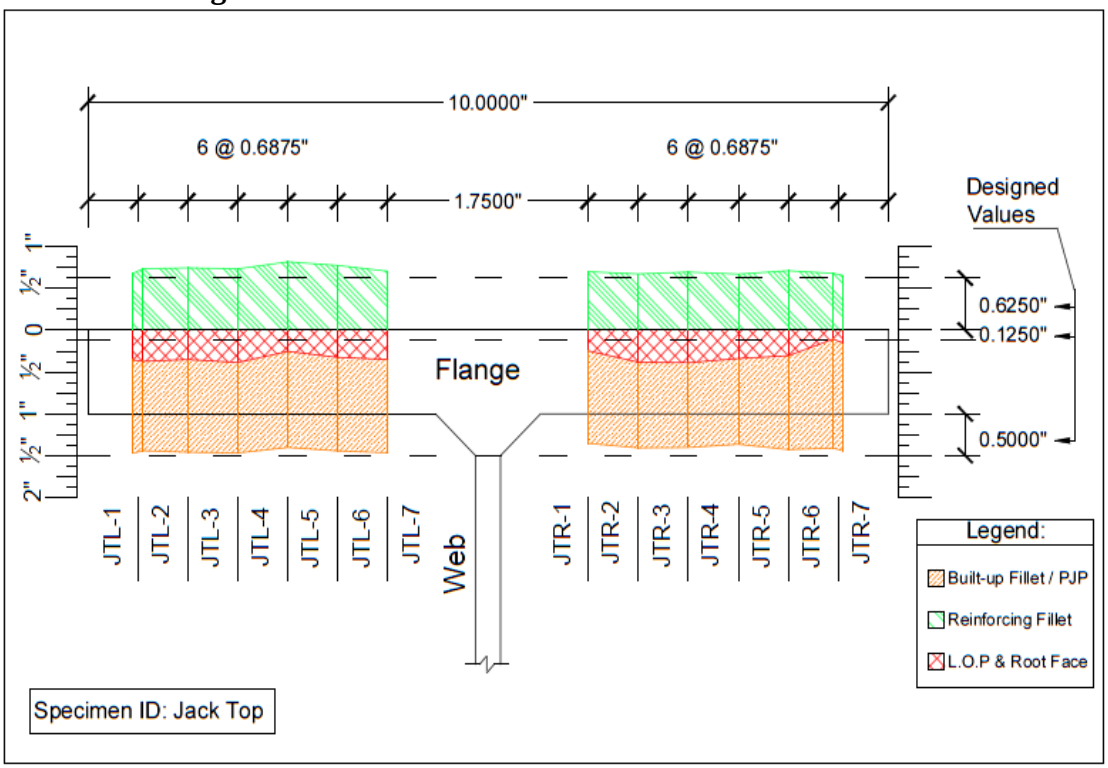

Figure 65. JT- Cross Sectional Weld PenetrationView

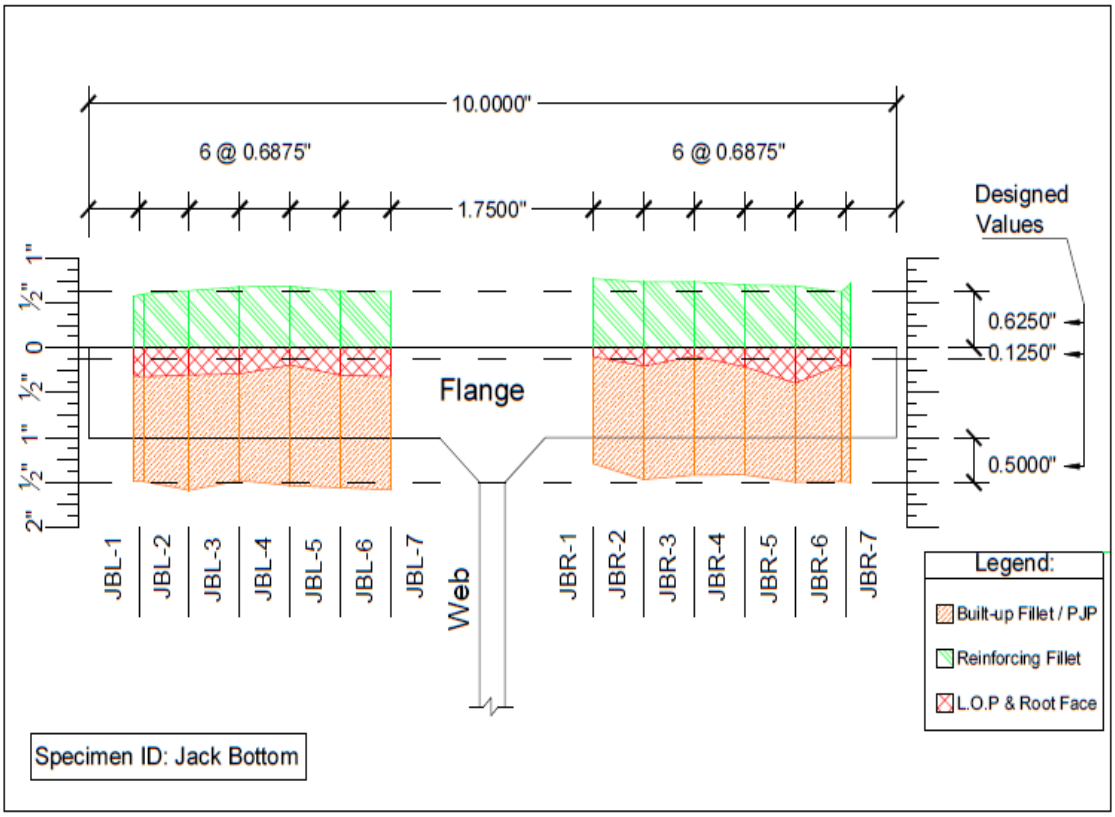

Figure 66. JB- Cross Sectional Weld PenetrationView

Table 16 and Figure 63 through Figure 66 provide good insight on the LOP, root face, and the length of the weld legs along the end-plate portion of our specimens. However, the destructive process implemented to obtain these dimensions cannot be performed in production. A non-destructive quality control methodology is needed in actual production. In production a certified weld inspector examines and passes judgment on the welds.

5.3.1.2. Theoretical Weld Throats

To complement the cross-sectional analysis a certified weld inspector measured the fillet sizes of the flange to end-plate welds using fillet measuring gauges. For convenience measurements were taken at each cross sectional cut. Four measurements were taken at each cut. Measurements of the following were taken:

- The leg of the outside built-up PJP fillet weld running parallel to the end-plate (OE)
- The leg of the outside built-up PJP fillet weld running parallel to the flange (OF)
- The leg of the inside reinforcing fillet weld running parallel to the end-plate (IE)
- The leg of the inside reinforcing fillet weld running parallel to the flange (IF)

Tables of each fillet leg size can be found in appendix E though H. The average of each flange dimensions, the designed values, and a comparison between the actual values divided design can be seen below in Table 18. Figure 67 shows a typical diagram of the fillets' legs and the accompanying labeling system used by Table 18 and the tables in Appendix E – H.

Table 18. Averaged Fillet Sizes of Flange to End-plate Welds Measured from Gauges

Specimen ID:	Outside (Groove Side)		Inside	
	Flange Side (OF)	End-plate Side (OE)	Flange Side (IF)	End-plate Side (IE)
Designed Vals. (in.)	**0.5000**	**0.5000**	**0.6250**	**0.6250**
Jack Bottom	0.9196	0.5268	0.9554	0.6161
Actual/Design (in.)	**1.839**	**1.054**	**1.529**	**0.986**
Jack Top	0.9375	0.5000	0.9420	0.6607
Actual/Design (in.)	**1.875**	**1.000**	**1.507**	**1.057**
King Bottom	0.8795	0.4955	0.8661	0.6607
Actual/Design (in.)	**1.759**	**0.991**	**1.386**	**1.057**
King Top	0.8929	0.5179	0.8304	0.6429
Actual/Design (in.)	**1.786**	**1.036**	**1.329**	**1.029**
Total Avg. Actual/Design	**1.814**	**1.020**	**1.4375**	**1.032**

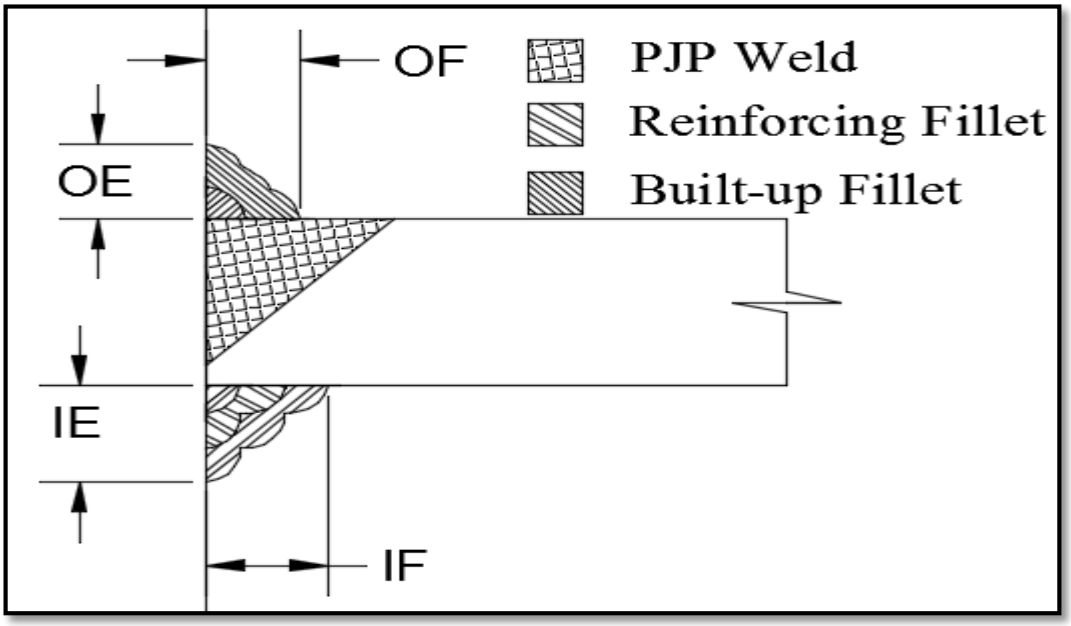

Figure 67. Labeling System for the Measured Fillets

As it can be seen in Table 18 the welds made on the flanges' surfaces (OF & OE), ranged from 32 to 83% larger than the engineering design. This increase in weld size impacted the strength of the test specimen's flange to end-plate connections above the engineering design value. These strengths can be seen in Table 19, and will be discussed later. While the implementation of oversized welds in industry is typically not an issue, when testing designs, actual structures should be as close to the designed values as possible. The strength of our sliced welds will serve as a reference for the development of design criteria for these connections. If the welds made on our specimen are over or under the initial engineered designed value this must be accounted for in our design analysis. Consequently this new measured value will become the "new" design value in the design of these connections.

5.3.2. Examination of Flange to End-plate's Connections Strength

As mentioned, it is important to solve for the actual strength of our test specimens' flange to end-plate connection. The true flange to end-plate strengths was obtained by measuring the effective throats of our demand critical welds, T_{fo}, and $T_{fi,}$ the throat of the outside and inside welds. These values were obtained from slicing open our welds measuring the shortest effective weld throat. These averaged throat lengths can be seen in Table 16. T_{fo} and T_{fi} are multiplied by design equations to give the strength of each welds, R_{not}, and R_{nit}. The strength of the outside flange weld (R_{not}) and the strength of the inside flange weld (R_{nit}) sum to the total strength of the flange weld (R_{nt}). The total strength of the flange welds can be seen in equation E9.0.

$$R_{nt} = R_{not} + R_{nit} \qquad \text{[E9.0]}$$

$R_{nt} = Total\ Strength\ of\ Flange\ Weld, Detirmined\ from\ Measured\ Throats$

$R_{not} = Strength\ of\ PJP\ \&\ Built - up\ Fillet, Detirmined\ \ from\ Measured\ Throats$
$R_{nit} = Strength\ of\ Fillet\ Weld\ Fillet, Detirmined\ from\ Measured\ Throats$

The strength of the individual flange welds needs to be solved for. This is done by solving for the strength of the weld on the outside of the flange (R_{not}) and the strength of the welds on the inside of the flange (R_{nit}). The equations used to solve for these strengths were in accordance with the *AISC's 14th Edition of the Steel Construction Manual* (2012) for weld design. The equations for these welds' strengths are as follows:

$$R_{not} = .6 * F_{EXX} * T_{fo} * L \qquad \text{[E10.0]}$$

$R_{not} = Strength\ of\ PJP\ \&\ Built - up\ Fillet\ Detirmined\ from\ Measured\ Throat$
$F_{EXX} = Strength\ of\ Weld\ Electrode$
$T_{fo} = Length\ of\ Outside\ Weld's\ Effictive\ Throat$
$L = Length\ of\ Weld\ Along\ Width\ of\ Flange$

$$R_{nit} = .6 * F_{EXX} * T_{fi} * L \ \ * F_{SF} \qquad \text{[E11.0]}$$

$R_{nit} = Strength\ of\ Fillet\ Weld\ Fillet\ Detirmined\ from\ Measured\ Throat$
$T_{fi} = Length\ of\ Inside\ Weld's\ Effictive\ Throat$
F_{SF}= *1.5 Strength Factor Increase for Transversely Loaded Fillet Welds*

The strength of each flange to end-plate connection was calculated using the averaged shortest effective throat (directly measured weld throats), these strength values can be found in Table 19. These design values made use of the weld slices. Since these weld throats values are a direct measurement they give the true design strength of these welds. It should be stated that while these procedures give the true strength of our welds this destructive testing is not practical in industry. Since in industry welds will not be cut open and examined, it was deemed prudent that an approximate strength of our

welds would be calculated using the average fillet sizes from Table 18. Using known initial values (groove size), the measured fillets after the welds were completed, and design equations E4.0, E5.0, E6.0, the strengths were calculated. These design equations use the fillet welds measured leg sizes and calculate the shortest effective throat of each weld. However there is a big assumption made when calculating the weld's strength this way. This assumption is that the root face and LOP values are true engineering design value. Using these values the strength of each flange to end-plate connection that was calculated using fillet measuring gauges can be seen in Table 19. In Table 19 the following will be examined:

- Initial design strength
- Strength determined from measuring fillet sizes after welding using fillet measuring gauges
- Strength determined from cutting the connection and measuring the effective throat

Table 19 highlights the difference between the calculated strengths of the welds as determine by directly measuring the weld throats to that of production inspection values (theoretical weld throats). Table 20 shows the ratio of the strength calculated from directly measuring the effective throat divided by the initial design strength.

Table 19. Averaged Strengths of Flange to End-plate Welds

Avg.	Means of Calculating Strength:	Strength of Inside Flanges (Kips)	Strength of Outside Flanges (Kips)	Total Strength (Kips)
	Designed Vals.	269.68	423.26	692.95
Jack Bottom	Strength from Measured Fillets*	315.99	510.87	826.86
	Strength from Measured Throats **	289.60	443.35	732.95
Jack Top	Strength from Measured Fillets*	330.13	509.56	839.69
	Strength from Measured Throats **	308.92	397.94	706.86
King Bottom	Strength from Measured Fillets*	320.60	501.50	822.10
	Strength from Measured Throats **	321.11	379.65	700.76
King Top	Strength from Measured Fillets*	310.24	506.04	816.28
	Strength from Measured Throats **	318.91	396.26	715.17
Avg.	Strength from Measured Fillets*	319.24	506.99	826.23
	Strength from Measured Throats **	309.64	404.30	713.94

* Values taken from certified welding inspector's fillet gauge measurements (Figure 67)
** Values taken from cross sectional cuts T_{fo}, and T_{fi} (Figure 62)

Table 20. True Strength (Measured Throat) / Design Strength of Flange to End-plate Welds

Measured Throat Strength / Design Strength			
Location:	Inside Flange	Outside Flange	Total
Jack Bottom	1.07	1.05	1.06
Jack Top	1.15	0.94	1.02
King Bottom	1.19	0.9	1.01
King Top	1.18	0.94	1.03
Avg.	1.15	0.96	1.03

5.3.3. Discussion of Fillet Welds

Referencing Table 16 through Table 20 and Figure 63 through Figure 66 a few statements can be made. On average the fillet's legs on the end-plate side of the flange to end-plate welds are very close to engineered values. However the legs of the fillet welds along the flanges are consistently larger than the requested design. The fillet's leg along the flange on the grooved side of the weld ranged from 76% to 88% larger than engineered. The fillet's leg along the flange on the non-grooved side of the weld ranged from 38% to 53% larger than engineered. While these values are considerably larger than the engineered values, the strength's obtained from measuring the throat of the welds is close to that of the design value. This can be seen by the measured throat to design ratio in Table 20. These ratios ranged from 0.90 to 1.10 while the total strength's ratios of the welded connection ranged from 1.01 to 1.06. This can be accounted to the facts that a large LOP and a larger than designed root face were present in our welds, this will be examined and discussed in further detail later. It cannot be ignored that welds made on the flange portion of the connection are consistently larger than called out. Also it is worth noting that if these welds were inspected by using the fillet weld size (assumed strength from gauge measured fillets), these welds would have a design strength almost 25% larger than initially engineered, which is not the case. This highlights the significance LOP and root face sizes effect design strength.

After testing was completed a discussion was had with the welder who made these welds. It was discovered that he tried to build up the weld along the end-plate, which required him to typically lay half an inch of extra material to build up enough

weld metal to get the desired leg on the end-plate portion of the weld. Thus explaining the higher than expected size of the welds along the flanges.

5.3.4. Discussion of Root Face and LOP

The effects of the LOP and root face had on the strength of our connections was significant. The root face and LOP are easily discernable when looking at the cross sectional cuts of our welds, see Figure 61. The root face of our specimens, ranged from 36 to 98% larger than engineered. On average the LOP was 0.140 inches, where it was engineered to be zero.

This unfused portion of the weld is essentially an un-propagated crack in the weld. A brief discussion on crack propagation will be presented to assess the effect this larger than designed weld flaw will have on the stress of the tip of the weld flaw. In Figure 68, Schreurs (2012) illustrates an elliptical hole with a uniform stress (σ) being applied perpendicular to the length of the ellipse. The applied stress (σ), causes a magnified stress to occur at the tips of the ellipse $\sigma_{yy.}$ This magnified stress is a factor of the applied stress (σ), the length of the ellipse (a), and the radius of the ellipse (ρ). The length (crack length) and radius of the ellipse (crack tip radius) control the magnification of the stress at the ellipse's tip.

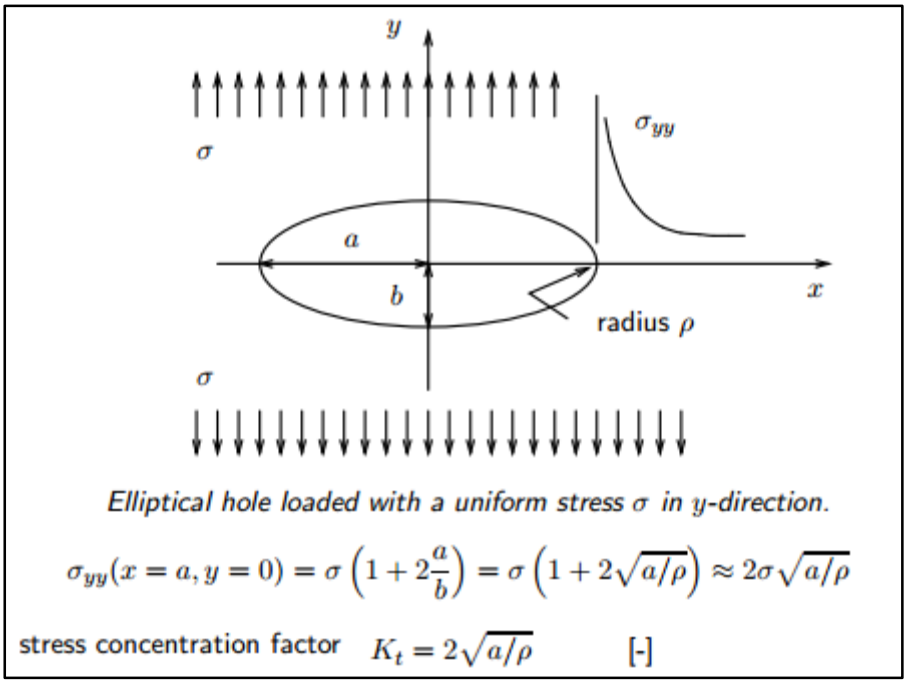

Figure 68. Stress at Crack's Tip (Schreurs, 2012)

The findings from the experimental investigation show that the LOP and root face were 2.2 times large than the designed value. Meaning the initial flaw in the weld was larger than anticipated. Figure 68 shows us that the longer the unfused flaw become (a), the higher the stresses become at the tip of the unfused portion. For our experiment, this means the stresses at the unfused portion tip was larger than the anticipated by design. In production, the presence of a 2x stress concentration would be undesirable, however our experimental testing revealed little degradation in performance. . Our results provide confidence that if original design values are implemented in further production that the weld metal should be strong enough to resist the high stress concentration at the unfused portions tip.

Beveling plates is something that is readily controllable. This typically should affect the strength of the welds less than other welding parameters. This is because

beveled joints are easy to inspect. Typically the root face should be held to some tolerance. If this required value is not met it should be corrected before the welding process is allowed to be completed. However in our rafter this was not the case. This can be seen in Figure 62 in which the bevel is actually curved which left our specimen with oversized root faces. The over sizing of these test specimen's root faces significantly impacted strength. As long as care is taken during the beveling and fit up process concerns about significant increase to the size of the root face should be alleviated. It is suggested that for PJP welds some amount of quality control should be implemented when beveling plates. For instance when a plate is beveled for a determined root face this should be compared to a nominal plate thickness of the desired root face dimension. If the root face is wider than the plate's thickness these spots should be marked and fixed until the designed root face is achieved.

Based on the measured LOP in our test specimens, it seems that the feasibility of depositing weld metal perfectly into the root of the welds on a 45° bevel with a GMAW is not practical. Our understanding is that deposition of weld metal into the root due to the poor bevel process was the main culprit for LOP in PJP connections. The *AISC's 14th Edition of the Steel Construction Manual* (2012) on prequalified welded joints for partial joint penetration groove welds states that 45° PJP groove welds made in the overhead and vertical welding position receive an eighth of an inch reduction from effective throat length. However welds made in the flat and horizontal position are not subject to this reduction. When examining the welding position used on the flange to end-plate connection of our test specimen they were made in the flat position and therefore were designed with no reduction to effective throat.

It can be seen from our cross section cuts of the flange to end-plate connections, photos like Figure 62, that there is significant LOP present in our welds. Other good examples can be viewed in Appendix E though H. The reduction of an extra eighth of an inch regardless of welding position might be a good design practice for all 45° PJP groove welds. As long as this additional eighth inch section is removed from our PJP weld design the assumed LOP should be conservative in nature. This should relieve concerns about LOP due to workmanship and fabrication.

5.3.5. Discussion of Size Effects on Connection

This study examined one inch flanges with a seven-eighths inch groove at a 45° angle. That means the root face makes up twelve and a half percent of the thickness of the flange. However if the prequalification of this modified PJP connection is used on flanges of lesser thickness, concerns arise when the size of the root face becomes a significant percentage of the total flanges thickness. It is for this reason that root faces shall be limited in size. The root face used in built-up welds shall be limited to twelve and a half percent of the thickness of the flange. While this may be conservative in nature this study only considered one root face size. This may change if an array of testing is completed on the size effect of the root face.

5.3.6. Final Remarks on Connection Performance

During cyclic testing the flanges yielded and the LOP/root face inside the welds did not propagate a crack. This shows how well the weld metal absorbs energy. The use of highly tough and ductile weld metal alleviates concerns about the strength of the weld. Since the major changes to the design criteria for steel connections following the 1995 Northridge Earthquakes, brittle failure of high toughness electrode material such

as this one would be highly uncharacteristic. Finally since there is more metal at this flange to end-plate connection when compared to the flange, this means the force can be distributed over this larger area. In distributing these forces over a larger area the stress over this location decreases.

6. Summary and Conclusions

The 6 bolt extended multiple-row moment end-plate connection with modified PJP welds were tested to investigate the strength of the connection and the modified PJP weld used on the connection. Below is a summary of our findings from the research:

1. It is recommend that a quality control check of the root face be implemented, in doing so the root face should be equal to or smaller than the designed value before welding is completed.
2. When considering effects of LOP:
    - It is recommended that an extra eighth of an inch be subtracted, during design, from the effective throat of the grooved side of the modified PJP connection for any LOP that may be present or
    - It is recommended that after the reinforcing fillet on the inside of the flange is made, this should be brushed before the built-up PJP weld is made.
3. The 6-bolt extended multiple-row moment end-plate connection with modified PJP welds were tested to investigate the strength of the modified PJP weld, and in turn passed all the needed criteria to prequalify this modified PJP weld for use as demand critical welds in IMFs and less stringent frame types, if the following conditions are met:
    - Modified PJP welds are designed for **six percent larger** than expected flexural strength of the beam per the *2010 AISC Seismic Provision.*
    - The root face should be **12.5% or less of the flange thickness.**

- Thick end-plate condition are observed and should be **37% larger than the minimum required** end-plate thickness per the *AISC End-plate Design Guides.*
- Unstiffened column flange thickness should be **42% larger than the minimum required column** flange thickness per the *AISC End-plate Design Guides.*

4. While no specimen failed from weld cracking it is extremely important that care be taken in the preparation, and welding of the joint.

7. Further PJP Weld Design Considerations / Recommendations

While this round of testing achieved prequalification of the use of PJP welds on IMF demand critical connection there are still a couple concerns with implementation of PJP welds. First, the true design strength of the modified PJP connection needs to be examined. Others research resulted in the implementation of liberal design equations and liberal effective throats, which is understandable considering the AISC's design equation for PJP welds were developed in the early 60s. However this research only examined a few gauges of metal. An extensive array and a larger number of samples must be examined before a true design strength can be proposed. Finally, the potential size effects of these welds needs to be examined before varying root faces and varying depths of penetration are implemented. Having mentioned these items, it is noteworthy to say that the conditions implemented in this testing was favorable and there is no reason why PJP welds should be restricted in use.

References:

AISC Committee on Specifications. *Seismic Provisions for Structural Steel Buildings*. Vol. 1. Chicago, 2010. pp. 402. Print.

AISC's Steel Construction Manual. 14th ed. Chicago. pp. 16-1 399., 2012. Print.

Azuma, Koji, Yoshiaki Kurobane, and Yuji Makino. "Cyclic Testing of Beam-to-Column Connections with Weld Defects and Assessment of Safety of Numerically Modeled Connections from Brittle Fracture." *Engineering Structures* 22.12 (2000): pp. 1596–1608. *ScienceDirect*. Web. 25 Feb. 2015.

Bond, D.E. and Murray, T.M. "Analytical and Experimental Investigation of a Flush Moment End-Plate Connection with Six Bolts at the Tension Flange," *Research Report No.CE/VPI-ST-89/10*, Dept, of Civil Engineering, Virginia Polytechnic Institute and State University, Blacksburg, VA. (1989)

Chen, Yiyi, and Sufang Wang. "Research on End-Plate Connection with Non-Completely Penetrated Welds." *Journal of Constructional Steel Research* 65.1 (2009): pp. 228–236. *ScienceDirect*. Web. 25 Feb. 2015.

Disque, R.O. "End-Plate Connections," *National Engineering Conference Proceedings* Disque, R.O. (1962) "End-Plate Connections," National Engineering Conference Proceedings (1962): pp. 30-37. Print.

Dubina, D, and A Stratan. "Behavior of Welded Connections of Moment Resisting Frames Beam-to-Column Joints." *Engineering Structures* 24.11 (2002): pp. 1431–1440. *ScienceDirect*. Web. 17 Feb. 2015.

"Effect of Local Details on Ductility of Welded Moment Connections." *Journal of Structural Engineering* 127.9 (2001): pp. 1036–1044. *ASCE*. Web. 18 Feb. 2015.

Federal Energency Management Agency. *Recommended Seismic Design Criteria foNew Steel Moment-Frame Buildings, FEMA-350*. SAC, 2000. Text.

Gagnon, Darrel P., and D. J. Laurie Kennedy. "Behavior and Ultimate Tensile Strength of Partial Joint Penetration Groove Welds." *Canadian Journal of Civil Engineering* 16.3 (1989): pp. 384–399. *NRC Research Press*. Web. 23 Feb. 2015.

Gomez, Ivan Ricardo. "Behavior and Design of Column Base Connections." Ph.D. University of California, Davis, 2010. *ProQuest*. Web. 26 Feb. 2015.

Kennedy, N.A., S. Vinnakota, and A.N. Shelbourne. "Yield-Line Analysis of End-Plate Connections With Bolt Force Predictions." *Proceedings of the International Conference on Joints in Structural Steelwork* (1981): pp. 2.138-.157. Print.

Kukreti, A. R., and R. Prasad. “Hysteretic Behavior Prediction of Full and Partial Penetration Transverse Groove Welded Joints.” *Computers & Structures* 59.1 (1996): pp. 1–11. *ScienceDirect*. Web. 25 Feb. 2015.

Kurobane, Yoshiaki, Koji Azuma and Yuji Makino. "Applicability of PJP Groove welding to Beam-Column Connection Under Seismic Loading." *Connection is Steel Structures V* (2004): pp. 367-380.

Mao, Changshi, James Ricles, Le-Wu Lu, and John Fisher. "Effect of Local Details on Ductility of Welded Moment Connections." *Journal of Structural Engineering*. 127th ed. Vol. 2001. pp. 1033-1044. Print.

McCormac, Jack C., and Stephen F. Csernak. *Structural Steel Design*. Boston: Prentice Hall, 2012. pp. 478. Print.

Meng, R. L. and Murray, T. M., “Seismic performance of Bolted end-Plate Moment Connections.” *Proceedings of, AISC National Steel Construction Conference* (1997), pp. 7-9, 30-1 to 30-14. Print

Miazga, Gregory S., and D. J. Laurie Kennedy. “Behaviour of Fillet Welds as a Function of the Angle of Loading.” *Canadian Journal of Civil Engineering* 16.4 (1989): pp. 583–599. *NRC Research Press*. Web. 17 Feb. 2015.

Murray, Thomas M. “Recent Developments for the Design of Moment End-Plate Connections.” *Journal of Constructional Steel Research* 10 (1988): pp. 133–162. *ScienceDirect*. Web. 26 Feb. 2015.

Murray, T. M. *AISC Design Guide Series 4, Extended End-Plate Moment Connections,* American Institute of Steel Construction, Chicago. (1990)

Murray, Thomas, and Emmet Summner. *Extended End-Plate Moment Connections, Design Guide 4*. 2nd ed. Chicago, Ill.: American Institute of Steel Construction, 2003. pp. 158. Print.

Murray, Thomas, and W. Lee Shoemaker. *Flush and Extended Multiple-Row Moment End-Plate Connections , Design Guide 16*. Chicago, Ill.: American Institute of Steel Construction, 2002. Print.

Myers, A. T. et al. “Effect of Weld Details on the Ductility of Steel Column Baseplate Connections.” *Journal of Constructional Steel Research* 65.6 (2009): pp. 1366–1373. *ScienceDirect*. Web. 17 Feb. 2015.

Ricles, J.M., J.W. Fisher, Le-Wu Lu, and E.J. Kaufmann. "Development of Improved Weld Moment Connections for Earthquake-Resisting Design." *Journal of Construction Steel Research* 58 (2002): pp. 565-604. Print.

Schreurs, P.J. G., Dr. "Fracture Mechanics." Fracture Mechanics (2012): n.p. 6 Sept. 2012. Web. 3 May 2016.

Sato, Atsushi, James D. Newell and Chia-Ming Uang. "Cyclic Behavior and Seismic Design of Bolted Flange Plate Steel Moment Connection." *Engineering Journal* (2008): pp. 221-232.

SATOH, Kunihiko et al. “Experimental Study on the Mechanical Behavior and the Tensile Strength of Partial Penetration Groove Welded Joint.” *Transactions of the Japan Welding Society* 5.2 (1974): pp. 198–206. Print.

Shaw, Sean Michael. “Seismic Performance of Partial Joint Penetration Welds in Steel Moment Resisting Frames.” Ph.D. University of California, Davis, 2013. *ProQuest*. Web. 17 Feb. 2015.

Srouji, R., A.R. Kukreti, and T.M. Murray. "Yield-Line Analysis of End-Plate Connections With Bolt Force Predictions,." *Research Report FSEL/MBMA*(1983): pp. 83-105. Print

Sumner, Emmett A. Unified Design of Extended End-Plate Moment Connections Subject to Cyclic Loading. Diss. Virginia Polytechnic Institute and State U, 2003.: n.p., n.d. Print.

Appendix A – Design Calculations
A.1 – Test Specimen Design

CALCULATED STRENGTHS

CONNECTION: Six-Bolt Extended Unstiffened Moment End-Plate Connection 44B1016E w/12 in End-Plate

DATE: July 20,2015 — Dennis P. Watson

Modifed: Aug 11,2015 — Samuel Sherry

Specified Grade for: Flange and Web = ASTM A572, Grade 50
End-Plate = ASTM A36, Grade 36

$\phi_p := 0.75$ $\phi_b := 0.90$ $E := 29000 \cdot ksi$

MEASURED PROPERTIES-BEAM

$F_{uspec} := 65 \cdot ksi$ $F_{yspec} := 50 \cdot ksi$

$d := 44.00 \cdot in$ $t_p := 2.00 \cdot in$ $p_{fo} := 4.00 \cdot in$ $d_e := 2.00 \cdot in$

$b_{fb} := 10.00 \cdot in$ $F_{yf} := 62.5 \cdot ksi$ $b_p := 12.00 \cdot in$ $p_{fi} := 4.00 \cdot in$ $p_b := 4.00 \cdot in$

$t_{fb} := 1.00 \cdot in$ $F_{uf} := 79 \cdot ksi$ $L_p := 70.0 \cdot in$ $gage := 5.50 \cdot in$

$k_{1b} := 0.50 \cdot in$ $F_{yw} := 78 \cdot ksi$ $F_{yp} := 50.5 \cdot ksi$ $h_w := d - 2 \cdot t_{fb}$

$t_w := 0.3125 \cdot in$ $F_{uw} := 80.0 \cdot ksi$ $F_{up} := 72.0 \cdot ksi$

$k_c := \frac{4}{\sqrt{\frac{h_w}{t_w}}}$ $k_c = 0.3$

CALCULATED PROPERTIES

$s_{dim} := \frac{1}{2} \cdot \sqrt{b_p \cdot gage}$ $s_{dim} = 4.1 \cdot in$ $p_{ext} := d_e + p_{fo}$

Higher Plate Strength when d_e greater than s_{dim}. $d_e = 2 \cdot in$ $s_{dim} = 4.1 \cdot in$

PROPERTIES OF COLUMN

36B1232I

$d_c := 38 \cdot in$ $k_{fillet} := 0.50 \cdot in$

Assume stiffener plate thickness:

For flange, use Fy and Fu of end-plate.

$t_{wc} := 0.75 \cdot in$ $F_{yc} := 55.0 \cdot ksi$

$b_{fc} := 12.0 \cdot in$ $F_{uc} := 70.0 \cdot ksi$ $k_{1c} := 0.5 \cdot in$

$t_{fc} := t_p$ $Z_{xc} := b_{fc} \cdot t_{fc} \cdot (d_c - t_{fc}) + \frac{1}{4} \cdot t_{wc} \cdot (d_c - 2 \cdot t_{fc})^2$ $Z_{xc} = 1080.7 \cdot in^3$

$t_{fc} = 2 \cdot in$ $h_c := d_c - 2 \cdot t_{fc}$ $h_c = 34 \cdot in$

$phiR_v := 0.9 \cdot 0.6 \cdot F_{yc} \cdot d_c \cdot t_{wc}$

$phiR_v = 846.5 \cdot kip$ 1

SPECIFIED PROPERTIES OF BOLTS

$d_b := 1.375 \cdot in$ $\quad F_{t325} := 90 \cdot ksi$ $\quad F_{t490} := 113 \cdot ksi$

$R_y := 1.1$ $\quad P_t := \frac{\pi \cdot d_b^2 \cdot F_{t490}}{4}$ $\quad P_t = 167.8 \cdot kip$

BEAM YIELD STRENGTH using Assumed Fy, Mp

Solve for Ixx of each area of section using .xls

$Ixx_{Flange} := 4623.33 \cdot in^4$ $\quad Ixx_{Web} := 1929.375 in^4$

$Sxx_{Flanges} := \frac{(Ixx_{Flange} \cdot 2)}{22 \cdot in}$ $\quad Sxx_{Web} := \frac{(Ixx_{Web})}{21 \cdot in}$

$Sxx_{Flanges} = 420.3 \cdot in^3$ $\quad Sxx_{Web} = 91.9 \cdot in^3$

$Mp_e := Sxx_{Flanges} \cdot F_{yspec} + Sxx_{Web} \cdot F_{yspec}$ $\quad Mp_e = 2134.1 \cdot kip \cdot ft$

BEAM Expected Flexural STRENGTH @ Hinge, assumed Fy & AISC 2010 Seismic Provision

$Z_x := b_{fb} \cdot t_{fb} \cdot (d - t_{fb}) + \frac{1}{4} \cdot t_w \cdot (d - 2 \cdot t_{fb})^2$ $\quad Z_x = 567.8 \cdot in^3$

$Mp_{AISC2010} := (Z_x \cdot F_{yspec}) \cdot (R_y)$ $\quad Mp_{AISC2010} = 2602.5 \cdot kip \cdot ft$

Estimate Location of Plastic Hinge

$L_{pdim} := \min\left(\frac{d}{2}, 3 \cdot b_{fb}\right)$ $\quad L_{pdim} = 22 \cdot in$

Moment at the face of the column. (Connection design moment.)

Assume Test Ram Force Applied at 18'-4" from Col. Face

$V_u := \frac{Mp_{AISC2010}}{18.34 \cdot ft}$ $\quad V_u = 141.9 \cdot kip$

$M_{uc} := Mp_{AISC2010} + V_u \cdot L_{pdim}$

$M_{uc} = 2862.6 \cdot kip \cdot ft$

2

BEAM MOMENT STRENGTH, Mb, Check Element Slenderness, AISC Table B4.1b

$\frac{b_{fb}}{2 \cdot t_{fb}} = 5$ $\quad 0.38 \cdot \sqrt{\frac{E}{F_{yspec}}} = 9.2$ $\quad \sqrt{\frac{E}{F_{yspec}}} = 24.1$ $\quad$ Flange is compact.

$\frac{h_w}{t_w} = 134.4$ $\quad 3.76 \cdot \sqrt{\frac{E}{F_{yspec}}} = 90.6$ $\quad 5.7 \cdot \sqrt{\frac{E}{F_{yspec}}} = 137.3$ $\quad$ Web is noncompact.

BEAM SECTION PROPERTIES

$I_x := 2 \cdot t_{fb} \cdot b_{fb} \cdot \left(\frac{d}{2} - \frac{t_{fb}}{2}\right)^2 + \frac{1}{12} \cdot t_w \cdot h_w^3$ $\quad I_x = 11174.4 \cdot in^4$ $\quad S_x := \frac{I_x}{0.5 \cdot d}$ $\quad S_x = 507.9 \cdot in^3$

$a_r := \frac{h_w \cdot t_w}{b_{fb} \cdot t_{fb}}$ $\quad m := \frac{55}{55}$ $\quad R_e := \frac{12 + a_r \cdot (3 \cdot m - m^3)}{12 + 2 \cdot a_r}$ $\quad R_e = 1$

BEAM MOMENT STRENGTH, Mb (CONT'D)

$I_T := \frac{1}{12} \cdot \left(\frac{0.5 \cdot d}{3}\right) \cdot t_w^3 + \frac{1}{12} \cdot t_{fb} \cdot b_{fb}^3$ $\quad I_T = 83.4 \cdot in^4$

$A_T := \left(\frac{0.5 \cdot d}{3}\right) \cdot t_w + t_{fb} \cdot b_{fb}$ $\quad A_T = 12.3 \cdot in^2$ $\quad r_T := \sqrt{\frac{I_T}{A_T}}$ $\quad r_T = 2.6 \cdot in$

Required L_b: $\quad L_b := 40.4 \cdot r_T$ $\quad L_b = 8.8\,ft$

If the unbraced length is less than L_b: $\quad F_{cr} := F_{yf}$

$R_{PG} := 1 - \left(\frac{a_r}{1200 + 300 \cdot a_r}\right) \cdot \left(\frac{h_w}{t_w} - 5.7 \cdot \sqrt{\frac{29000 \cdot ksi}{F_{cr}}}\right)$ $\quad R_{PG} = 1$

$M_b := S_x \cdot R_{PG} \cdot R_e \cdot F_{cr}$ $\quad M_b = 2620.1 \cdot kip \cdot ft$

END-PLATE STRENGTH, Mpl

$d_0 := d - \frac{t_{fb}}{2} + p_{fo}$ $\quad d_0 = 47.5 \cdot in$ $\quad h_0 := d_0 + \frac{t_{fb}}{2}$ $\quad h_0 = 48 \cdot in$

$d_1 := d - \frac{t_{fb}}{2} - t_{fb} - p_{fi}$ $\quad d_1 = 38.5 \cdot in$ $\quad h_1 := d_1 + \frac{t_{fb}}{2}$ $\quad h_1 = 39 \cdot in$

$d_2 := d - \frac{t_{fb}}{2} - t_{fb} - p_{fi} - p_b$ $\quad d_2 = 34.5 \cdot in$ $\quad h_2 := d_2 + \frac{t_{fb}}{2}$ $\quad h_2 = 35 \cdot in$

$s_{dim} = 4.1 \cdot in$

Higher Plate Strength when d_e greater than s_{dim}. $\quad d_e = 2 \cdot in$ $\quad s_{dim} = 4.1 \cdot in$

FOR SIX BOLT EXTENDED END-PLATE
AISC DG 16, p. 35 same as PhD Dissertation, Ron Meng, 2003, p. 85.

Note : Use $p_{fi} = s$, if $p_{fi} > s$ $\quad p_{fimin} := \min(s_{dim}, p_{fi})$ $\quad p_{fimin} = 4 \cdot in$

$$Y := \frac{b_p}{2} \cdot \left[h_1 \cdot \left(\frac{1}{p_{fimin}} \right) + h_2 \cdot \left(\frac{1}{s_{dim}} \right) + h_0 \cdot \left(\frac{1}{p_{fo}} \right) - \frac{1}{2} \right] \ldots$$
$$+ \frac{2}{gage} \cdot \left[h_1 \cdot \left(p_{fimin} + \frac{3p_b}{4} \right) + h_2 \cdot \left(s_{dim} + \frac{p_b}{4} \right) \right] + \frac{gage}{2}$$

$Y = 345.6 \cdot in$

$M_{PL} := t_p^{\,2} \cdot F_{yp} \cdot Y$ $\quad M_{PL} = 5818.4 \cdot kip \cdot ft$

BOLT STRENGTH WITHOUT PRYING, Mnp

$M_{NP} := 2 \cdot P_t \cdot (d_0 + d_1 + d_2)$ $\quad M_{NP} = 3369.8 \cdot kip \cdot ft$

COLUMN SIDE

For Stiffened Column Flange

$s_c := \frac{1}{2} \cdot \sqrt{b_{fc} \cdot gage}$ $\quad s_c = 4.1 \cdot in$ $\quad p_{si} := p_{fi}$ $\quad p_{so} := p_{fo}$

$$Y_c := \frac{b_{fc}}{2} \cdot \left[h_1 \cdot \left(\frac{1}{p_{si}} \right) + h_2 \cdot \left(\frac{1}{s_c} \right) + h_0 \cdot \left(\frac{1}{p_{si}} \right) - \frac{1}{2} \right] \ldots + \frac{2}{gage} \cdot \left[h_1 \cdot \left(p_{si} + \frac{3p_b}{4} \right) + h_2 \cdot \left(s_c + \frac{p_b}{4} \right) \right] + \frac{gage}{2}$$

$Y_c = 345.6 \cdot in$

Determine Reduced Stiffened Column Flange Thickness.

$t_{fcreq} := \sqrt{\frac{1.11 \cdot \phi_p \cdot M_{NP}}{\phi_b \cdot F_{yc} \cdot Y_c}}$ $\quad t_{fcreq} = 1.403 \cdot in$ $\quad t_{fc} = 2 \cdot in$

Calculate Factored Beam Flange Force

$F_{fu} := \frac{M_{uc}}{(d - t_{fb})}$ $\quad F_{fu} = 878.8 \cdot kip$

Calculate Strength of Unstiffened Column Flange to Determine Stiffener Design Force

$phiM_{cf} := \phi_b \cdot F_{yc} \cdot Y_c \cdot t_{fc}^2$ $\quad phiM_{cf} = 68438.1 \cdot kip \cdot in$

$phiR_{nflg} := \frac{phiM_{cf}}{d - t_{fb}}$

$phiR_{nflg} = 1591.6 \cdot kip$ $\quad F_{fu} = 878.8 \cdot kip$

Calculate Local Web Yielding Strength

$C_t := 1.0$ Assume connection is not at top of column.

$k_{fillet} = 0.5 \cdot in$

$N_{dim} := t_{fb} + 2 \cdot k_{fillet}$ $N_{dim} = 2 \cdot in$

$phiR_{nyield} := C_t \cdot (6 \cdot k_{fillet} + N_{dim} + 2 \cdot t_p) \cdot F_{yc} \cdot t_{wc}$

$phiR_{nyield} = 371.3 \cdot kip$ $F_{fu} = 878.8 \cdot kip$ ***Column Stiffeners Required.***

Calculate Web Buckling Strength

$$phiR_{nbuck} := \frac{\phi_b \cdot 24 \cdot t_{wc}^3 \cdot \sqrt{E \cdot F_{yc}}}{h_c}$$

$phiR_{nbuck} = 338.5 \cdot kip$ $F_{fu} = 878.8 \cdot kip$ ***Column Stiffeners Required.***

Calculate Web Crippling Strength

$$phiR_{ncrip} := \phi_p \cdot 0.80 \cdot t_{wc}^2 \cdot \left[1 + 3 \cdot \left(\frac{N_{dim}}{d_c}\right) \cdot \left(\frac{t_{wc}}{t_{fc}}\right)^{1.5}\right] \cdot \sqrt{\frac{E \cdot F_{yc} \cdot t_{fc}}{t_{wc}}}$$

$phiR_{ncrip} = 721.3 \cdot kip$ $F_{fu} = 878.8 \cdot kip$ ***Column Stiffeners Required.***

Determine Column Stiffener Design Force

$F_{cu} := F_{fu} - \min(phiR_{nflg}, phiR_{nyield}, phiR_{nbuck}, phiR_{ncrip})$

$F_{cu} = 540.3 \cdot kip$

Calculate the Transverse Stiffener Force

Eq. 4.2-1 Required Transverse Strength of Web is:

$$t_{pmins} := \frac{F_{fu} - phiR_v}{0.9 \cdot 0.6 \cdot F_{yc} \cdot h_c}$$ $t_{pmins} = 0.032 \cdot in$ $t_{wc} = 0.75 \cdot in$

Design Transverse Stiffeners and Their Welds: $F_{ys} := F_{yp}$

Required area of stiffener:

$F_{cu} = 540.3 \cdot kip$ $\quad A_{sreq} := \frac{F_{cu}}{F_{yc}}$ $\quad A_{sreq} = 9.8 \cdot in^2$

Minimum Stiffener Width:

$b_{stiff} := Floor\left(\frac{b_{fc} - t_{wc}}{2}, 1.0 \cdot in\right)$ $\quad b_{stiff} = 5 \cdot in$

$b_{smin} := \frac{b_{fc}}{3} - \frac{t_{wc}}{2}$ $\quad b_{smin} = 3.6 \cdot in$

Stiffener Thickness, use larger of:

$\frac{t_p}{2} = 1 \cdot in$ and $b_{stiff} \cdot \frac{\sqrt{\frac{F_{yc}}{ksi}}}{95} = 0.4 \cdot in$

$t_{smin} := max\left(\frac{t_p}{2}, b_{stiff} \cdot \frac{\sqrt{\frac{F_{yc}}{ksi}}}{95}\right)$ $\quad t_{smin} = 1 \cdot in$

Stiffener Length:

$L_s := d_c - 2 \cdot t_{fc}$ $\quad L_s = 34 \cdot in$

Provided area of stiffeners:

$A_{sprov} := 2 \cdot b_{stiff} \cdot t_{smin}$ $\quad A_{sprov} = 10 \cdot in^2$

Check stiffener slenderness:

$maxslender := \frac{95}{\sqrt{\frac{F_{ys}}{ksi}}}$ $\quad maxslender = 13.4$ $\quad \frac{b_{stiff}}{t_{smin}} = 5$

Stiffener weld to column flange:

$P_{stiff} := F_{cu}$

$L_{wflg} := \left[\frac{b_{fc}}{2} - \left(k_{1c} + 0.25 \cdot in\right)\right] \cdot 4$ $\qquad L_{wflg} = 21 \cdot in$

$f_{wflg} := \frac{P_{stiff}}{L_{wflg}}$ $\qquad f_{wflg} = 25.7 \cdot \frac{kip}{in}$

$filletflg := \frac{f_{wflg}}{\left(\frac{70 \cdot ksi \cdot 0.30 \cdot 0.707 \cdot 1.5}{\frac{16}{in}}\right)}$ $\qquad filletflg = 18.5$ Use groove weld.

Stiffener weld to column web:

$P_{stiff} = 540.3 \cdot kip$

$L_{web} := \left[d_c - \left(k_{1c} + 0.25 \cdot in\right)\right] \cdot 4$ $\qquad L_{web} = 149 \cdot in$

$f_{wweb} := \frac{P_{stiff}}{L_{web}}$ $\qquad f_{wweb} = 3.6 \cdot \frac{kip}{in}$

$filletweb := \frac{f_{wweb}}{\left(\frac{70 \cdot ksi \cdot 0.30 \cdot 0.707}{\frac{16}{in}}\right)}$ $\qquad filletweb = 3.9$ Use 5/16 inch fillet NS and FS.

A.2 – Weld Design

CALCULATED STRENGTHS

For Built up PJP & Reinforcing Fillet at Flange to Endplate Connection

DATE: Aug. 13, 2015 Samuel T. Sherry

Specified Grade for: Flange and Web = ASTM A572, Grade 50
End-Plate = ASTM A36, Grade 36

WELD INFO:

$F_{yspec} := 50 \cdot ksi$ $F_{uspec} := 65 \cdot ksi$ $F_{Exx} := 70 \cdot ksi$ $E := 29000 \cdot ksi$

$Flg_t := 1 \cdot in$ $Rt_{Face} := .125 \cdot in$ $Fil_{built} := .5 \cdot in$ $Fil_{rein} := .625 \cdot in$ $Flg_w := 10 \cdot in$

$T_{web} := .3125 \cdot in$

CALCULATED PROPERTIES:

$P := Flg_t - Rt_{Face}$ $P = 0.875 \cdot in$

$Effective_{Throat} := \sqrt{\left(P^2 + Fil_{built}^{\ 2}\right)}$ $Effective_{Throat} = 1.0078 \cdot in$

Available Strenght of PJP & Built-up Fillet:

$Rno := .6 \cdot F_{Exx} \cdot Effective_{Throat} \cdot Flg_w$

$Rno = 423.3 \cdot kip$

Available Strenght of Reinforcing Fillet:

$Rni := .6 \cdot F_{Exx} \cdot (.707) \cdot Fil_{rein} \cdot 1.5\left(Flg_w - T_{web}\right)$

$Rni = 269.682 \cdot kip$

Strenght of Flange Welds:

$Rn := Rni + Rno$

$Rn = 692.95 \cdot kip$

1

Appendix B – Material Properties

Tested Metal Certificates & Data Sheets:

METALAB - McClure Engineering, Inc.

129 NW 132nd St. Oklahoma City, OK 73114
Main: 405-848-8378 • Fax: 405-848-8311 • Email: info@metalab-okc.com

Tensile Test Certificate

ASTM A370/ASTM E8-08, Rounded per ASTM E29-06b

Issued to: BC Steel 9900 NW 10th St. Okc, Ok 73127	Sample: Structural Steel Description: Specification: A370
Purchase Order: Verbal	Date Received: 6/17/2015 Date Issued: 7/01/2015 Lab No.: 1151040

Sample I.D. Structural Steel (Flat)		5/16" Sample	1/2" Sample
Test Sample Dimension (in.)	Width	0.499	0.498
	Thick	0.276	0.461
Ultimate Tensile (ksi)		80.0	78.5
Yield* (ksi)		78.0	64.0
Elongation (% in 2")		31	35
Reduction of Area (%)		---	---

*Determined at 0.2% offset.

Sample I.D. Structural Steel (Rounded)		1" Sample	2" Sample	Weld Tensile Sample (API 1104)
Test Sample Dimension (in.)	Dia.	0.499	0.498	0.496
	Dia. Final	0.266	0.314	0.244
Ultimate Tensile (ksi)		79.0	72.0	77.0
Yield* (ksi)		62.5	50.5	66.5
Elongation (% in 2")		32	31	33
Reduction of Area (%)		72	60	76

*Determined at 0.2% offset.

Douglas A. McClure, P.E.
Senior Metallurgical Engineer

METALAB - McClure Engineering, Inc.
129 NW 132nd St., Oklahoma City, OK 73114
Main: 405-848-8378 • Fax: 405-848-8311 • Email: info@metalab-okc.com

Charpy Impact Test Certificate

ASTM A370

Issued to: B&C Steel Buildings Dennis Watson 9900 NW. 10th St. Oklahoma City, OK 73127	Part Number: Structural Steel Weld Metal Heat Number: NG Specification: ASTM A370 / E23 CVN: (AWS D1.8 Annex A.)
B&C Steel P.O. No.: Verbal Min. (Full size): 17.93 ft/sec: Impact Velocity	Date Received: 6/17/2015 Date Issued: 7/22/2015 Lab No.: 1151040

Sample –Weld Metal(CVN) Longitudinal (-20°F)

(Five samples were tested; samples of highest and lowest "Energy Absorbed" results not reported according to Annex A/A7.)

Sample I.D.	Requirements	Sample 1	Sample 2	Sample 5
Width (in.)	0.391-0.397 (Full Size)	0.395	0.395	0.395
Depth (in.)	0.391-0.397	0.395	0.395	0.395
Notch Depth (in.)	0.079-0.081	0.079	0.079	0.079
Notch Radius (in.)	0.009-0.011	0.010	0.010	0.010
Temperature (°F)	-20	-20	-20	-20
Energy Absorbed (ft-lbs.)	Report	161	178	173
Lateral Expansion (in.)	Report	0.091	0.081	0.088
Percent Shear (%)	Report	80	80	80

Method: ASTM A370, Charpy Impact

Douglas A. McClure, P.E.
Principal Metallurgical Engineer

Appendix C – King End Plots & Photos

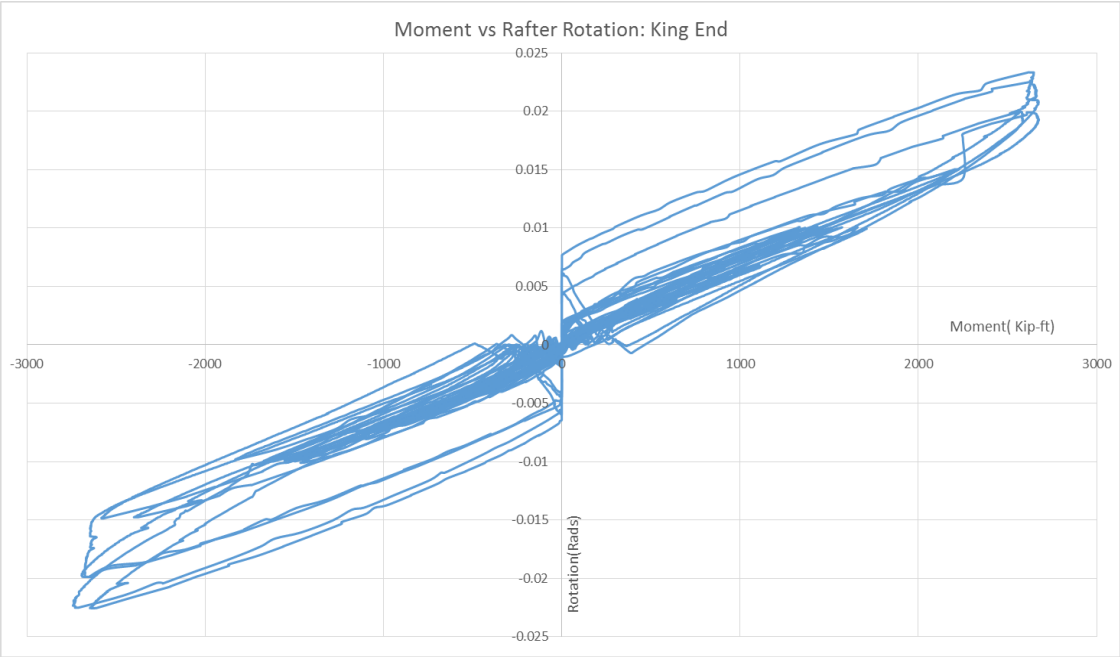

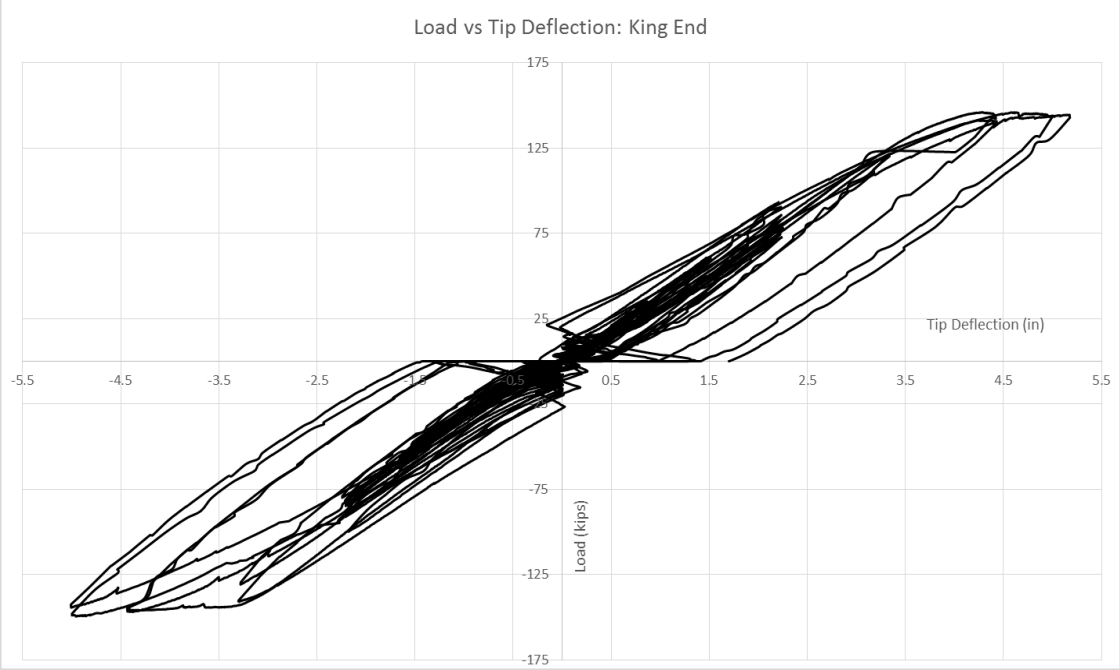

King End Prior to Testing:

West Flange Outside

King End 0.00375 radians:

No Discernable Changes

King End 0.005 radians:

No Discernable Changes

King End: End of Cycle 0.0075 radians:

King Flange Outside

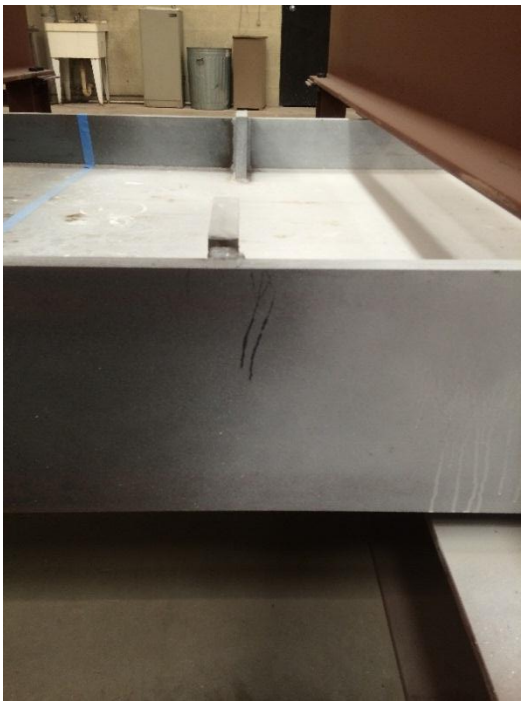

West Flange Outside @ Pick Point

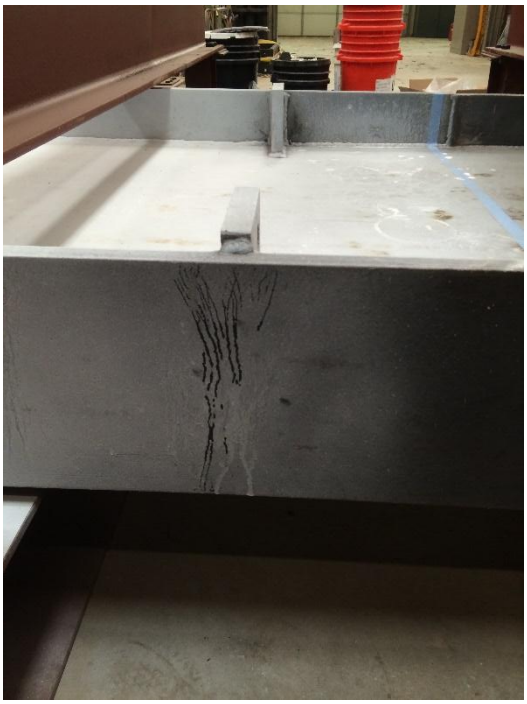

East Flange Outside @ Pick Point

King End: End of Cycle 0.01 radians

East Flange Inside

East Flange Outside

West Flange Inside

West Flange Outside

King End: End of Cycle 0.015 radians

East Flange Inside

East Flange Outside

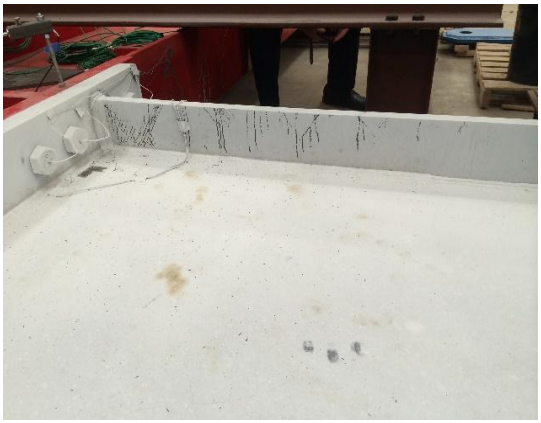

West Flange Inside

West Flange Outside

King End: End of Cycle 0.02 radians

East Flange Inside

East Flange Outside

West Flange Inside

West Flange Outside

King End: End of Cycle 0.0225 radians

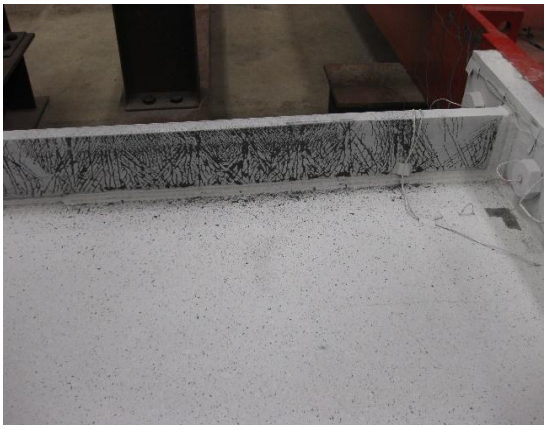

East Flange Inside

East Flange Outside

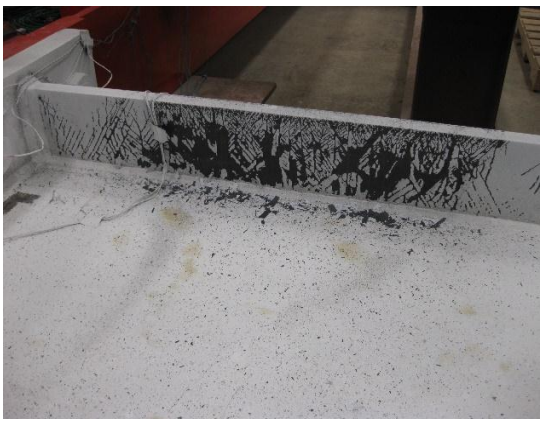

West Flange Inside

West Flange Outside

Web Deflection

Appendix D - Jack End Plots & Photos

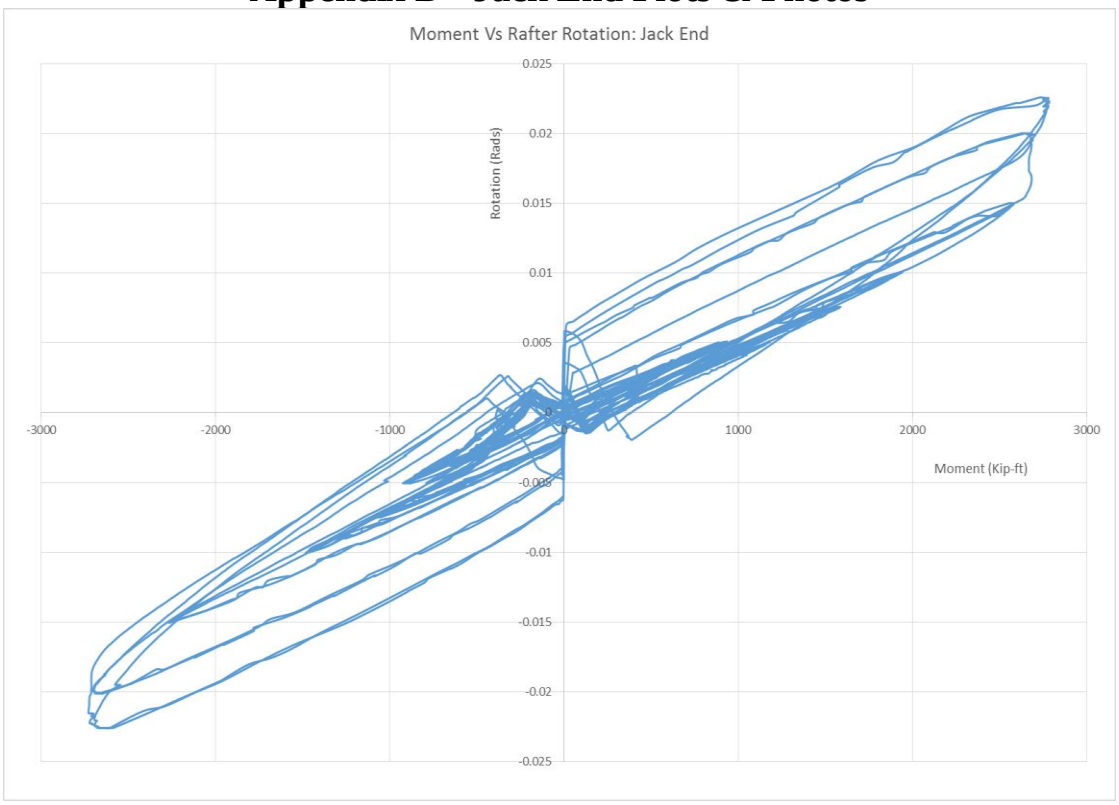

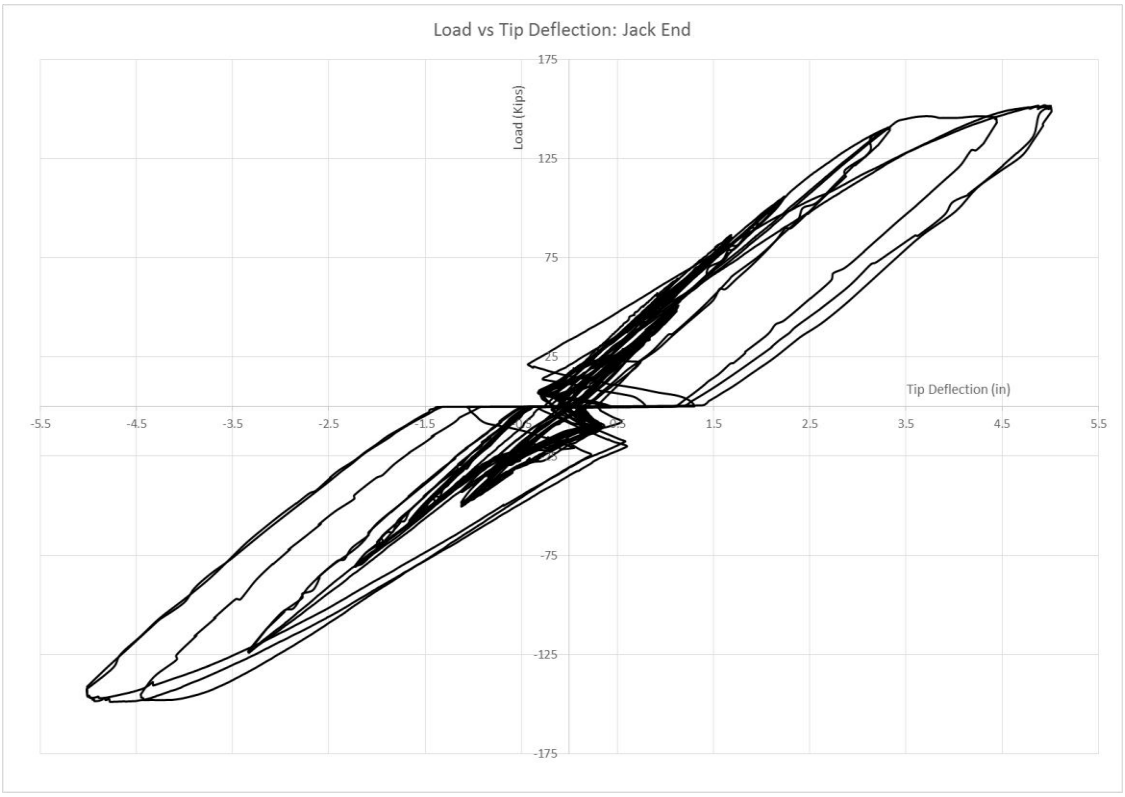

Jack End Prior to Testing:

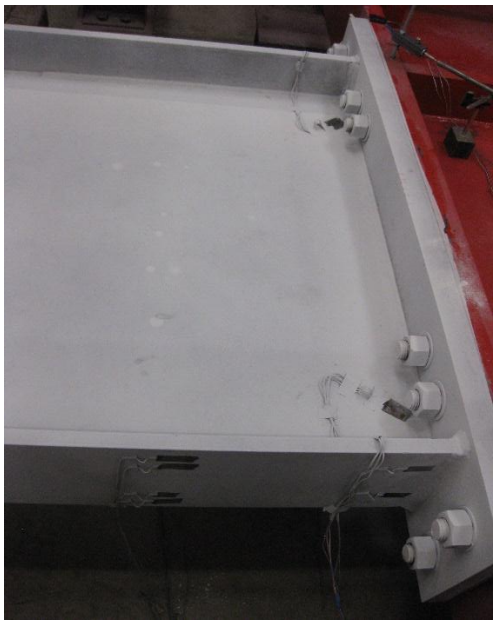

West Flange Outside **Web**

Jack End 0.00375 radians

No Discernable Changes

Jack End 0.005 radians

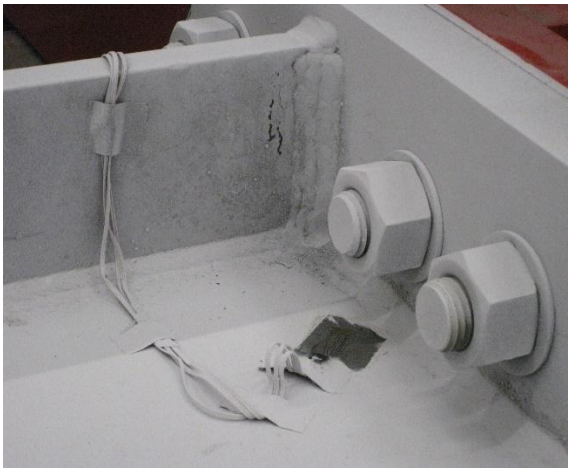

East Flange Inside **West Flange Outside**

Jack End: End of Cycle 0.0075 radians

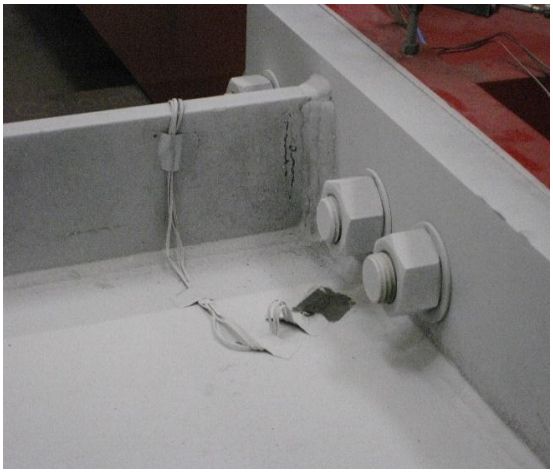

East Flange Inside

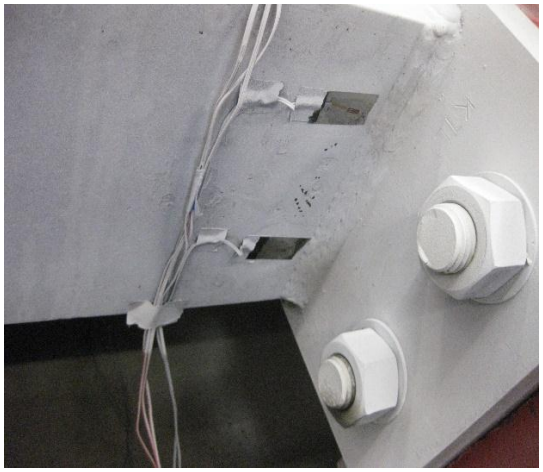

West Flange Outside

West Flange Outside @ Pick Point

Jack End: End of Cycle 0.01 radians

No Discernable Change from 0.0075 radians

Jack End: End of Cycle 0.015 radians

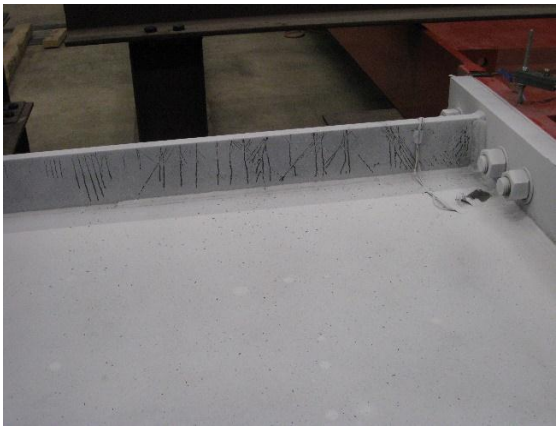

East Flange Inside

East Flange Outside

West Flange Outside

East Flange Outside

Jack End: End of Cycle 0.02 radians

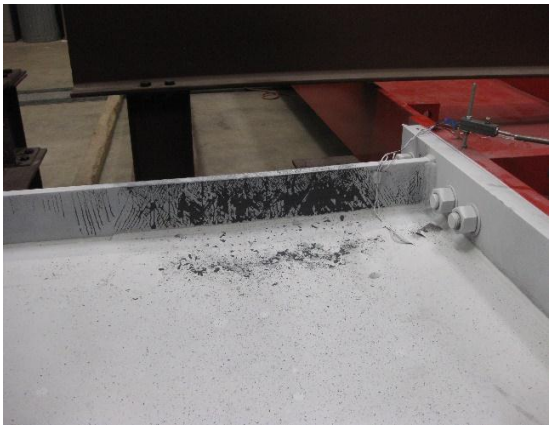

East Flange Inside

East Flange Outside

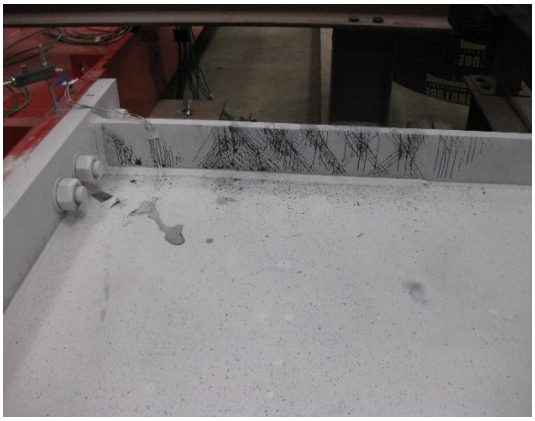

West Flange Inside

West Flange Outside

Jack End: End of Cycle 0.0225 radians

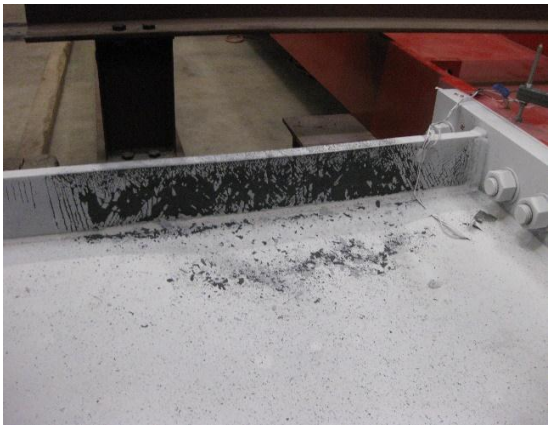

East Flange Inside

East Flange Outside

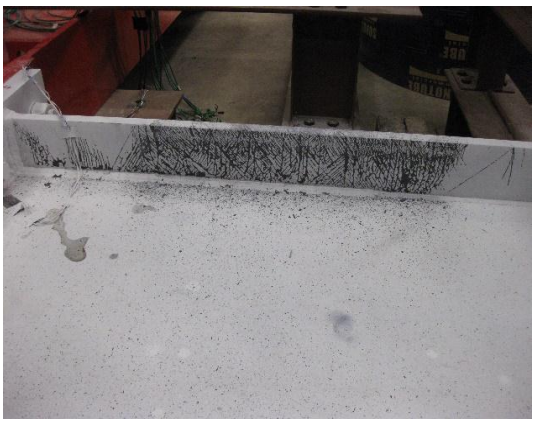

West Flange Inside

West Flange Outside

Web Deflection

Appendix E – Bottom Side of Jack End Weld Cuts

Flange to End-plate Modified PJP Weld's Cross Sectional Cuts

Test: Jack End **Flange: JB**

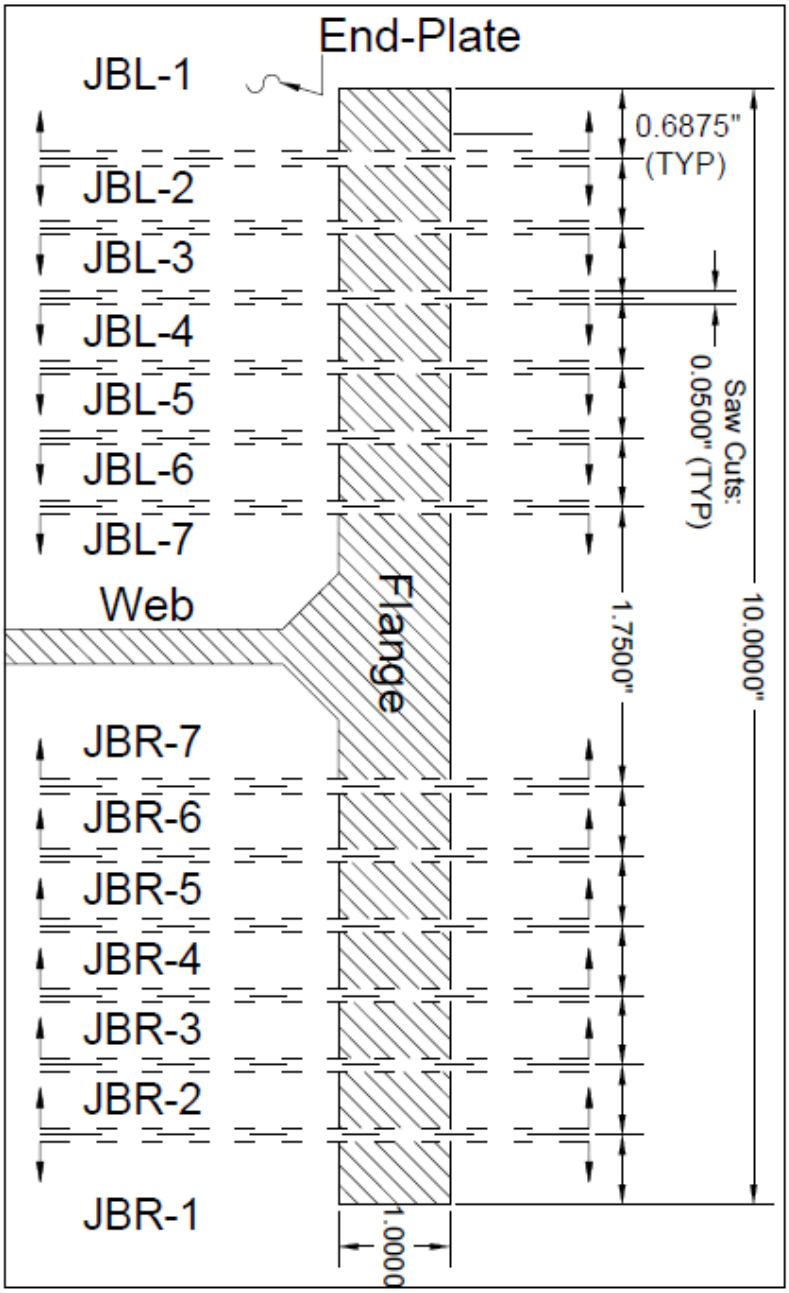

Test End: Jack Bottom						Flush With EP	
Weld Cut ID:	**PJP Weld Leg A (in.)**	**Root Face & Lack of Penetration B (in.)**	**Reinforcing Fillet Leg C (in.)**	**Measured Effective Throat T_{fo} (in.)**	**Measured Effective Throat T_{fi} (in.)**	**LOP Measured Along EP (in.)**	**Approx. Measured Root Face Along EP (in.)**
JBL-1	1.1765	0.3215	0.5759	1.0732	0.4558	0.0896	0.2336
JBL-2	1.1623	0.3209	0.6022	1.0099	0.4595	0.1235	0.1921
JBL-3	1.2852	0.3009	0.6388	1.1	0.4447	0.0869	0.2193
JBL-4	1.1891	0.2901	0.6801	1.0943	0.4697	0.0898	0.1884
JBL-5	1.346	0.1894	0.6879	1.1253	0.4689	0.0222	0.1879
JBL-6	1.255	0.3055	0.6305	1.1878	0.4383	0.1689	0.1228
JBL-7	1.2629	0.3191	0.625	1.0837	0.4821	0.1282	0.1885
Average:	**1.2396**	**0.2925**	**0.6343**	**1.0963**	**0.4599**	**0.1013**	**0.1904**
JBR-7	1.1946	0.0973	0.7732	1.0433	0.5132	0.0973	0.1503
JBR-6	1.2631	0.2046	0.733	1.0257	0.5502	0.2061	0*
JBR-5	1.3269	0.0192	0.7373	1.1169	0.4785	0.0912	0*
JBR-4	1.2051	0.2095	0.7017	0.9842	0.475	0.2095	0*
JBR-3	1.1025	0.3935	0.6914	0.7913	0.4747	0.3935	0*
JBR-2	1.3	0.1887	0.6225	1.0764	0.4615	0.1887	0*
JBR-1	1.288	0.2113	0.7183	1.0663	0.4711	0.2113	0*
Average:	**1.2400**	**0.1892**	**0.7111**	**1.0149**	**0.4892**	**0.1997**	**0.1503**
Total Avg:	**1.2398**	**0.2408**	**0.6727**	**1.0556**	**0.4745**	**0.1505**	**0.1703**
						*** Denotes Poor Fitup**	

Fillet sizes of flange to end-plate welds				
Specimen ID:	**Outside (Groove Side)**		**Inside**	
JBL	**Flange Side (OF)**	**End-plate Side (OE)**	**Flange Side (IF)**	**End-plate Side (IE)**
1	1	1/2	1	1/2
2	1	1/2	1	5/8
3	1	1/2	1	5/8
4	7/8	5/8	7/8	5/8
5	7/8	5/8	7/8	5/8
6	7/8	1/2	1	5/8
7	7/8	1/2	1	5/8
Avg	0.9286	0.5357	0.9643	0.6071
Design	0.5000	0.5000	0.6250	0.6250
Avg/Design	**1.8571**	**1.0714**	**1.5429**	**0.9714**
Specimen ID:	**Outside (Groove Side)**		**Inside**	
JBR	**Flange Side (OF)**	**End-plate Side (OE)**	**Flange Side (IF)**	**End-plate Side (IE)**
1	1	1/2	7/8	5/8
2	1	1/2	7/8	5/8
3	7/8	5/8	1	5/8
4	7/8	1/2	1	5/8
5	7/8	1/2	1	5/8
6	7/8	1/2	7/8	5/8
7	7/8	1/2	1	5/8
Avg	0.9107	0.5179	0.9464	0.6250
Design	0.5000	0.5000	0.6250	0.6250
Avg/Design	**1.8214**	**1.0357**	**1.5143**	**1.0000**

Test: Jack End Bottom **Flange: JBL-1**

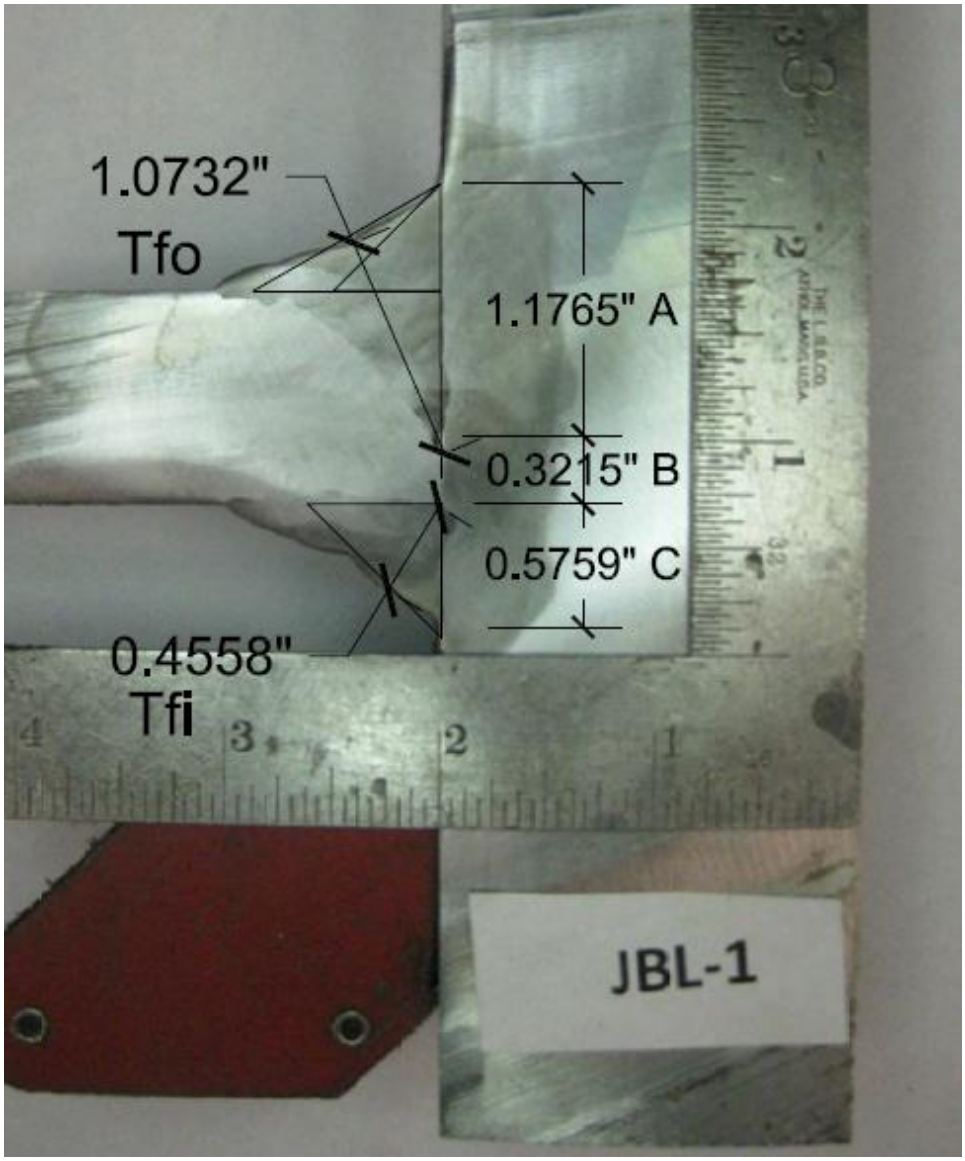

A = Built-up PJP Fillets

B = Lack of Penetration, LOP , Weld Root

C = Reinforcing Fillets

T_{fo} = Throat of A, PJP Fillets

T_{fi} = Throat of C, Reinforcing Fillets

Test: Jack End Bottom **Flange: JBL-2**

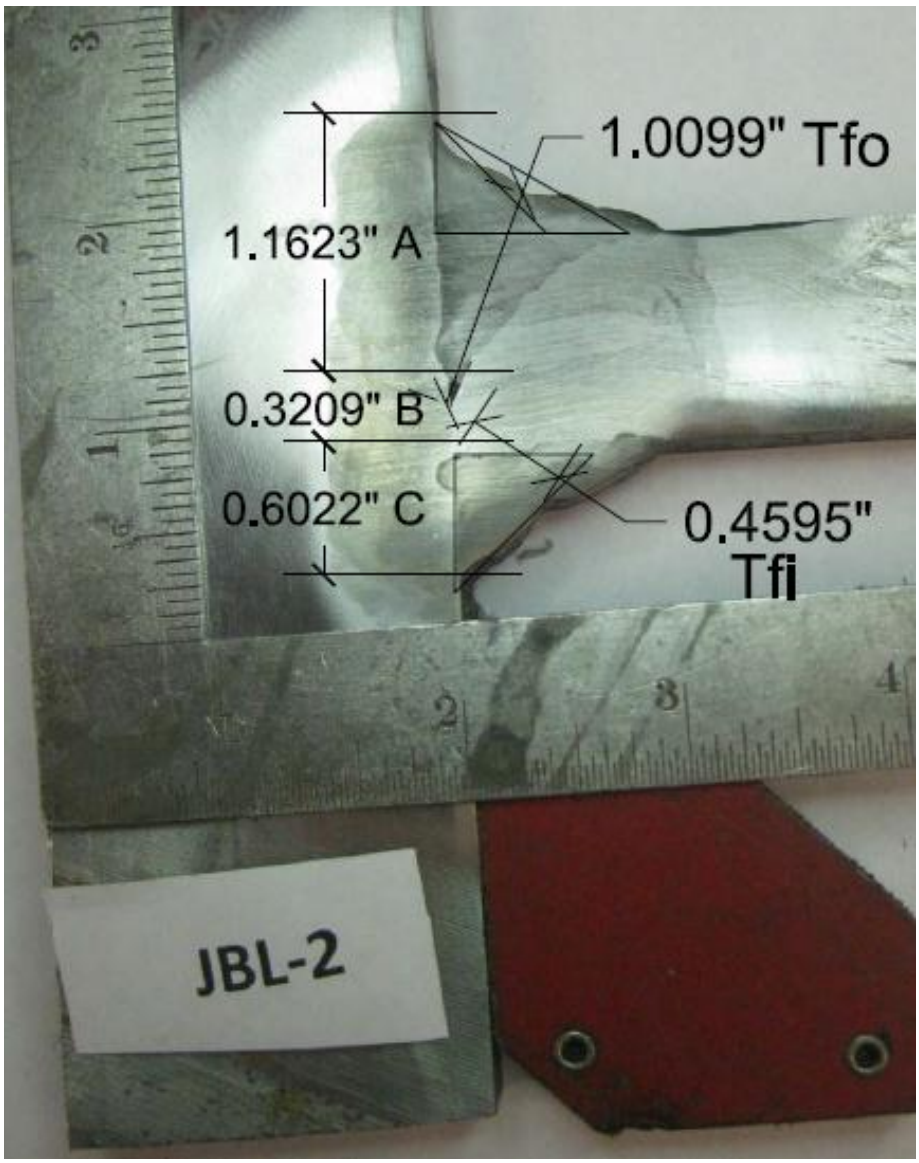

A = Built-up PJP Fillets

B = Lack of Penetration, LOP , Weld Root

C = Reinforcing Fillets

T_{fo} = Throat of A, PJP Fillets

T_{fi} = Throat of C, Reinforcing Fillets

Test: Jack End Bottom **Flange: JBL-3**

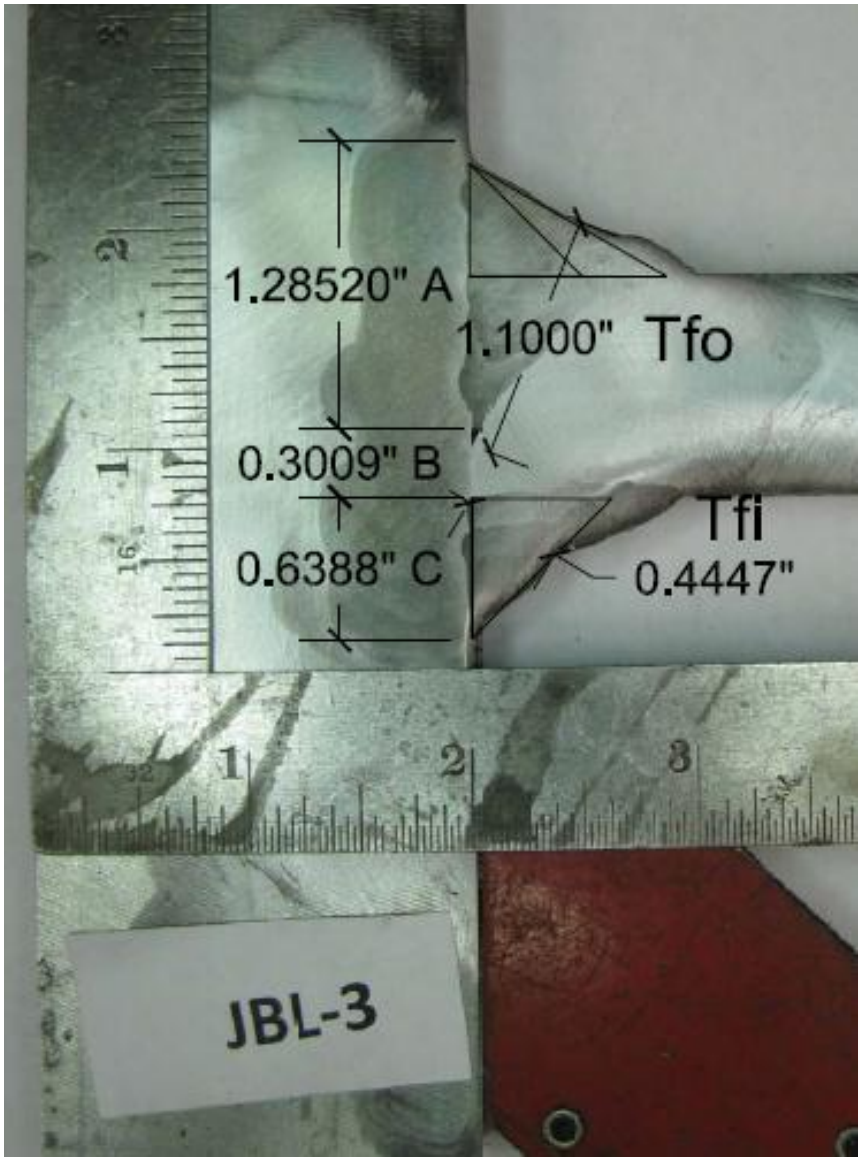

A = Built-up PJP Fillets

B = Lack of Penetration, LOP , Weld Root

C = Reinforcing Fillets

T_{fo} = Throat of A, PJP Fillets

T_{fi} = Throat of C, Reinforcing Fillets

Test: Jack End Bottom **Flange: JBL-4**

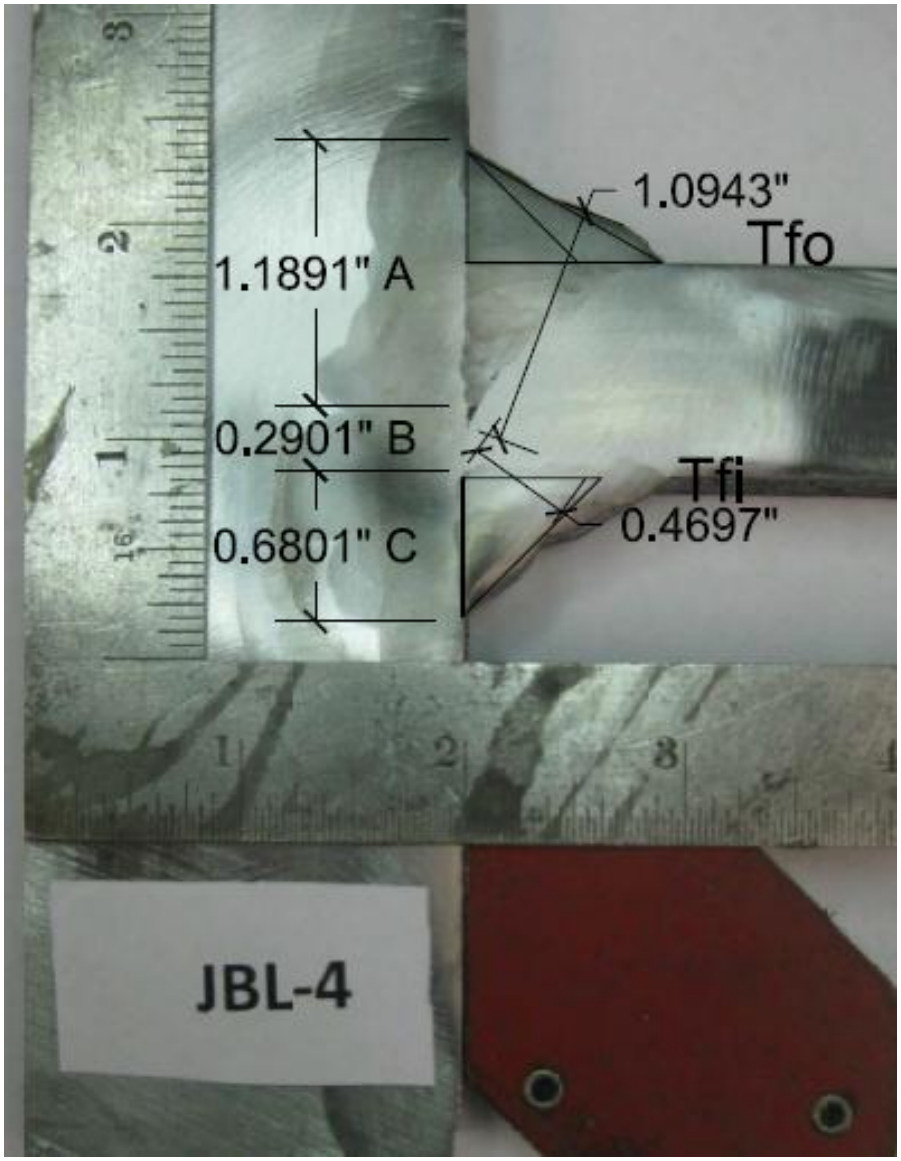

A = Built-up PJP Fillets

B = Lack of Penetration, LOP , Weld Root

C = Reinforcing Fillets

T_{fo} = Throat of A, PJP Fillets

T_{fi} = Throat of C, Reinforcing Fillets

Test: Jack End Bottom **Flange: JBL-5**

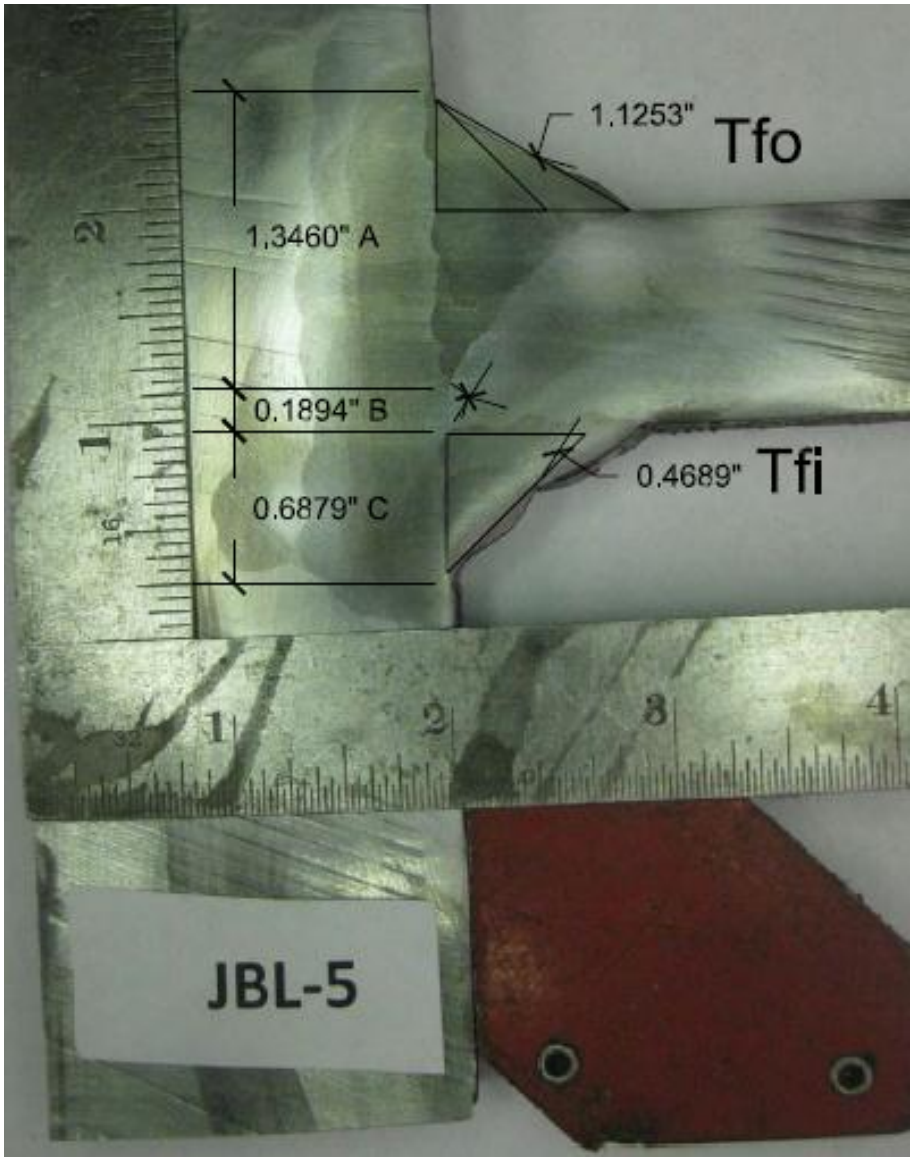

A = Built-up PJP Fillets

B = Lack of Penetration, LOP , Weld Root

C = Reinforcing Fillets

T_{fo} = Throat of A, PJP Fillets

T_{fi} = Throat of C, Reinforcing Fillets

Test: Jack End Bottom **Flange: JBL-6**

A = Built-up PJP Fillets

B = Lack of Penetration, LOP , Weld Root

C = Reinforcing Fillets

T_{fo} = Throat of A, PJP Fillets

T_{fi} = Throat of C, Reinforcing Fillets

Test: Jack End Bottom **Flange: JBL-7**

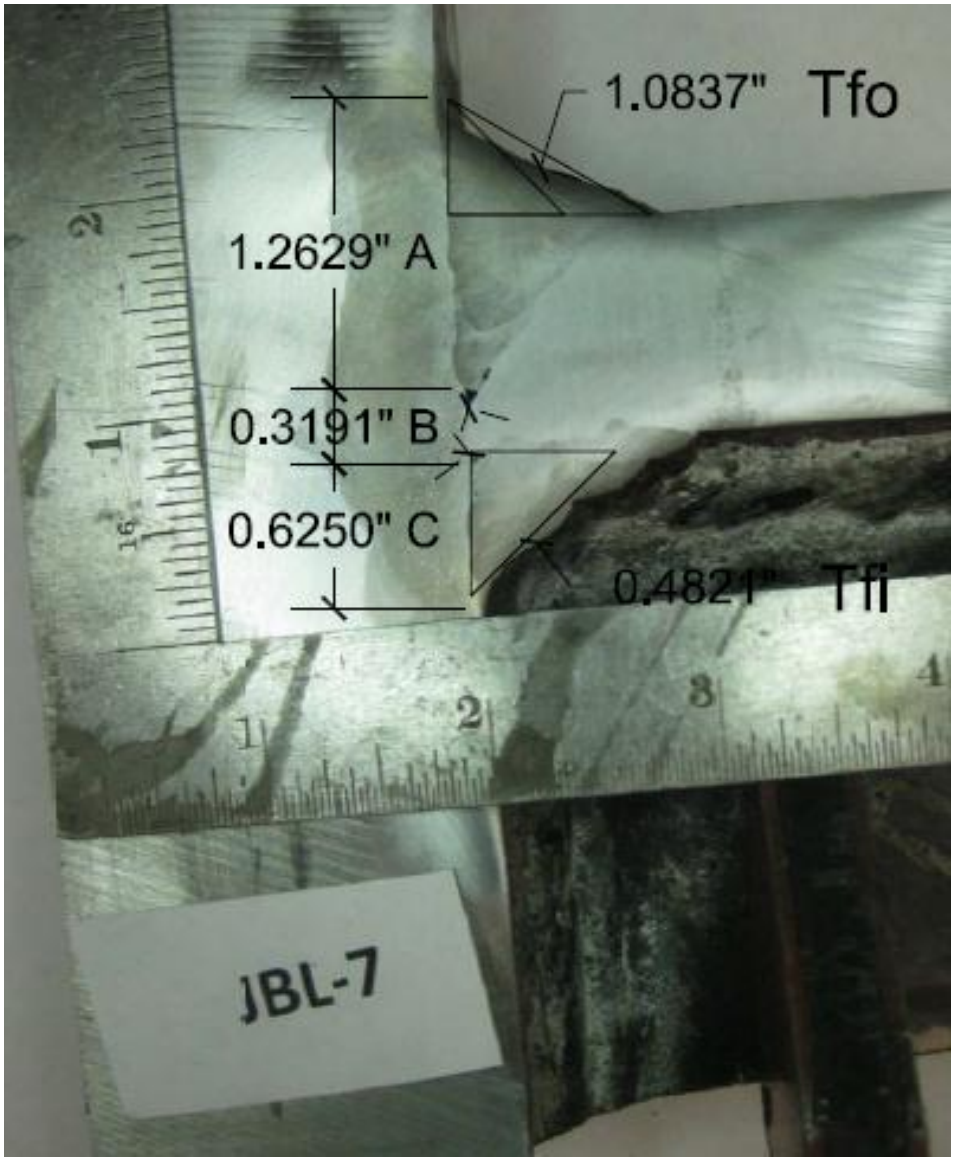

A = Built-up PJP Fillets

B = Lack of Penetration, LOP , Weld Root

C = Reinforcing Fillets

T_{fo} = Throat of A, PJP Fillets

T_{fi} = Throat of C, Reinforcing Fillets

Test: Jack End Bottom **Flange: JBR-7**

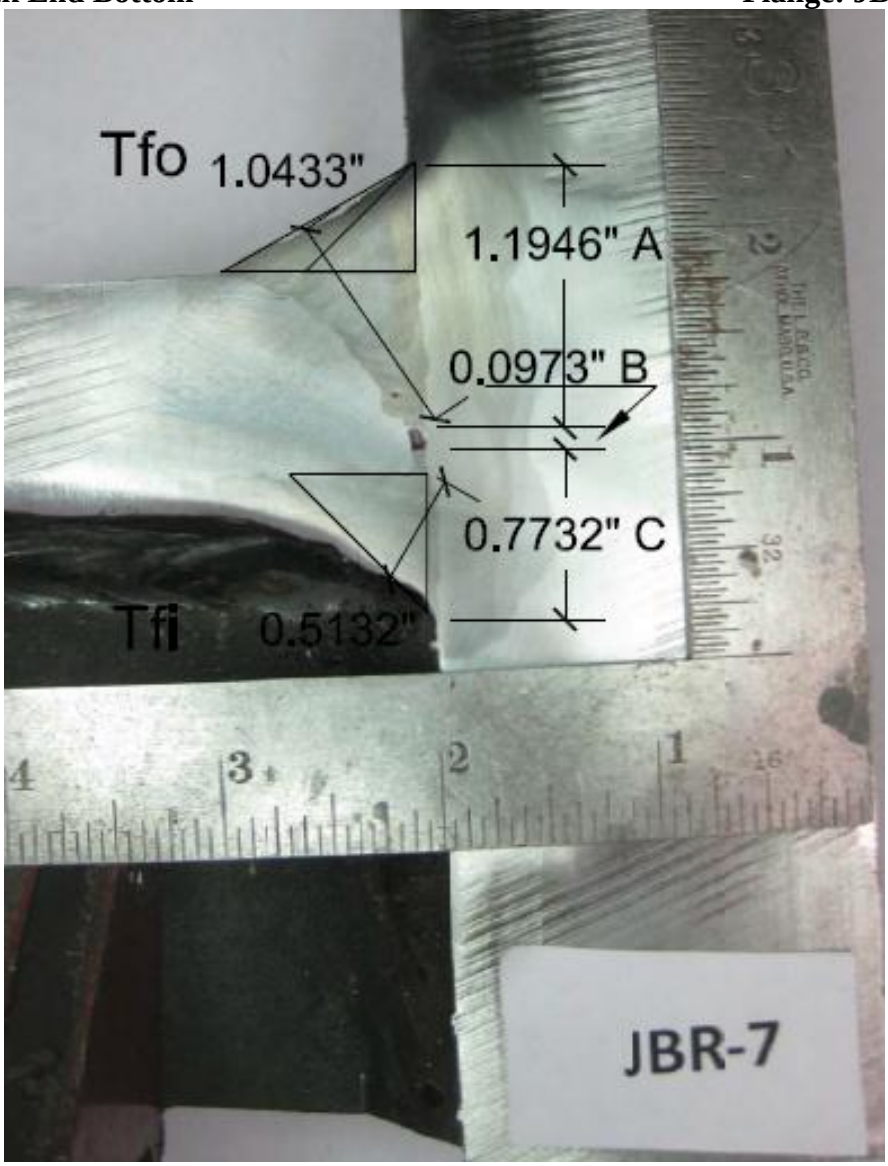

A = Built-up PJP Fillets

B = Lack of Penetration, LOP , Weld Root

C = Reinforcing Fillets

T_{fo} = Throat of A, PJP Fillets

T_{fi} = Throat of C, Reinforcing Fillets

Test: Jack End Bottom **Flange: JBR-6**

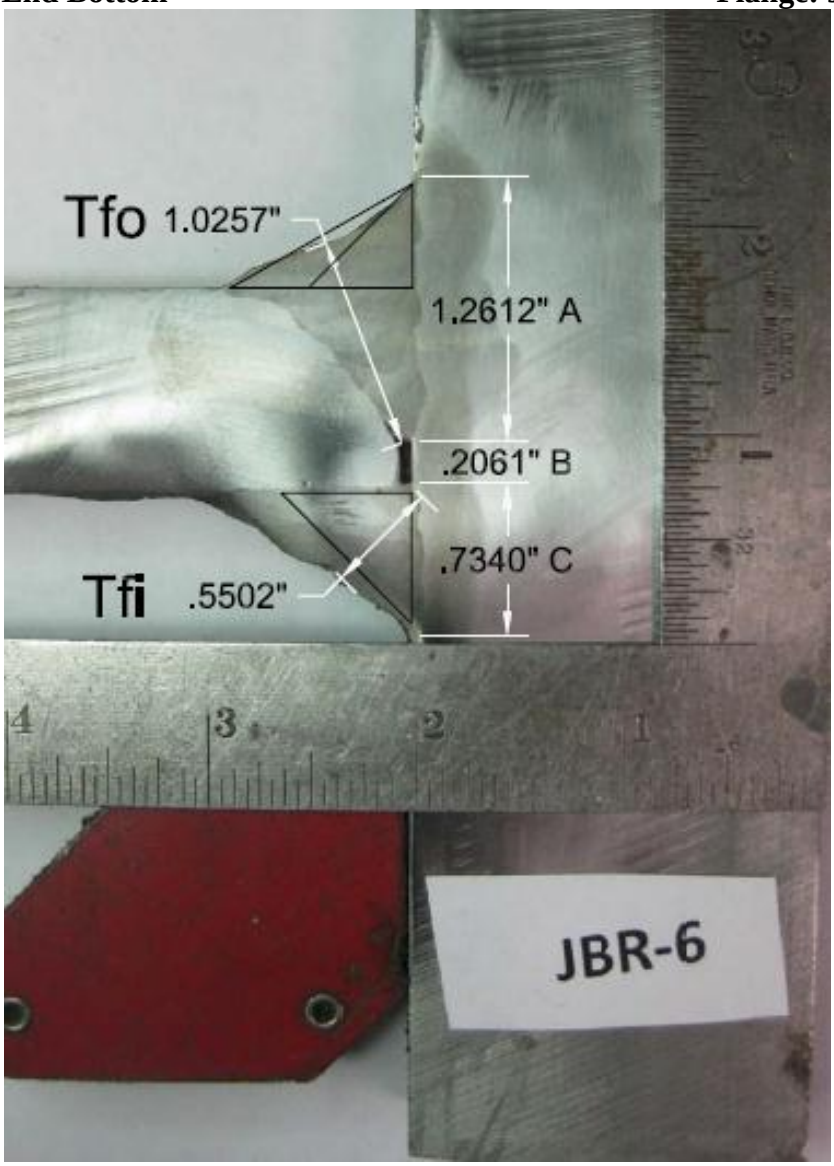

A = Built-up PJP Fillets

B = Lack of Penetration, LOP , Weld Root

C = Reinforcing Fillets

T_{fo} = Throat of A, PJP Fillets

T_{fi} = Throat of C, Reinforcing Fillets

Test: Jack End **Flange: JBR-5**

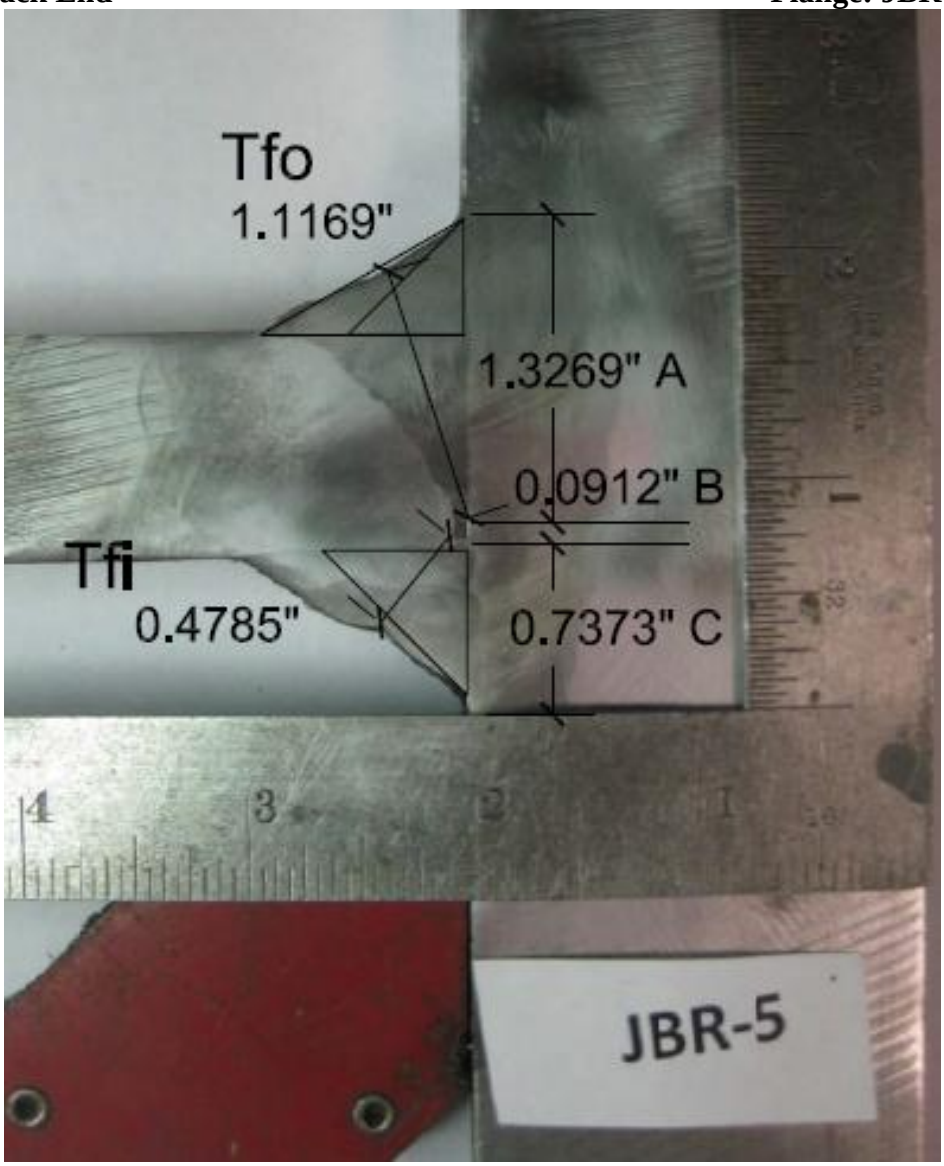

A = Built-up PJP Fillets

B = Lack of Penetration, LOP , Weld Root

C = Reinforcing Fillets

T_{fo} = Throat of A, PJP Fillets

T_{fi} = Throat of C, Reinforcing Fillets

Test: Jack End Bottom **Flange: JBR-4**

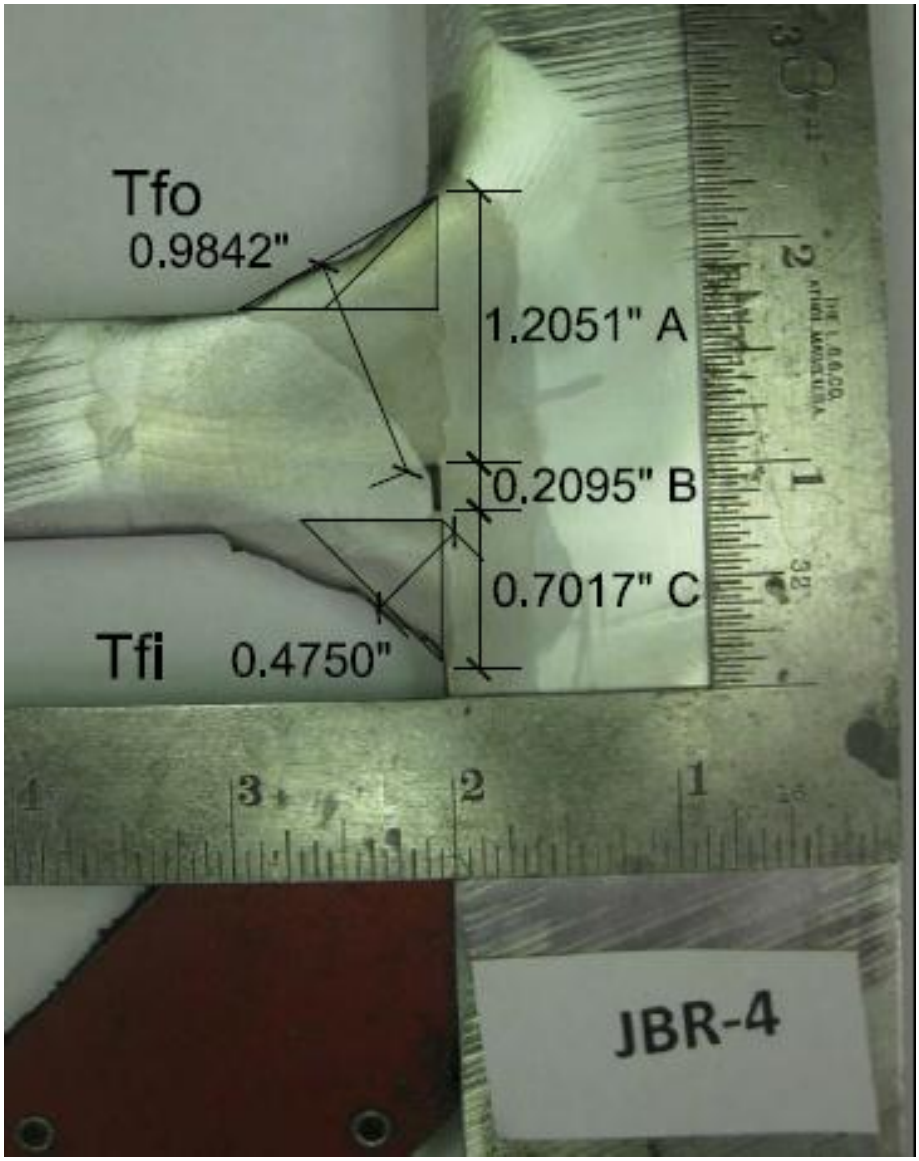

A = Built-up PJP Fillets

B = Lack of Penetration, LOP , Weld Root

C = Reinforcing Fillets

T_{fo} = Throat of A, PJP Fillets

T_{fi} = Throat of C, Reinforcing Fillets

Test: Jack End Bottom **Flange: JBR-3**

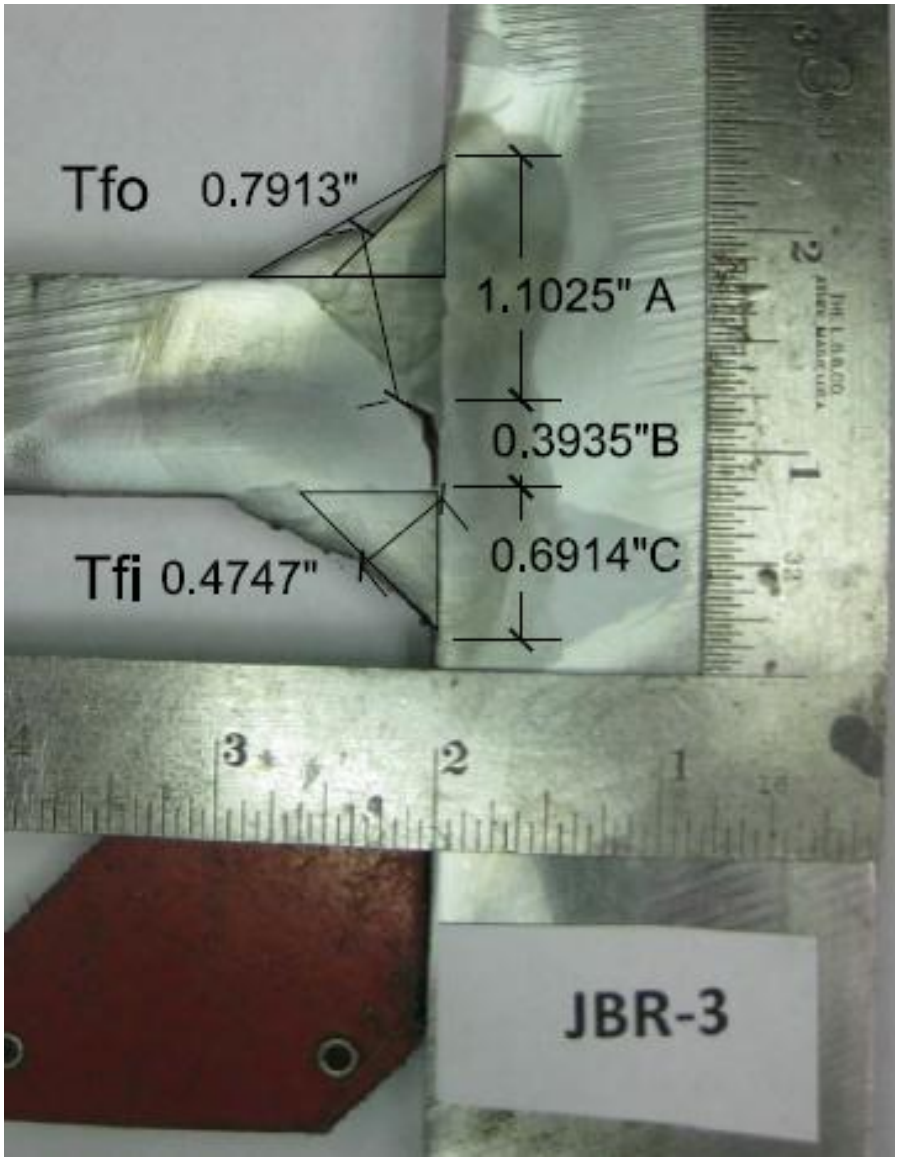

A = Built-up PJP Fillets

B = Lack of Penetration, LOP , Weld Root

C = Reinforcing Fillets

T_{fo} = Throat of A, PJP Fillets

T_{fi} = Throat of C, Reinforcing Fillets

Test: Jack End Bottom **Flange: JBR-2**

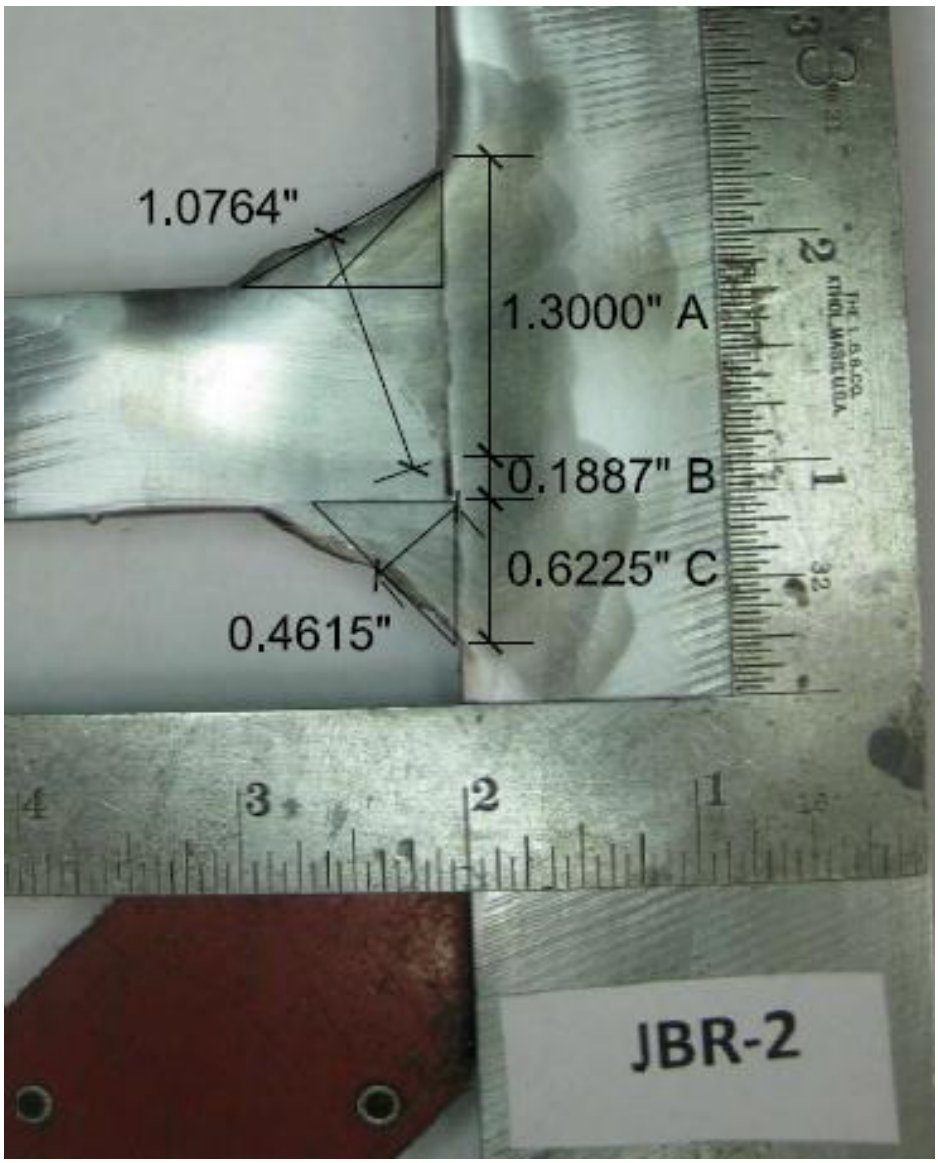

A = Built-up PJP Fillets

B = Lack of Penetration, LOP , Weld Root

C = Reinforcing Fillets

T_{fo} = Throat of A, PJP Fillets

T_{fi} = Throat of C, Reinforcing Fillets

Test: Jack End Bottom **Flange: JBR-1**

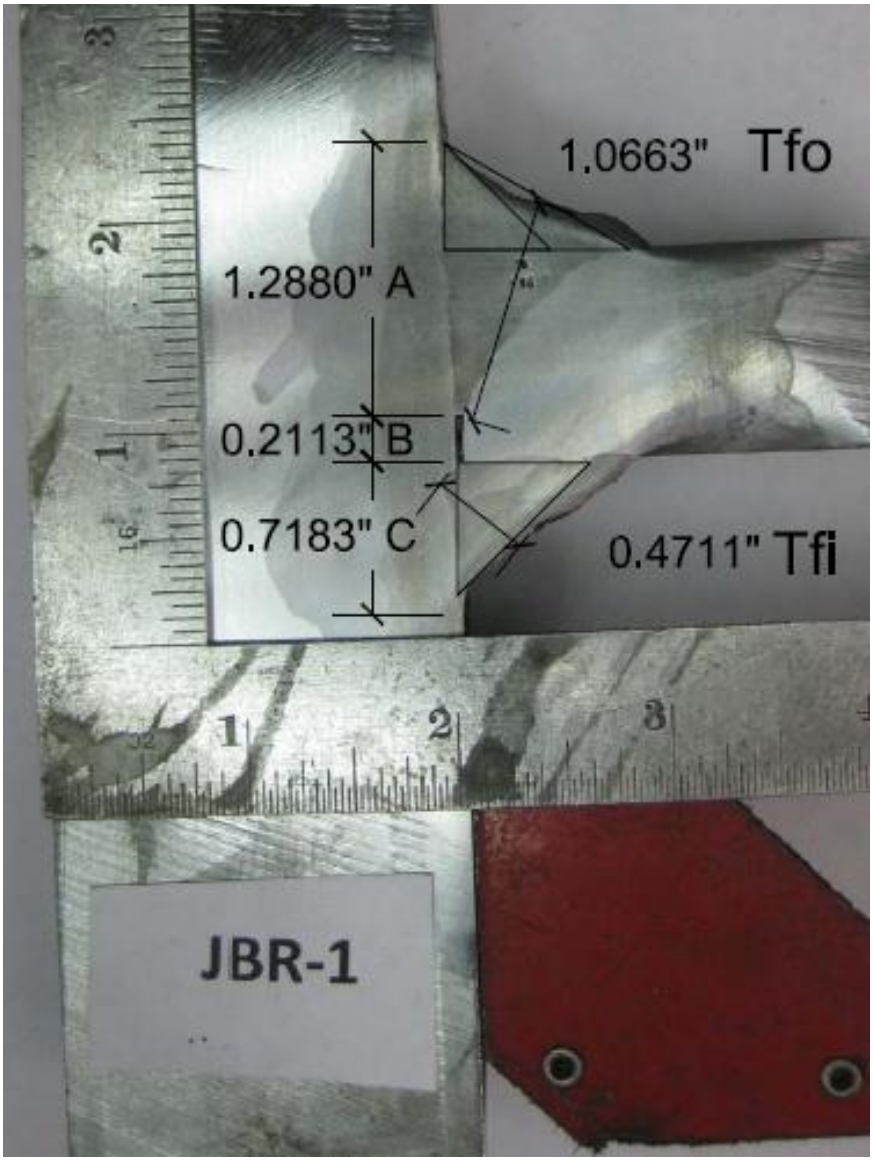

A = Built-up PJP Fillets

B = Lack of Penetration, LOP , Weld Root

C = Reinforcing Fillets

T_{fo} = Throat of A, PJP Fillets

T_{fi} = Throat of C, Reinforcing Fillets

Appendix F - Top Side of Jack End Weld Cuts

Flange to End-plate Modified PJP Weld's Cross Sectional Cuts

Test: Jack End Top **Flange: JT**

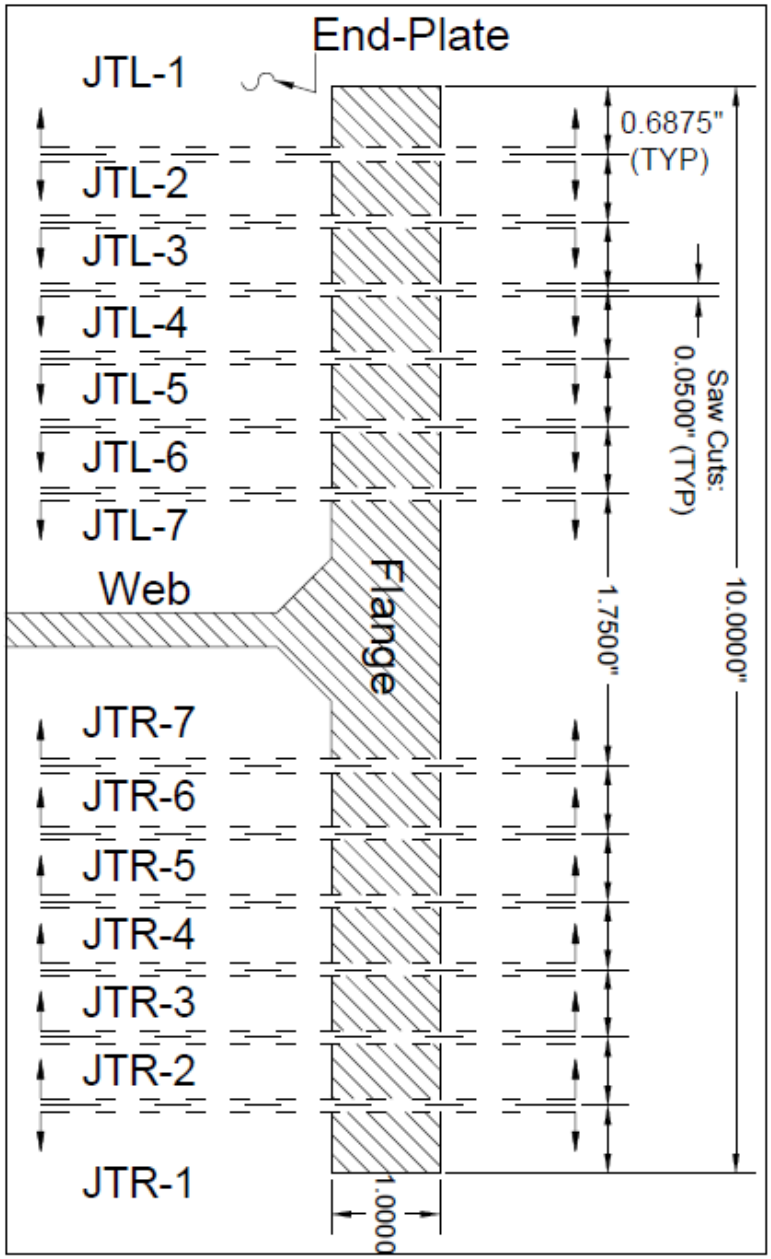

Test End: Jack Top						Flush With EP	
Weld Cut ID:	PJP Weld Leg A (in.)	Root Face & Lack of Penetration B (in.)	Reinforcing Fillet Leg C (in.)	Measured Effective Throat T_{fo} (in.)	Measured Effective Throat T_{fi} (in.)	LOP Measured Along EP (in.)	Approx. Measured Root Face Along EP (in.)
JTL-1	1.1202	0.354	0.6787	1.0286	0.5577	0.354	0
JTL-2	1.068	0.3727	0.7339	0.9069	0.5484	0.1854	0.1854
JTL-3	1.1115	0.3492	0.7455	0.9628	0.5159	0.1045	0.2499
JTL-4	1.0834	0.3856	0.7343	0.8962	0.5312	0.1183	0.2681
JTL-5	1.1503	0.2527	0.8194	0.9313	0.5401	0.0485	0.2527
JTL-6	1.1196	0.3252	0.7756	0.9447	0.5474	0	0.3252
JTL-7	1.1163	0.3503	0.7057	0.9084	0.5016	0.1065	0.2662
Average:	**1.1099**	**0.3414**	**0.7419**	**0.9398**	**0.5346**	**0.1310**	**0.2579**
JTR-7	1.1059	0.247	0.7013	0.9813	0.6155	0	0.247
JTR-6	1.0253	0.3823	0.6729	0.8532	0.4546	0.1296	0.251
JTR-5	1.0153	0.389	0.6959	0.8432	0.4471	0.1351	0.2578
JTR-4	1.0257	0.3386	0.6707	0.8569	0.4437	0.0941	0.2466
JTR-3	1.1227	0.3057	0.7132	0.9335	0.4188	0.3057	0
JTR-2	1.3047	0.1059	0.6799	1.0976	0.4806	0.1059	0.1826
JTR-1	1.291	0.1526	0.6525	1.1201	0.4837	0.1526	0
Average:	**1.1272**	**0.2744**	**0.6838**	**0.9551**	**0.4777**	**0.1319**	**0.2370**
Total Avg:	**1.1186**	**0.3079**	**0.7128**	**0.9475**	**0.5062**	**0.1314**	**0.2475**
						* Denotes Poor Fitup	

Fillet sizes of flange to end-plate welds				
Specimen ID:	**Outside (Groove Side)**		**Inside**	
JTL	**Flange Side (OF)**	**End-plate Side (OE)**	**Flange Side (IF)**	**End-plate Side (IE)**
1	1	1/2	1 1/16	5/8
2	1	1/2	1	3/4
3	1	1/2	1	3/4
4	1	1/2	1	3/4
5	1	1/2	1	3/4
6	1	1/2	1	3/4
7	1	1/2	1	5/8
Avg	1.0000	0.5000	1.0089	0.7143
Design	0.5000	0.5000	0.6250	0.6250
Avg/Design	**2.0000**	**1.0000**	**1.6143**	**1.1429**
Specimen ID:	**Outside (Groove Side)**		**Inside**	
JTR	**Flange Side (OF)**	**End-plate Side (OE)**	**Flange Side (IF)**	**End-plate Side (IE)**
1	7/8	1/2	7/8	5/8
2	7/8	1/2	7/8	5/8
3	7/8	1/2	7/8	5/8
4	7/8	1/2	7/8	5/8
5	7/8	1/2	7/8	5/8
6	7/8	1/2	7/8	5/8
7	7/8	1/2	7/8	1/2
Avg	0.8750	0.5000	0.8750	0.6071
Design	0.5000	0.5000	0.6250	0.6250
Avg/Design	**1.7500**	**1.0000**	**1.4000**	**0.9714**

Test: Jack End Top **Flange: JTL-1**

A = Built-up PJP Fillets

B = Lack of Penetration, LOP , Weld Root

C = Reinforcing Fillets

T_{fo} = Throat of A, PJP Fillets

T_{fi} = Throat of C, Reinforcing Fillets

Test: Jack End Top **Flange: JTL-2**

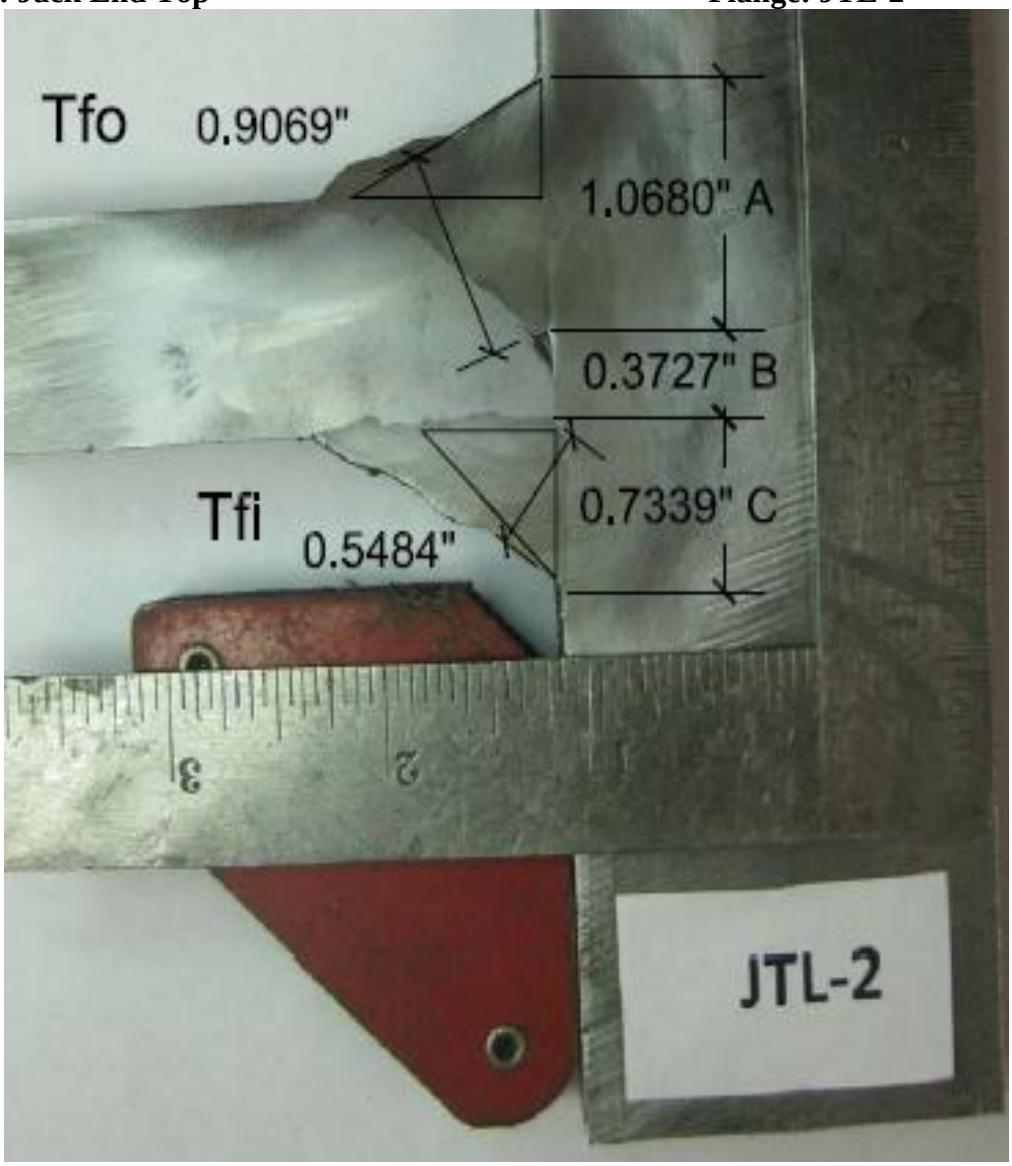

A = Built-up PJP Fillets

B = Lack of Penetration, LOP , Weld Root

C = Reinforcing Fillets

T_{fo} = Throat of A, PJP Fillets

T_{fi} = Throat of C, Reinforcing Fillets

Test: Jack End Top **Flange: JTL-3**

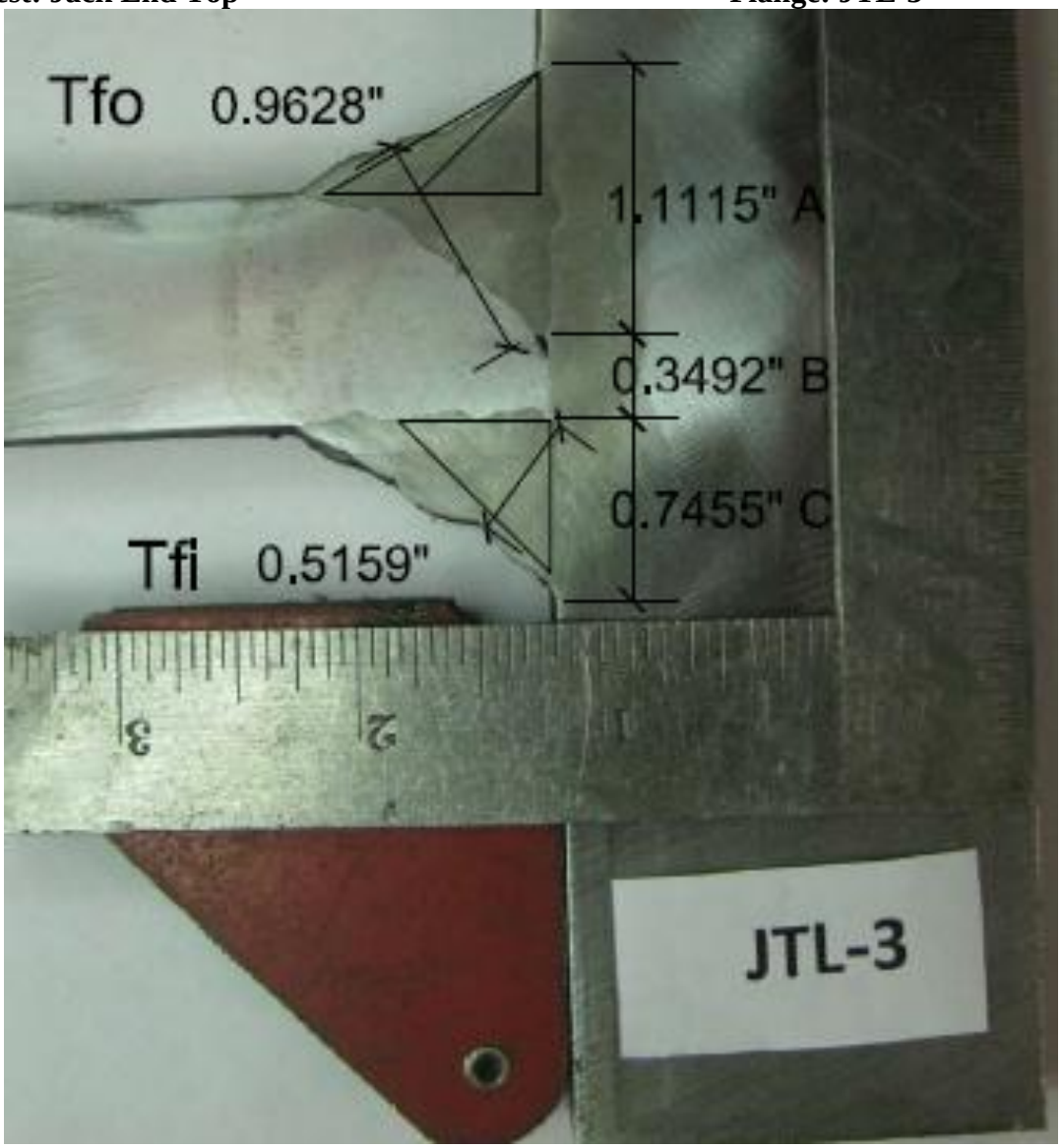

A = Built-up PJP Fillets

B = Lack of Penetration, LOP , Weld Root

C = Reinforcing Fillets

T_{fo} = Throat of A, PJP Fillets

T_{fi} = Throat of C, Reinforcing Fillets

Test: Jack End Top **Flange: JTL-4**

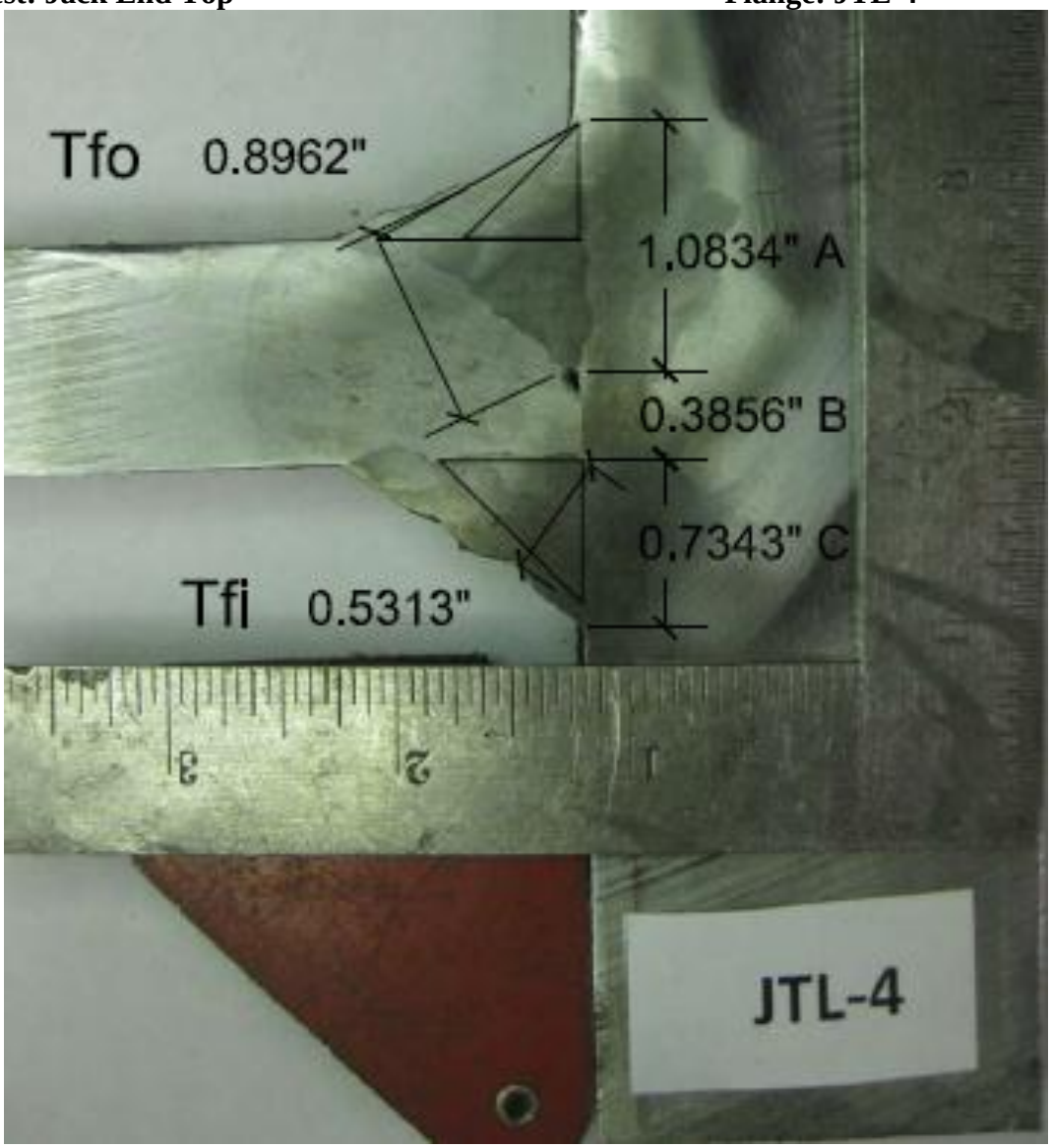

A = Built-up PJP Fillets

B = Lack of Penetration, LOP , Weld Root

C = Reinforcing Fillets

T_{fo} = Throat of A, PJP Fillets

T_{fi} = Throat of C, Reinforcing Fillets

Test: Jack End Top **Flange: JTL-5**

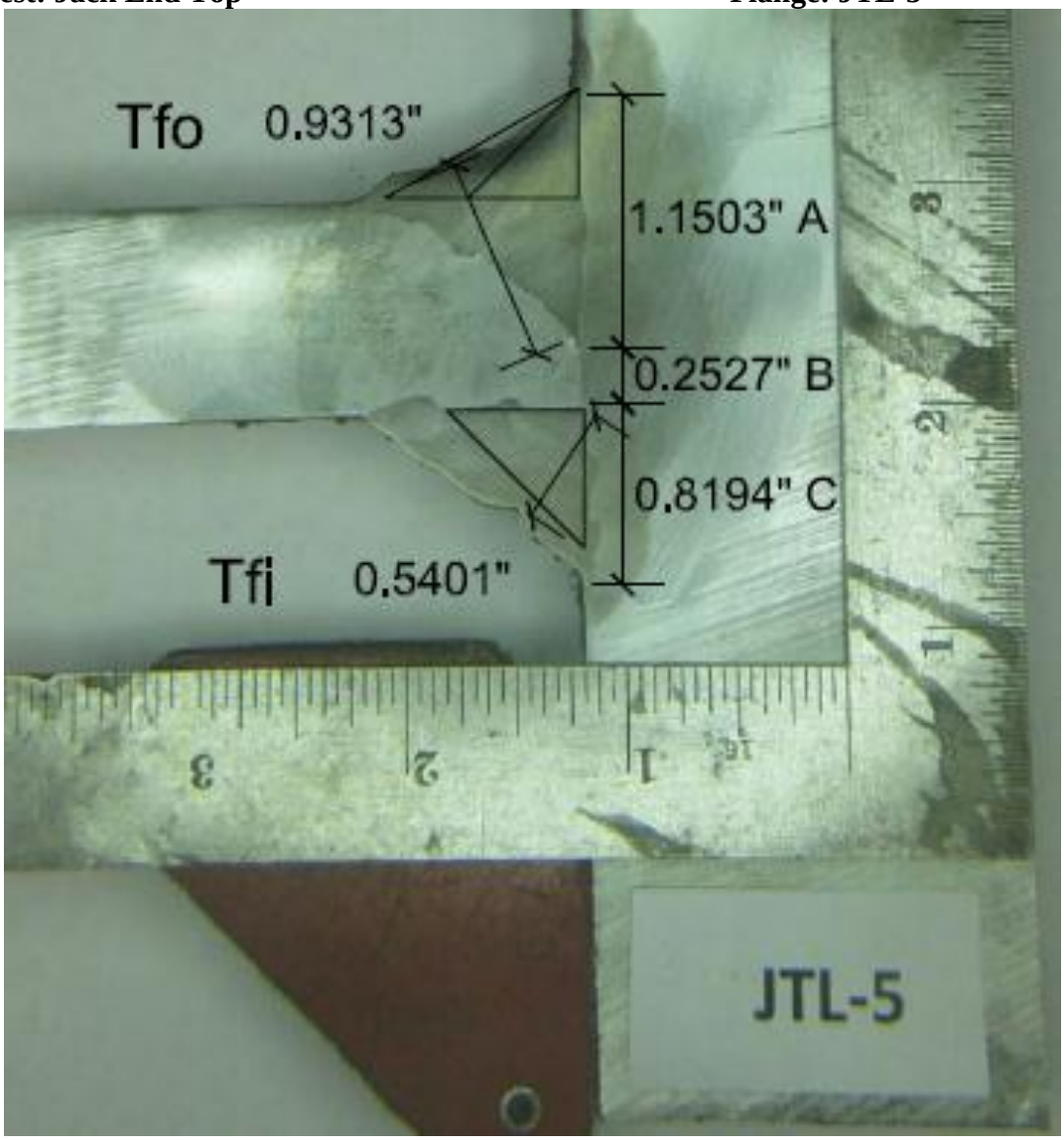

A = Built-up PJP Fillets

B = Lack of Penetration, LOP , Weld Root

C = Reinforcing Fillets

T_{fo} = Throat of A, PJP Fillets

T_{fi} = Throat of C, Reinforcing Fillets

Test: Jack End Top **Flange: JTL-6**

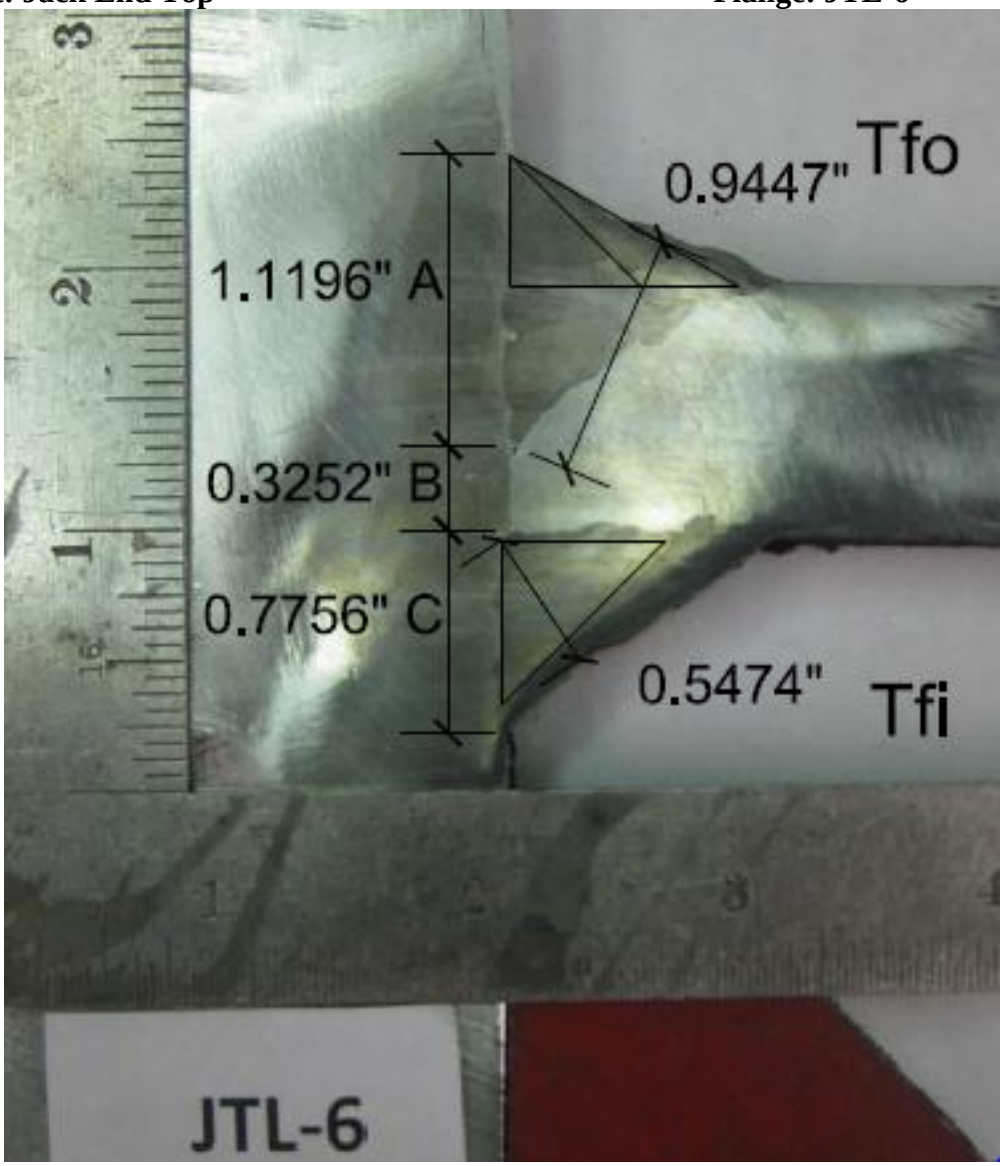

A = Built-up PJP Fillets

B = Lack of Penetration, LOP , Weld Root

C = Reinforcing Fillets

T_{fo} = Throat of A, PJP Fillets

T_{fi} = Throat of C, Reinforcing Fillets

Test: Jack End Top **Flange: JTL-7**

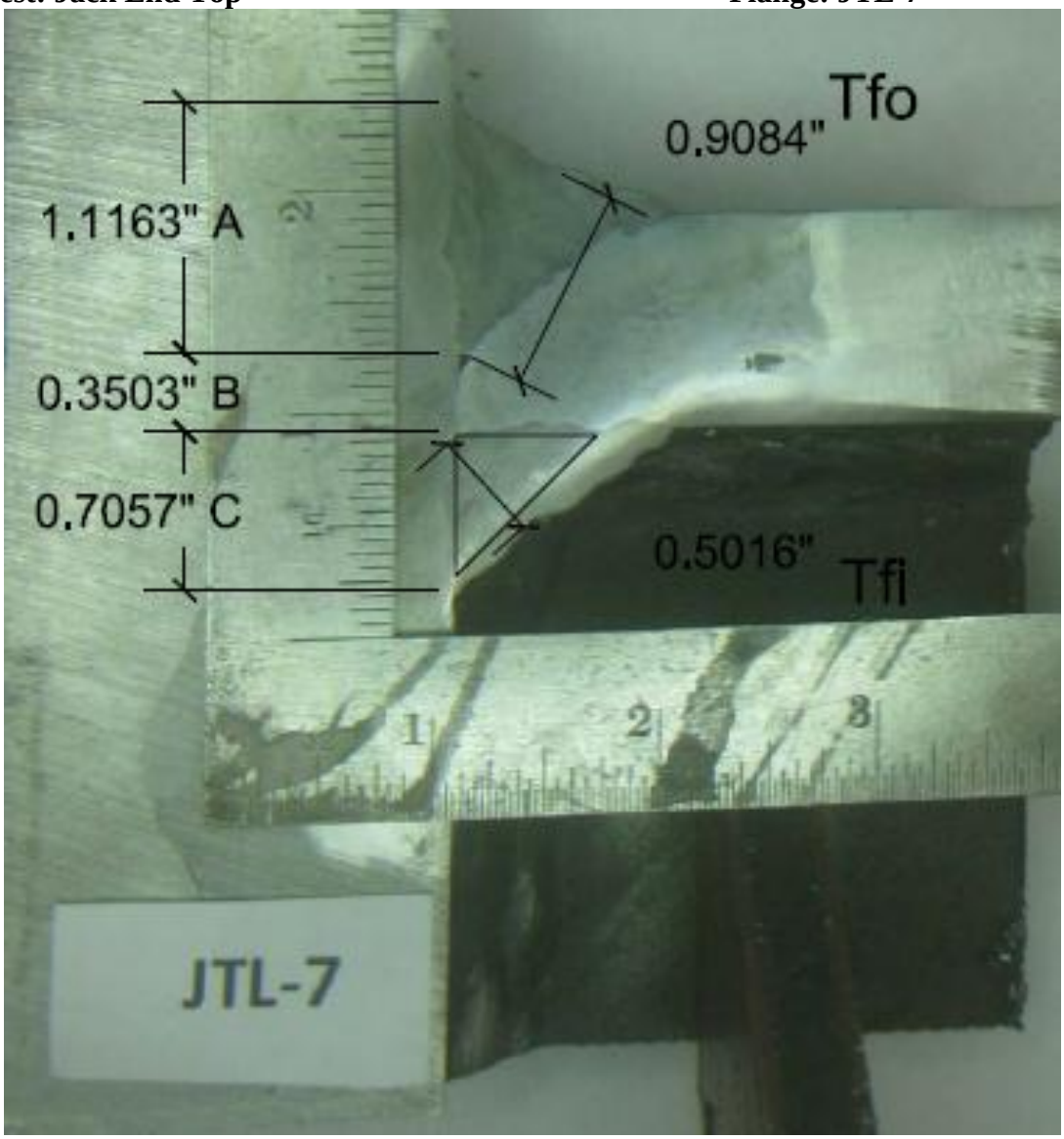

A = Built-up PJP Fillets

B = Lack of Penetration, LOP , Weld Root

C = Reinforcing Fillets

T_{fo} = Throat of A, PJP Fillets

T_{fi} = Throat of C, Reinforcing Fillets

Test: Jack End Top **Flange: JTR-7**

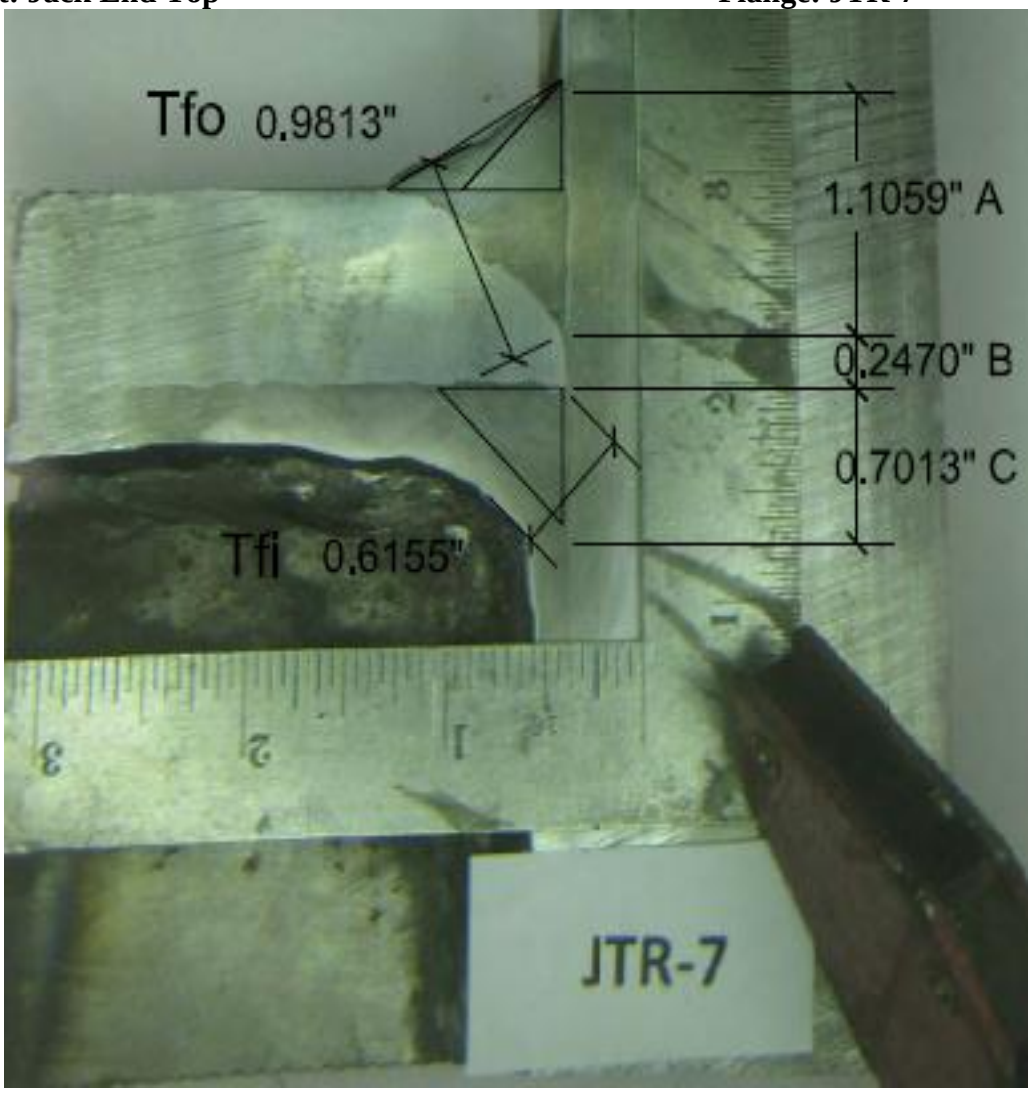

A = Built-up PJP Fillets

B = Lack of Penetration, LOP , Weld Root

C = Reinforcing Fillets

T_{fo} = Throat of A, PJP Fillets

T_{fi} = Throat of C, Reinforcing Fillets

Test: Jack End Top **Flange: JTR-6**

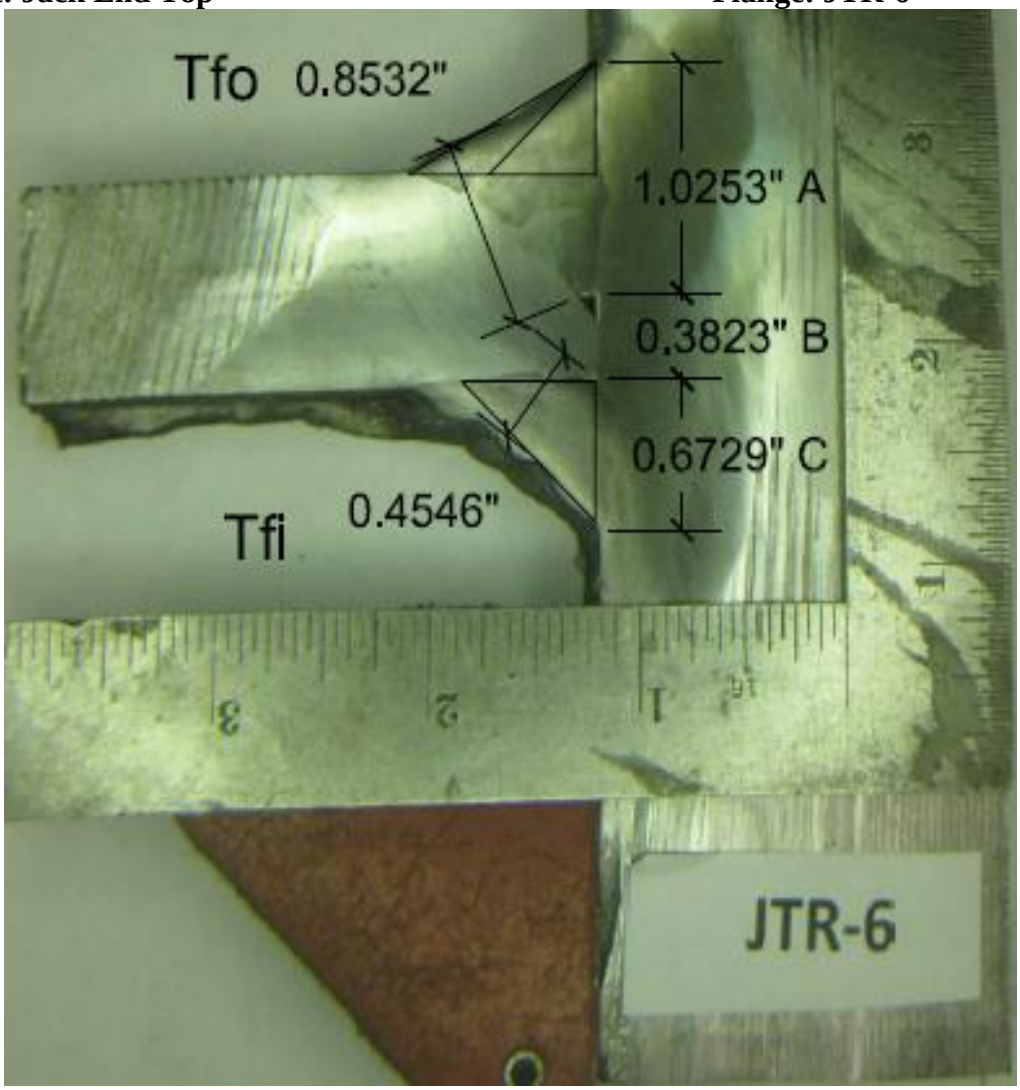

A = Built-up PJP Fillets

B = Lack of Penetration, LOP , Weld Root

C = Reinforcing Fillets

T_{fo} = Throat of A, PJP Fillets

T_{fi} = Throat of C, Reinforcing Fillets

Test: Jack End Top **Flange: JTR-5**

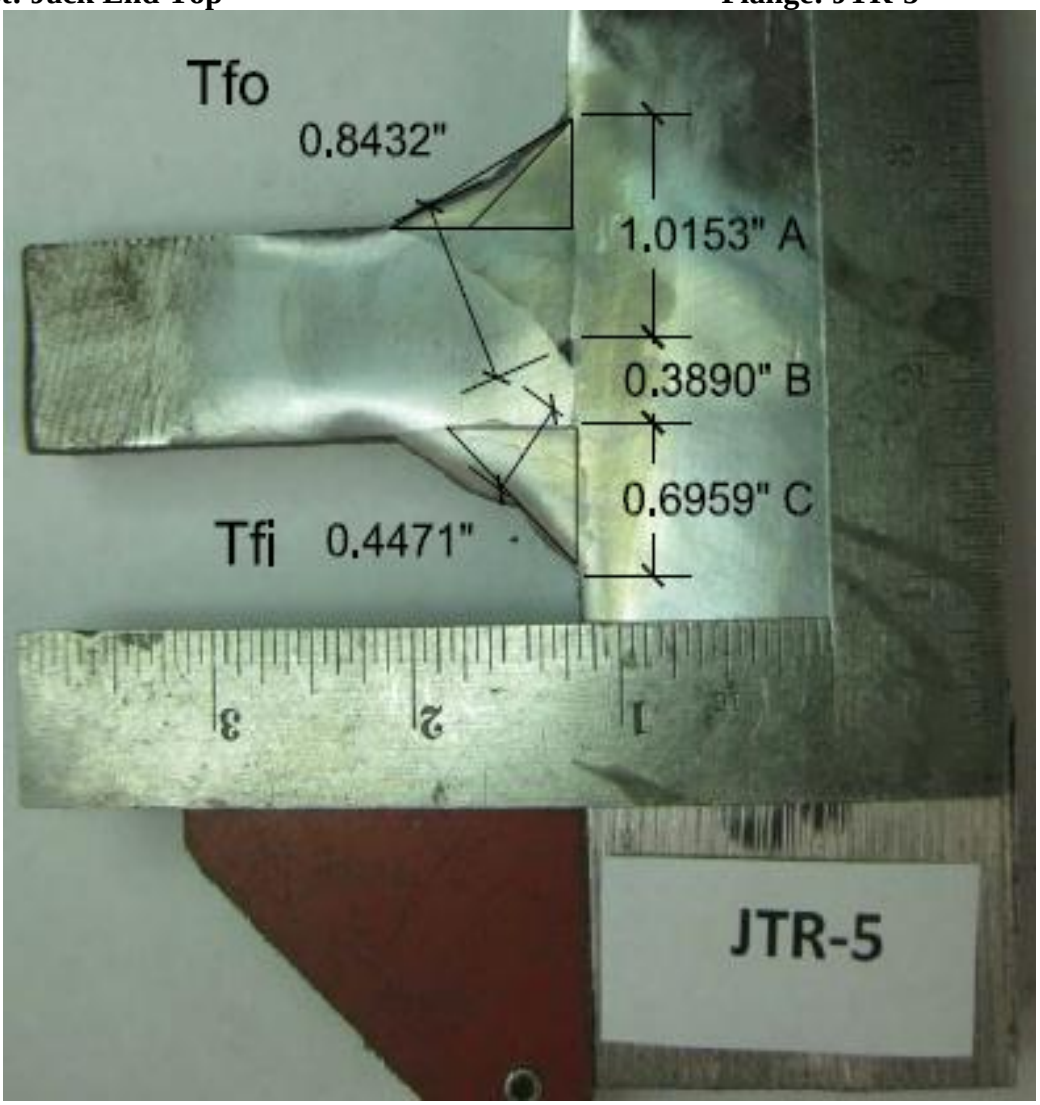

A = Built-up PJP Fillets

B = Lack of Penetration, LOP , Weld Root

C = Reinforcing Fillets

T_{fo} = Throat of A, PJP Fillets

T_{fi} = Throat of C, Reinforcing Fillets

Test: Jack End Top **Flange: JTR-4**

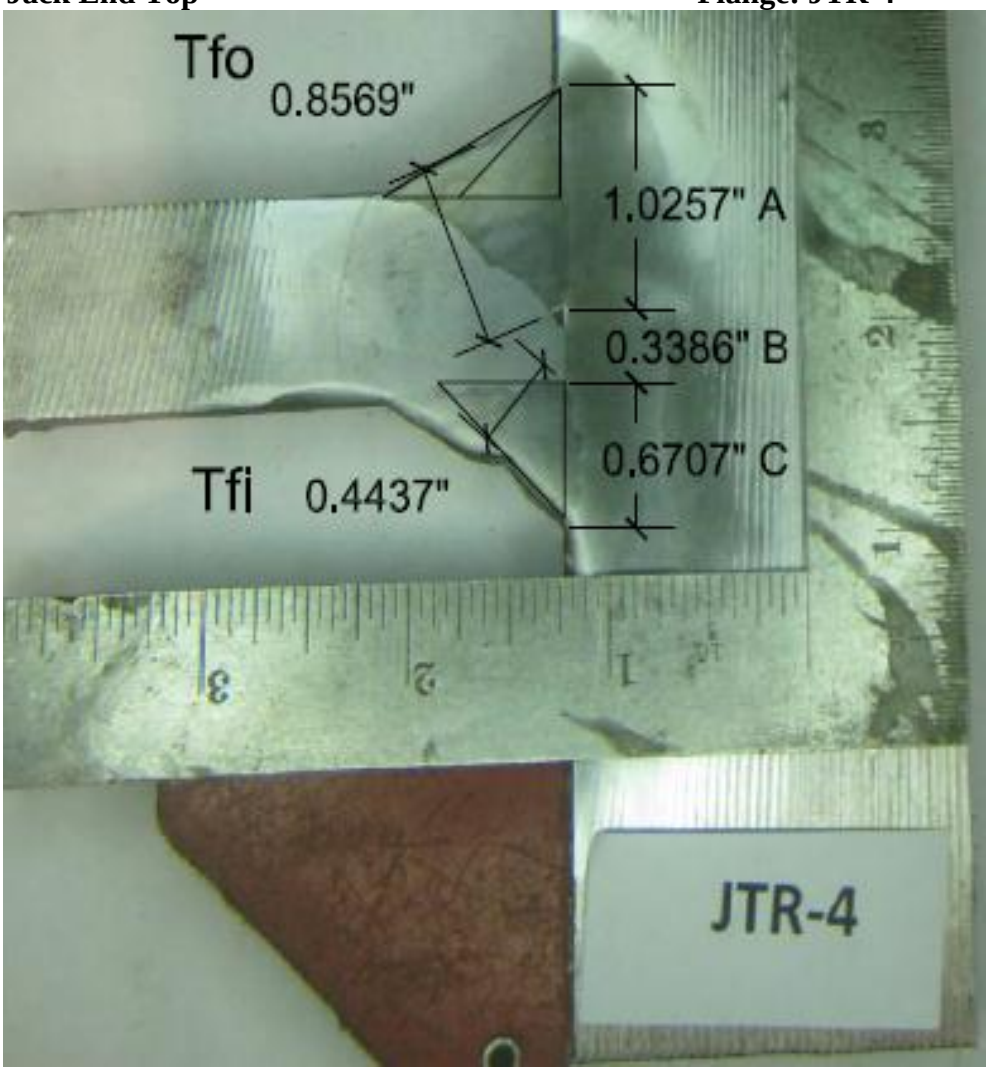

A = Built-up PJP Fillets

B = Lack of Penetration, LOP , Weld Root

C = Reinforcing Fillets

T_{fo} = Throat of A, PJP Fillets

T_{fi} = Throat of C, Reinforcing Fillets

Test: Jack End Top **Flange: JTR-3**

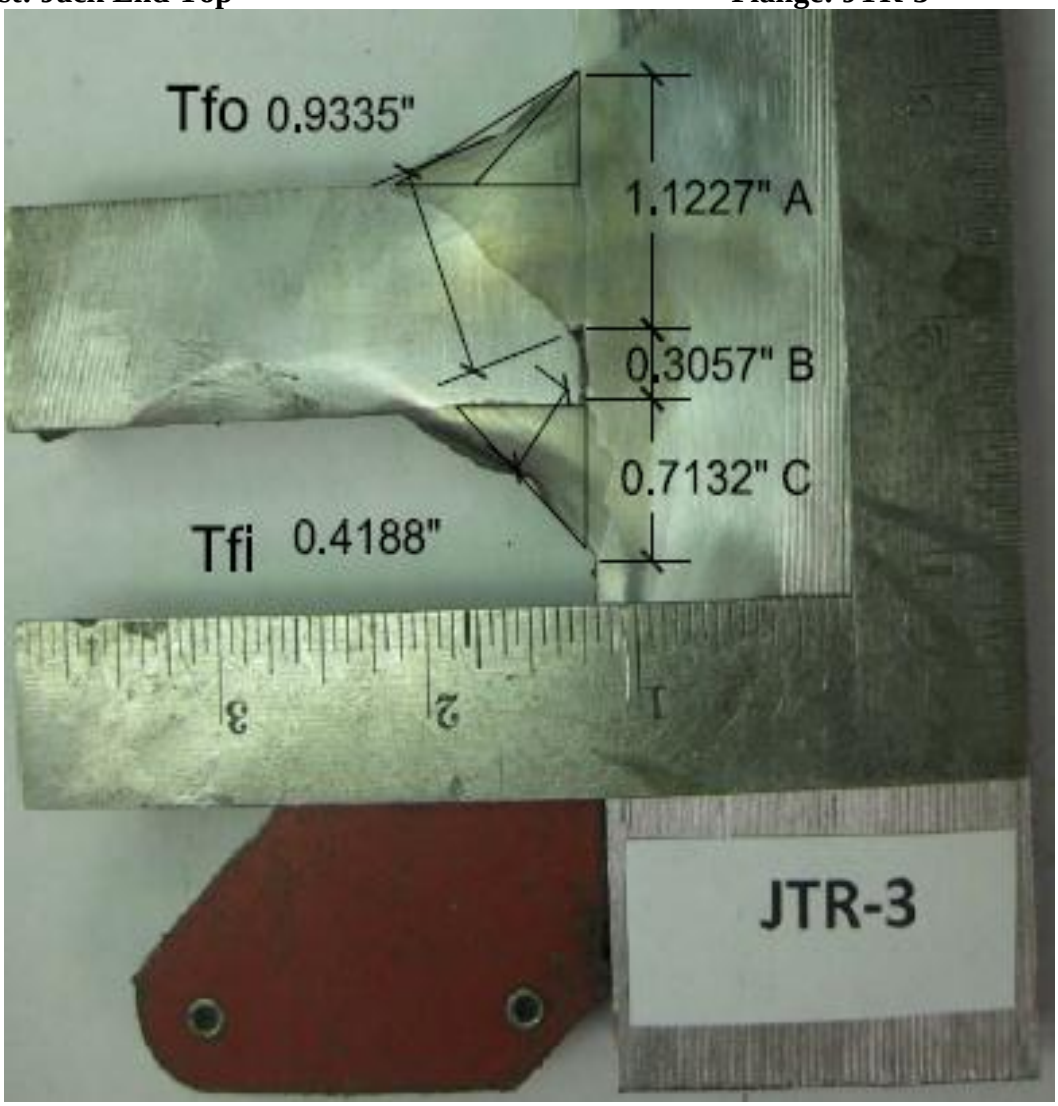

A = Built-up PJP Fillets

B = Lack of Penetration, LOP , Weld Root

C = Reinforcing Fillets

T_{fo} = Throat of A, PJP Fillets

T_{fi} = Throat of C, Reinforcing Fillets

Test: Jack End Top **Flange: JTR-2**

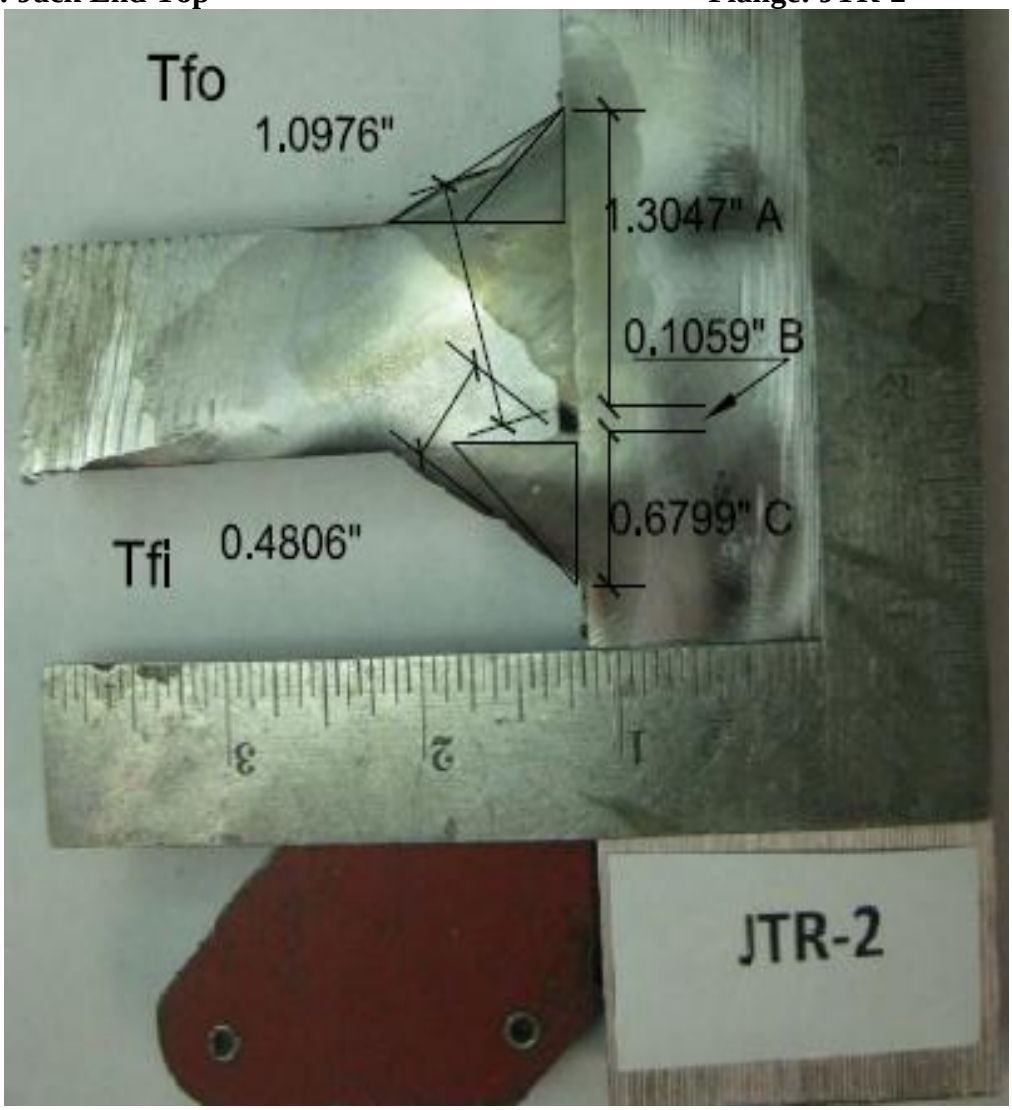

A = Built-up PJP Fillets

B = Lack of Penetration, LOP , Weld Root

C = Reinforcing Fillets

T_{fo} = Throat of A, PJP Fillets

T_{fi} = Throat of C, Reinforcing Fillets

Test: Jack End Top **Flange: JTR-1**

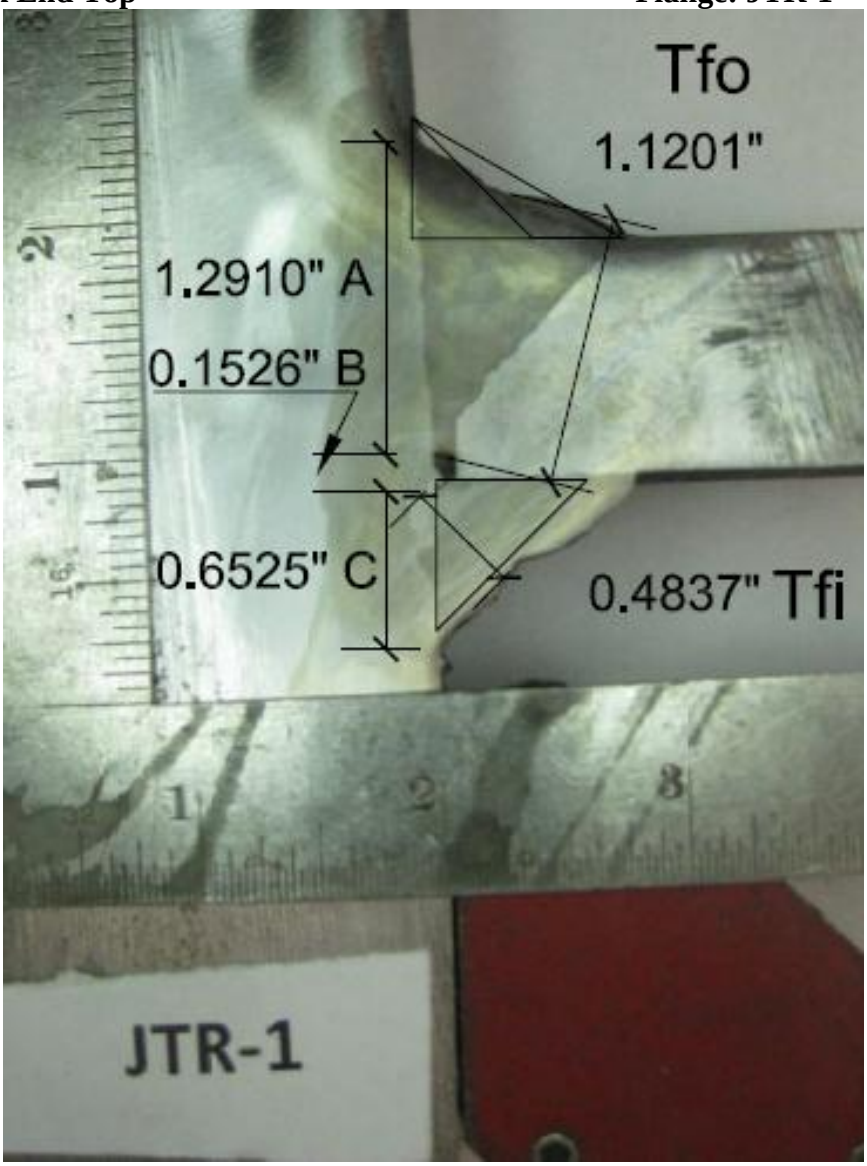

A = Built-up PJP Fillets

B = Lack of Penetration, LOP , Weld Root

C = Reinforcing Fillets

T_{fo} = Throat of A, PJP Fillets

T_{fi} = Throat of C, Reinforcing Fillets

Appendix G - Bottom Side of King End Weld Cuts

Flange to End-plate Modified PJP Weld's Cross Sectional Cuts

Test: King End Bottom **Flange: KB**

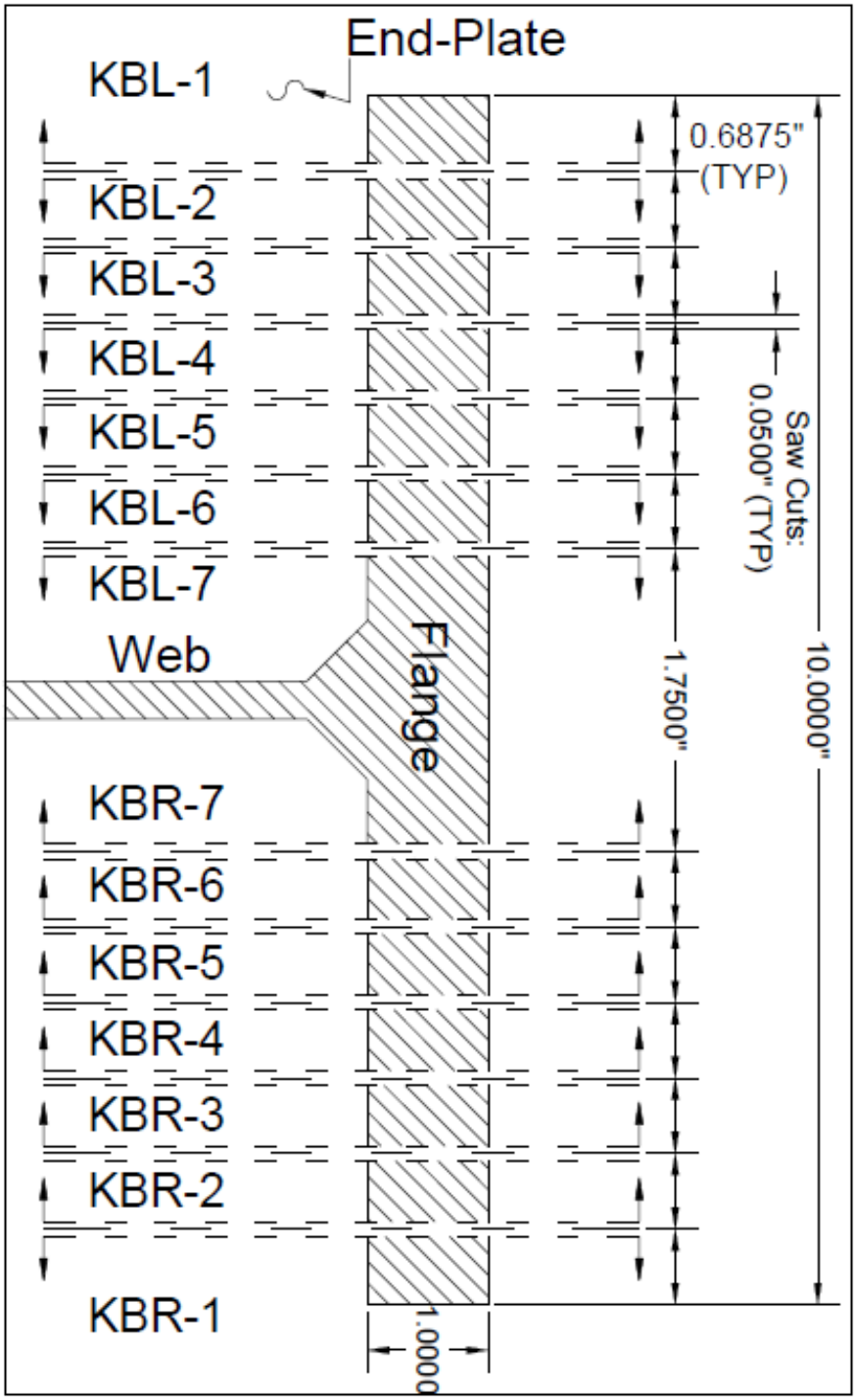

Test End: King Bottom						Flush With EP	
Weld Cut ID:	**PJP Weld Leg A (in.)**	**Root Face & Lack of Penetration B (in.)**	**Reinforcing Fillet Leg C (in.)**	**Measured Effective Throat T_{fo} (in.)**	**Measured Effective Throat T_{fi} (in.)**	**LOP Measured Along EP (in.)**	**Approx. Measured Root Face Along EP (in.)**
KBL-1	1.0407	0.4294	0.6695	0.8667	0.4954	0.178	0.2597
KBL-2	1.002	0.4112	0.641	0.8493	0.4928	0.1626	0.2535
KBL-3	1.0926	0.3777	0.6309	0.9328	0.5142	0.1301	0.255
KBL-4	1.1474	0.3133	0.6861	0.9029	0.544	0.095	0.2218
KBL-5	1.0374	0.3371	0.6871	0.8722	0.5161	0.1041	0.2169
KBL-6	1.1679	0.3396	0.7191	0.8954	0.5652	0.1447	0.1975
KBL-7	1.0962	0.3156	0.7609	0.8944	0.6206	0.1467	0.164
Average:	**1.0835**	**0.3606**	**0.6849**	**0.8877**	**0.5355**	**0.1373**	**0.2241**
KBR-7	1.2157	0.1977	0.7519	0.9749	0.5721	0.0884	0.1489
KBR-6	1.0873	0.3218	0.722	0.8633	0.4782	0.14	0.1935
KBR-5	1.071	0.3297	0.7763	0.856	0.4745	0.3297	0*
KBR-4	1.1229	0.2736	0.6994	0.8942	0.5322	0.2736	0*
KBR-3	1.2117	0.2274	0.6578	0.9991	0.4951	0.2274	0*
KBR-2	1.219	0.1961	0.7099	0.8951	0.5267	0.1961	0*
KBR-1	1.1808	0.1962	0.679	0.9588	0.5388	0.1962	0*
Average:	**1.1583**	**0.2489**	**0.7138**	**0.9202**	**0.5168**	**0.2073**	**0.1712**
Total Avg:	**1.1209**	**0.3047**	**0.6994**	**0.9039**	**0.5261**	**0.1723**	**0.1976**
						*** Denotes Poor Fitup**	

Fillet sizes of flange to end-plate welds				
Specimen ID:	**Outside (Groove Side)**		**Inside**	
KBL	**Flange Side (OF)**	**End-plate Side (OE)**	**Flange Side (IF)**	**End-plate Side (IE)**
1	1	7/16	7/8	5/8
2	1	1/2	15/16	5/8
3	15/16	1/2	15/16	5/8
4	1	1/2	7/8	3/4
5	7/8	1/2	7/8	3/4
6	7/8	1/2	7/8	3/4
7	7/8	1/2	1	5/8
Avg	0.9375	0.4911	0.9107	0.6786
Design	0.5000	0.5000	0.6250	0.6250
Avg/Design	**1.8750**	**0.9821**	**1.4571**	**1.0857**
Specimen ID:	**Outside (Groove Side)**		**Inside**	
KBR	**Flange Side (OF)**	**End-plate Side (OE)**	**Flange Side (IF)**	**End-plate Side (IE)**
1	7/8	1/2	7/8	5/8
2	7/8	1/2	7/8	5/8
3	7/8	1/2	7/8	5/8
4	3/4	1/2	3/4	5/8
5	3/4	1/2	7/8	5/8
6	3/4	1/2	3/4	3/4
7	7/8	1/2	3/4	5/8
Avg	0.8214	0.5000	0.8214	0.6429
Design	0.5000	0.5000	0.6250	0.6250
Avg/Design	**1.6429**	**1.0000**	**1.3143**	**1.0286**

Test: King End Bottom **Flange: KBL-1**

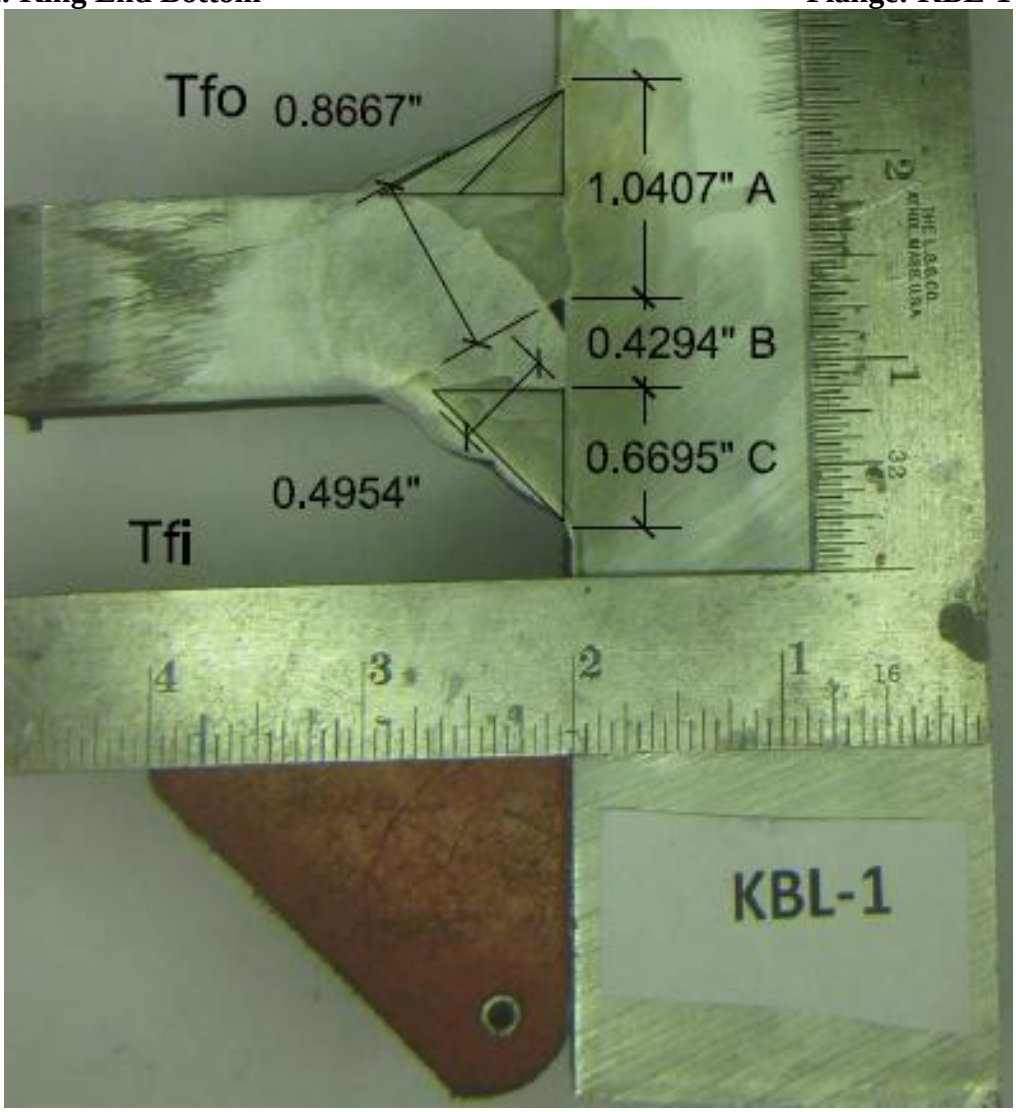

A = Built-up PJP Fillets

B = Lack of Penetration, LOP , Weld Root

C = Reinforcing Fillets

T_{fo} = Throat of A, PJP Fillets

T_{fi} = Throat of C, Reinforcing Fillets

Test: King End Bottom **Flange: KBL-2**

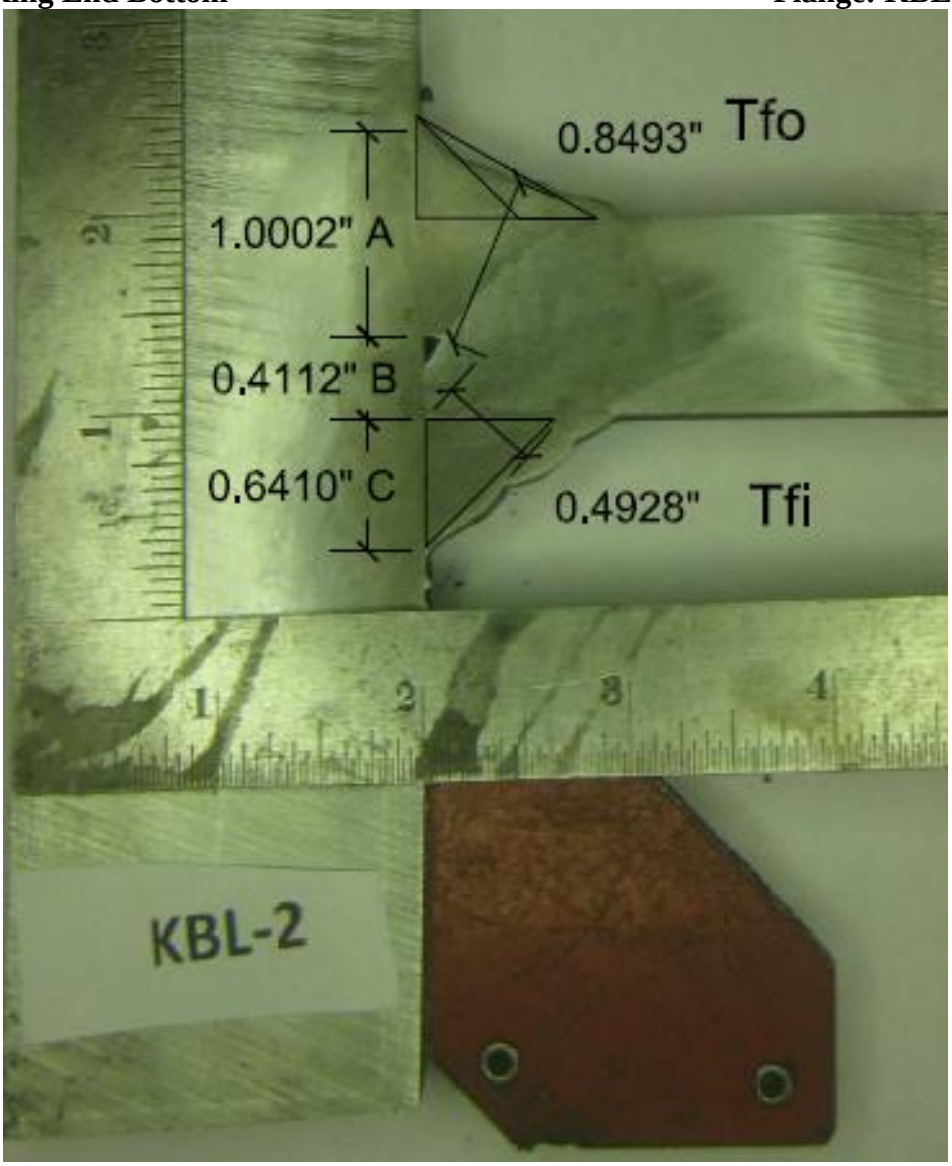

A = Built-up PJP Fillets

B = Lack of Penetration, LOP , Weld Root

C = Reinforcing Fillets

T_{fo} = Throat of A, PJP Fillets

T_{fi} = Throat of C, Reinforcing Fillets

Test: King End Bottom **Flange: KBL-3**

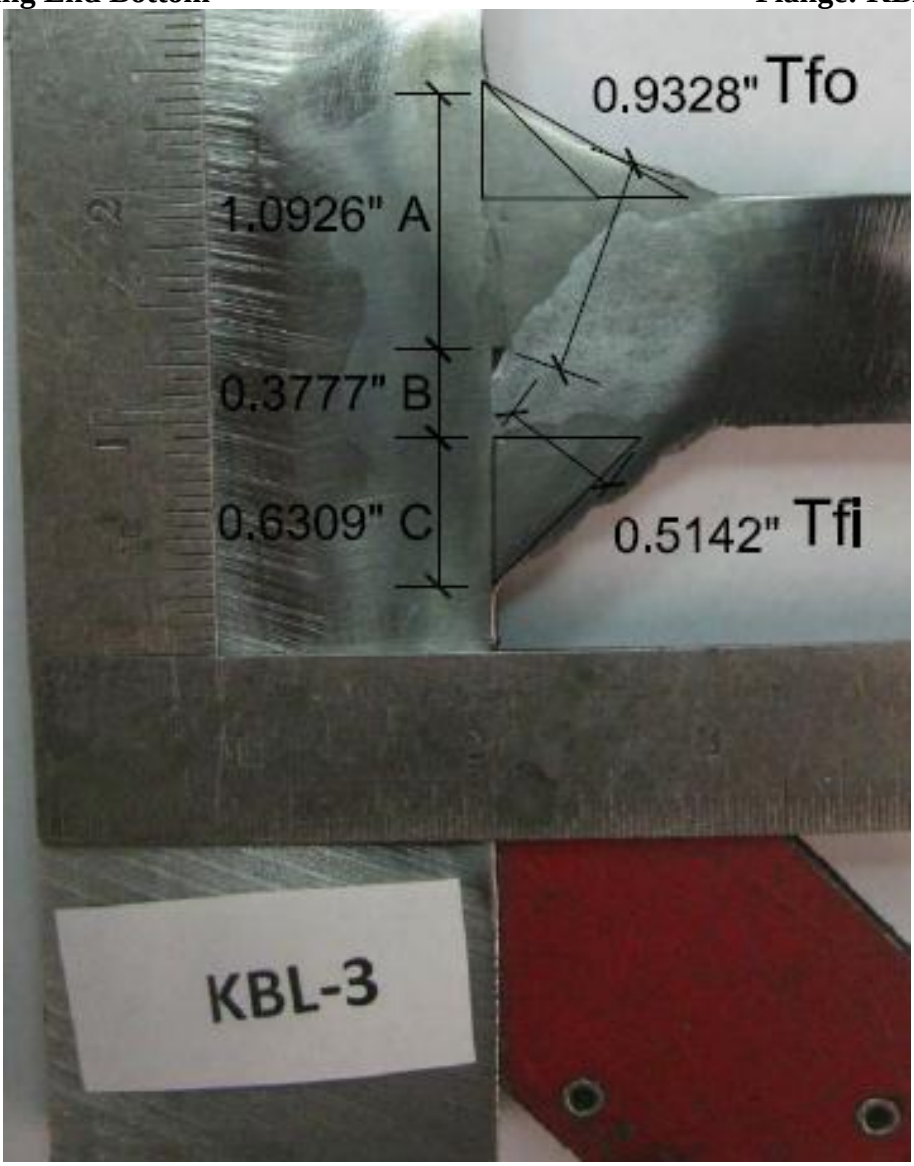

A = Built-up PJP Fillets

B = Lack of Penetration, LOP , Weld Root

C = Reinforcing Fillets

T_{fo} = Throat of A, PJP Fillets

T_{fi} = Throat of C, Reinforcing Fillets

Test: King End Bottom **Flange: KBL-4**

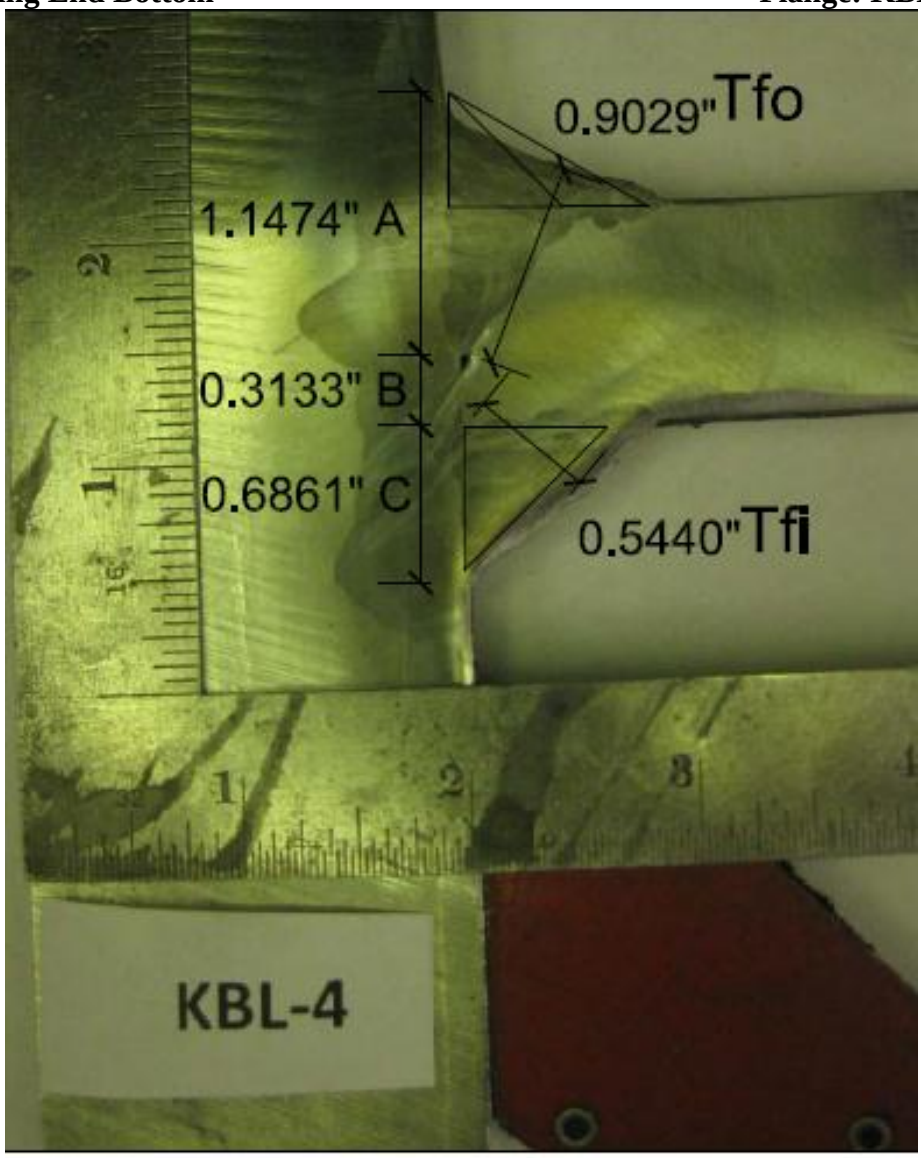

A = Built-up PJP Fillets

B = Lack of Penetration, LOP , Weld Root

C = Reinforcing Fillets

T_{fo} = Throat of A, PJP Fillets

T_{fi} = Throat of C, Reinforcing Fillets

Test: King End Bottom **Flange: KBL-5**

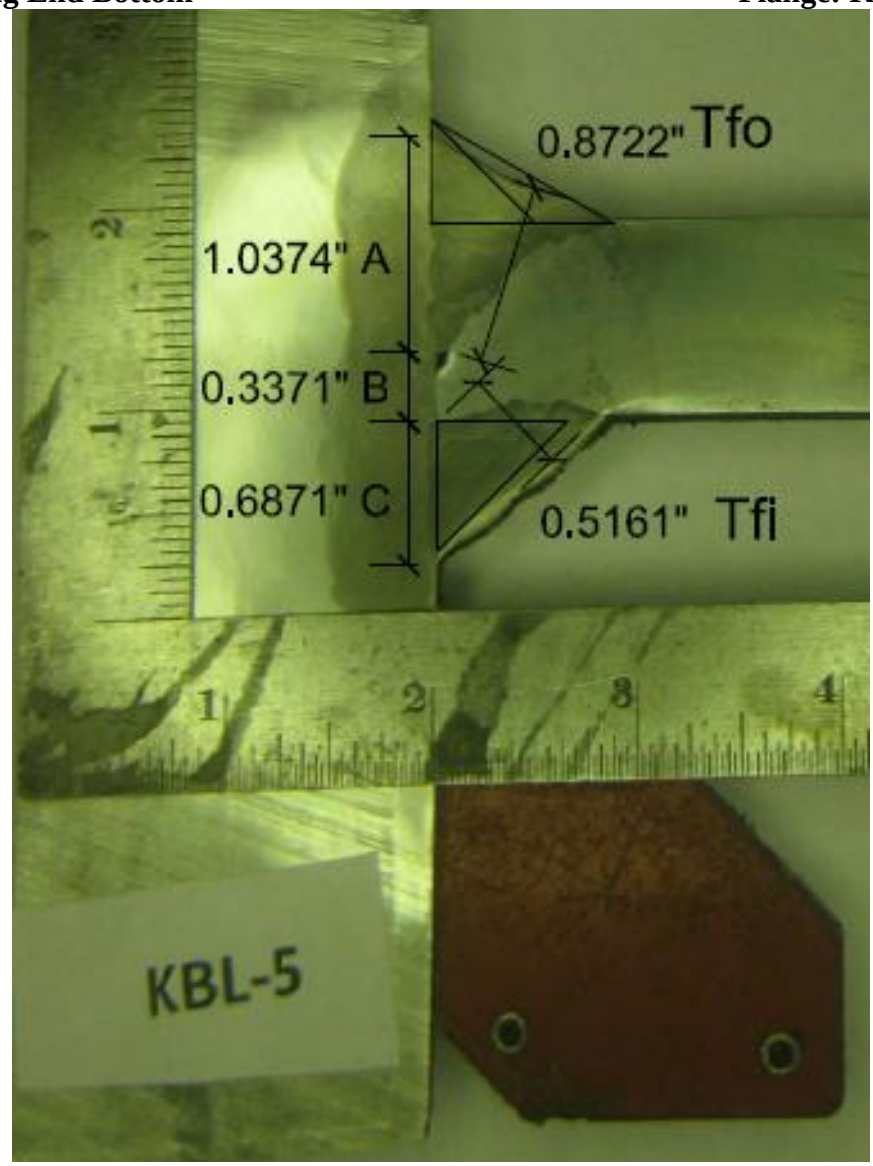

A = Built-up PJP Fillets

B = Lack of Penetration, LOP , Weld Root

C = Reinforcing Fillets

T_{fo} = Throat of A, PJP Fillets

T_{fi} = Throat of C, Reinforcing Fillets

Test: King End Bottom **Flange: KBL-6**

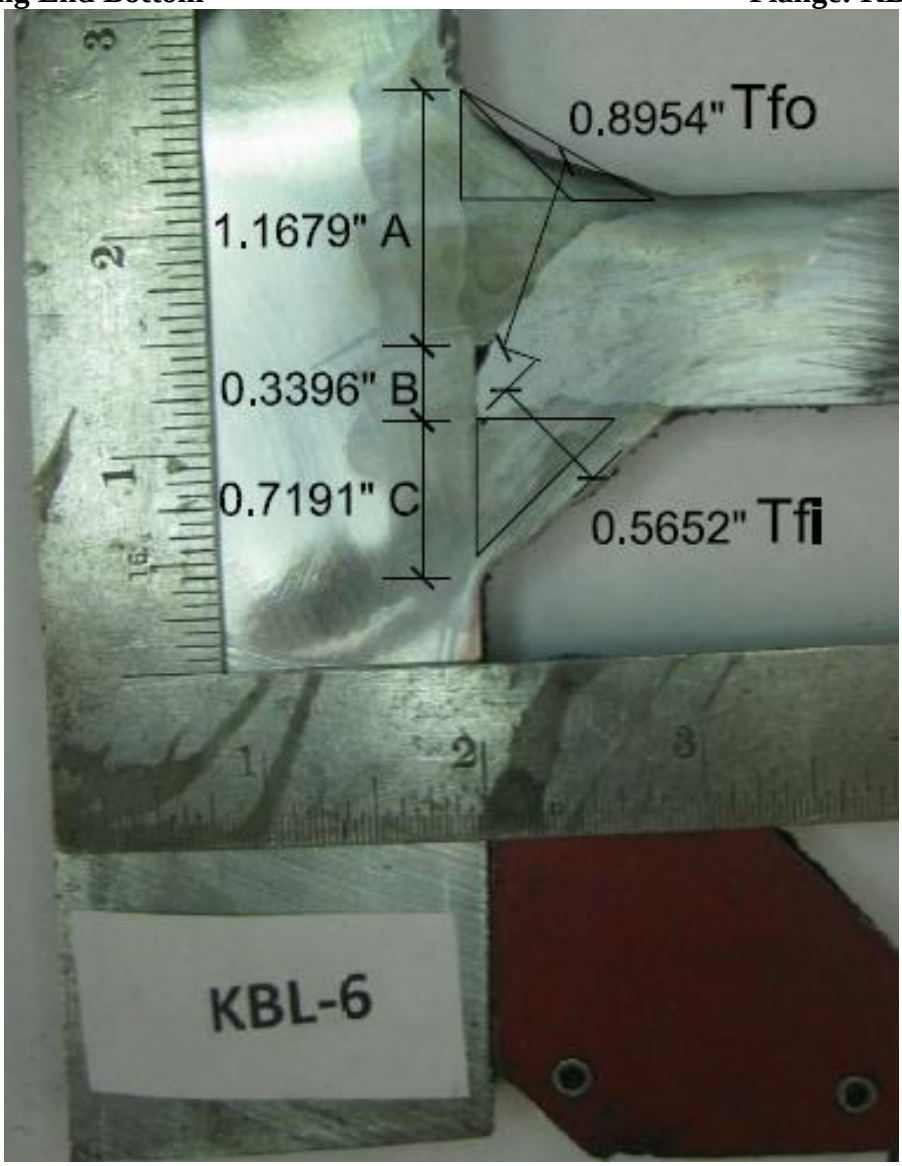

A = Built-up PJP Fillets

B = Lack of Penetration, LOP , Weld Root

C = Reinforcing Fillets

T_{fo} = Throat of A, PJP Fillets

T_{fi} = Throat of C, Reinforcing Fillets

Test: King End Bottom **Flange: KBL-7**

A = Built-up PJP Fillets

B = Lack of Penetration, LOP , Weld Root

C = Reinforcing Fillets

T_{fo} = Throat of A, PJP Fillets

T_{fi} = Throat of C, Reinforcing Fillets

Test: King End Bottom **Flange: KBR-7**

A = Built-up PJP Fillets

B = Lack of Penetration, LOP , Weld Root

C = Reinforcing Fillets

T_{fo} = Throat of A, PJP Fillets

T_{fi} = Throat of C, Reinforcing Fillets

Test: King End Bottom **Flange: KBR-6**

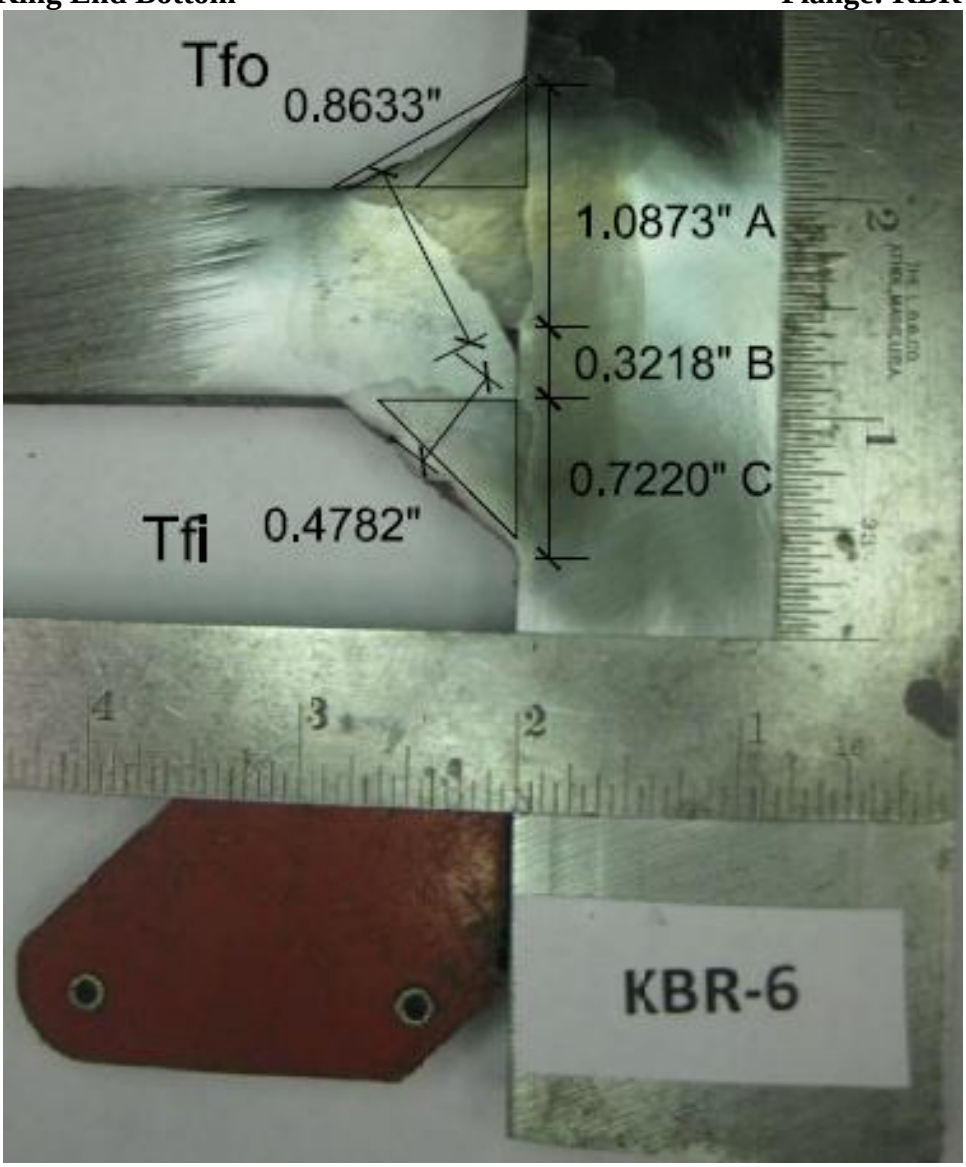

A = Built-up PJP Fillets

B = Lack of Penetration, LOP , Weld Root

C = Reinforcing Fillets

T_{fo} = Throat of A, PJP Fillets

T_{fi} = Throat of C, Reinforcing Fillets

Test: King End Bottom **Flange: KBR-5**

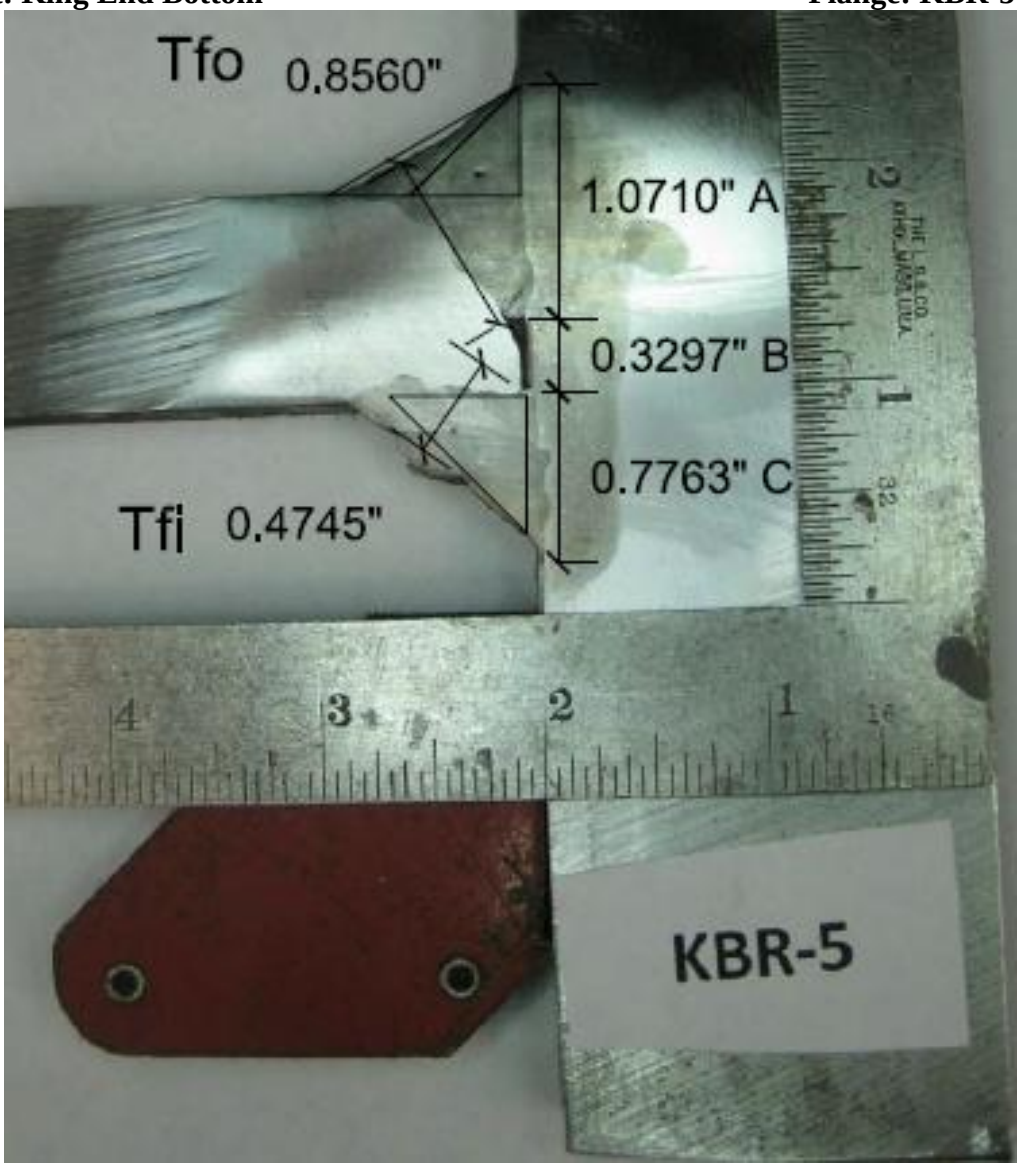

A = Built-up PJP Fillets

B = Lack of Penetration, LOP , Weld Root

C = Reinforcing Fillets

T_{fo} = Throat of A, PJP Fillets

T_{fi} = Throat of C, Reinforcing Fillets

Test: King End Bottom **Flange: KBR-4**

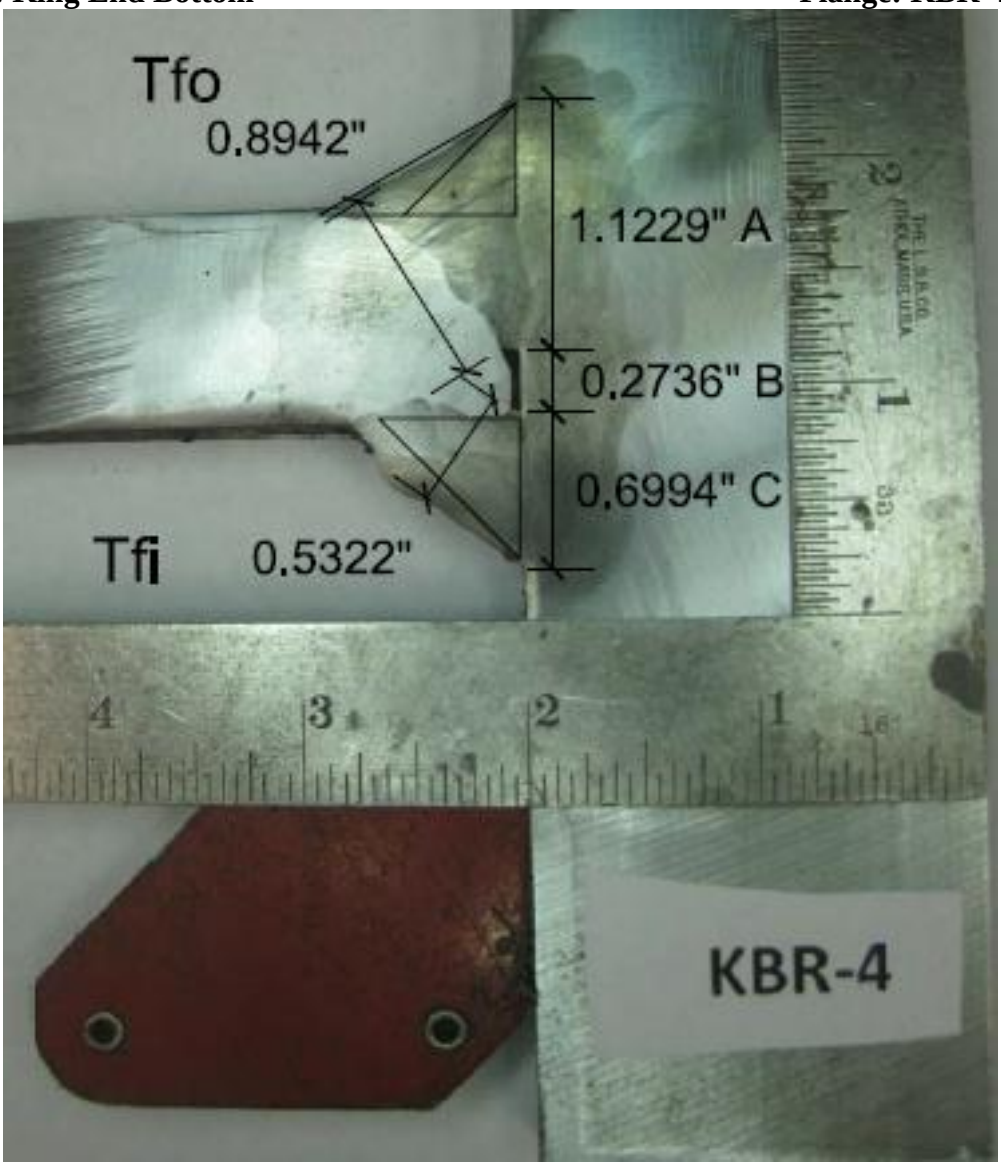

A = Built-up PJP Fillets

B = Lack of Penetration, LOP , Weld Root

C = Reinforcing Fillets

T_{fo} = Throat of A, PJP Fillets

T_{fi} = Throat of C, Reinforcing Fillets

Test: King End Bottom **Flange: KBR-3**

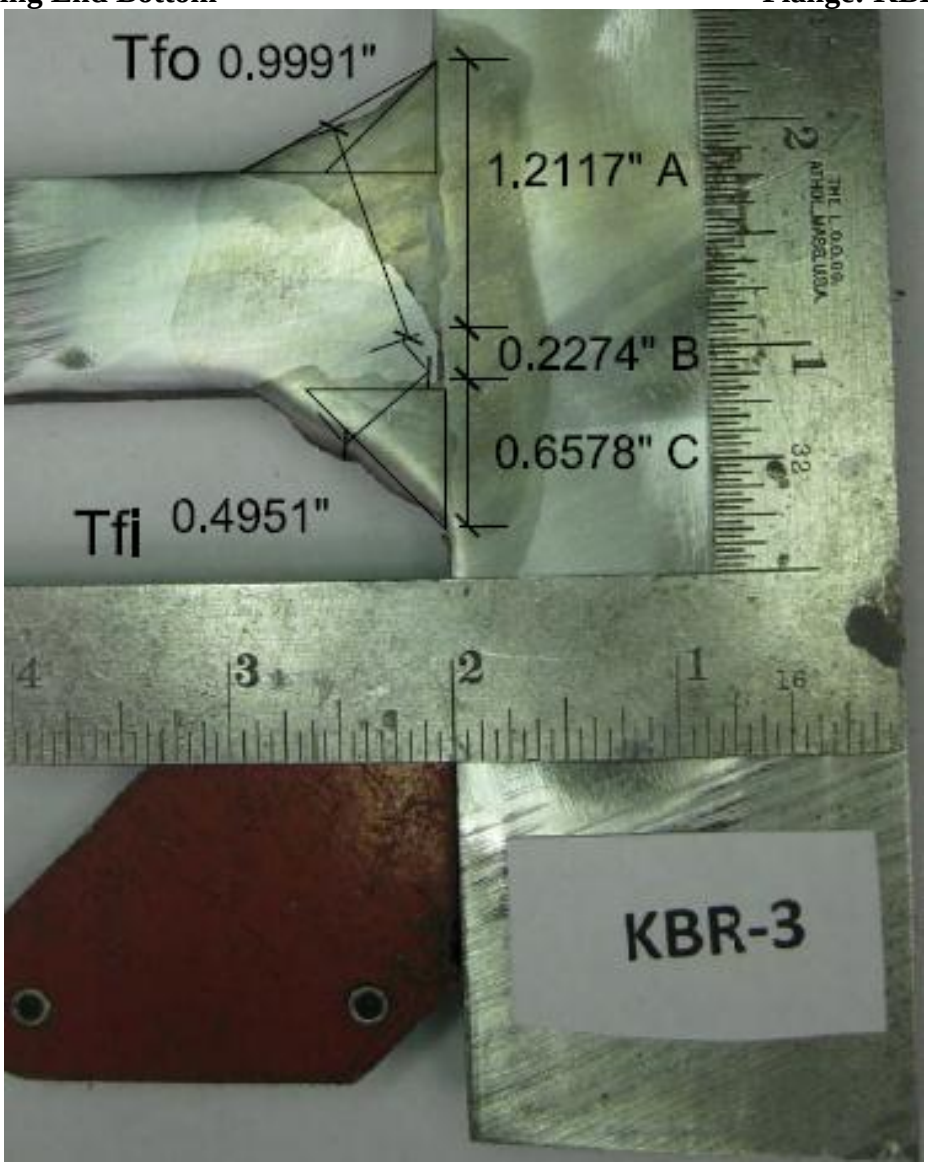

A = Built-up PJP Fillets

B = Lack of Penetration, LOP , Weld Root

C = Reinforcing Fillets

T_{fo} = Throat of A, PJP Fillets

T_{fi} = Throat of C, Reinforcing Fillets

Test: King End Bottom **Flange: KBR-2**

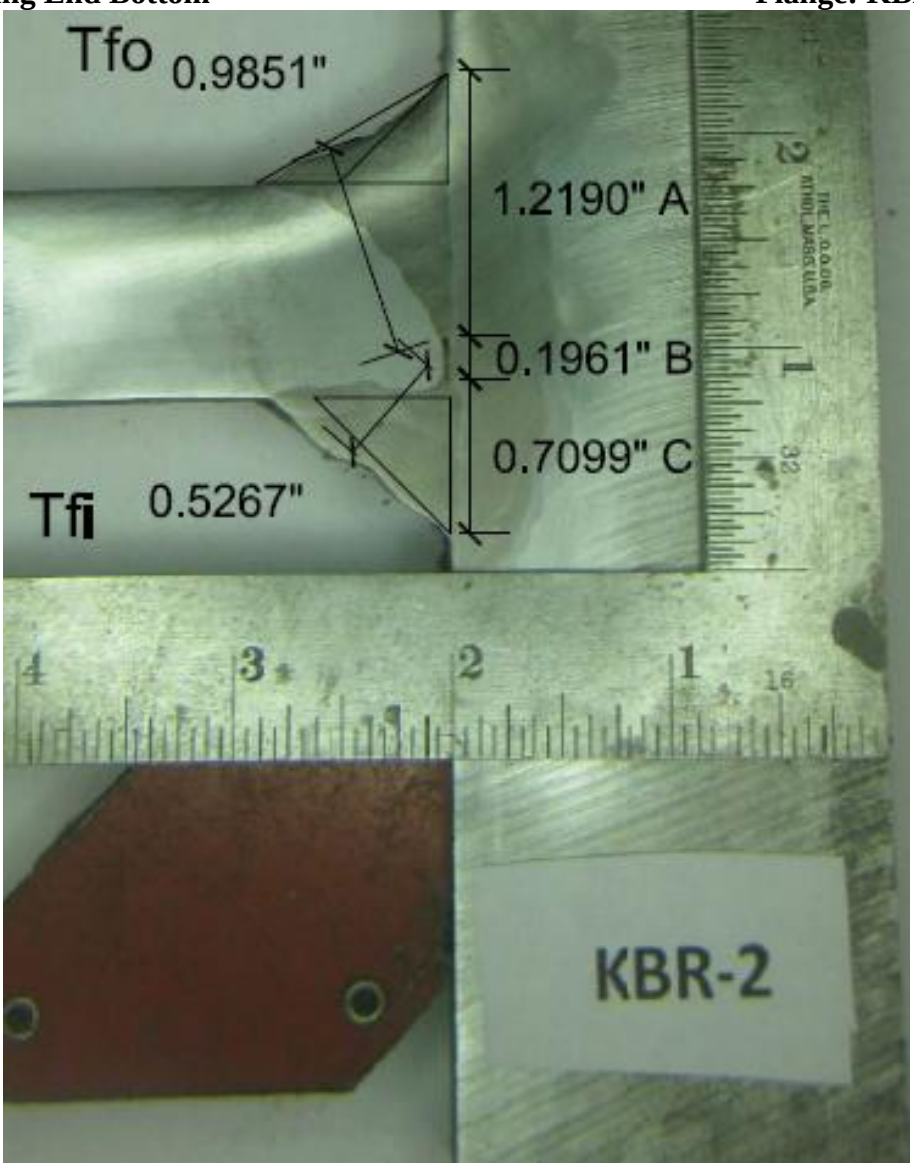

A = Built-up PJP Fillets

B = Lack of Penetration, LOP , Weld Root

C = Reinforcing Fillets

T_{fo} = Throat of A, PJP Fillets

T_{fi} = Throat of C, Reinforcing Fillets

Test: King End Bottom **Flange: KBR-1**

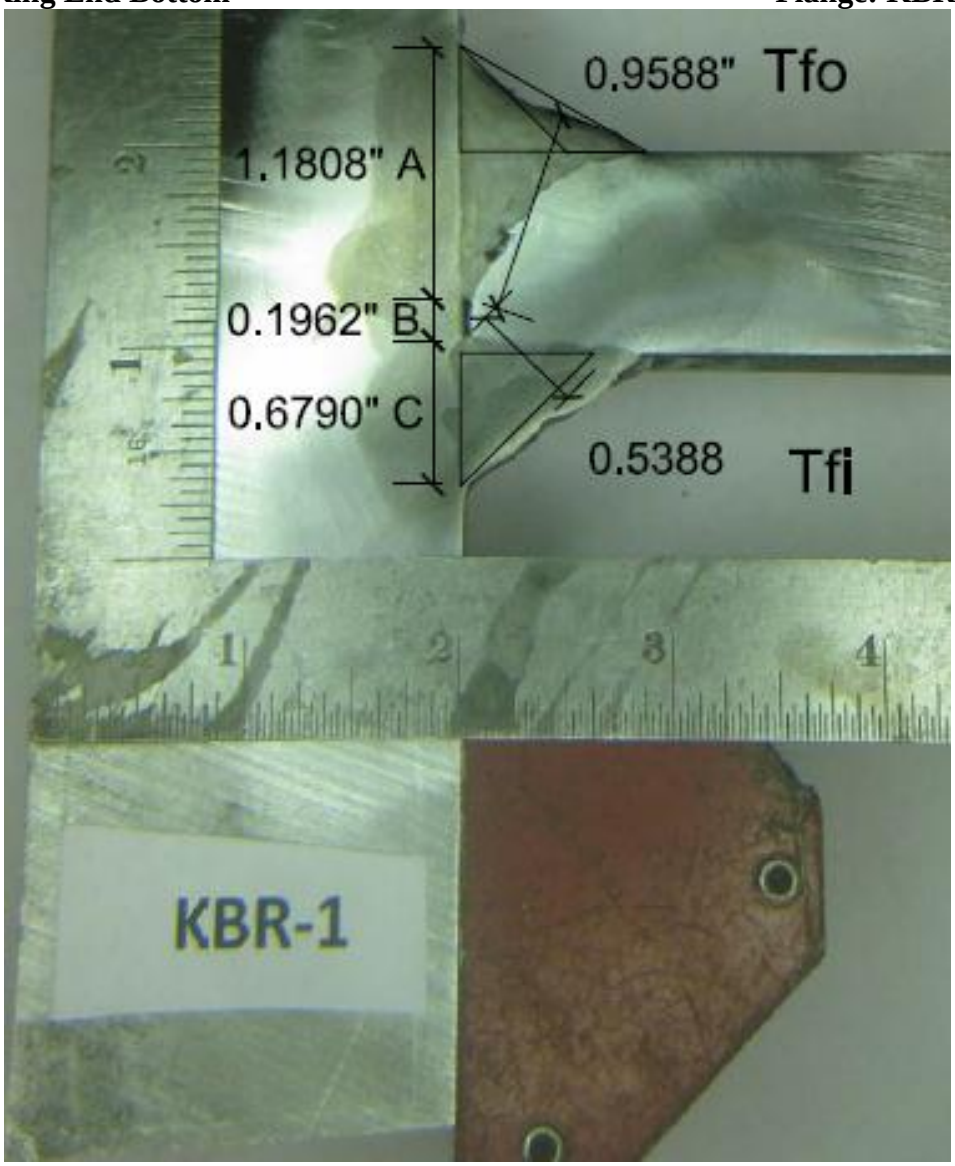

A = Built-up PJP Fillets

B = Lack of Penetration, LOP , Weld Root

C = Reinforcing Fillets

T_{fo} = Throat of A, PJP Fillets

T_{fi} = Throat of C, Reinforcing Fillets

Appendix H - Top Side of King End Weld Cuts

Flange to End-plate Modified PJP Weld's Cross Sectional Cuts

Test: King End Top **Flange: KT**

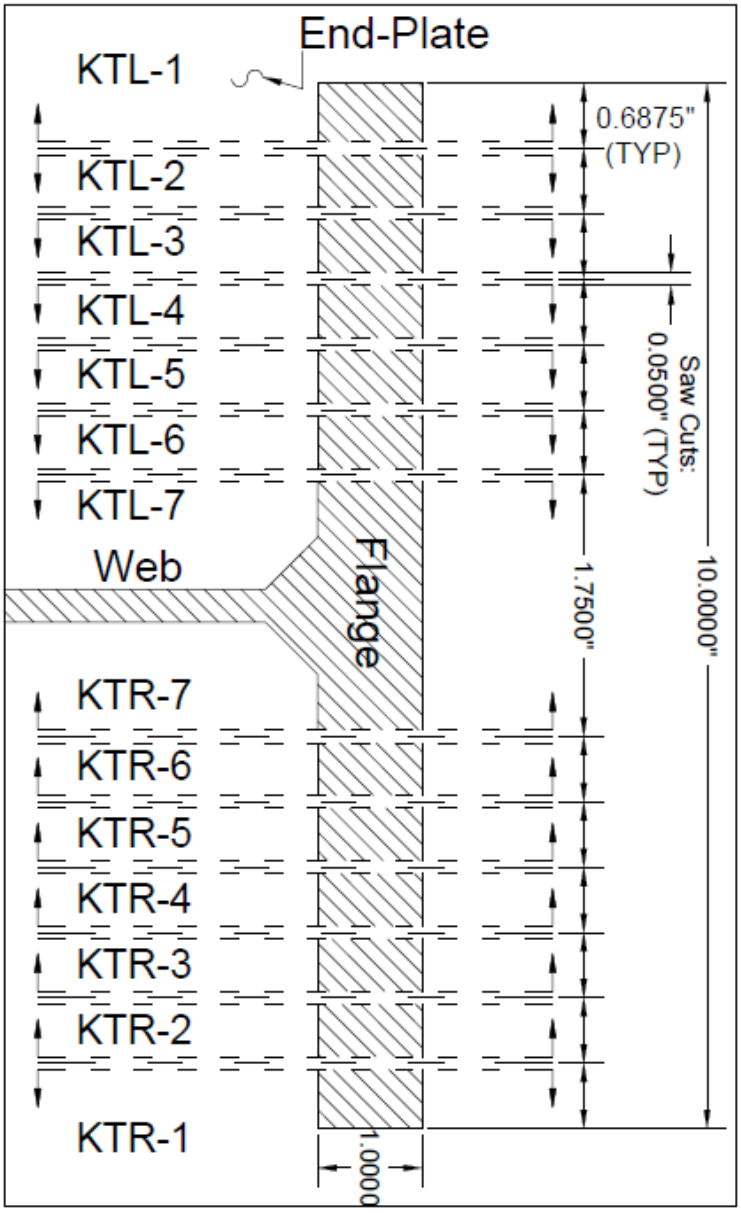

Test End: King Top						Flush With EP	
Weld Cut ID:	**PJP Weld Leg A (in.)**	**Root Face & Lack of Penetration B (in.)**	**Reinforcing Fillet Leg C (in.)**	**Measured Effective Throat T_{fo} (in.)**	**Measured Effective Throat T_{fi} (in.)**	**LOP Measured Along EP (in.)**	**Approx. Measured Root Face Along EP (in.)**
KTL-1	1.4021	0	0.7085	1.1222	0.5734	0	0
KTL-2	1.2774	0.0479	0.7978	1.0886	0.5343	0.0479	0*
KTL-3	1.1357	0.3109	0.7272	0.9116	0.4978	0.1848	0.1235
KTL-4	1.1297	0.3642	0.6859	0.8898	0.4559	0.1605	0.1755
KTL-5	1.2349	0.2367	0.7369	0.9782	0.4579	0	0.2367
KTL-6	1.1657	0.2558	0.7332	0.9753	0.5496	0.0681	0.2126
KTL-7	1.0755	0.3817	0.7258	0.8245	0.547	0.2509	0.2319
Average:	**1.2030**	**0.2282**	**0.7308**	**0.970028571**	**0.516557143**	**0.1017**	**0.1960**
KTR-7	1.0821	0.3304	0.6932	0.8238	0.5311	0.1351	0.2001
KTR-6	1.1657	0.302	0.6802	0.897	0.5249	0.1091	0.2055
KTR-5	1.0009	0.3544	0.6628	0.9549	0.4691	0.1337	0.2223
KTR-4	1.1296	0.2744	0.6503	0.9135	0.5086	0.1271	0.1613
KTR-3	1.2843	0.1031	0.6332	1.0746	0.543	0	0.1031
KTR-2	1.0654	0.4042	0.705	0.7689	0.5409	0.2537	0.1623
KTR-1	1.2378	0.2126	0.8153	0.9856	0.5821	0	0.2126
Average:	**1.1380**	**0.2830**	**0.6914**	**0.9169**	**0.528528571**	**0.1084**	**0.1810**
Total Avg:	**1.1705**	**0.2556**	**0.7111**	**0.943464286**	**0.522542857**	**0.1051**	**0.1885**
						*** Denotes Poor Fitup**	

Fillet sizes of flange to end-plate welds				
Specimen ID:	**Outside (Groove Side)**		**Inside**	
KTR	**Flange Side (OF)**	**End-plate Side (OE)**	**Flange Side (IF)**	**End-plate Side (IE)**
1	7/8	1/2	7/8	3/4
2	7/8	1/2	7/8	3/4
3	7/8	1/2	3/4	5/8
4	7/8	1/2	3/4	5/8
5	7/8	1/2	3/4	5/8
6	7/8	1/2	3/4	5/8
7	7/8	1/2	3/4	5/8
Avg	0.8750	0.5000	0.7857	0.6607
Design	0.5000	0.5000	0.6250	0.6250
Avg/Design	**1.7500**	**1.0000**	**1.2571**	**1.0571**
Specimen ID:	**Outside (Groove Side)**		**Inside**	
KTL	**Flange Side (OF)**	**End-plate Side (OE)**	**Flange Side (IF)**	**End-plate Side (IE)**
1	1	1/2	7/8	3/4
2	7/8	3/4	7/8	1/2
3	7/8	1/2	7/8	5/8
4	7/8	1/2	7/8	5/8
5	7/8	1/2	7/8	5/8
6	1	1/2	7/8	5/8
7	7/8	1/2	7/8	5/8
Avg	0.9107	0.5357	0.8750	0.6250
Design	0.5000	0.5000	0.6250	0.6250
Avg/Design	**1.8214**	**1.0714**	**1.4000**	**1.0000**

Test: King End Top **Flange: KTL-1**

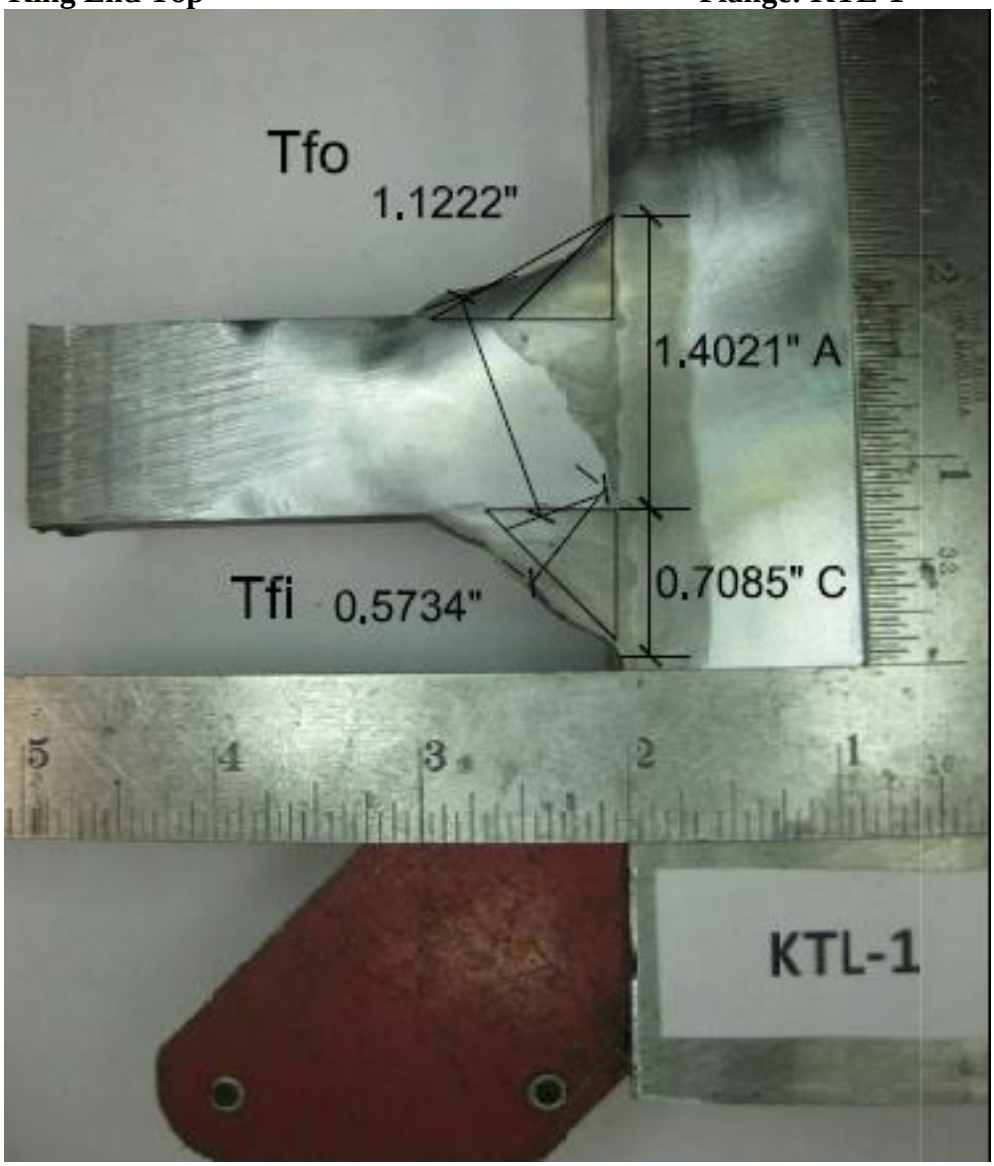

A = Built-up PJP Fillets

B = Lack of Penetration, LOP , Weld Root

C = Reinforcing Fillets

T_{fo} = Throat of A, PJP Fillets

T_{fi} = Throat of C, Reinforcing Fillets

Test: King End Top **Flange: KTL-2**

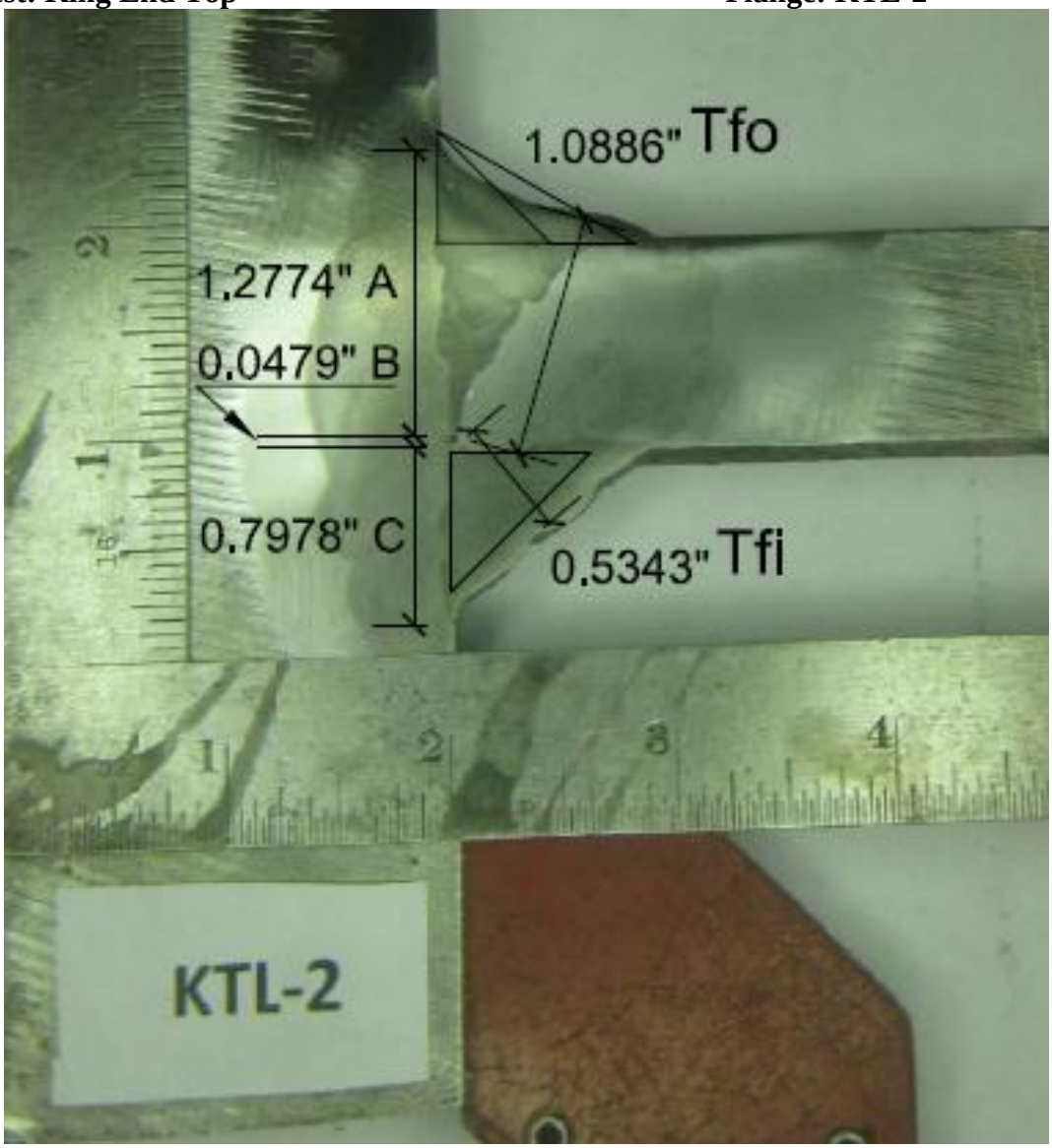

A = Built-up PJP Fillets

B = Lack of Penetration, LOP , Weld Root

C = Reinforcing Fillets

T_{fo} = Throat of A, PJP Fillets

T_{fi} = Throat of C, Reinforcing Fillets

Test: King End Top **Flange: KTL-3**

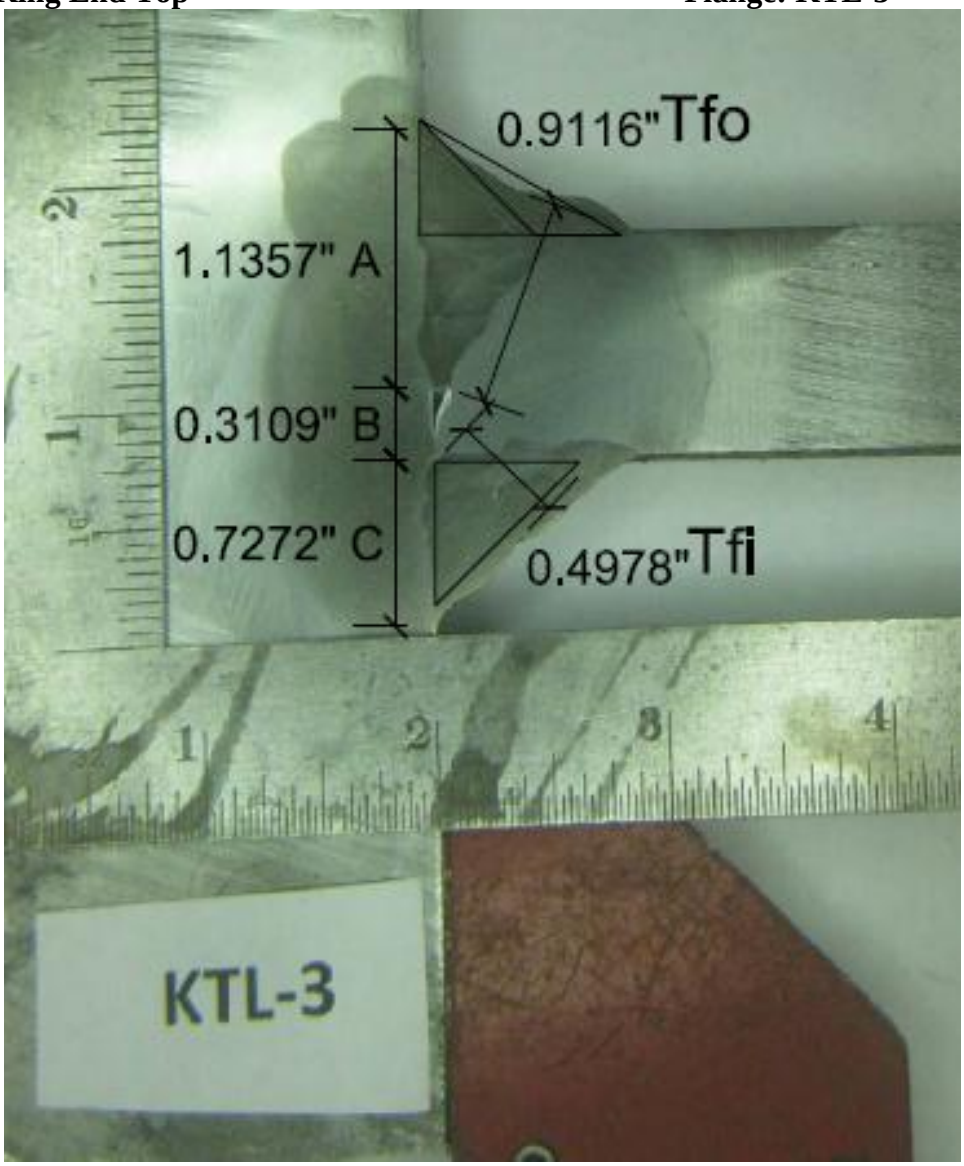

A = Built-up PJP Fillets

B = Lack of Penetration, LOP , Weld Root

C = Reinforcing Fillets

T_{fo} = Throat of A, PJP Fillets

T_{fi} = Throat of C, Reinforcing Fillets

Test: King End Top **Flange: KTL-4**

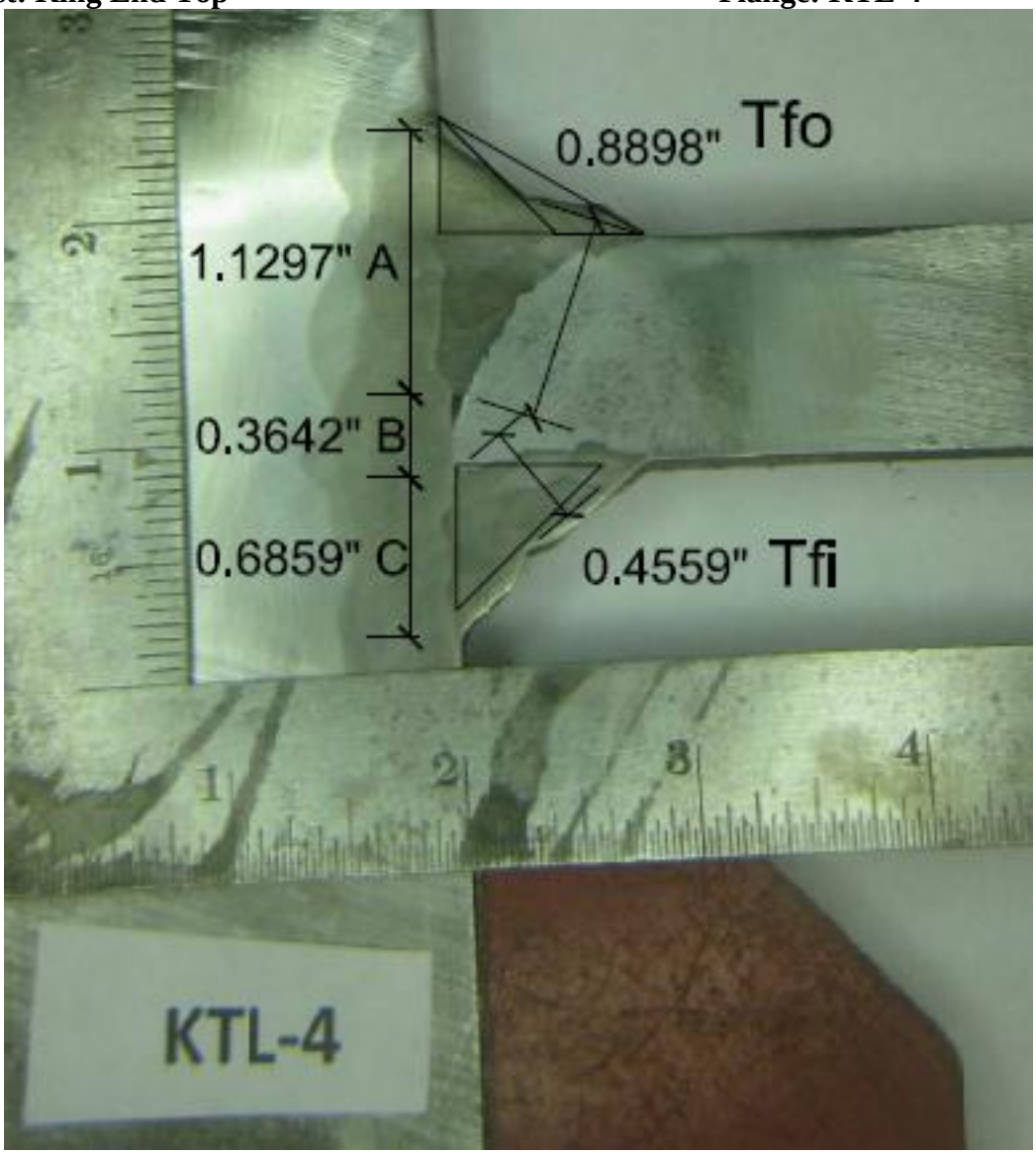

A = Built-up PJP Fillets

B = Lack of Penetration, LOP , Weld Root

C = Reinforcing Fillets

T_{fo} = Throat of A, PJP Fillets

T_{fi} = Throat of C, Reinforcing Fillets

Test: King End Top **Flange: KTL-5**

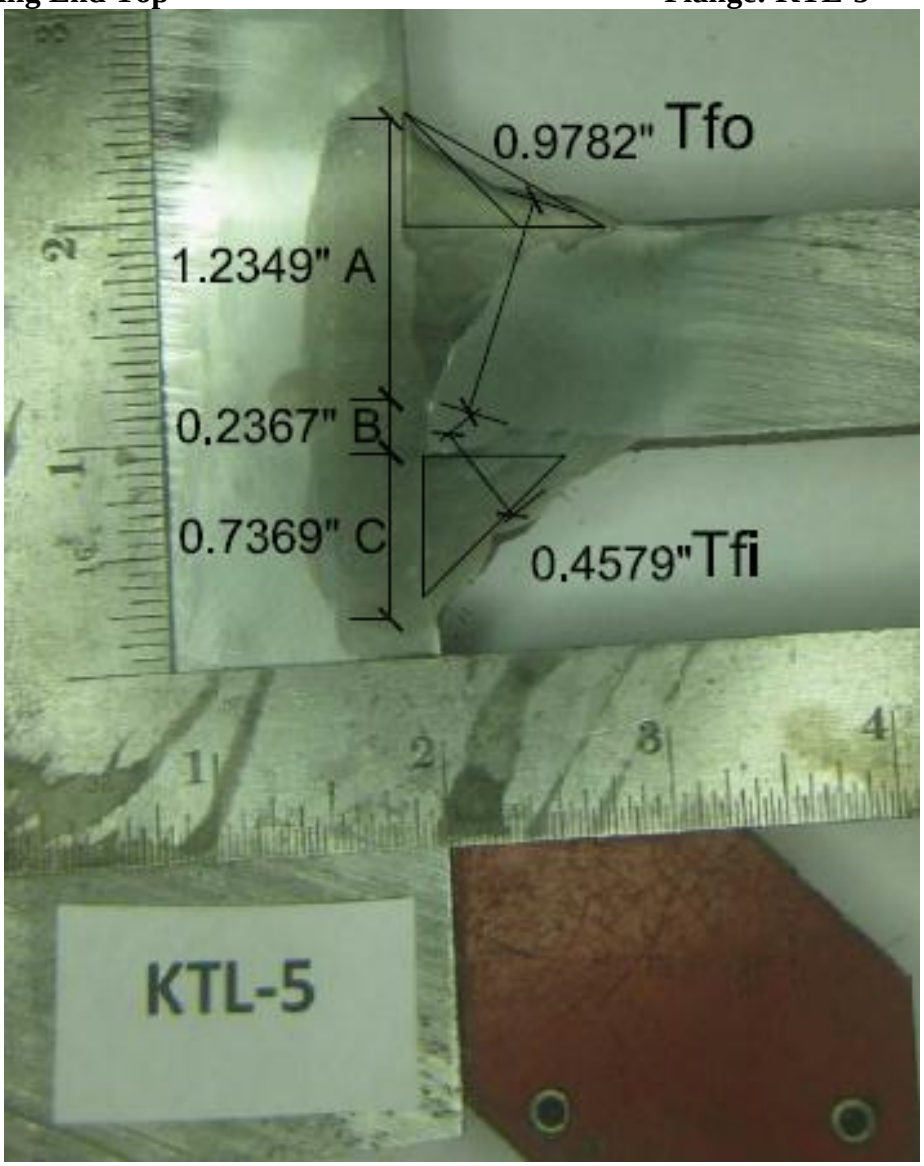

A = Built-up PJP Fillets

B = Lack of Penetration, LOP , Weld Root

C = Reinforcing Fillets

T_{fo} = Throat of A, PJP Fillets

T_{fi} = Throat of C, Reinforcing Fillets

Test: King End Top **Flange: KTL-6**

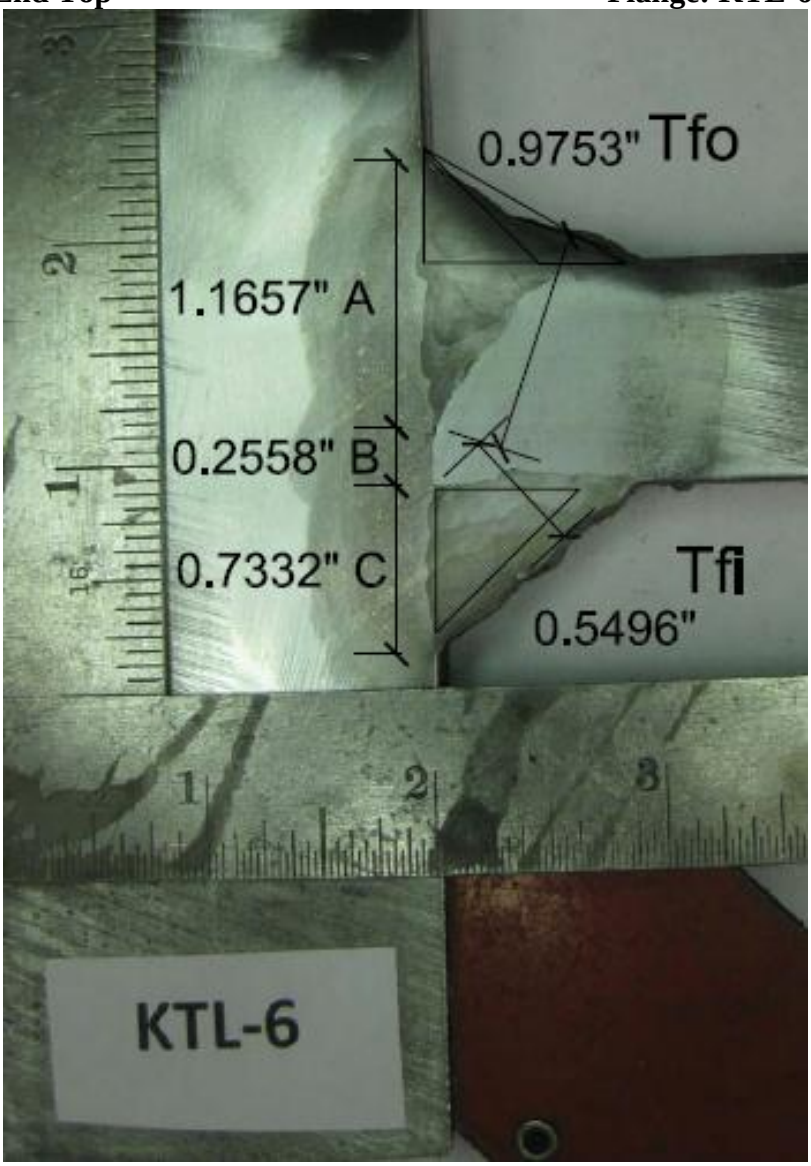

A = Built-up PJP Fillets

B = Lack of Penetration, LOP , Weld Root

C = Reinforcing Fillets

T_{fo} = Throat of A, PJP Fillets

T_{fi} = Throat of C, Reinforcing Fillets

Test: King End Top **Flange: KTL-7**

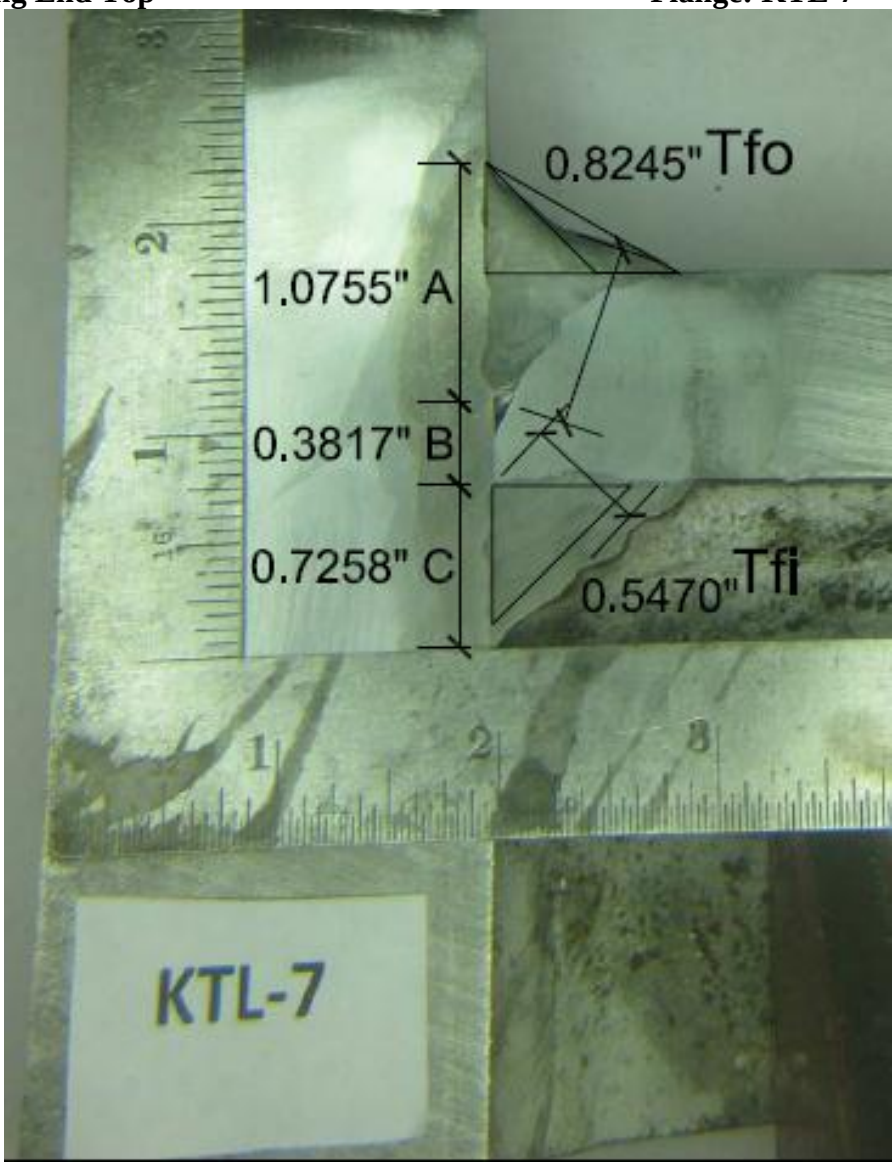

A = Built-up PJP Fillets

B = Lack of Penetration, LOP , Weld Root

C = Reinforcing Fillets

T_{fo} = Throat of A, PJP Fillets

T_{fi} = Throat of C, Reinforcing Fillets

Test: King End Top **Flange: KTR-7**

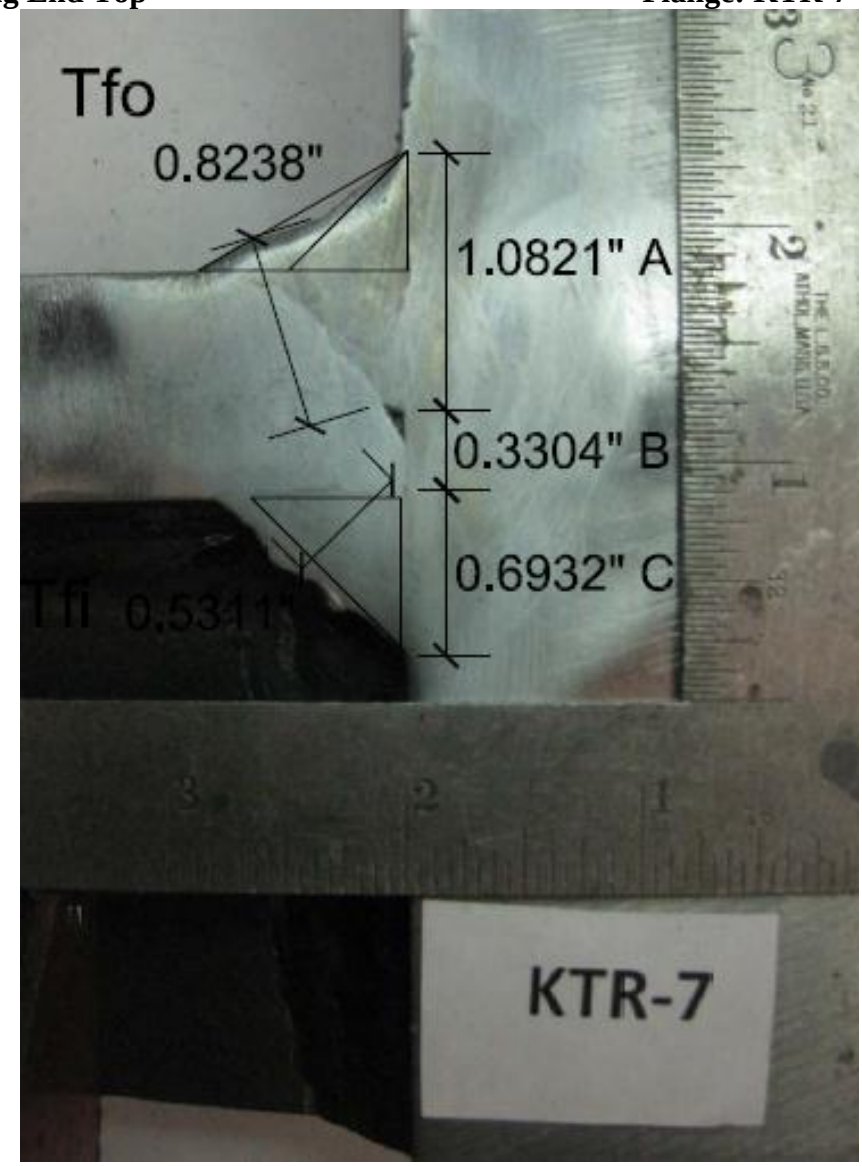

A = Built-up PJP Fillets

B = Lack of Penetration, LOP , Weld Root

C = Reinforcing Fillets

T_{fo} = Throat of A, PJP Fillets

T_{fi} = Throat of C, Reinforcing Fillets

Test: King End Top **Flange: KTR-6**

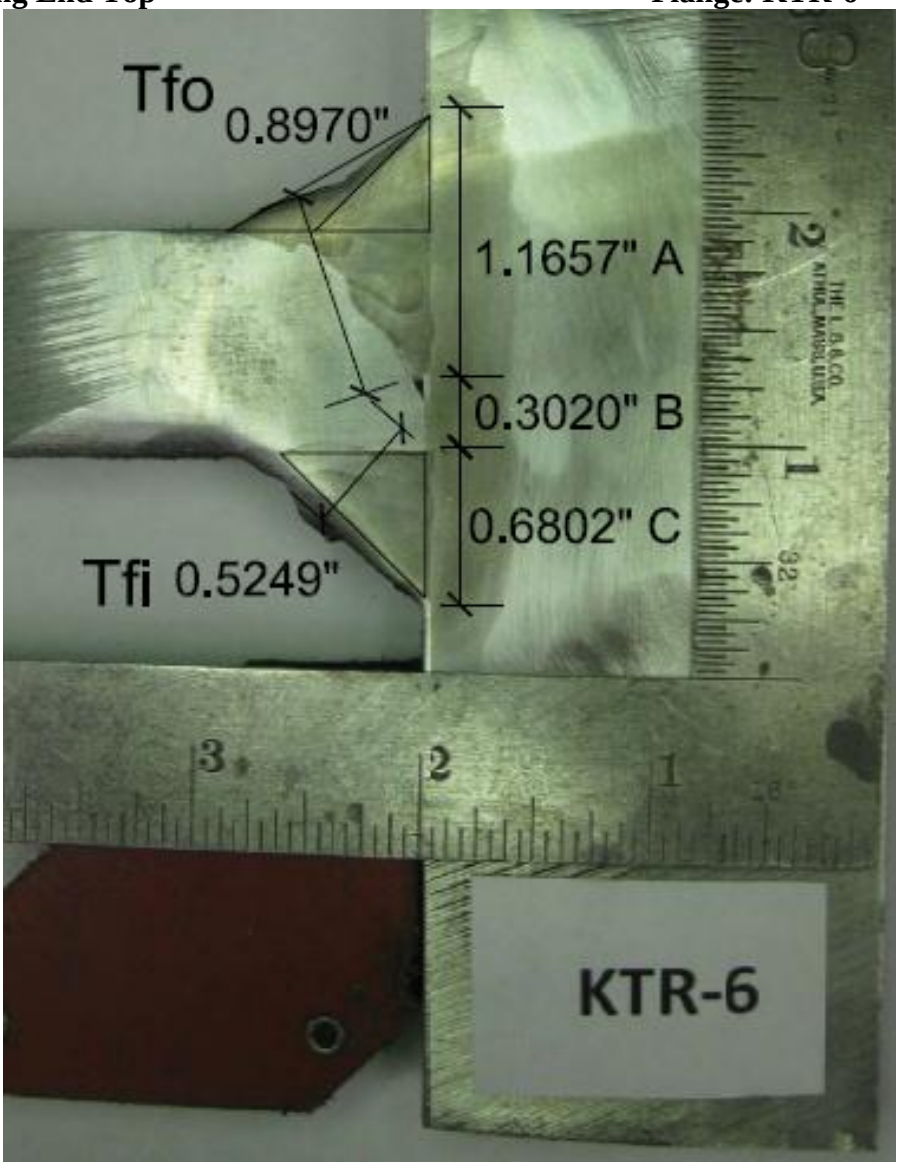

A = Built-up PJP Fillets

B = Lack of Penetration, LOP , Weld Root

C = Reinforcing Fillets

T_{fo} = Throat of A, PJP Fillets

T_{fi} = Throat of C, Reinforcing Fillets

Test: King End Top **Flange: KTR-5**

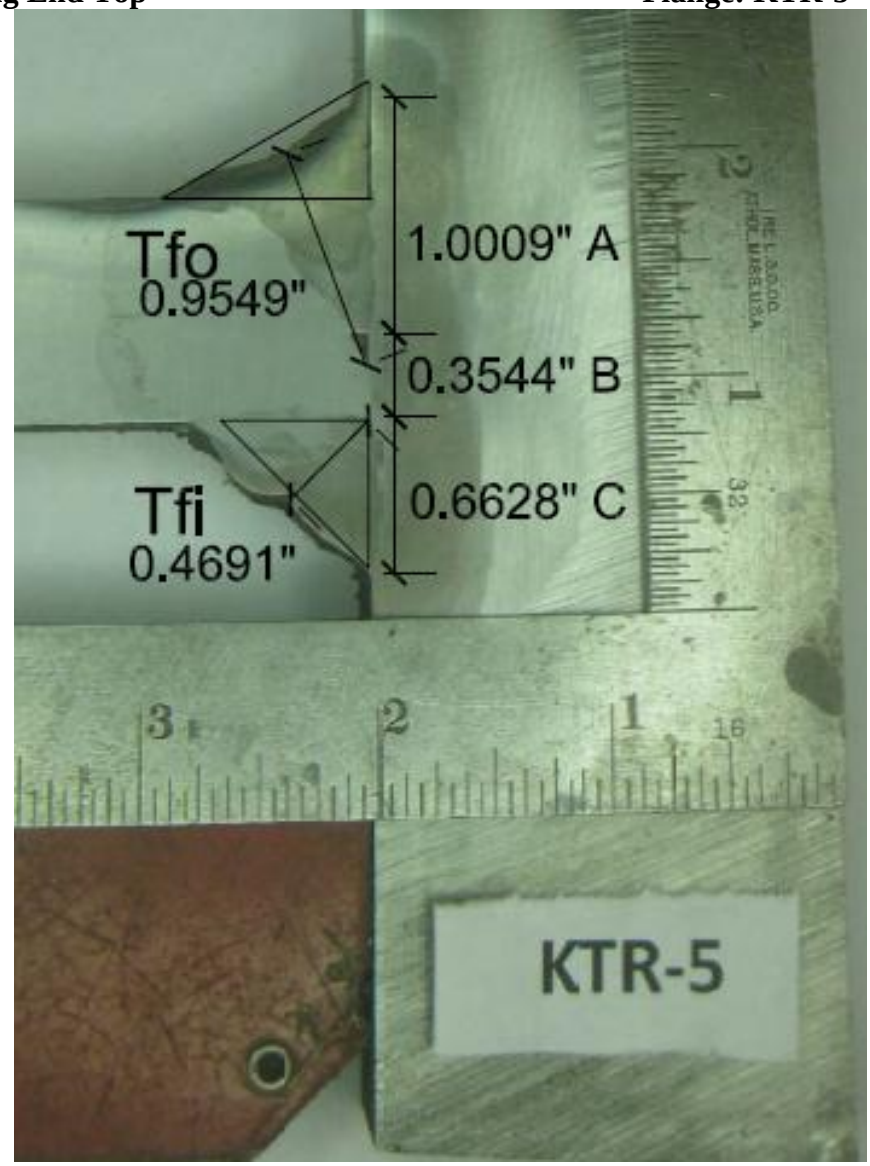

A = Built-up PJP Fillets

B = Lack of Penetration, LOP , Weld Root

C = Reinforcing Fillets

T_{fo} = Throat of A, PJP Fillets

T_{fi} = Throat of C, Reinforcing Fillets

Test: King End Top **Flange: KTR-4**

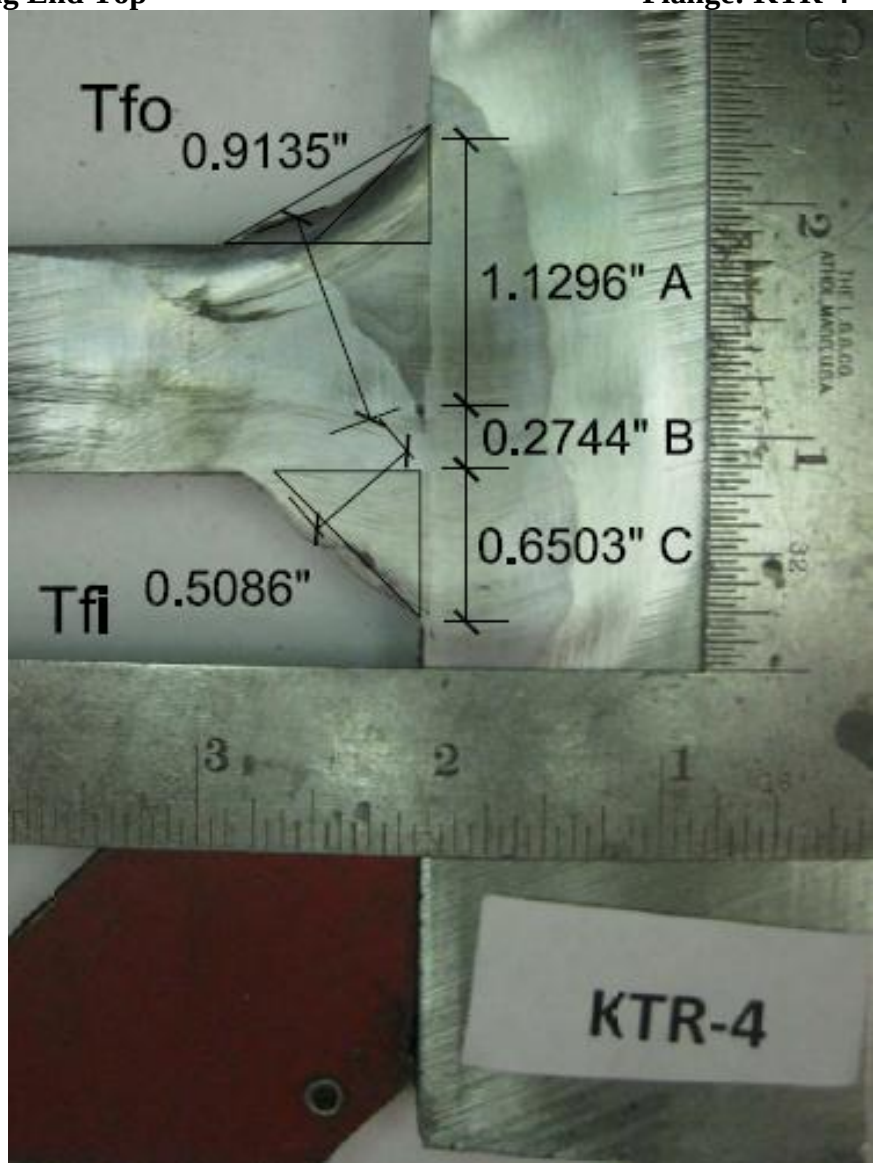

A = Built-up PJP Fillets

B = Lack of Penetration, LOP , Weld Root

C = Reinforcing Fillets

T_{fo} = Throat of A, PJP Fillets

T_{fi} = Throat of C, Reinforcing Fillets

Test: King End Top **Flange: KTR-3**

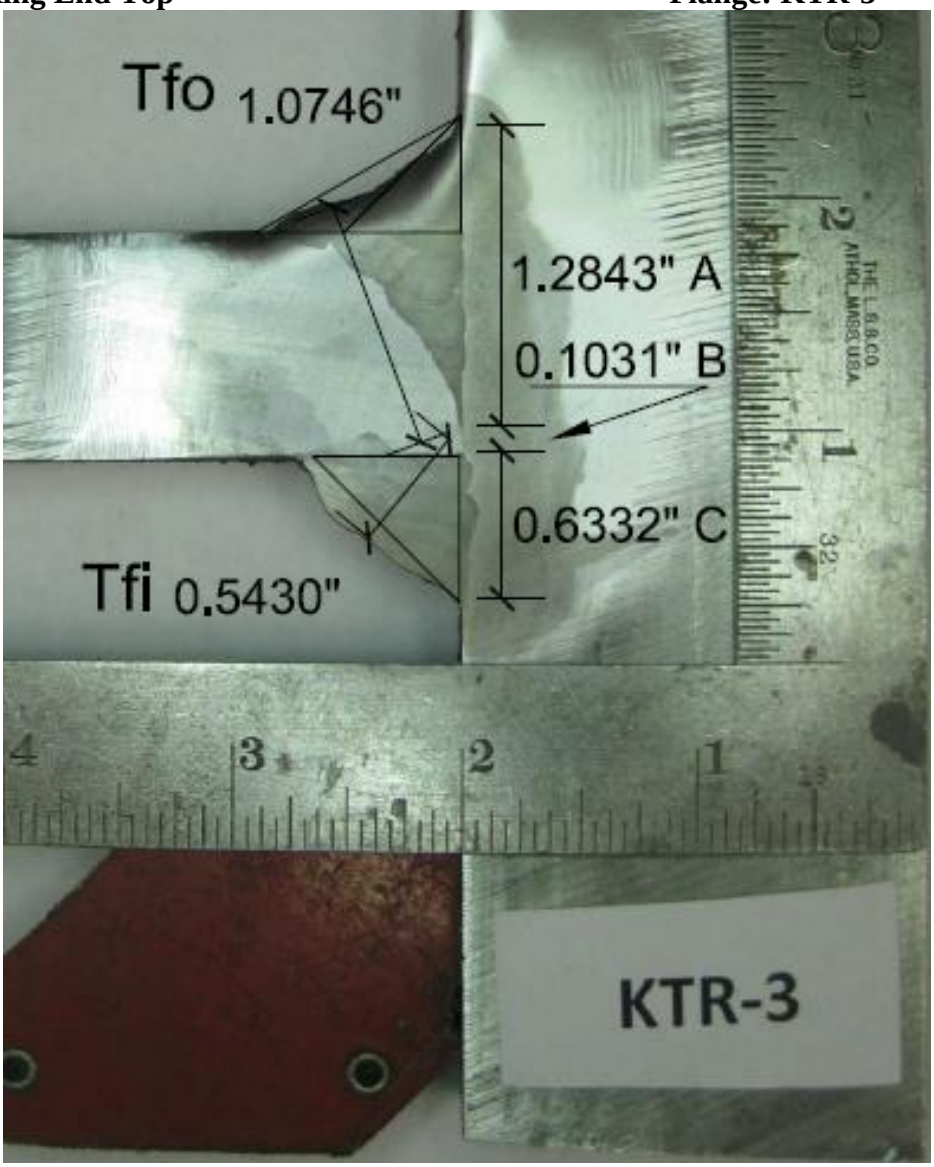

A = Built-up PJP Fillets

B = Lack of Penetration, LOP , Weld Root

C = Reinforcing Fillets

T_{fo} = Throat of A, PJP Fillets

T_{fi} = Throat of C, Reinforcing Fillets

Test: King End Top **Flange: KTR-2**

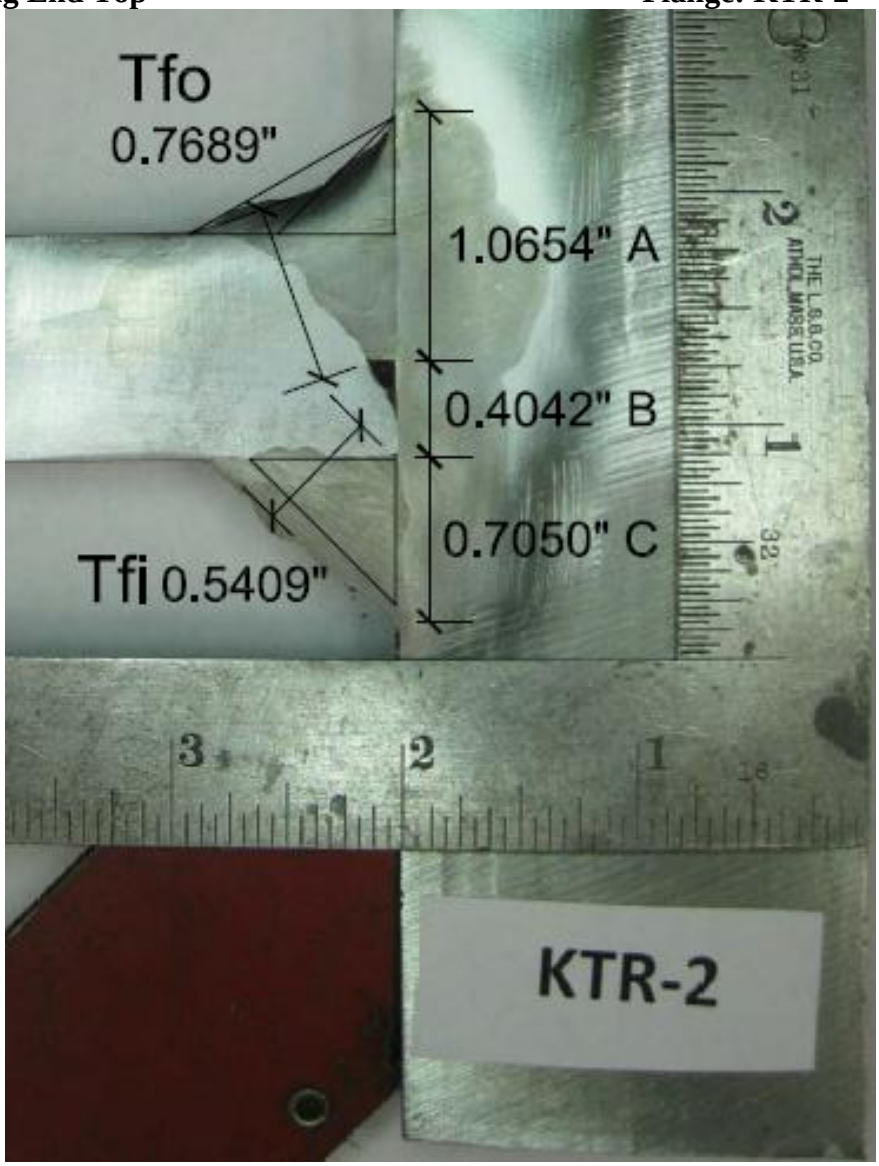

A = Built-up PJP Fillets

B = Lack of Penetration, LOP , Weld Root

C = Reinforcing Fillets

T_{fo} = Throat of A, PJP Fillets

T_{fi} = Throat of C, Reinforcing Fillets

Test: King End Top **Flange: KTR-1**

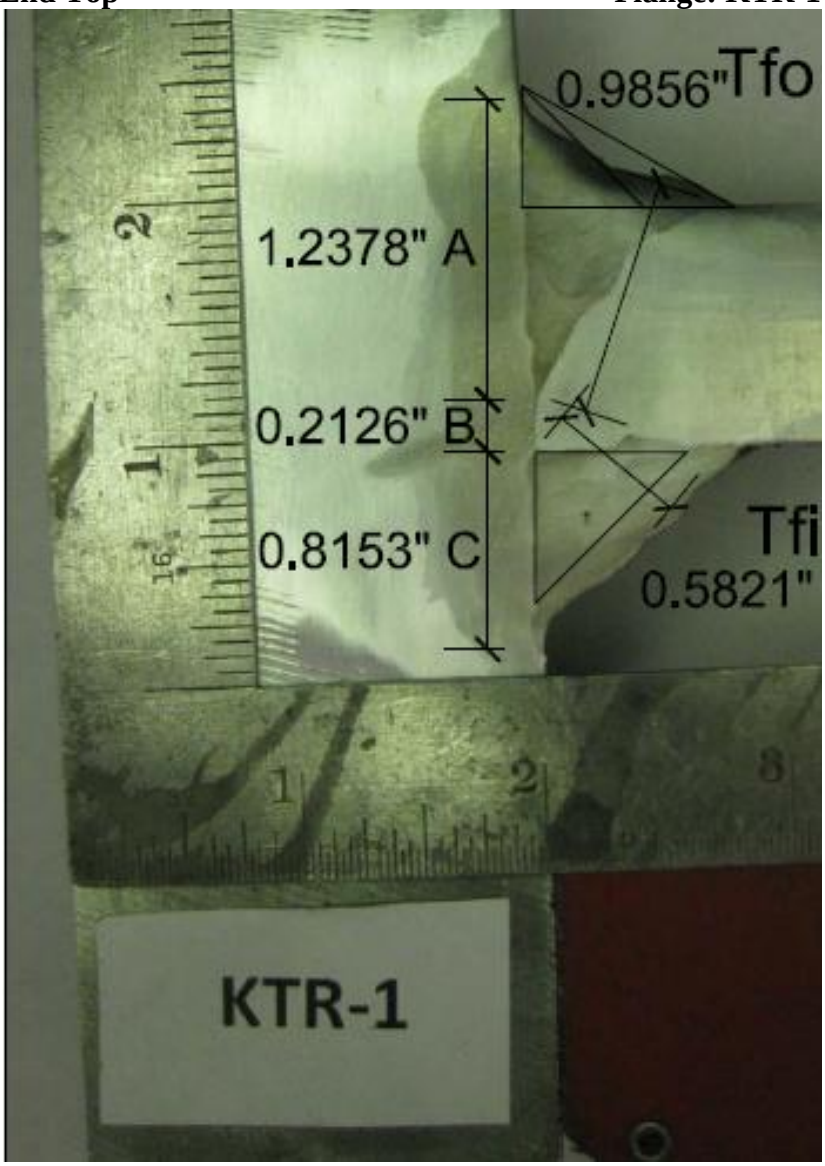

A = Built-up PJP Fillets

B = Lack of Penetration, LOP , Weld Root

C = Reinforcing Fillets

T_{fo} = Throat of A, PJP Fillets

T_{fi} = Throat of C, Reinforcing Fillets